

**The Regulation of Mucilage Production in the Seed Coat Mucilage
Secretory Cells of *Linum usitatissimum* (Flax) and the Genetic Model
*Arabidopsis thaliana***

Bronwen A. Forward

Department of Biology

McGill University, Montreal

August 2016

A thesis submitted to McGill University in partial fulfillment of the requirements of the
degree of Doctor of Philosophy

© Bronwen Forward 2016

ABSTRACT

The trait known as myxospermy is seen across many plant species encompassing a wide range of environmental contexts, whereby the seed coat epidermal cells differentiate to become mucilage secretory cells (MSCs). These cells produce large amounts of mucilage, which consists largely of hydrophilic polysaccharides that swell and burst from the cells upon contact with water. This resulting gel-like capsule surrounding the seed is proposed to confer a number of evolutionary adaptations such as facilitating or preventing seed dispersal, and promoting seed germination under favourable conditions. Mucilage composition varies substantially across species, with pectins and hemicelluloses (i.e. the cell wall matrix polysaccharides) being the primary components. The best studied MSCs are those of the genetic model *Arabidopsis thaliana*, which has become a model system to identify genes involved in cell wall polysaccharide synthesis, secretion, modification and regulation of these processes. One of the few pectin biosynthetic enzymes shown to directly affect mucilage production is *MUCILAGE-MODIFIED 4/RHAMNOSE SYNTHASE 2 (MUM4/RHM2)*, which provides UDP-L-rhamnose for the synthesis of the most abundant pectin in *Arabidopsis* mucilage, rhamnogalacturonan I. In addition to the role of mucilage as an ecological adaptation of the seed, it is also an important agricultural commodity. Linseed flax (*Linum usitatissimum*) mucilage has been characterized in terms of its composition and physical properties, as it is used in soluble dietary fibre supplements, human nutrition, medical adhesives, pharmaceuticals, and texturizing agents in foods. The detailed study of flax MSC differentiation revealed a patterned deposition of mucilage, with a higher concentration of acidic polymers deposited in the outer mucilage region, while more neutral polymers accumulate in the inner region. This pattern correlates with both a change in Golgi stack morphology and the differential upregulation of putative UDP-L-

rhamnose and UDP-D-xylose synthases. These nucleotide sugar synthases are substantially upregulated in flax seed coats during mucilage production, suggesting a potential role in providing the required substrates for mucilage production in flax. Bioinformatic analysis of the flax RHM gene family revealed great divergence between family members compared to that seen in *Arabidopsis* and other species. In addition to investigating mucilage production in flax, we further expand our understanding of mucilage production and regulation using the *Arabidopsis* MSC model. *MUM4 ENHANCER 4 (MEN4)* is identified as a novel putative transcription factor that localizes to the nucleus and is homologous to *TATA-BINDING PROTEIN-ASSOCIATED FACTOR 8*, a component of the general transcription machinery and other regulatory complexes. *men4* mutants produce approximately 30% of the mucilage produced by wild-type seeds, and also appear to produce smaller seeds. The additive phenotype of the *mum4 men4* double mutant suggests that MEN4 affects mucilage production via factors independent of, and possibly in addition to, MUM4, and preliminary qRT-PCR results suggest that potential downstream targets of MEN4 may include currently unknown factors.

RÉSUMÉ

Le trait de la myxospermie peut être observé à travers une large gamme de contextes environnementaux dans lesquels les cellules épidermales de l'écorce graineuse se différencient pour devenir des cellules de mucilage sécrétoires (CMS). Ces cellules produisent énormément de mucilage, qui consistant en majorité de polysaccharides qui gonflent et qui font éventuellement éclater les cellules en contact avec l'eau. La théorie courante indique que cette gélule qui encapsule la graine confère plusieurs adaptations évolutives telles que la promotion ou la prévention de la dispersion ainsi que la promotion de la germination sous conditions favorables. La composition du mucilage varie considérablement selon l'espèce avec les pectines et les hémicelluloses (les polysaccharides qui forment la matrice de la paroi cellulaire) comme constituants principaux. Les CMS les plus connues sont celles du modèle génétique *Arabidopsis thaliana*, qui est devenu un exemple idéal pour l'identification des gènes qui sont impliqués dans la régulation des processus de synthèse, de sécrétion et de modification des polysaccharides de la paroi cellulaire. Un des enzymes peu connus au substrat de pectine et qui a été identifié comme acteur direct dans la production du mucilage est le *MUCILAGE-MODIFIED 4/RHAMNOSE SYNTHASE 2 (MUM4/RHM2)* qui fournit le UDP-L-rhamnose pour la synthèse de la protéine de mucilage la plus abondante chez *Arabidopsis*, la rhamnogalacturonan I. En plus de son rôle dans l'adaptation écologique de la graine, il représente aussi une commodité agricole importante. Le mucilage des graines de lin (*Linum usitatissimum*) a déjà été caractérisé en termes de sa composition et de ses propriétés physiques, puisqu'il est utilisé dans les compléments de fibres diététiques solubles, dans le domaine de la nutrition humaine, dans les adhésifs médicaux, les pharmaceutiques et les agents de texturisation dans certains produits alimentaires. L'étude approfondie sur la différenciation dans les CMS du lin a révélé que la déposition du mucilage

s'effectue de façon particulière, avec une concentration plus élevée de polymères acides dans les régions externes du mucilage et une concentration de polymères neutres plus élevée en rentrant vers les régions de l'intérieur. Ce motif est en corrélation avec un changement de morphologie dans les dictyosomes de l'appareil de Golgi et d'une surexpression différentielle putatif des synthases de l'UDP-L-rhamnose et du UDP-D-xylose. La production des synthases de nucléotides à base de glucides est considérablement augmentée dans l'écorce de la graine de lin pendant la production du mucilage, ce qui suggère qu'ils jouent possiblement un rôle dans la procuration des substrats nécessaire pour la production du mucilage. L'analyse bioinformatique de la famille génétique *RHM* a révélé un écart considérable entre les membres de cette famille comparé à ce qui a été observé chez *Arabidopsis* et autres espèces. En plus de nos recherches sur la production du mucilage dans le lin, nous développons davantage notre compréhension sur la production du mucilage et de sa régulation en nous basant sur le modèle des CMS d'*Arabidopsis*. *MUM4 ENHANCER 4 (MEN4)* est identifié comme étant un nouveau facteur de transcription putatif qui se localise au niveau du noyau et qui est homologue au *TATA-BINDING PROTEIN-ASSOCIATED FACTOR 8*, qui est un constituant de la machinerie générale de transcription et d'autres complexes régulateurs. Les mutants du *men4* produisent à peine 30% du mucilage du genre déjanté ainsi que de plus petites graines. Le phénotype additif du double mutant *mum4 men4* suggère que *MEN4* exerce un effet sur la production du mucilage qui est indépendant et possiblement en concert avec *MUM4* et les résultats préliminaires du gRT-PCR démontrent que certaines cibles en aval du *MEN4* pourraient inclure des facteurs qui reste à découvrir.

ACKNOWLEDGEMENTS

First and foremost, I would like to express my sincere gratitude to my supervisor, Dr. Tamara Western. Her relentless guidance, enthusiasm, patience, and dedication to my training as a researcher have been invaluable, and I could not have accomplished this without her. Working with her has been a truly rewarding experience, and I cannot possibly thank her enough.

I would also like to thank my supervisory committee members, Dr. Greg Brown and Dr. Hugo Zheng, who generously gave their time to provide support and constructive insight over the course of my studies.

Throughout the years, I have had the privilege of working alongside some great graduate students, research assistants, undergraduate students, and postdoctoral fellows. I am thankful to my lab co-workers, past and present, for all of their advice, entertainment, and assistance in the many times I needed an extra set of hands. I would like to thank Mike Ogden and Jonathan Palozzi for their roles in the continuation of the project, and Sami Chaaban for his assistance and expertise in the chromatography work. There are so many others who have not been mentioned here, to whom I am also forever grateful to for all of their help.

I would like to thank the many wonderful friends who have been there to cheer me up or celebrate even small successes, depending on experimental outcomes that day. Thanks also to Dave, for the countless cups of coffee, and sometimes wine, that have been handed to me during the writing of this thesis.

Finally, my deepest thanks go to my Mom for nurturing my love of science from a very young age, and to my Dad and Stepmom for their constant reminders that “You can eat an elephant – one bite at a time.”

PREFACE AND CONTRIBUTIONS OF AUTHORS

This thesis is comprised of three chapters, the first of which is a review of the literature. Original contribution to knowledge in chapter two includes the development of flax mucilage secretory cells, the identification of both UDP-L-rhamnose and UDP-D-xylose synthase gene families, as well as their developmental expression pattern during mucilage production. Chapter three includes the further detailed characterization of the *men4* mutant phenotype, cell biology, and cloning of the *MEN4* locus, identifying this gene as a putative transcription factor involved in mucilage regulation in Arabidopsis.

Chapter 2: This chapter is in preparation for publication, and is expected to be submitted in the coming weeks. All work was carried out by myself, with the following exceptions: T. Western was responsible for the chemical fixation and resin-embedding of flax seed coats presented in Figure 2.1. A. Abdeen provided the *GL2promoter::GUSPlus* construct, and M. Jordan performed the flax transformations with this construct to provide the transgenic flax lines used in this study.

Chapter 3: This chapter identifies *MEN4* as a novel putative mucilage regulator, and is in preparation for publication pending further work characterizing its molecular role. All work was carried out by myself, with the following exceptions: A. Arsovski performed the phenotypic analysis of ruthenium red and immunostained seeds, toluidine blue stained seed sections, and seed size measurements presented in Figures 3.1, 3.2, and 3.4. T. Western and A. Arsovski performed the chemical analyses of mucilage polysaccharides presented in Tables 3.1 and 3.2, and sample fixation for TEM imaging. ErYang Li assisted with the creation of the *MEN4::GFP* and *35S::HA::MEN4* constructs.

TABLE OF CONTENTS

ABSTRACT	3
RESUME.....	5
ACKNOWLEDGEMENTS	7
PEFACE AND CONTRIBUTIONS OF AUTHORS	9
TABLE OF CONTENTS	11
LIST OF FIGURES.....	15
LIST OF TABLES	16
LIST OF ABBREVIATIONS	17
CHAPTER1: Literature Review: Introduction to the prevalence, function, cell biology, and genetics of seed coat mucilage secretory cells (MSCs), and the synthesis of matrix polysaccharides	19
1.1 INTRODUCTION.....	21
1.2 MYXOSPERMY.....	23
1.2.1 Definition, prevalence, and ecological function.....	23
1.2.2 Composition of seed coat mucilages	24
1.2.3 Cell Biology of Mucilage Production.....	25
1.3 CELL WALL MATRIX POLYSACCHARIDES AND THEIR SYNTHESIS	31
1.3.1 Overview of the matrix polysaccharides	31
1.3.2 Pectins	32
1.3.2.1 Homogalacturonan.....	33
1.3.2.2 Xylogalacturonan.....	34
1.3.2.3 Rhamnogalacturonan II	34
1.3.2.4 Rhamnogalacturonan I.....	35
1.3.3 Hemicellulose	36
1.3.3.1 Xyloglucan.....	36
1.3.3.2 Xylans.....	37
1.3.3.3 Mannans.....	37

1.3.3.4 Mixed linkage glucans.....	38
1.3.4 The enzymatic components of matrix polysaccharide biosynthesis.....	38
1.3.4.1 NSEs	39
1.3.4.2 NSTs	41
1.3.4.3 GTs	42
1.3.4.4 Golgi-localized polysaccharide synthase complexes	44
1.3.5 RG I Biosynthesis.....	46
1.3.6 Arabinoxylan biosynthesis	49
1.4 THE GENETICS OF MUCILAGE PRODUCTION AND ITS REGULATION	54
1.4.1 The Arabidopsis MSC model system.....	54
1.4.1.1 Outer integument differentiation	54
1.4.1.2 Mucilage synthesis and secretion	55
1.4.1.3 Mucilage polysaccharide modification.....	59
1.4.1.4 Mucilage structure	62
1.4.2 Genes in seed coat development and mucilage production in other species.....	65
1.5 RESEARCH GOALS.....	66
Link between Chapter 1 and 2.....	79
CHAPTER 2: The cell biology, patterning, and regulation of mucilage production in the seed coat mucilage secretory cells of <i>Linum usitatissimum</i> (Linseed flax)	81
ABSTRACT	83
2.1 INTRODUCTION.....	85
2.2 MATERIALS AND METHODS	91
2.2.1 Plant materials and growth conditions	91
2.2.2 Staging of flower age	91
2.2.3 Microscopy.....	92
2.2.4 Dot blots	93
2.2.5 Separation of flax mucilage.....	94
2.2.6 Sequence alignments and bioinformatics	94
2.2.7 Quantitative RT-PCR	95
2.2.8 Beta-glucuronidase (GUS) assay.....	96

2.3 RESULTS.....	96
2.3.1 Mucilage secretory cell differentiation in flax	96
2.3.2 Cell biology and ultrastructural features of mucilage production in flax MSCs.....	98
2.3.3 Patterned deposition of polymers in flax mucilage secretory cells	99
2.3.4 <i>UDP-L-RHAMNOSE SYNTHASE</i> homologs in flax	103
2.3.5 <i>UDP-D-XYLOSE SYNTHASE</i> homologs in flax.....	106
2.3.6 Expression of flax <i>RHM</i> homologs	107
2.3.7 Expression of flax <i>UXS</i> homologs.....	109
2.3.8 Exogenous protein expression in flax mucilage.....	110
2.4 DISCUSSION	111
2.4.1 Flax MSCs are specialized seed coat epidermal cells that fill entirely with mucilage	111
2.4.2 Changes in Golgi stack morphology during mucilage production.....	112
2.4.3 Deposited mucilage has striped regions of differential polysaccharide compositions.....	113
2.4.4 Upregulation of nucleotide sugar synthase genes potentially involved in the production of substrates for mucilage production.....	116
2.4.5 <i>RHM</i> genes in flax have undergone unique divergence compared to orthologs in other genomes.....	118
2.4.6 <i>RHM</i> , <i>UER</i> and <i>UXS</i> expression are correlated with both differential polysaccharide deposition and changes in Golgi stack morphology.....	120
2.4.6 Functional protein co-products can be secreted into flax mucilage	122
Link between Chapter 2 and 3.....	167
CHAPTER 3: The identification and characterization of <i>MUCILAGE-MODIFIED 4 ENHANCER</i> <i>4 (MEN4)</i> , a putative transcription factor involved in the regulation of mucilage production ...	169
ABSTRACT	171
3.1 INTRODUCTION.....	173
3.2 MATERIALS AND METHODS	178
3.2.1 Plant lines, mutagenesis and growth conditions.....	178
3.2.2 Microscopy	179

3.2.3 Seed Size Measurements	179
3.2.4 Chemical Analysis.....	180
3.2.5 Immunofluorescence	181
3.2.6 <i>MEN4</i> mapping and bioinformatics.....	181
3.2.7 <i>MEN4</i> cloning and fusion constructs.....	182
3.2.8 GUS expression assay	183
3.2.9 GFP imaging.....	184
3.2.10 Qualitative and quantitative (real-time) RT-PCR.....	184
3.3 RESULTS.....	185
3.3.1 <i>men4</i> mutants produce less mucilage	185
3.3.2 Additive phenotype of <i>men4 mum4</i> mutants	188
3.3.3 <i>men4</i> mutants have no gross defects in Golgi stack morphology	190
3.3.4 <i>men4</i> mutants have smaller seeds.....	191
3.3.5 <i>MEN4</i> encodes a novel putative transcription factor with homology to a TATA- Binding Protein-Associated Factor.....	191
3.3.6 <i>MEN4</i> is expressed in multiple tissues including the developing seed coat.....	193
3.3.7 <i>MEN4</i> localizes to the nucleus in Arabidopsis MSCs.....	195
3.3.8 <i>MEN4</i> may regulate mucilage production via transcriptional regulation of currently unknown targets.....	196
3.4 DISCUSSION	198
3.4.1 <i>MEN4</i> affects mucilage production	198
3.4.2 <i>MEN4</i> is a putative transcription factor and may be a tissue-specific paralog of a TATA-binding Protein Associated Factor (TAF)	200
3.4.3 Overview of the potential roles of <i>MEN4</i>	205
CONCLUSIONS AND FUTURE WORK	239
LITERATURE CITED	245

LIST OF FIGURES

Figure 1.1 Schematic diagram of MSC differentiation in Arabidopsis.....	75
Figure 1.2 Selection of nucleotide sugar interconversion reactions catalyzed by NSEs	77
Figure 2.1. Gross morphological features of flax MSC differentiation	127
Figure 2.2. TEM on high-pressure frozen flax MSCs to observe features of secretory apparatus during mucilage production	129
Figure 2.3. Antibodies for different cell wall polysaccharides bind to distinct domains of deposited flax mucilage.....	133
Figure 2.4. Protein alignment of Arabidopsis and seven putative RHM & UER homologs in flax.....	135
Figure 2.5. Protein motif structure of UXS, RHM, and UER orthologs in Arabidopsis and flax.....	139
Figure 2.6. Neighbor-joining tree of putative RHM genes across 33 species.....	141
Figure 2.7. Protein alignment of putative rhamnose synthases across 33 species	143
Figure 2.8. Protein alignment of Arabidopsis and thirteen putative UXS homologs in flax	145
Figure 2.9. Transcript expression of highly upregulated <i>UXS</i> , <i>RHM</i> , and <i>UER</i> orthologs in flax seed coat tissue	149
Figure 2.10. The Arabidopsis <i>GL2</i> promoter drives exogenous protein expression in the flax seed coat for secretion to the mucilage	151
Figure 2.11. Flax <i>RHM</i> and <i>UXS</i> homolog expression is correlated with the deposition of compositionally distinct mucilage regions and changes in Golgi stack morphology	153
Supplemental Figure 2.1. TEM on 13 and 16 DAF seed coats shows vesicles fusing with the plasma membrane.....	157
Supplemental Figure 2.2. Selected dot blots of flax mucilage and water soluble cell wall extracts	159
Supplemental Figure 2.3. Separation of flax mucilage on an anion exchange column into fractions containing polymers of increasing acidity	161
Supplemental Figure 2.4. Transcript expression of a selection of <i>RHM</i> and <i>UXS</i> genes tested for upregulation in seed coat.....	165
Figure 3.1. Ruthenium red staining and seed coat structure of <i>men4-1</i> versus wild-type Col-2 seeds	211

Figure 3.2. Immunofluorescence of developing Col-2 (WT), <i>men4-1</i> , <i>mum4-1</i> and <i>men4-1 mum4-1</i> seed coats and of mature whole seeds	217
Figure 3.3. Transmission electron micrographs of high-pressure frozen and freeze-substituted developing epidermal cells of Col-2 (WT), <i>men4-1</i> , <i>mum4-1</i> and <i>men4-1 mum4-1</i> seed coats.....	219
Figure 3.4. Comparison of seed size for Col-2 (WT) <i>men4-1</i> , <i>mum4-1</i> and <i>men4-1 mum4-1</i> seeds	221
Figure 3.5. <i>MEN4</i> encodes a novel putative transcription factor that contains domains similar to those of TATA-Binding Protein Associated Factors (TAFs).....	223
Figure 3.6. Alignment of MEN4 and AtTAF8 amino acid sequences	225
Figure 3.7. The <i>MEN4</i> promoter drives GUS expression in seedlings, inflorescence, leaves, and seeds	227
Figure 3.8. MEN4 localizes primarily to the nucleus in MSCs	229
Figure 3.9. Quantitative RT-PCR of mucilage-related genes in WT and <i>men4</i> mutant backgrounds	231
Supplemental Figure 3.1. Microarray data on <i>MEN4</i> and <i>AtTAF8</i> expression.....	235
Supplemental Figure 3.2. <i>MEN4promoter::GUS</i> and <i>GL2promoter::GUS</i> expression in seed coats versus embryos.....	237

LIST OF TABLES

Table 1.1: Genes involved in MSC differentiation	68
Table 2.1. Polysaccharide antibodies tested on flax mucilage.....	131
Supplemental Table 2.1. Flax homologs of <i>UXS</i> , <i>RHM</i> , and <i>UER</i> tested for expression levels by qRT-PCR.....	163
Table 3.1. Neutral monosaccharide quantification of mucilage extracted from <i>men4-1</i> , <i>mum4-1</i> and <i>men4-1 mum4-1</i> versus wild-type seeds.....	213
Table 3.2 Monosaccharide quantification of mucilage extracted from <i>men4-1</i> , <i>mum4-1</i> and <i>men4-1 mum4-1</i> versus wild-type seeds using carbodiimide reduction to identify uronic acids	215

LIST OF ABBREVIATIONS

BTP - bromodomain transcription factors and PHD domain-containing proteins

DAF - days after flowering

DPA - days post anthesis

EST - expressed sequence tag

GT - glycosyltransferase

HG - homogalacturonan

IRX - irregular xylem

MEN - MUM enhancer

MSC - mucilage secretory cell

MUM - mucilage-modified

NSE - nucleotide sugar interconversion enzyme

NST - nucleotide sugar transporter

PME - pectin methylesterase

RG I/II - rhamnogalacturonan I/II

RHM - rhamnose synthase

TAF - TATA-binding protein-associated factor

TAPD - TAF65-PRODOS

TBP - TATA-binding protein

TEM - transmission electron microscopy

TGN - trans-Golgi network

UDP - uridine diphosphate

UXS - UDP-xylose synthase

XG - xyloglucan

CHAPTER 1

Literature Review: Introduction to the prevalence, function, cell biology, and genetics of seed coat mucilage secretory cells (MSCs), and the synthesis of matrix polysaccharides

1.1 INTRODUCTION

In flowering plants (angiosperms), pollination and double fertilization leads to not only the initiation of embryogenesis and the formation of the nutrient-rich endosperm, but also to the differentiation of the ovule integument into the mature seed coat, which forms a protective barrier around the embryo until it germinates under favourable conditions. This seed coat can be specialized in a number of ways, conferring specific adaptive properties to the seed. One feature found across a broad variety of seeds in a wide range of environments is the production of large amounts of hydrophilic mucilage, an umbrella term for a pectin-rich polysaccharide gel-matrix that is released from the epidermal cells upon hydration. (Esau 1977; Fahn 1979; Haughn and Western 2012; Western 2012).

Seed coat mucilage has long been commodified in a number of industries based on its soluble fibre content and hydrogel-like properties (Zwieniecki et al. 2001; Zohuriaan-Mehr, M.J. and Kabiri 2008). In the food industry, the mucilaginous seed husks from species such as linseed flax (*Linum usitatissimum*) and *Salvia hispanica* (commonly known as Chia) are widely sold as sources of dietary fibre, binding agents, or egg-substitutes in health foods. Flax mucilage is also highly valued and well characterized as a texturizer, thickener, emulsifying agent, and chemical stabilizer in food products, foams, moisturizers, and medical adhesives, due to its high viscosity, water-retention capabilities, and hypo-allergenic properties (Mazza and Biliaderis 1989; Fedeniuk and Biliaderis 1994; Anttila et al. 2008; Khalloufi et al. 2009; Ganorkar and Jain 2013; Kaewmanee et al. 2014). The seed coat of *Plantago*, or Psyllium husk, is sold as Metamucil®, a digestive aid, and its mucilage is also an efficient pharmaceutical binder that can slow drug release in capsule form (Saeedi et al. 2010). The mucilage of *Solanum viarum*, a member of the nightshade

family, is valued not for its polysaccharide content, but for its co-production of solasodine, a glycoalkaloid that serves as raw material for a number of steroid drugs (Srinivas et al. 1998).

In addition to its variety of uses in human consumption and commercial products, the production of seed coat mucilage provides a powerful model system to study the regulation of cell wall biosynthesis, secretion, and modification, as the polysaccharides occurring in mucilages are also common components of primary and secondary plant cell walls. This has been well-established over the past 15 years through the study of the seed coat mucilage secretory cells (MSCs) of the genetic model plant *Arabidopsis thaliana* (*Arabidopsis*). Currently, over 50 genes involved in ovule integument differentiation, matrix polysaccharide and cellulose biosynthesis, polysaccharide secretion, modifications of these polymers, and their regulation have been identified using this system (Table 1.1; recently reviewed in Western 2012; North et al. 2014; Francoz et al. 2015; Voiniciuc, Yang, et al. 2015). As novel genes continue to be identified in mucilage production, a growing complexity is observed in terms of the polymers present in this specialized cell wall, and how they interact to affect cell wall structure, suggesting that many more mucilage-related genes likely exist, with functions yet to be investigated.

This literature review begins with an overview of the myxospermy trait, its prevalence among the angiosperms, its proposed functions, and the developmental cell biology of seed coat mucilage secretory cells (MSCs). A brief overview of the most prevalent matrix polysaccharides (pectins and hemicelluloses) found in mucilage will also be discussed. This will be followed by an examination of the synthesis of these cell wall polymers, including the types of molecular machinery required to produce a diverse array of polysaccharides, and how they regulate cell wall production. Finally, the genetics of mucilage production and MSC development will be discussed,

with a focus on the *Arabidopsis* genetic model, as it is by far the most extensively characterized system/species. This section will also include known evidence of possible conservation of the mucilage production pathway in myxospermous crop plants.

1.2 MYXOSPERMY

1.2.1 Definition, prevalence, and ecological function

Myxodiaspory refers to an adaptive trait in angiosperms whereby a specialized cell type of the developing seed coat or pericarp (fruit) produces hydrophilic, pectinaceous mucilage, which is secreted to the apoplast (Grubert 1974; Fahn 1979; Boesewinkel and Bouman 1984). This trait has been identified in species spanning a broad number of families, occurring across a wide range of environments. Pericarpal mucilage produced in the fruiting body of seeds is prevalent among the Asteraceae, Lamiaceae, Moraceae, Urticaceae and Poaceae, while seed coat mucilage (myxospermy) is found in a larger number of families including the Acanthaceae, Brassicaceae (including plant model *Arabidopsis thaliana*), Linaceae, Plantaginaceae, and Solanaceae (Kraemer 1898; Witztum et al. 1969; Swarbrick 1971; Young and Evans 1973; Grubert 1974; Bouman 1975; Bushway et al. 1981; Fahn 1982a; Schnepf and Deichgraber 1983a; Gowda 1984; Goto 1985; Sharma and Koul 1986; Eskin 1992; Oomah et al. 1995; Duletiæ-Lauševič and Marin 1999; Ryding 2001; Diederichsen et al. 2006; Kreitschitz and Vallès 2007; Huang et al. 2008; Inceer 2011). Complete lists of known myxospermous species have been assembled in over 100 plant families (Grubert 1974; Grubert 1981; Western 2012). This review will focus mainly on

those that produce seed coat versus pericarpal mucilage, and will incorporate examples from those that have been characterized to some extent.

An interesting feature of the myxospermous angiosperms is their prevalence over a broad range of environments, with particularly high frequencies in both arid and humid habitats (Ryding 2001), suggesting that mucilage likely plays a versatile role in terms of seed adaptation, depending on the environmental context. A number of ecological roles for seed mucilage have been proposed. As myxospermy is rather common in arid regions, it is predicted to aid in seed hydration, as the hydrophilic properties of mucilage allow it to draw and hold water tightly to the seed. Here, it may also act as a water reservoir for germination and seedling development under water and salt stress (Harper and Benton 1966; Grubert 1974; Mott 1974; Ellner and Shmida 1981; Fahn 1982; Penfield et al. 2001; Rautengarten et al. 2008; Arsovski et al. 2009; Kreitschitz et al. 2009; Yang et al. 2010). Seed hydration as a result of seed mucilage has also been implicated in the initiation of DNA repair mechanisms, which is essential when seeds have been subject to long periods of dormancy (Yang et al. 2010). Conversely, mucilage may also prevent germination under water-logged or flooded conditions by regulating oxygen entry into the seed (Heydecker and Orphanos 1968; Witztum et al. 1969; Fitch et al. 2007). Mucilage may also have a number of roles in seed dispersal, where it has been proposed to aid in sticking the seed to soil substrates to prevent washing away by water or wind, promoting adherence to soil near the mother plant where conditions are favourable, adherence to animal substrates (epizoochory), or to ease the passage of the seed through the digestive tract of animals (endozoochory) (Harper and Benton 1966; Fuller and Hay 1983; Lobova et al. 2003; Sun et al. 2012; Yang et al. 2012; Kreitschitz et al. 2015).

1.2.2 Composition of seed coat mucilages

Seed coat mucilages can be categorized as cellulosic or as ‘true slimes,’ where true slimes contain only matrix polysaccharides (pectins and hemicelluloses). Other mucilages contain cellulose, which can take the form of amorphous fibrils (Schnepf and Deichgraber 1983a; Gowda 1984; Haughn and Western 2012; Western 2012). MSCs can also have large secondary cell wall inclusions that are laid down spirally, such as the *Arabidopsis* columella, and cellulosic rays that aid in mucilage adherence to the seed through their interactions with other cell wall polymers. Mucilages are often characterized by the presence of the pectin rhamnogalacturonan I (RG I), however other matrix polysaccharides and cellulose are also prevalent and found in varying proportions in mucilage across species (reviewed in Western 2012; North et al. 2014). Unbranched RG I is the principal component of *Arabidopsis* mucilage, with much smaller amounts of the pectin homogalacturonan (HG), as well as hemicelluloses xyloglucan, glucomannan and arabinoxylan (Voiniciuc, Yang, et al. 2015; Voiniciuc, Schmidt, et al. 2015; Voiniciuc, Guenl, et al. 2015; Hu et al. 2016; Ralet et al. 2016). Conversely, flax mucilage has highly branched RG I, but is primarily composed of double-branched arabinoxylan, with a small amount of HG found in various amounts depending on ecotype (Naran et al. 2008; Kaewmanee et al. 2014; Pavlov et al. 2014). *Blepharis persica* mucilage, like *Arabidopsis*, is composed primarily pectins, but contains mostly HG rather than RG I (Witztum et al. 1969). *Plantago ovata* has mucilage that is primarily composed of the hemicellulose arabinoxylan (Sharma and Koul 1986; Naran et al. 2008). *Plantago psyllium* is thought to also contain a higher proportion of pectins, as Ca⁺ treatment can affect the gel properties of the mucilage, which is characteristic of pectins (Harper and Benton 1966; Grubert 1974; reviewed in Western 2012).

1.2.3 Cell Biology of Mucilage Production

MSCs are a specialized cell type that synthesizes copious amounts of mucilage that is secreted to the apoplast, a region of cell wall deposition outside the cell membrane. In this section, the cell biology of mucilage production in *Arabidopsis* will be described in detail, as it has been investigated most thoroughly, followed by a comparison of the developmental features observed in various other myxospermous species that have been characterized at the cellular level to some extent.

Following fertilization in *Arabidopsis*, the MSC differentiation process (Figure 1.1) begins with expansion of the vacuole, constraining the cytoplasm to the outer edges of the cell (Western et al. 2000). Starch granules are also seen throughout the cytoplasm, and these eventually localize to the distal region of the cell. At this point, differentiation continues as mucilage begins to accumulate via polarized secretion to the apoplast, at the junctions between the distal and radial cell walls, resulting in a ring-shaped secretion zone (Western et al. 2000). As a result of the continued mucilage secretion into the outer edges of the cell, at approximately seven days post anthesis (7 DPA), the starch granule-rich cytoplasm is pushed into the middle of the cell, creating a volcano-shaped column, with the plasma membrane still contacting the basal and lower radial cell walls, as well as a smaller region in the centre of the distal cell wall. Once mucilage secretion to the apoplast has finished, there is deposition of a secondary cell wall that rigidifies the inner column, resulting in a cellulosic structure called a columella. Secondary cell wall production becomes visible by 9 DPA, and is accompanied by shrinkage of the starch granules (Beeckman et al. 2000; Western et al. 2000; Windsor et al. 2000). This observation, along with the evidence that both starchless and excess starch mutants have abnormally-shaped columellae, suggests that these starch reserves may be required in the deposition of cell wall polymers in the columella rather than the mucilage (Western et al. 2000; Windsor et al. 2000). Secondary cell wall deposition

within the columella continues until the cytoplasm undergoes programmed cell death, and eventually the mucilage pocket within the mature MSC desiccates, forming a donut-shaped trough around the columella. Upon hydration, the hydrophilic mucilage swells quickly, breaking the outer tangential cell wall and releasing this mucilage to form a gel-like capsule that envelops the seed. The extrusion of mucilage from the Arabidopsis seed coat results in the formation of two distinct mucilage layers: an outer, water-soluble layer, which can be largely removed upon agitation, and an adherent inner layer, which remains tightly associated with the seed coat (Western *et al.*, 2000). These layers can be easily visualized using the stain ruthenium red, which strongly stains pectic polysaccharides and acidic polymers (Sterling 1970). In both layers, the most abundant pectic polysaccharide is RG I, which is largely unbranched in the outer mucilage layer (Penfield *et al.* 2001; Macquet *et al.* 2007). The inner adherent layer also contains the methylesterified pectin HG (Willats, Orfila, *et al.* 2001; Macquet, *et al.* 2007). In the adherent layer, primary cell wall remnants from the rupture of the MSCs remain attached at the edges of radial and distal cell walls, along with visible rays of crystalline cellulose (Beeckman *et al.* 2000; Western *et al.* 2000; Windsor *et al.* 2000). These cellulose microfibrils are thought to interact directly with pectins and hemicelluloses, tightly adhering mucilage to the seed coat in this region (Macquet *et al.* 2007; Dick-Pérez *et al.* 2011; Haughn and Western 2012; Voiniciuc *et al.* 2015; Hu *et al.* 2016; Ralet *et al.* 2016).

Arabidopsis MSCs have also been studied at the ultrastructural level with transmission electron microscopy (TEM) in order to observe cellular features including the secretory apparatus during mucilage synthesis (Western *et al.* 2000; McFarlane *et al.* 2008; Young *et al.* 2008). Immunogold labelling with an anti-RG I (pectin) antibody (CCRC-M36), which was raised against Arabidopsis mucilage, confirmed that mucilage is synthesized in the Golgi apparatus, as labelling

was found in the trans-Golgi network (TGN), secretory vesicles carrying cargo to the plasma membrane, and in the apoplastic mucilage pocket (McFarlane et al. 2008; Young et al. 2008). Investigation of MSC Golgi stacks also revealed ultrastructural changes in Golgi morphology and quantity at the onset of mucilage production. Prior to mucilage synthesis, Golgi stacks appeared long, thin, and cup-shaped with lightly staining cisternae, along with a small TGN associated with the stack. At 7 DPA, concurrent with the rapid production of mucilage, Golgi stacks had shortened cisternae with swollen margins, and a conspicuous cis-trans polarity, whereby staining was darker in the cisternae towards the TGN due to the presence of the electron-rich pectins present in the luminal margins, where mucilage is accumulated. In addition, large TGNs were present at this stage, and many secretory vesicles were seen associated with the Golgi stacks and throughout the cytoplasm (Young et al. 2008). In addition to a change in Golgi stack morphology during mucilage production, the number of Golgi stacks doubled in number, as demonstrated by both counting stacks in ultrathin-sectioned images, and by counting fluorescently labelled stacks in live cells using confocal microscopy (Young et al. 2008). This increase in Golgi stack number appears to be developmentally regulated rather than mucilage production-dependent, as a mutant that produces very little mucilage also exhibited this increase in Golgi stack number (Young et al. 2008). However, the Golgi stack morphology appears to be affected by the amount of mucilage made, as the same mucilage reduced mutants have very thin, fenestrated and lightly stained Golgi stacks at the stage of MSC differentiation corresponding to mucilage production (Western et al. 2000; Young et al. 2008). Another feature observed in this study was that Golgi stacks were evenly distributed throughout the cells during mucilage production, rather than accumulating near the mucilage pocket. This is in contrast to what is seen in other instances of Golgi-mediated cell wall production, such as cell plate formation in dividing cells or at the tips of growing cells, where

Golgi stacks aggregate near the site of cell wall deposition (Jürgens 2005; Cole and Fowler 2006; Campanoni and Blatt 2007). This suggests that mucilage secretion is a dynamic process where Golgi stacks are mobilized to deposit vesicles and then move away, or that polar secretion of mucilage vesicles are targeted to these cell edges through other factors. At 9 DPA, after mucilage synthesis has finished, the Golgi stacks maintain their swollen appearance, and look similar to that seen at 7 DPA. The anti-RG I antibody does not localize to Golgi at this stage, and it is thought that Golgi vesicles are largely carrying cellulose synthase complexes to the plasma membrane at this point, where they aid in the production of the columellae (Wightman and Turner 2010; Griffiths et al. 2015).

The cytoskeleton of *Arabidopsis* MSCs has also been studied. While actin microfilaments were evenly distributed throughout the MSCs, cortical microtubules (MTs) were mainly found lining the mucilage pocket during mucilage synthesis using both fluorescently-labelled anti-tubulin antibodies and TEM of seed coat cross sections (McFarlane et al. 2008). Interestingly, temperature-sensitive *mor1-1* mutants, which exhibit disorganized MT arrangement, appear to have normal MSC differentiation compared to wild-type, with no visible alterations to mucilage production or columella formation. However, 40% of these mutants exhibited mucilage extrusion defects (McFarlane et al. 2008). These cortical microtubules are believed to be ‘tracks’ which guide cellulose synthase (CESA) complexes to move unidirectionally in a circular manner around the cytoplasmic column, depositing cellulose into the apoplast in a helical array (Griffiths et al. 2015). It has been proposed that the spiral array of cellulose deposited in the mucilage acts like a spring upon water imbibition, aiding in MSC rupture, which may explain the *mor1-1* extrusion defect (Griffiths et al. 2015).

The cell biology of mucilage production in MSCs of other species is fairly limited. Other species that have been examined at the ultrastructural level include *Brassica campestris*, *Plantago ovata*, and *Solanum viarum*, which lack secondary cell wall inclusions and cellulose fibers in the mucilage, and subsequently are not found to have microtubules lining the plasma membrane at secretion sites. Many Golgi stacks accumulate in the cytoplasm, which accumulates in the upper face of the MSCs, forming a secretion zone flat across the plasma membrane. Additionally, these species contain starch granules which appear to shrink during mucilage production, as they are not required to form any cellulosic inner structure (Hyde 1970; Van Caesele et al. 1981; Srinivas et al. 1998). Bright field microscopy suggests this is also the case for the MSCs of flax (Boesewinkel 1980).

At the gross morphological level, secondary cell inclusions resembling the Arabidopsis columellae are seen in *Salvia hispanica* (Chia), *Camelina sativa*, and in many other species of the Brassicaceae (reviewed in Vaughan and Whitehouse 1971; Muñoz et al. 2012; Western 2012; North et al. 2014). Other internal cellulosic structures exist that can vary in form substantially, as seen in *Collomia grandiflora*, where MSCs contain spiral-shaped secondary cell wall fibers that expand upon wetting. A number of *Ruellia* species have long, hair-like MSCs containing mucilage with spiral-shaped fibers that also expand with mucilage release (Hsiao and Chuang 1981; Schnepf and Deichgraber 1983a; Schnepf and Deichgraber 1983b). Cellulose fibers are deposited into the mucilage of developing *Cydonia oblonga* MSCs, and as coiled threads in *Artemisia campestris* and several species of *Salvia* (Abeysekera and Willinson 1988; Kreitschitz 2009). Those species that contain secondary cell wall inclusions that have been studied cytologically have also been found to have cortical microtubules lining the plasma membrane at the site of secretion, as seen

in Arabidopsis, reflecting their likely role in cellulose synthesis (Hsiao and Chuang 1981; Schnepf and Deichgraber 1983a; Schnepf and Deichgraber 1983b; Young et al. 2008).

1.3 CELL WALL MATRIX POLYSACCHARIDES AND THEIR SYNTHESIS

1.3.1 Overview of the matrix polysaccharides

The plant cell wall is a dynamic extracellular network that mediates all aspects of plant growth, development, and stress response. The compounds found in this complex, interaction-rich network include cellulose, hemicelluloses, a diverse group of acidic polysaccharides known collectively as pectins, polysaccharide-active enzymes, and smaller amounts of both glycoproteins and proteoglycans. Cellulose is an integral component of all cell walls, and has been found to interact directly with both hemicelluloses and pectins in the cell wall matrix (Zykwinska et al. 2005; Zykwinska et al. 2007; Zykwinska et al. 2008; Dick-Pérez et al. 2011; Wang et al. 2015). The matrix polysaccharides include both hemicelluloses and pectins, which are synthesized in the Golgi apparatus. Cellulose is synthesized by complexes located in the plasma membrane. Cellulose structure, biosynthesis, and regulation have been well characterized, and extensively reviewed recently, and will not be covered in this review (Li et al. 2014 and McFarlane et al. 2014). Matrix polysaccharides are the main cell wall components found in characterized mucilages, and require a multitude of enzymes for their controlled synthesis. Enzymatic modifications of these polymers are also common within the deposited wall, changing their cross-linking capacity and affecting cell wall properties. This section begins with a structural description of the so-called matrix polysaccharides, followed by an overview of the enzymatic machinery

required for their synthesis in the Golgi apparatus, and control points in their production. Finally, a detailed description of RG I and arabinoxylan synthesis will be covered as an example of both pectin and hemicellulose production, respectively.

1.3.2 Pectins

Pectins are a structurally diverse group of acidic polysaccharides that are characterized by the presence of galacturonic acid (GalA). Along with hemicelluloses, these comprise the matrix polysaccharides within which the cellulose network is embedded (reviewed in Harholt et al. 2010; Yapo 2011; Atmodjo et al. 2013). Primary cell walls of dicotyledonous plants tend to contain a higher proportion of pectin than secondary cell walls and are the main non-cellulosic component, while secondary cell walls and the cell walls of grasses contain very little pectin. However, mucilage appears to be a specialized type of secondary cell wall that can be pectin-rich in a number of species (reviewed in Western 2012). Pectins undergo extraordinary amounts of production in MCSs, but are also a fundamental component of other cell types, as they form the middle lamellae and are the first cell wall components, along with callose, synthesized to form new cell walls during cell division (reviewed in Mohnen 2008). They also undergo constant modification, allowing them to mediate cell wall structure, properties, integrity, loosening, and susceptibility to pathogens. Cell wall models have long portrayed pectins as an amorphous gel-like matrix in which the structural load-bearing cellulose and hemicellulose network is embedded. However, more recent studies strongly suggest that pectins have a far more important load-bearing role than was originally thought, whereby pectins have been recently found to make many direct contacts with cellulose and have a discernible impact on cell wall properties (Zykwinska et al. 2005; Zykwinska

et al. 2007; Zykwinska et al. 2008; Dick-Pérez et al. 2011; Wang et al. 2015; Bidhendi and Geitmann 2015).

Pectins can be categorized into three main structural groups: Homogalacturonan (HG), the substituted HGs rhamnogalacturonan II and xylogalacturonan, and rhamnogalacturonan I (RG I). It is important to note that the study of polysaccharides relies on assays of monosaccharide composition and linkage analysis of polymers that are capable of being solubilized from cell wall preparations and purified to various degrees, creating some limitations in our ability to fully understand the nature of these polymers as they occur in the cell wall. For instance, it is not fully understood whether these pectin groups occur as individual molecules, or as part of a long continuous backbone comprised of pectin structural domains, providing a possible explanation for the difficulty in purifying these compounds into distinct fractions (reviewed in Mohnen 2008; Caffall and Mohnen 2009; Atmodjo et al. 2013; Anderson 2015). Another interesting possibility is that these pectic domains are linked to polypeptides that nucleate their biosynthesis and linkage to other polysaccharides. The discovery of *ARABINOXYLAN PECTIN ARABINOGALACTAN PROTEIN 1 (APAPI)* illustrated the existence of a peptidoglycan structure where HG, RG I, galactan, and xylan domains were linked to a single protein (Tan et al. 2013). It is unclear whether more complexes like this exist and have yet to be purified, or if this is a specialized subpopulation of polysaccharide cell wall components.

1.3.2.1 Homogalacturonan

HG is the most abundant pectic polysaccharide, and consists of a straight chain of unbranched, α -(1,4)-linked GalA residues. The GalA residues can be acetylated at the O-2 or O-3 position, while the C-6 position is readily methylesterified (Willats, Orfila, et al. 2001; Atmodjo

et al. 2013). Methylesterification of pectins, particularly HG, exerts a great effect on cell wall properties by affecting their crosslinking capabilities with other HG molecules. HG tends to be secreted in a highly methylesterified form due to pectin methyltransferases in the Golgi cisternae (Willats, Orfila, et al. 2001; Ibar and Orellana 2007). These are then de-esterified to various extents upon deposition *in muro* by pectin methylesterases, which promote HG cross-linking via interactions with Ca^{2+} , depending on how many GalAs in a row are unesterified (Willats et al. 2000; Willats, Orfila, et al. 2001; Western et al. 2004; reviewed in Levesque-Tremblay et al. 2015).

1.3.2.2 Xylogalacturonan

Xylogalacturonan is a substituted form of HG, as it shares a backbone of α -(1,4)-linked galacturonic acid residues, which can be substituted at the O-3 branch point with a β -linked xylose, and sometimes β -(3,4)-linked xylose small chains. This polymer is mostly enriched in reproductive tissues, and has been proposed to promote protection of HG from pathogen attack by means of these xylose substitutions (Jensen et al. 2008; reviewed in Anderson 2015).

1.3.2.3 Rhamnogalacturonan II

Another highly substituted form of HG is rhamnogalacturonan II, and it is the most structurally complex of all the pectins. As in HG and XGA, RG II has a backbone of α -(1,4)-linked galacturonic acid residues, but is decorated with four evolutionarily conserved sidechains comprised of 12 different sugars arranged in over 20 different linkages. In the cell wall, RG II molecules exist as dimers that are cross-linked by borate diester bonds mediated by conserved apiose residues (O'Neill et al. 2004; Yapo 2011; Atmodjo et al. 2013). While there are relatively

few studies regarding RG II, the high degree of evolutionary conservation suggests its importance in mediating cell wall properties. This is confirmed in studies of mutants causing even subtle changes in branch structure, which have major implications in plant morphology, where plants are often dwarfed as a result (reviewed in Mohnen 2008).

1.3.2.4 Rhamnogalacturonan I

RG I is the second most abundant pectin, and is a primary component of many seed coat mucilages across species (reviewed in Western 2012; North et al. 2014). RG I has an alternating backbone of α -(1,2)-linked rhamnose (Rha) and α -(1,4)-linked GalA residues. The Rha backbone residues can be frequently substituted with sidechains, and the degree of branching is highly variable based on species, cell type, and stage of development. In general, these sidechains are attached to the Rha subunits at the O-4 position, and consist of arabinose and galactose (Willats, McCartney, et al. 2001; Mohnen 2008). RG I sidechains can be individual, linear, or branched. They can contain α -(1,5)-linked arabinans with 2- and 3-linked arabinose or arabinan branching. They may also consist of β -(1,4)-linked D-galactan, where these galactan chains contain 3-linked L-arabinans. Some branches also contain β -(1,3)-linked D-galactan with β -6-linked galactan or arabinan branching (reviewed in Mohnen 2008; Caffall and Mohnen 2009; Anderson 2015). RG I branch structure often varies across species. For example, in flax mucilage, RG I is unusually branched by a single non-reducing L-galactose residues at the O-3 position instead of the typical O-4 position (Naran et al. 2008), whereas galactan residues are bound solely to arabinan sidechains in potato tuber cell walls (ØBro et al. 2004). Conversely, RG I is largely unbranched in *Arabidopsis* mucilage, with infrequent branching of both 1,5-linked arabinans and non-reducing terminal galactosyl residues (Penfield et al. 2001; Naran et al. 2008).

1.3.3 Hemicellulose

Hemicelluloses are a group of neutral to slightly acidic compounds found in plant cell walls that have been characterized by their β -D-(1,4)-linked pyranosyl backbone residues, which give them a cellulose-like conformation that allows hydrogen bonding to occur between these polymers and cellulose microfibrils. These compounds are found in different proportions between primary and reinforced secondary cell walls, and can be organized into four main types: xyloglucans, mannans, xylans, and mixed-linkage glucans.

1.3.3.1 Xyloglucan

Xyloglucan is an abundant, neutral polysaccharide found most commonly in the primary cell walls of many dicotyledonous species. It consists of a β -D-(1,4)-glucan backbone that is decorated with side chains containing α -D-xylosyl, -galactosyl-xylosyl, and -fucosyl-galactosyl-xylosyl residues at regular intervals at the O-6 position. O-acetylation is also prevalent at these sites (Lerouxel et al. 2006; Manabe et al. 2011; Park and Cosgrove 2015). Xyloglucan is thought to form cross-links with cellulose microfibrils due to its cellulose-like backbone, with which it can form hydrogen bonds. This network of xyloglucan and cellulose was long thought to be the major load-bearing feature of plant cell walls, however the role of xyloglucan, its importance to cell wall structure, and its interaction strength with cellulose are currently under debate as new evidence suggests that xyloglucan is more dispensible than was previously thought. The removal of xyloglucan through the use of cell wall mutants has very little effect on cell wall function (Cavalier et al. 2008; Zabolina et al. 2012), and furthermore, NMR studies and adsorption assays reveal that pectins directly interact with cellulose far more frequently than with xyloglucan (Zykwinska et al.

2005; Zykwinska et al. 2007; Zykwinska et al. 2008; Dick-Pérez et al. 2011; Park and Cosgrove 2015; Wang et al. 2015).

1.3.3.2 Xylans

Xylans are predominating hemicelluloses in secondary cell walls of dicotyledonous plants, but some occur in primary cell walls as well. The backbone is composed of β -(1,4)-linked xylose, which can be acetylated, possibly increasing its affinity for cellulose (Busse-Wicher et al. 2014). In a number of species, the reducing end of xylan polymers has a conserved tetrasaccharide of 4- β -D-Xyl-(1,4)- β -D-Xyl-(1,3)- α -L-Rha-(1,2)- α -D-GalA-(1,4)-D-Xyl. The function of this sequence is not fully understood, however it has been proposed that it may act as either an initiator or terminator of xylan backbone synthesis (York and O'Neill 2008; Rennie and Scheller 2014). Xylose residues can also be substituted at the O-2 or O-3 position. Substitutions often consist of α -(1,2)-galactosyl and glucuronyl groups that can be unmodified or methylated. Arabinoxylan has a xylan backbone that is decorated with 2, 3, and double 2,3-linked arabinose residues, and sometimes α -L-arabinofuranosyl substitutions (Caffall and Mohnen 2009). In grasses, arabinose residues of arabinoxylan can also be feruloylated, which may affect its ability to cross-link with other arabinoxylan molecules and lignin (Grabber 2005). While arabinoxylan is found to a lesser extent in cell walls overall, it is often found in mucilages across many different species (Sharma and Koul 1986; Naran et al. 2008; Hao and Mohnen 2014; Rennie and Scheller 2014; Zhong and Ye 2015).

1.3.3.3 Mannans

A relatively minor group of dicotyledonous secondary cell wall components, with the exception of sugar storage tissues, are mannans. This group is comprised of galactomannans and galactoglucomannans, which are also similar in structure to cellulose, and are important in both cell wall structure and as sugar storage polysaccharides. Galactomannans have a backbone of β -(1,4)-D-mannose and β -(1,4)-D-glucose at irregular intervals. In galactoglucomannans, 1,6-galactose sidechains are attached to the mannose residues, while, in other variations, the mannose residues can also be acetylated (reviewed in Zhong and Ye 2015).

1.3.3.4 Mixed linkage glucans

Mixed linkage glucans consist of an unsubstituted backbone of glucosyl residues that contain β -(1,3) and β -(1,4) linkages, where stretches of β -(1,4) linked glucose residues are separated by a single β -(1,3) linkage, conferring polymer flexibility in those regions. These are found predominately in monocot primary cell walls (Caffall and Mohnen 2009; Burton et al. 2010).

1.3.4 The enzymatic components of matrix polysaccharide biosynthesis

Like all polysaccharides, pectins and hemicelluloses are synthesized by glycosyltransferases that use activated nucleotide sugars as their substrates. Their synthesis takes place in the lumen of the Golgi apparatus, from which these large polymers are secreted to the plasma membrane and deposited to the apoplast via secretory vesicles (Dupree and Sherrier 1998; Sterling et al. 2001; Young et al. 2008; Driouich et al. 2012). Pectin and hemicellulose synthesis requires the co-operation of a plethora of nucleotide sugar substrate-specific enzymes categorized into three main functional roles: 1) nucleotide sugar interconversion enzymes (NSEs), which

synthesize the activated sugar building blocks, 2) nucleotide sugar transporters (NSTs) to channel those sugar monomers made in the cytoplasm into the Golgi lumen, and 3) glycosyltransferases (GTs) to catalyse glycosidic linkages between the donor sugar and the acceptor polysaccharide chain.

1.3.4.1 NSEs

Glycan synthesis in the Golgi apparatus requires an abundance of activated sugar donors to be added to the growing polysaccharide chain. NSEs catalyze the synthesis of the 30 different nucleotide sugars found in plants through the conversion of the precursor NDP-glucose, which is the primary product of photosynthesis. These enzymes carry out conversion reactions through a combination of epimerase, decarboxylase, dehydrogenase, and reductase activities, which are specific to a particular NDP-sugar substrate, causing changes in sugar conformation and structure (examples shown in Figure 1.2) (reviewed in Bar-peled and Neill 2011). At least 100 NSE genes have been predicted in the genetic model plant *Arabidopsis*, and many more have been identified in other species through biochemical, genetic, and bioinformatic approaches (Reiter 2008; Yin et al. 2011). These interconversion reactions, along with a sugar salvage pathway, which converts free sugars to nucleotide sugars in reactions catalyzed by sugar kinases and UDP-sugar pyrophosphorylases, provide the substrate for the synthesis of all polysaccharides and glycoproteins of the plant (reviewed in Seifert 2004; Bar-peled and Neill 2011). Eleven NSE families have been identified in plants, all of which are represented in *Arabidopsis*, where multiple isoforms can exist for a particular enzymatic activity. These often have overlapping expression and functional redundancy, while some have tissue-specific upregulation. This is the case for the synthesis of Rha, through the conversion of UDP-D-Glc to UDP-L-Rha, where there are three

RHAMNOSE SYNTHASE genes, *RHMI*, 2, and 3, in addition to *NUCLEOTIDE RHAMNOSE SYNTHASE/EPIMERASE-REDUCTASE (NRS/ER)*, also known as *UER1*, which can perform two of the three catalytic reactions of the RHM proteins (Usadel et al. 2004; Watt et al. 2004; Western et al. 2004; Diet et al. 2006; Oka et al. 2007). NSE isoforms can also have different catalytic efficiencies and NAD⁺ cofactor requirements, as seen in the UDP-D-glucose/UDP-D-galactose 4-epimerase genes (*UGE1-5*) (Barber et al. 2006). A number of NSEs contain transmembrane domains which anchor them to the Golgi apparatus with their catalytic domains facing the lumen.

For example, *UGE4*, one of five UDP-D-Gal synthase isoforms in the UDP-D-glucose/UDP-D-galactose 4-epimerase family, has a Golgi-localized transmembrane domain, whereas the others are cytoplasmic (Barber et al. 2006). Half of the UDP-xylose synthase isoforms and a number of the glucuronate 4-epimerases (GAEs) that synthesize GalA also have transmembrane domains, while others are localized to the cytoplasm. Rhamnose synthases, on the other hand, are all predicted to localize to the cytoplasm, as none of them contain a predicted transmembrane domain (Harper and Bar-Peled 2002; Gu and Bar-Peled 2004; Mølhøj et al. 2004; Pattathil et al. 2005; Barber et al. 2006; reviewed in Atmodjo et al. 2013).

The availability of the correct amount of the proper nucleotide sugar is a key factor in maintaining the right levels of pectins and hemicelluloses. For this reason, NSEs can act as regulators of polysaccharide biosynthesis at the substrate level. The transcript level expression of a particular isoform in a particular tissue and developmental stage can have dramatic effects on plant phenotype. For example, *UGE* mutant plants have defects in pollen development, general plant growth, and root growth, depending on which isoforms are mutated, due to altered XG levels in different plant tissues (Rösti et al. 2007). Further regulation via NSEs is seen at the protein

level, where sugar substrates can inhibit enzymatic activity of their own NSE, or NSEs of other sugar substrates. For example, rhamnose and xylose synthases are both mutually inhibited by UDP-L-Rha and UDP-D-Xyl *in vitro* (Hinterberg et al. 2002; Turner and Botha 2002; Oka et al. 2007).

1.3.4.2 NSTs

As many NSEs are cytoplasmic, the action of NSTs is required to channel activated sugars into the Golgi lumen where they can be accessible to glycosyltransferases for the incorporation into polysaccharide chains. NSTs are hydrophobic proteins with between six and ten transmembrane domains, and were first discovered in plants at the biochemical level using Golgi vesicles isolated from pea (*Pisum sativum*) (Munoz et al. 1996). Presently, over 50 transporter members in six clades have been identified and confirmed for sugar substrates such as GDP-mannose, UDP-rhamnose/UDP-galactose, UDP-glucose, and UDP-xylose (reviewed in Reyes and Orellana 2008; Rautengarten et al. 2014; Ebert et al. 2015). All transporters discovered thus far appear to have discrete substrate specificities and can similarly affect polysaccharide synthesis at the substrate level. In rice, a UDP-glucose transporter mutant *brittle culm14 (bc14)* had pleiotropic effects on plant biomechanical properties, and indirectly modulate cellulose content in cell walls by a reduction in the matrix polysaccharides (Zhang et al. 2011). The more recent development of a technique for NST characterization using NST expression in liposomes and subsequent measurement of sugar uptake via mass spectroscopy lead to the discovery of a UDP-rhamnose/UDP-galactose transporter (URGT2) that regulates RG I production at the substrate level, and mutants exhibit decreased mucilage, much like *mum4/rhm2* rhamnose synthase mutants

(Usadel et al. 2004; Western et al. 2004; Rautengarten et al. 2014). This technique also resulted in the identification of at least three UDP-xylose transporters. As half of the UDP-xylose synthases are localized to the Golgi apparatus via their transmembrane domain, generating a pool of xylose in the Golgi lumen, it may seem redundant to have xylose-specific Golgi transporters. However, mutations in *UDP-XYLOSE TRANSPORTER1 (UXT1)* result in a 30% reduction in xylose in stem cell walls, indicating that both cytoplasmic and Golgi-synthesized pools of UDP-xylose are important in maintaining proper xylose levels for polysaccharide synthesis (Ebert et al. 2015). Though few have been studied, NST expression resembles that of NSEs, whereby transcript levels are fairly ubiquitous throughout all tissues, with some isoforms being upregulated in particular tissues. For example, while both *URGT* and *UXT* genes exhibit ubiquitous expression throughout the plant, *URGT2* has the highest expression in seeds (Rautengarten et al. 2014), and *UXT3* is the most abundant transcript in its family, particularly in pollen and flowers (Ebert et al. 2015).

1.3.4.3 GTs

Once the nucleotide sugars are synthesized and transported to the Golgi lumen, GTs catalyze the formation of glycosidic linkages between activated nucleotide sugar monomers and the polysaccharide chain acceptor molecule. Matrix polysaccharide biosynthesis requires a large array of unique GTs in order to produce the diverse array of molecules found in plant cell walls. Assuming that unique enzymes are needed to catalyze each unique glycosidic linkage in these polymers, it is estimated that at least 53 distinct GT enzymatic activities would be required in pectin synthesis alone (Mohnen 2008; Harholt et al. 2010). Both pectin and hemicellulose GTs have been identified in *Arabidopsis*, both bioinformatically and biochemically while a number have also been predicted in other species using purified enzyme extracts with measured enzymatic

activities on specific sugar substrates (reviewed in Caffall and Mohnen 2009; Gorshkova et al. 2012; Atmodjo et al. 2013; Zhong and Ye 2015). The identification and characterization of GT activities and their encoding genes is difficult, as reconstitution of their enzymatic conditions is hindered by the challenge of obtaining pure active enzyme preparations and obtaining the proper substrates for the reactions (Atmodjo et al. 2013). While relatively few GTs have been confirmed and characterized in terms of their biochemical function, those that have all localize to Golgi membranes, with many having predicted and proven membrane domains (reviewed in Oikawa et al. 2013). The expression of GTs at the transcript level resembles that seen in NSE and NST families, where isoforms exhibit fairly ubiquitous expression with one or more showing upregulation in particular tissues. For example, HG backbone synthesis is mediated by several GT8 family members, the *GALACTURONOSYLTRANSFERASE (GAUT)* and *GALACTURONOSULTRANSFERASE-LIKE (GATL)* gene families. Gene family members of both are expressed transcriptionally in all tissues in Arabidopsis, while *GATL4* is specific to pollen grains and elongating pollen tubes (Kong et al. 2011). The RHAMNOGALACTURONAN XYLOSYLTRANSFERASES (RGXTs) 1-4 add UDP-Xyl onto L-Fuc of RG II sidechains (Egelund et al. 2006; Egelund et al. 2008; Petersen et al. 2009). *RGXT1* and 2 are expressed in seedlings and vegetative tissue in mature plants, while *RGXT 3* is only expressed in leaves and siliques of mature plants. *RGXT4*, however, is the most abundantly expressed and is found in all tissues (Egelund et al. 2006; Egelund et al. 2008; Liu et al. 2011).

Acetyltransferases (ATs) and methyltransferases (MTs) are also involved in the synthesis of matrix polysaccharides in the Golgi apparatus. ATs and MTs modify these polymers during their synthesis through facilitating the addition of acetyl and methyl groups, respectively, to sugar monomers of hemicelluloses and pectins. These modifications rely on the import of donors acetyl

Co-enzyme A and S-adenyl-L-methionine, respectively, to the Golgi lumen through Golgi-localized co-enzyme transporters (Lee et al. 2011). Although there are currently no known ATs for pectin specifically, several DUF231-containing *TRICHOME BIREFRINGENCE LIKE (TBL)* genes with xylan-acetyltransferase activity have been investigated and found to affect acetylation levels of xylan, with mutations having prominent effects on plant morphology (reviewed in Gibeaut 2000; Scheible and Pauly 2004; Caffall and Mohnen 2009; Yin et al. 2010; Atmodjo et al. 2013; Yuan et al. 2013; Yuan, Teng, Zhong, and Ye 2016a; Yuan, Teng, Zhong, Haghghat, et al. 2016; Yuan, Teng, Zhong, and Ye 2016b; Schultink et al. 2015). Mutations in a putative pectin MT gene with sequence similarity to known MTs led to the identification of QUASIMODO-2/TUMOROUS SHOOT DEVELOPMENT-2 (QUA2/TSD2). *qua2/tsd2* mutants have decreased cell adhesion and reduced levels of HG (Krupková et al. 2007; Mouille et al. 2007). While the catalytic activity of QUA2/TSD2 has not been confirmed, its mutant phenotype is similar to *qual*, a putative HG GT (HG:GalAT), suggesting it functions in pectin synthesis (Bouton et al. 2002).

1.3.4.4 Golgi-localized polysaccharide synthase complexes

Matrix polysaccharide biosynthesis requires the coordination of many NSEs, NSTs, and GTs. Thus it has been proposed that they can form multi-subunit complexes in the Golgi apparatus that can pass acceptor substrates to one another and incorporate nucleotide sugars into the growing polymers (Atmodjo et al. 2013; Oikawa et al. 2013). Evidence for complex formation is fairly well documented, particularly within the GTs. The galacturonosyltransferases *GAUT1* and *GAUT7* act in a non-redundant fashion, and both are involved in catalyzing the formation of the HG backbone. Co-immunoprecipitation assays indicate that these form a complex in the Golgi membrane (Atmodjo et al. 2011). Interestingly, *GAUT1* has a transmembrane domain that is

removed *in vivo* through proteolytic cleavage, but maintains its transferase activity. GAUT7, inversely, appears to lack catalytic function when expressed alone, but maintains its membrane anchor, indicating that these may be required to function together via anchoring to the Golgi membrane by GAUT7 (Atmodjo et al. 2011). QUASIMODO3 (QUA3), a putative HG methyltransferase (Miao et al. 2011), also purifies with the GAUT1/GAUT7 complex (Atmodjo et al. 2011). Similarly, co-immunoprecipitation, Fluorescence Resonance Energy Transfer (FRET), and Bi-molecular Fluorescence Complementation (BiFC) assays confirmed that the arabinosyltransferase ARAD1 interacts in complex with itself and with family member ARAD2 to facilitate the addition of arabinan sidechains to pectins (Harholt et al. 2012). Hemicellulose synthases appear to form complexes as well, as seen with the xylan backbone synthases IRREGULAR XYLEM (IRX) 9, 10, and 14, which may be enriched with different IRX isoforms in a tissue-specific manner, as different proportions of these enzymes co-purify with each other depending on tissue and species (Wu et al. 2010; Chiniquy et al. 2013; reviewed in Hao and Mohnen 2014; Ren et al. 2014; Lund et al. 2015). Biosynthetic complex formation has also been implicated in xyloglucan synthesis, where BiFC confirmed interactions between a CESA-like glucan synthase and several xylosyl transferases that putatively add xylosyl residues to the glucan backbone (Chou et al. 2012; Lund et al. 2015).

Mounting evidence for these complexes includes the use of novel methods of reconstitution and characterization of these complexes *in vivo* using BiFC (Lund et al. 2015). Results strongly suggest the formation of multi-protein ‘metabolons’ acting in a temporal and tissue-specific manner that requires the right amount of sugar substrates along with the proper transferase isoforms specific to that sugar. These may act in one of two proposed models of polysaccharide biosynthesis in the Golgi lumen. In one mechanism, GT complexes pass acceptor

chains back and forth in a subsequent fashion, adding sugars that it receives from NSTs and membrane-bound NSEs. The alternative theory is that distinct polysaccharide domains are synthesized by the different complexes en bloc, and are subsequently linked together by yet unknown ‘oligotransferases’ which facilitate linkage of longer lengths of donor and acceptor molecules (reviewed in Atmodjo et al. 2013).

1.3.5 RG I Biosynthesis

RG I is comprised of an alternating backbone of Rha and GalA, with a variety of arabinan, galactan, and arabinogalactan sidechains, and it has been estimated that its synthesis requires as many as 35 GTs (Mohnen 2008). Most of the NSEs, NSTs and GTs involved in polysaccharide synthesis exist as large multi-gene families with functional redundancy, making genetic dissection of pectin and hemicellulose production difficult. While several key enzymatic activities required in RG I synthesis have been identified in a number of species (reviewed in Mohnen 2008; Caffall and Mohnen 2009; Atmodjo et al. 2013), few genes encoding RG I biosynthetic enzymes have been characterized compared to how many likely exist, according to this estimate. This review will mainly focus on biosynthetic genes studied in *Arabidopsis*, as these have been investigated in most detail, and have made use of insertional mutants to determine the effect of mutations on plant phenotypes and cell wall composition.

Nucleotide sugars UDP-L-Rha and UDP-D-GalA are the building blocks of the RG I backbone. The conversion of UDP-D-Glc to UDP-D-GalA requires both UDP-Glc dehydrogenase and UDP-Glc 4-epimerase enzymatic activities, however no genes in either of these families have been directly implicated in RG I synthesis. Three *RHAMNOSE SYNTHASE (RHM)* genes are found in *Arabidopsis*, which all encode a tri-functional enzyme that catalyzes the conversion

of UDP-D-Glc to UDP-L-Rha via a UDP-Glc 4,6-dehydratase domain in the N-terminus, and a C-terminal combined 3,5-epimerase / 4-keto-reductase domain that performs the latter parts of the reaction using the UDP-4-keto-deoxy-Glc intermediate as a substrate (Reiter and Vanzin 2001; Oka et al. 2007). Two *RHMs* have been directly linked to RG I synthesis. *RHM2/MUCILAGE MODIFIED 4 (RHM2/MUM4)* provides the UDP-Rha substrate for RG I production in seed coat mucilage, and mutants have mucilage with decreased Rha and GalA (Usadel et al. 2004; Western et al. 2004; Oka et al. 2007). *RHMI* has also been implicated in RG I synthesis in Arabidopsis root hair cell walls, where a similar decrease in Rha and GalA is observed (Diet et al. 2006; Wang et al. 2009). Rhamnose synthases are cytoplasmic and therefore require transporters to move rhamnose from the cytoplasm to the Golgi lumen. A family of six UDP-L-Rha/UDP-D-Gal transporters (*URGTs*) were investigated for transporter activity on a number of sugar substrates. The *urgt2* mutant was found to have decreased mucilage, and linkage analysis confirmed that, while RG I structure was unaffected, RG I size and amount was reduced, indicating that this transporter may channel the proper amount of rhamnose to synthesize the correct levels of RG I (Rautengarten et al. 2014). There are currently no known GTs that have been confirmed to catalyze glycosidic linkages between the UDP-L-Rha and UDP-D-GalA residues of the RG I backbone. The GT8 enzyme *GALACTURONOSYLTRANSFERASE-LIKE 5 (GATL5)* resembles the galacturonosyltransferases seen in HG backbone synthesis (reviewed in Atmodjo et al. 2013; Anderson 2015). *gatl5* mutants exhibit seed coat mucilage defects wherein both GalA and Rha are both decreased and less RG I is produced in general, but this RG I is larger in size than that extracted from wild-type seeds. Unlike other known galacturonosyltransferases (*GAUTs*), *GATL5* does not have a transmembrane domain, despite its localization to the Golgi apparatus, suggesting that it is likely recruited to the Golgi membrane via interactions with other GTs. While *gatl5*

mutants exhibit reduced Rha and GalA in mucilage, the protein did not appear to have GalAT activity *in vitro*, and may instead regulate RG I size through some other function (Kong et al. 2013).

A number of enzymatic activities and genes involved in RG I sidechains have also been identified. β -(1,4)-GalT activity affecting RG I galactan sidechains have been identified in a number of species. Purified extracts from plant endomembrane preparations in pea, flax, soybean, mung bean, and potato have the enzymatic capacity to elongate pre-existing galactans (Goubet and Morvan 1993; Geshi et al. 2000; Baydoun et al. 2001; Peugnet et al. 2001; Geshi et al. 2002; Abdel-Massih et al. 2003; Geshi et al. 2004; Ishii et al. 2004; Konishi et al. 2007). For example, membrane preparations from mung bean can elongate existing galactans through the addition of galactopyranose onto 1,4-galactan acceptors up to approximately 25 subunits in length, resembling native galactan sidechains (Ishii et al. 2004). While these enzymes are capable of adding to a growing galactan chain, a separate enzyme may be needed to create a glycosidic linkage between the galactan chain and the rhamnose residues of the RG I backbone. This specific activity was isolated from potato membrane preparations, which was able to add galactose to the C-4 residue of UDP-L-Rha. Interestingly, glycosidic linkages were only possible when the RG I substrate had low levels of pre-existing galactan sidechains, while RG I substrates with no galactans or many galactans were not acceptors for this GalT activity (Geshi et al. 2002). In *Arabidopsis*, three putative GT92 members GALACTAN SYNTHASE (GALS) 1, 2, and 3 were identified, and GALS1 was confirmed biochemically as a β -(1,4)-galactan β -(1,4)-galactosyltransferase that acts on RG I sidechains (Liwanag et al. 2012). *gals1* mutants have decreased galactose content in their cell walls, while overexpression results in an increase. *gals2* and *gals3* T-DNA insertional mutants also exhibit reduced cell wall galactose, and therefore may

have similar roles in RG I synthesis. Arabinosyltransferase activity promoting linkage of arabinan side chains has also been identified. In mung bean preparations of Golgi membranes, both 1,5-AraT and lower levels of 1,3-AraT activity has been detected (Ishii, Konishi, et al. 2005; Konishi et al. 2006). In one study in mung bean, AraT activity was confirmed where arabinans could be added directly to β -galactan side chains on the RG I backbone, forming arabinogalactan branches (Ishii, Ono, et al. 2005). In *Arabidopsis*, *ARABINAN DEFICIENT 1 (ARAD1)* and its homolog *ARAD2* are two of seven GT47 protein family members implicated in pectin arabinan biosynthesis, and mutants exhibit decreased cell wall arabinans by approximately 70%, despite maintaining normal overall plant morphology (Harholt and Jensen 2006; Harholt et al. 2012). *ARAD1* and *ARAD2* can form homo- and heterodimers with one another (Lund et al. 2015) and function non-redundantly, as neither can rescue the mutant phenotype of the other (Harholt et al. 2012). Mutant analysis and immunostaining with various anti-pectin antibodies suggest that these are putative RG I: AraTs, but their precise biochemical function has yet to be confirmed.

1.3.6 Arabinoxylan biosynthesis

Xylans are highly abundant in dicot secondary cell walls and exist with a number of variable side chain modifications (Faik 2010; Rennie and Scheller 2014; Zhong and Ye 2015). Arabinose substitution of the xylan backbone is relatively less prevalent in cell walls overall, however there are exceptions in both monocot primary cell walls and in mucilage of myxospermous plants (Muralikrishna et al. 1987; Naran et al. 2008). As xylans comprise a large portion of secondary cell walls, and their abundance and structure has major implications in cell wall properties and agricultural extractability, considerable effort has gone into investigating the genes involved in xylan biosynthesis.

Arabinoxylan synthesis requires pools of both UDP-D-Xyl and UDP-L-Araf for the backbone and sidechains, respectively. UDP-D-Xyl production largely relies on the activity of *UDP-XYLOSE SYNTHASE (UXS)* genes, six of which have been identified in Arabidopsis, with orthologs found in other species including poplar, cotton, and tobacco (Harper and Bar-Peled 2002a; Bindschedler et al. 2007; Du et al. 2013). These act as UDP-D-GlcA decarboxylases, which convert UDP-D-GlcA to UDP-D-Xyl. In Arabidopsis, the cytoplasmic isoform *UXS3* is the only *UXS* gene implicated in the synthesis of xylans thus far, as *uxs3* mutants are affected in secondary cell wall production (Harper and Bar-Peled 2002a; Zhong and Ye 2012). In cotton, one cytosolic and two membrane-bound *UXS* homologs are transcriptionally upregulated during secondary cell wall production in fiber cells, and were confirmed to all have UDP-D-GlcA decarboxylase activity when expressed in bacteria, suggesting these play a role in xylan biosynthesis (Pan et al. 2010). Several *UXS* genes in tobacco were also implicated in xylan synthesis, as their downregulation resulted in a decrease in cell wall xylan compared to other cell wall polymers that also contain xylose (Bindschedler et al. 2007). As half of the *UXS* genes in Arabidopsis are localized to the Golgi apparatus membrane via a conserved transmembrane domain, it may seem redundant for xylose synthesis to require transporters to import cytoplasmic UDP-D-Xyl, however, a family of three *UDP-XYLOSE TRANSPORTER (UXT)* genes were recently identified, where *uxt1* mutants had a 30% xylose reduction in stem cell walls, indicating the importance in maintaining both cytoplasmic and Golgi lumen pools of UDP-D-Xyl (Ebert et al. 2015). Currently, there are no known arabinose synthases that have been specifically linked to arabinoxylan biosynthesis, however, a putative glucuronoarabinoxylan synthase complex purified from wheat contained putative XylIT, AraT, and GlcAT activity in addition to UDP-arabinose mutase activity that

catalyzes the conversion of arabinopyranose to arabinofuranose, which is essential prior to being incorporated onto the xylan backbone (Zeng et al. 2010).

At the centre of xylan backbone biosynthesis is a putative complex comprised of several GT43 and GT47 xylosyltransferases. IRREGULAR XYLEM 9 (IRX9), IRX10, and IRX14 interact in Arabidopsis, along with their functionally redundant paralogs IRX9-LIKE (IRX9-L), IRX10-L and IRX14-L. Double mutants between any gene pair result in severe cell wall-related defects such as dwarfing, reduced XylT activity, and little to no xylan in cell walls (Brown et al. 2007; Lee et al. 2007; Brown et al. 2009; Faik 2010; Lee et al. 2010; Wu et al. 2010; Lee et al. 2012). It is thought that these IRX proteins form a xylan synthase complex located in the Golgi membrane that may vary in terms of the types and relative amounts of IRX isoforms present. In a putative glucuronoarabinoxylan synthase complex purified from wheat endosperm, members from GT47, GT43, and GT75 immunoprecipitated together, including functional homologs of both IRX10 and IRX14, but not IRX9 (Zeng et al. 2010). Conversely, an IRX9 ortholog from rice copurifies with IRX9-L and IRX14, and the overexpression of IRX9 alone is sufficient to increase xylan content in Arabidopsis cell walls (Chiniquy et al. 2013). In psyllium (*Plantago ovata*), whose seed coat produces almost pure arabinoxylan, *IRX10* and a number of *IRX10* paralogs were transcriptionally enriched in mucilaginous tissue, while *IRX9* and *IRX14* homologs were nearly undetectable, indicating either tissue-dependent complex formation or evolutionary divergence of xylan synthesis pathways (Harholt and Jensen 2006; Jensen et al. 2013; Jensen et al. 2014). More recently, the novel GT61 *MUCILAGE-RELATED 21 (MUCI21)/MUCILAGE-MODIFIED 5 (MUM5)* was found to be co-expressed during mucilage production in Arabidopsis along with *IRX14*, where they are both required in the synthesis of a highly branched xylan. In this specialized highly branched form of xylan, MUCI21/MUM5 adds xylose substitutions to the straight xylan

backbone produced at least in part by IRX14 (Voiniciuc, Guenl, et al. 2015; Hu et al. 2016; Ralet et al. 2016). Despite the ability of IRX9 and IRX14 to promote xylan synthesis via XylT activity in both *Arabidopsis* and tobacco (Wu et al. 2010; Lee et al. 2012), these isoforms lack the conserved amino acid motifs required for enzymatic activity in mammalian GT43 proteins, while maintaining their transmembrane domains that localize them to the Golgi membrane (Ren et al. 2014). It is possible that these remain an essential component of xylan synthesis due to their structural role in the xylan synthase complex, where they may aid in anchoring the complex in the Golgi membrane and/or confer substrate specificity through the substrate binding domains maintained in these proteins (Ren et al. 2014). IRX10 and its paralog IRX10-L are currently the only isoforms confirmed biochemically to synthesize xylan *in vitro*, and may form the core of many xylan synthase complexes (Jensen et al. 2014; Urbanowicz et al. 2014).

A number of additional GT mutants have been identified that affect xylan backbone synthesis beyond IRX10 and its previously described complex partners. Mutations in *IRX7/FRA8*, *IRX7-L/F8H*, *IRX8/GAUT12*, and *PARVUS/GATL1* cause decreased levels of xylan, where existing xylans have a larger molecular weight and also lack the reducing end tetrasaccharide common to most xylans (York and O'Neill 2008; reviewed in Rennie and Scheller 2014). This led to the hypothesis that these GTs are involved in the addition of this oligosaccharide and that it acts as a terminator of xylan backbone elongation (York and O'Neill 2008). However, homologs of *IRX8*, *IRX7*, and *PARVUS* exist in both *Physcomitrella* and grasses, which do not have this reducing end in the xylan backbone (Kulkarni et al. 2012), and therefore the precise functions of these enzymes have yet to be determined.

There are currently no GTs confirmed *in vitro* to synthesize the 1,2- and 1,3-linkages of arabinose residues on the xylan backbone, but there is evidence that these exist and may exist in complex with xylan synthases. In wheat, a putative glucuronoarabinoxylan synthase complex was immunoprecipitated, and contained putative GTs from GT43, GT47, and GT75 families exhibiting XylT, AraT, GlcT and Araf mutase activity. However, the precise enzymatic activities of these GT family members have not been defined (Zeng et al. 2010). In addition, a number of GT61 family members from wheat endosperm were confirmed to have AraT activity, and caused a decrease in α -(1,3)-linked arabinose (Chiniquy et al. 2012). Overexpression of these wheat orthologs in *Arabidopsis* also resulted in increased arabinose substitutions (Anders et al. 2012), however their homologs have not yet been investigated in *Arabidopsis*.

Modifiers of the xylan backbone and its branches have also been investigated. The *REDUCED WALL ACETYLATION* genes *RWAI-4* encode acetyl coenzyme A transporters, which move cytosolic acetyl donors to the Golgi lumen (Lee et al. 2011; Manabe et al. 2011). The DUF231 domain-containing *TBR29/ESKIMO1 (ESK1)* was found to affect levels of 2-O and 3-O-acetylation of xylosyl residues, where mutants had substantially less acetylation, and xylans were more accessible to and digested by endoxylanases (Yuan et al. 2013; Urbanowicz et al. 2014). *ESK1* acts in conjunction with a number of other *TBR-like* proteins including *TBL3*, and *TBL31–35*, where double and triple mutants were even more severely affected in xylan acetylation levels (Yuan, Teng, Zhong, and Ye 2016a; Yuan, Teng, Zhong, Haghghat, et al. 2016; Yuan, Teng, Zhong, and Ye 2016b). Hemicellulose acetyltransferases are of particular interest in agricultural applications, as acetylation is a hindrance for the use of plant biomass as biofuels. In addition to xylan acetylation, esterification of arabinoxylan with ferulic acid via an ester linkage to arabinose side chains can alter cell wall recalcitrance through the formation of ferulate dimers,

which are thought to cross link arabinoxylan polymers in the cell wall. A feruloyltransferase homolog from rice, *BdAT1*, was exogenously expressed in the grass *Brachypodium distrachyon*, resulting in increased ferulate levels (Buanafina et al. 2015), but these homologs have not yet been investigated in *Arabidopsis*.

1.4 THE GENETICS OF MUCILAGE PRODUCTION AND ITS REGULATION

1.4.1 The Arabidopsis MSC model system

The MSCs of *Arabidopsis* have been extensively exploited as a model system in which to screen for genes involved in various aspects of cell wall biosynthesis, modification, structure, polar secretion and the tight regulation of these processes. The primary function of these specialized cells is to produce great amounts of mucilage, and this trait provides an easily screenable means of determining even subtle phenotypes resulting from mutations in genes affecting mucilage production and properties, and their regulation. There are currently over 50 genes that have been identified through genetic analyses of *Arabidopsis* MSCs (summarized in Table 1.1) (reviewed in Western 2012; North et al. 2014; Francoz et al. 2015; Voiniciuc, Yang, et al. 2015).

1.4.1.1 Outer integument differentiation

Outer integument differentiation establishes the cell fate of the MSCs and is controlled by a number of factors. Their loss via mutation results in loss of or severe defects in MSC differentiation. Unsurprisingly, these have severe effects on mucilage production and mutants

make very little to no mucilage. The pleiotropic regulator *APETALA 2 (AP2)* and two redundantly functioning NAC family transcription factors (TFs) *NARSI* and *NARS2* act early in the establishment of inner and outer integument differentiation, and mutations in these genes result in the absence of MSC differentiation (Bowman, J.L. and Koornneef 1994; Jofuku et al. 1994; Debeaujon 2000; Western et al. 2001; Kunieda et al. 2008). In addition to these master regulators, the YABBY protein *INNER NO OUTER (INO)*, a class III homeodomain leucine zipper protein *REVOLUTA (REV)*, and two functionally redundant KANADI family TFs *KANI* and *KAN2* also contribute to the proper formation of the outer integument, and mutants have severely arrested MSC differentiation (McAbee et al. 2006; Kelley et al. 2009).

1.4.1.2 Mucilage synthesis and secretion

Many of the genes currently characterized in the Arabidopsis MSC system were discovered due to their reduced mucilage mutant phenotypes. Genes involved in the production and secretion of mucilage, and their transcriptional regulators, produce less mucilage overall, often with notable reductions in both Rha and GalA, representing the backbone subunits of the pectin RG I. Since RG I is the most abundant pectin in Arabidopsis mucilage, Rha and GalA quantification is a means to determine mucilage production defects in these mutants.

To date, relatively few of the known MSC genes have been verified as pectin biosynthetic enzymes. The best characterized biosynthetic gene required for mucilage production is *MUM4/RHM2* (Usadel et al. 2004; Western et al. 2004; Oka et al. 2007; Arsovski et al. 2009), which catalyzes the conversion of UDP-D-Glc into UDP-L-Rha (see previous section) (Oka et al. 2007). All three Arabidopsis *RHM* genes are expressed ubiquitously, however *MUM4/RHM2* is specifically upregulated in the seed coat at the time of mucilage production (Western et al. 2004).

mum4 mutants produce approximately one tenth of the quantity of mucilage found in wild-type seeds when quantified by Rha and GalA levels, indicating that *MUM4/RHM2* is a key limiting factor of mucilage production at the RG I substrate level (Western et al. 2004; A. a. Arsovski et al. 2009). Since RHMs are cytoplasmic, an NST is necessary to import Rha into the lumen of the Golgi apparatus for RG I backbone synthesis. A bi-functional UDP-L-Rha / UDP-D-Gal transporter URGT2 was recently discovered that is able to transport UDP-L-Rha in reconstituted liposomes, and mutants have a reduced mucilage phenotype (Rautengarten et al. 2014). One mutant allele of *URGT2* also exhibited decreased UDP-D-Gal in extracted mucilage, suggesting that this NST is able to transport both substrates (Rautengarten et al. 2014). Two putative GTs GALACTURONOSYL-TRANSFERASE-LIKE 5 (GATL5) and GALACTURONOSYLTRANSFERASE 11 (GAUT11) were also identified to have mucilage production defects in the mutants, and may be involved in pectin synthesis (Caffall et al. 2009; Kong et al. 2013). *gat15* mutants exhibit a more subtle reduction in mucilage production than *mum4* mutants (Kong et al., 2013). The RG I present in *gat15* mutants is approximately 60% higher in molecular weight than that of wild-type, suggesting that the role of *GATL5* in RG I production involves more than GalAT activity, and may regulate RG I molecular size (Kong et al. 2013). One mutant allele of *gaut11* produces somewhat reduced mucilage, with a decrease in GalA levels exclusively, suggesting this has an effect on HG rather than RG I (Caffall et al., 2009).

To achieve precise levels of mucilage production, the differentiation of Arabidopsis MSCs is under tight regulation by a number of transcriptional regulators working in multiple pathways. A number of regulators beyond *AP2* and other outer integument differentiation genes have been identified by their reduced mucilage phenotypes, and at least three separate transcriptional pathways have been identified that modulate the expression of downstream targets involved in

mucilage production and modification. *GLABRA2* (*GL2*) and *TRANSPARENT TESTA GLABRA 1* (*TTG1*) have been demonstrated via transcriptional analysis to regulate *MUM4/RHM2*, and are required for the specific upregulation of *MUM4/RHM2* in MSCs during mucilage production (Western et al. 2004). *TTG1*, *TRANSPARENT TESTA 2* (*TT2*), *TT8*, *GLABRA 2* (*GL2*), *ENHANCER OF GLABRA 3* (*EGL3*), and *MYB5* also exhibit reduced mucilage phenotypes when mutated, and their encoded proteins have been found to form a TTG1-MYB-bHLH complex that regulates *GL2* expression (Koorneef 1981; Debeaujon 2000; Zhang et al. 2003; Western et al. 2004; Gonzalez et al. 2009; Li et al. 2009). These genes form a TF network whereby the homeobox TF *GL2* upregulates the expression of *MUM4*, while *GL2* in turn is regulated by AP2 in addition to the TTG1-MYB-bHLH complex (Rerie et al. 1994; Walker et al. 1999; Gonzalez et al. 2009; Li et al. 2009; Ranocha et al. 2014). Both of these regulators (AP2 and the TTG1-MYB-bHLH complex) also regulate *TRANSPARENT TESTA GLABRA 2* (*TTG2*), a gene encoding a WRKY TF that is also required for mucilage production, though it does not do so via transcriptional control of *MUM4* (Western et al. 2004). An additional R2R3 MYB, *MYB61*, defines a third pathway regulating mucilage production that is also independent of *MUM4* (Penfield et al. 2001; Western et al. 2004). Interestingly, *GATL5* appears to be regulated by all three transcriptional pathways, as its expression decreases in *gl2*, *ttg2*, and *myb61* mutants, indicating that some cross talk likely exists between these regulatory networks (Kong et al. 2013). Additional TFs found to regulate mucilage production include *DNA-BINDING WITH ONE FINGER 4* (*DOF4*) and *DE1 BINDING FACTOR 1* (*DF1*), but their positions relative to other transcriptional pathways have yet to be determined (Vasilevski et al. 2012; Zou et al. 2013). *DOF4* mutants have collapsed MSCs in addition to reduced mucilage, and may negatively regulate the cell wall-loosening expansin gene *AtEXPA9* (Zou et al. 2013). *DF1*, a MYB-like tri-helix TF, also

regulates mucilage production through unknown targets, though mutant analysis suggests it functions downstream of *TTG2* (Voiniciuc, Yang, et al. 2015).

The large accumulation of mucilage in the apoplast of developing MSCs has also allowed the identification of factors affecting polar secretion of the matrix polysaccharides, as pectin production occurs in the Golgi apparatus and must be transported to the plasma membrane for release into the apoplast. *RADIAL SWELLING 3 (RSW3)* encodes a subunit of glucosidase II, which processes *N*-glycans. This processing is required for proper protein folding, and these have been implicated in cell wall deposition in that *rsw3* mutants are unable to extrude their seed coat mucilage (Burn et al. 2002). It is not known whether RSW3 plays a direct role in mucilage secretion or in the proper folding of Golgi-localized proteins required in mucilage production (Burn et al. 2002). *echidna (ech)* mutants have MSCs that produce mis-targeted mucilage within the cell (McFarlane et al. 2013). ECH forms a complex in the TGN with two YPT/RAB GTPase Interacting Proteins (YIPs) YIP4a and YIP4b (Gendre et al. 2013). Transmission electron microscopy of MSCs in both *ech* and *yip4a yip4b* double mutants determined that mucilage accumulates in the vacuole and ER (Gendre et al. 2013; McFarlane et al. 2013). SEC8 and EXO70A1 are both subunits of the exocyst complex, which mediates fusion of Golgi-derived vesicles with the plasma membrane (Žárský et al. 2009; Kulich et al. 2010; Žárský et al. 2013). Both *sec8* and *exo708a* mutants exhibit a reduced mucilage phenotype, however neither of these mutants have been investigated at the cytological level (Kulich et al. 2010). Yeast two-hybrid analysis determined that ROH1, a DUF793 protein family member, interacts with exocyst subunit EXO70A1, and gain-of-function mutants of *roh1* also exhibited pectin production phenotypes (Kulich et al. 2010).

As it is likely that more biosynthetic genes are required in mucilage biosynthesis and secretion, efforts have been made to determine other key players through mutant screens. One such forward-genetic screen was performed by mutagenizing a population in the *mum4* mutant background and screening for enhancer mutations (Arsovski et al. 2009). Many biosynthetic genes exist in large gene families with varying degrees of functional redundancy, and therefore mutant screens in a sensitized background may be able to pick up more subtle mucilage phenotypes that may not be apparent in single mutants. This *mum4* enhancer screen resulted in the identification of six novel genes named *MUM ENHANCER (MEN) 1–6* (Arsovski et al. 2009). Double mutants of *mum4* and *men1*, *men4*, or *men5* resulted in lower mucilage production than the *mum4* mutant alone, and the *men4* mutant exhibited a single mutant phenotype with a ~60% reduction in mucilage, indicating that these three *MEN* genes likely have a role in the biosynthesis, secretion, or regulation of mucilage production, which has yet to be determined (Arsovski et al. 2009).

1.4.1.3 Mucilage polysaccharide modification

A number of genes have also been identified through the investigation of mucilage release phenotypes, whereby mutants produce mucilage in amounts similar to wild-type seeds, but are defective in releasing the mucilage upon seed hydration. Proper mucilage extrusion from the MSCs upon water imbibition has been found to require an array of cell wall polymer modifications. These modifications appear to establish both correct swelling properties of the mucilage within the mucilage pocket, and weakening of the primary cell wall to facilitate mucilage swelling-induced cell wall rupture (Dean et al. 2007; Macquet et al. 2007; Arsovski et al. 2009; Bui et al. 2011; Walker et al. 2011; Voiniciuc et al. 2013). One key pectin modification is methylesterification of GalA subunits, seen most commonly in the HG backbone (Willats, Orfila,

et al. 2001; Miao et al. 2011; Saez-Aguayo et al. 2013; Levesque-Tremblay et al. 2015). Pectins are secreted from the Golgi apparatus in a highly methylesterified form due to the presence of pectin methyltransferases (MTs), and these methyl groups are removed to various extents in the cell wall by pectin methylesterases (PMEs) (reviewed in Willats, Orfila, et al. 2001; reviewed in Levesque-Tremblay et al. 2015). The de-methylesterification of GalA by PMEs creates negatively charged regions on the pectin backbone, which, if in long stretches, can form Ca²⁺ crosslinks between pectin molecules, and rigidifying the cell wall matrix (Willats, Orfila, et al. 2001; Willats, McCartney, et al. 2001; Saez-Aguayo et al. 2013; Ranocha et al. 2014; Turbant et al. 2016). *PECTIN METHYLESTERASE INHIBITOR 6 (PMEI6)*, *AtSUBTILASE 1.7 (AtSBT1.7)*, and *FLYING SAUCER 1 (FLYI)* are all required for proper mucilage extrusion, and mutants exhibit a phenotype whereby normal primary cell wall breakage is affected. They all act as negative regulators of PMEs, and their mutants display decreased levels of pectin methylesterification. PMEI6 and subtilisin-like serine protease AtSBT1.7 likely act directly on PMEs by binding and degrading them, respectively, thus preventing them from removing methylesters from the HG backbone (Rautengarten et al. 2008; Saez-Aguayo et al. 2013). *FLYI* encodes a transmembrane RING E3 ubiquitin ligase that may ubiquitinate PMEs for degradation. While each plays a role in maintaining proper levels of HG methylesterification, direct targets for each of these genes have yet to be determined (Voiniciuc et al. 2013). Both *ADENOSINE KINASE 1 (ADK1)* and *PECTIN METHYLESTERASE 58 (PME58)* are also required for proper HG methylesterification in mucilage, but are not required for mucilage release (Moffatt et al. 2002; Turbant et al. 2016). PME58 is thought to modulate molecular interactions between HG and other polysaccharides in the inner mucilage layer (Turbant et al. 2016), while *adk1* mutants had substantially decreased methylesterification of mucilage polysaccharides (Moffatt et al. 2002), indicating that the de-

esterification of precise polysaccharides at certain developmental time points may be key in regulating mucilage properties and extrusion.

MUM2/BGAL6 and *BETAXYLOSIDASE 1 (BXL1)* encode RG I sidechain modifiers required for proper mucilage release, and may affect both mucilage swelling and cell wall weakening. *MUM2/BGAL6* encodes a β -galactosidase essential for trimming of the RG I sidechains galactose, galactans and arabinogalactans. *mum2* mutants are unable to release any mucilage without sodium carbonate treatment and have increased galactose, arabinose, and RG I branchpoints (Dean et al. 2007; Audrey Macquet, M.-C. Ralet, et al. 2007). *BXL1* encodes a bi-functional β -xylosidase / α -arabinofuranosidase that also trims RG I sidechains by removing arabinans, as arabinose is increased in the mutants, and arabinans were increased in mucilage and cell walls (Arsovski et al. 2009). PEROXIDASE 36 (*PER36*) is a member of the class III peroxidase family that weakens the primary cell wall by creating reactive oxygen species, which may degrade pectins. *PER36* is expressed most strongly in the outer tangential cell wall, and *per36* mutations result in sheet-like peeling of the primary cell wall upon mucilage extrusion (Kunieda et al. 2013). *MEN2* and *MEN6*, which were identified from the mutant screen in the *mum4* mutant background, may also play a role in mucilage and/or primary cell wall modification, as these mutants affect mucilage release rather than quantity (Arsovski et al. 2009). Their precise roles have not yet been determined.

Mucilage modification may be regulated through additional transcriptional networks, although some cross talk is possible. *MUM1/LEUNIG HOMOLOG (LUH)*, a groucho/TUP1 family co-repressor protein, controls mucilage release while making normal amounts of mucilage, and does so independently of the TTG1-bHLH-MYB complex (Bui et al. 2011; Huang et al. 2011;

Walker et al. 2011). *luh* mutants exhibit improper mucilage swelling, inability to release mucilage without cation chelator or alkali treatments, as well as increased RG I sidechains and HG methylesterification (Huang et al. 2011). Its homolog *LEUNIG (LUG)* interacts in complex with LUH, but is not required for mucilage release as seen for *LUH* (Huang et al. 2011). LUH was found to activate transcription of mucilage modifiers *PMEI6*, *SBT1.7*, *BXL1*, and *MUM2/BGAL6* (Huang et al. 2011; Saez-Aguayo et al. 2013).

1.4.1.4 Mucilage structure

While the pectins RG I and HG comprise the major components of Arabidopsis mucilage, smaller amounts of highly branched hemicelluloses xylan and heteromannan are also present, and are thought to mediate mucilage adherence in the inner layer through interactions with cellulose microfibrils that span the inner domain (Yu et al. 2014; Voiniciuc, Guenl, et al. 2015; Voiniciuc, Schmidt, et al. 2015; Hu et al. 2016; Ralet et al. 2016). Genes involved in cellulose and hemicellulose biosynthesis and organization have been identified based on their mucilage structure phenotypes (Sullivan et al. 2011; Yu et al. 2014; Voiniciuc, Schmidt, et al. 2015; Hu et al. 2016; Ralet et al. 2016). These mutants produce wild-type amounts of mucilage, but the relative proportions of adherent versus non-adherent mucilage layers are affected, often resulting in less adherent mucilage, and more of the total mucilage being allocated to the outer diffuse layer (Harpaz-Saad et al. 2011; Sullivan et al. 2011).

Cellulose synthases act in heteromeric complexes in the plasma membrane that deposit cellulose into the cell wall. CELLULOSE SYNTHASE 5 (*CESA5*) is involved in the production of mucilage cellulose, which extends as rays into the inner adherent domain (Smadar Harpaz-Saad et al. 2011; Mendu et al. 2011; Sullivan et al. 2011). *CESA3* mutants are similarly affected in

mucilage cellulose, and it was determined that CESA5, CESA3, and CESA10 interact in the plasma membrane lining the mucilage pocket during mucilage synthesis (Griffiths et al. 2015). CESA5 and CESA10 may also work with with alternate synthases CESA2 and CESA9, which do not exhibit mucilage phenotypes, but affect columella formation rather than cellulosic rays of the mucilage (Stork et al. 2010; Mendu et al. 2011). *COBRA-LIKE 2 (COBL2)* is a GPI-anchored protein predicted to facilitate cellulose deposition, and is co-expressed with cellulose synthase genes involved in mucilage production (Ben-Tov et al. 2015). *cobl2* mutants similarly exhibit the mucilage attachment phenotype as a result of having substantially reduced crystalline cellulose deposited in the mucilage (Ben-Tov et al. 2015). Mutations in receptor-like kinase *FEI2*, and the GPI-anchored fasciclin-type arabinogalactan protein *SALT-OVERLY SENSITIVE 5 (SOS5)* are also required for proper mucilage structure (Harpaz-Saad et al. 2011; Sullivan et al. 2011; Harpaz-Saad et al. 2012). It was initially reported that SOS5, FEI2 and CESA5 function in the same pathway involved in cellulose synthesis (Harpaz-Saad et al. 2011; Harpaz-Saad et al. 2012). However, evidence suggests that, while SOS5 and FEI2 do indeed interact genetically in a pathway promoting seed adherence through SOS5 glycosylation (Basu et al. 2016), SOS5 is thought to affect mucilage adherence and/or structure independently of CESA5 through mediation of pectin adherence to cellulose, rather than cellulose production directly (Griffiths et al. 2014).

IRREGULAR XYLEM 14 (IRX14) is a GT48 family xylosyltransferase thought to be involved in the incorporation of UDP-D-Xyl residues into the xylan backbone in mucilage (Catalin Voiniciuc et al. 2015; Hu et al. 2016; Ralet et al. 2016). Linkage analysis revealed that xylan is the most abundant xylose-rich component of mucilage, and that IRX14 is essential for xylan backbone synthesis, while another GT61 family xylosyltransferase, *MUCILAGE-RELATED21/MUCILAGE-MODIFIED 5 (MUCI21/MUM5)*, is required to add UDP-D-Xyl

residues directly to the xylan backbone (Voiniciuc et al. 2015; Hu et al. 2016; Ralet et al. 2016). This highly branched xylan is essential in maintaining normal mucilage adherence (Voiniciuc et al. 2015a; Hu et al. 2016; Ralet et al. 2016). Biochemical analyses and in vitro binding assays showed that adherent and non-adherent mucilage structure is based on the direct interaction of xylan and RG I, which is required to mediate the adsorption of RG I onto cellulose (Ralet et al. 2016).

CELLULOSE SYNTHASE-LIKE A2 (CSLA2) is involved in galactoglucomannan backbone synthesis, and its mutation results in a compacted inner mucilage domain, despite normal amounts of mucilage present in the adherent layer (Yu et al. 2014). Mutations in another GT34 family α -1,6-galactosyltransferase *MUCILAGE-RELATED 10 (MUCI10)* shares the compact adherent mucilage layer phenotype with *csla2*, although slightly less severe (Voiniciuc et al. 2015b). In *muci10* mutants, mucilage contains decreased levels of galactose, with an additional 50% decrease in mannose, suggesting that the presence of these galactose branches to the glucomannan backbone is required for proper backbone synthesis (Voiniciuc et al. 2015b). These studies demonstrate that the loss of heteromannan in mucilage changes the spatial distribution of mucilage cellulose, with a reduction in the formation of crystalline cellulose and an almost complete reduction of the cellulosic rays (Yu et al. 2014). Finally, the homeodomain TF *KNOTTED-LIKE HOMEODOMAIN OF ARABIDOPSIS THALIANA 7 (KNAT7)* is a negative regulator of secondary cell wall deposition in stems and roots, and mutants have thickened secondary cell walls in these tissues (Bhargava et al. 2013; Liu and Douglas 2015). *knat7* mutants also have a structural defect in mucilage, with subtle reductions in minor components that could be part of hemicellulose, indicating that KNAT7 may regulate hemicellulose production in MSCs (Romano et al. 2012; Voiniciuc, Yang, et al. 2015)

1.4.2 Genes acting in seed coat development and mucilage production in other species

The discovery of potential mucilage-related genes in other myxospermous species has largely relied on transcriptomic profiling and EST library construction specific to seed coat tissues. A study in a variety of cultivated *Plantago ovata* looked at GTs that are potentially involved in the formation of xylan synthase complexes, as *Plantago* mucilage is composed almost entirely of AX (Jensen et al. 2013). Four developmental stages of seed coat layers containing both MSCs and endosperm, as well as one stage of stem tissue, were transcriptionally profiled using RNA-seq. This revealed the upregulation of a number of highly divergent homologs of *IRX10*, as well as several GTs from other families that may be involved in the synthesis of xyloglucan, and HG. Mannan synthases were also highly expressed, but this is likely due to their function in storage tissues of the endosperm layer. Interestingly, little to no expression of other known xylosyltransferases *IRX9*, *IRX14*, or their paralogs were significantly expressed in MSCs, while *IRX* homologs in *Plantago* stem tissue closely resemble those seen in Arabidopsis and other dicots (Jensen et al. 2013). They propose that this *IRX10* isoform divergence in *Plantago* seed coats may be the result of selective pressure due to the various xylan structures found in its mucilage that may have different biochemical roles than that found in secondary cell walls of other tissues (Jensen et al. 2013). *De novo* transcriptome sequencing has been performed more recently in *Plantago* ovaries over a large developmental time-scale, which identified a number of other transcripts enriched in the seed coat with potential roles in mucilage biosynthesis and regulation (Kotwal et al. 2016). Orthologs of Arabidopsis genes including *GAUT1/PARVUS* and 11, *GATL3*, 6, and 5, *MUM4*, *RSW3*, *UDP-XYLOSE/APIOSE SYNTHASE (MUR4)*, *TTG1*, and *AP2* were all identified in this screen and their enrichment was confirmed with quantitative reverse transcription PCR (Kotwal et al. 2016). A study of flax seed development using EST libraries constructed across

various tissues including seed coats at early stages in mucilage biosynthesis confirmed the conservation of several potential mucilage-related genes (Venglat et al. 2011). Several putative *RHM* homologs were enriched, though none were considered orthologs of *RHM2/MUM4*, as well as a homolog of *BXLI*, and a number of galacturonosyltransferases that may be involved in RG I backbone synthesis (Venglat et al. 2011).

1.5 RESEARCH GOALS

Seed coat mucilage is a valuable economic commodity across a number of industries, based on its nutritional and physiochemical properties. *Arabidopsis* MSCs have become a model system to explore genes involved in cell wall production, modification, and the regulation of these cell wall processes in cell differentiation, and over 50 genes have been identified to date. Increasing our understanding of the factors affecting mucilage production using this model system is agriculturally useful, as we can apply this framework to other important crop species, potentially increasing their value. The goal of this thesis was to expand on our knowledge of mucilage production and regulation through both the study of a novel mucilage mutant in *Arabidopsis*, and the characterization of MSC development and mucilage production in the seed coat of flax. This was carried out specifically through:

- 1) The investigation of the cell biology and regulation of mucilage production in the MSCs of the crop plant *Linum usitatissimum* (flax). While a number of studies have characterized the chemical composition and properties of extracted flax mucilage, relatively little is known about

flax MSC differentiation, or how mucilage production might be regulated at the genetic level. This work provides the first detailed analysis of MSC differentiation and mucilage production in flax. We also establish key developmental time stages of mucilage deposition, which correlate with morphological changes in the secretory apparatus. As RG I production in Arabidopsis is controlled by the seed coat specific upregulation of NSE *MUM4/RHM2*, we predicted that mucilage-related NSEs might be similarly upregulated in seed coat tissue during mucilage production in flax. Transcriptional upregulation of putative Rha and Xyl NSE genes was observed at key time points in flax mucilage deposition, suggesting that these genes may play a role in mucilage biosynthesis. Finally, we provide evidence that flax mucilage can be exploited for manipulation through the expression of an exogenous protein co-product, whereby we successfully expressed a secretable reporter protein into flax mucilage using an Arabidopsis promoter.

2) The characterization of the *MUM4* enhancer gene *MEN4*. *mum4 men4* double mutants produce less mucilage than the *mum4* single mutant, indicating an enhancement of the *mum4* phenotype. Mutations in *MEN4* result in a single mutant phenotype as well, whereby seeds produce approximately 30% of the mucilage produced in wild-type. Based on this phenotype, we predicted that *MEN4* may act as a pectin biosynthetic enzyme, secretory factor, or a transcriptional regulator of pectin production. The location of the ethyl methanesulfonate-induced point mutation in *men4* was determined via Next-Generation Mapping, and revealed a mutation in a novel TF of unknown function, which shared sequence-based homology with a conserved TATA-binding Associated Factor (TAF). Along with its sub-cellular localization to the nucleus, these results support a putative role in gene regulation.

Table 1.1: Genes involved in MSC differentiation

Table 1.1

Gene	AGI number	Protein	Proposed role in mucilage production	Reference
REGULATION OF OUTER INTEGUMENT DIFFERENTIATION				
<i>APETALA2 (AP2)</i>	At4g36920	AP2 TF	Regulation of outer integument differentiation	1-6
<i>ABERRANT TESTA SHAPE (ATS)</i>	At5g42630	Kanadi-family TF	Regulation of ovule integument development	6-8
<i>KANADI 1 (KAN1)</i>	At5g16560	Kanadi-family TF	Regulation of outer integument differentiation	8,9
<i>KANADI 2 (KAN2)</i>	At1g32240	Kanadi-family TF	Regulation of outer integument differentiation	8,9
<i>INNER NO OUTER (INO)</i>	At1g23420	YABBY protein	Regulation of outer integument differentiation	9
<i>REVOLUTA (REV)</i>	At5g60690	class III homeodomain leucine zipper	Regulation of outer integument differentiation	9
<i>NAC REGULATED SEED MORPHOLOGY1 (NARS1) = NAC2</i>	At1g52880	NAC-like TF	Regulation of seed coat & embryo development	10
<i>NAC REGULATED SEED MORPHOLOGY2 (NARS2) = NAM</i>	At3g15510	NAC-like TF	Regulation of seed coat & embryo development	10
MUCILAGE SYNTHESIS & SECRETION				
<i>MUCILAGE-MODIFIED4 (MUM4)/RHAMNOSE SYNTHASE2 (RHM2)</i>	At1g53500	UDP-L-Rha synthase	Pectin biosynthesis (RG I)	3,4,11-13
<i>UDP-L-RHAMNOSE/UDP-D-GALACTOSE TRANSPORTER2 (URGT2)</i>	At1g21070	UDP-L-Rha/UDP-D-Gal transporter	Golgi membrane-localized transporter of UDP- L-Rha for RG I synthesis	14
<i>GAUT11</i>	At1g18580	Glycosyltransferase (GT8)	Pectin biosynthesis (HG?)	15
<i>GAUT1-LIKE 5 (GATL5)</i>	At1g02720	Glycosyltransferase (GT8)	Pectin biosynthesis (RG I?)	16
<i>RADIAL SWELLING3 (RSW3)</i>	At5g63840	Glucosidase II active in N-glycan processing in ER	Pectin biosynthesis/secretion?	17
<i>SEC8</i>	At3g10380	Subunit of exocyst	Mucilage secretion	18
<i>EXO70A1</i>	At5g03540	Subunit of exocyst	Mucilage secretion	18
<i>ROH1</i>	At1g63930	DUF793, interactor with Exo70a1	Regulator of mucilage secretion?	18
<i>YPT/RAB GTPASE INTERACTING PROTEIN 4a (YIP4a) & YIP4b</i>	At2g18840 At4g30260	YIP family proteins	Mucilage secretion	19

<i>ECHIDNA (ECH)</i>	At1g09330	TGN-localized protein	Mucilage secretion	19,20
<i>TRANSPARENT TESTA GLABRA1 (TTG1)</i>	At5g24520	WD40 repeat protein	Regulator of mucilage synthesis	2-4,6,7,21-23
<i>MYB5</i>	At3g13540	R2R3 MYB TF	Regulator of mucilage synthesis	24,25
<i>TRANSPARENT TESTA2 (TT2)</i>	At5g35550	R2R3 MYB TF	Regulator of mucilage synthesis	6,24
<i>TRANSPARENT TESTA8 (TT8)</i>	At4g09820	bHLH TF	Regulator of mucilage synthesis	6,26
<i>ENHANCER OF GLABRA3 (EGL3)</i>	At1g63650	bHLH TF	Regulator of mucilage synthesis	26
<i>GLABRA2 (GL2)</i>	At1g79840	Homeobox TF	Regulator of mucilage synthesis	2-4,27
<i>TTG2</i>	At2g37260	WRKY TF	Regulator of mucilage synthesis	4,28
<i>MYB61</i>	At1g09540	R2R3 MYB TF	Regulator of mucilage synthesis	4,21
<i>KNOTTED-LIKE HOMEODOMAIN OF ARABIDOPSIS THALIANA 7</i>	At1g62990	Homeodomain TF	Regulator of mucilage synthesis	29,30
<i>DE1 BINDING FACTOR 1 (DF1)</i>	At1g76880	MYB-like trihelix TF	Regulator of mucilage synthesis	31
<i>DNA-BINDING WITH ONE FINGER (DOF4.2)</i>	At4g21030	DNA-binding with one finger	Regulator of seed coat development and mucilage production	32
<i>ABSCISIC ACID1 (ABA1)</i>	At5g67030	Zeaxanthin epoxidase	ABA biosynthesis, hormone regulation of mucilage synthesis	33
<i>MUM ENHANCER1 (MEN1)</i>		Unknown	?	13
<i>MEN1</i>		Unknown	?	13
<i>MEN3</i>		Unknown	?	13
<i>MEN4</i>		Unknown	?	13
<i>MEN5</i>		Unknown	?	13

MUCILAGE STRUCTURE & MODIFICATION

<i>MUM5/MUCILAGE-RELATED 21 (MUCI21)</i>	At3g10320	Putative xylan xylosyltransferase	Branched xylan synthesis	34,35
<i>IRREGULAR XYLEM 14 (IRX14)</i>	At4g36890	Putative xylan xylosyltransferase	Xylan backbone synthesis	34,36
<i>CELLULOSE SYNTHASE-LIKE A 2 (CSLA2)</i>	At5g22740	Cellulose synthase like A family protein	Heteromannan synthesis	37
<i>MUCI10</i>	At2g22900	Putative GGM galactosyltransferase	Heteromannan synthesis	38
<i>MUM3/CELLULOSE SYNTHASE5 (CESA5)</i>	At5g09870	Cellulose synthase subunit	Mucilage structure (cellulose synthesis)	3,39-43
<i>CELLULOSE SYNTHASE 3 (CESA3)</i>	At5g05170	Cellulose synthase subunit	Mucilage structure (cellulose synthesis)	43

<i>SALT OVERLY SENSITIVE5 (SOS5) (FLA4)</i>	At3g46550	GPI-anchored fasciclin-type AGP(e)	Mucilage structure (pectin-mediated adherence)	39,40,44-46
<i>FEI2</i>	At2g35620	Leucine-rich receptor kinase	Mucilage structure (cellulose deposition?)	39,40,44,46
<i>COBRA-LIKE 2 (COBL2)</i>	At3g29810	GPI-anchored COBRA-like protein	Mucilage structure (cellulose deposition)	47
<i>MUM2</i>	At5g63800	Beta-galactosidase	Mucilage/primary cell wall modification	3,48,49
<i>AtBXL1</i>	At5g49360	Bifunctional beta-xylosidase / arabinofuranosidase	Mucilage/primary cell wall modification	50
<i>PEROXIDASE 36 (PER36)</i>	At3g50990	class III peroxidase family	Primary cell wall degradation	51
<i>AtSUBTILASE1.7 (AtSBT1.7)</i>	At5g67360	Serine protease (subtilase)	Negative regulator of pectin methylesterases in mucilage/primary cell wall	52
<i>ADENOSINE KINASE1 (ADK1)</i>	At3g09820	Adenosine kinase	Mucilage methylation	53
<i>PECTIN METHYLESTERASE INHIBITOR 6 (PMEI6)</i>	At2g47670	Pectin methylesterase inhibitor	Mucilage (HG) methylation	54
<i>FLYING SAUCER 1 (FLY1)</i>	At4g28370	Transmembrane RING E3 ubiquitin ligase	Regulator of pectin methylation	55
<i>PECTIN METHYLESTERASE 58 (PME58)</i>	At5g49180	Pectin methylesterase	Mucilage (HG) methylation	56
<i>MUM1/LEUNIG_HOMOLOG (LUH)</i>	At2g32700	Groucho/TUP1 family co-repressor	Regulation of mucilage/primary cell wall modification	3,57-59
<i>LEUNIG (LUG)</i>	At4g32551	Groucho/TUP1 family co-repressor	Regulation of mucilage/primary cell wall modification	59
<i>MEN2</i>		Unknown	?	13
<i>MEN6</i>		Unknown	?	13
<u>OTHER MSC DIFFERENTIATION</u>				
<i>CESA9</i>	At2g21770	Cellulose synthase subunit	MSC cell morphology & secondary cell wall synthesis	42,60
<i>DEFECTIVE IN CUTICULAR RIDGES (DCR) / PEL3</i>	At5g23940	Soluble BAHD acyltransferase,	Seed coat cutin synthesis, seed coat structure	61
<i>GIBBERELLIN-3 OXIDASE4 (AtGA3OX4)</i>	At1g80330	GA-3-oxidase	Promotion of starch degradation during MSC differentiation	62

<i>AtGID1a</i>	At3g05120	Gibberellin receptor	MSC cell morphology	63
<i>AtGID1b</i>	At3g63010	gibberellin receptor	MSC cell morphology	63
<i>GA1</i>	At4g02780	ent-copalyl diphosphate synthetase 1	GA synthesis, regulation of MSC differentiation	63
<i>MOR1</i>	At2g35630	MAP215 MT-associated protein	Mucilage composition? Guidance of cellulose synthesis for columella?	64

(1)Jofuku et al. 1994 (2)Bowman, J.L. and Koornneef 1994(3)Western et al. 2001 (4)Western et al. 2004 (5)Molina et al. 2008 (6)Debeaujon 2000 (7)Leon-Kloosterziel et al. 1994 (8)McAbee et al. 2006 (9)Kelley et al. 2009 (10)Kunieda et al. 2008 (11)Usadel et al. 2004 (12)Oka et al. 2007 (13) Arsovski et al. 2009 (14)Rautengarten et al. 2014 (15)Caffall et al. 2009 (16)Kong et al. 2013 (17)Burn et al. 2002 (18)Kulich et al. 2010 (19)Gendre et al. 2013 (20)McFarlane et al. 2013 (21)Penfield et al. 2001 (22)Walker et al. 1999 (23)Koornneef 1981 (24)Gonzalez et al. 2009 (25)Li et al. 2009 (26)Zhang et al. 2003 (27)Rerie et al. 1994 (28)Johnson et al. 2002 (29)Romano et al. 2012 (30)Bhargava et al. 2013 (31) Vasilevski et al. 2012 (32)Zou et al. 2013 (33)Karssen et al. 1983 (34)Western 2006 (34)Catalin Voiniciuc et al. 2015 (35)Ralet et al. 2016 (36)Hu et al. 2016 (37)Yu et al. 2014 (38)Cătălin Voiniciuc et al. 2015 (39)Harpaz-Saad et al. 2011 (40)Harpaz-Saad et al. 2012 (41)Sullivan et al. 2011 (42)Mendu et al. 2011 (43)Griffiths et al. 2015 (44)Xu et al. 2008 (45)Griffiths et al. 2014 (46)Basu et al. 2016 (47)Ben-Tov et al. 2015 (48)Dean et al. 2007 (49)Macquet et al. 2007 (50) Arsovski et al. 2009 (51)Kunieda et al. 2013 (52)Rautengarten et al. 2008 (53)Moffatt et al. 2002 (54)Saez-Aguayo et al. 2013 (55)Voiniciuc et al. 2013 (56)Turbant et al. 2016 (57)Walker et al. 2011 (58)Huang et al. 2011 (59)Bui et al. 2011 (60)Stork et al. 2010 (61)Panikashvili et al. 2009 (62)Kim et al. 2005 (63)Iuchi et al. 2007 (64)McFarlane et al. 2008

FIGURES

Figure 1.1 Schematic diagram of MSC differentiation in Arabidopsis

(A) Following fertilization, MSCs are mainly filled with a large central vacuole (shown in blue), which pushes the cytoplasm (shown in pale green) to the cell edges. (B) Cell growth occurs along with the appearance of large starch granules (SG) shown at the apical face of the cells. (C) At approximately 7 DPA, polarized secretion of mucilage (M) to the plasma membrane forces the cytoplasm and starch granules to move away from the distal and radial cell walls (dw and rw, respectively) to the centre of the cell, forming a cytoplasmic column. The vacuole also shrinks towards the basal face of the cell. (D) At approximately 9 DPA, starch granules are depleted as a cellulosic secondary cell wall is deposited at the plasma membrane. This process continues as the cytoplasm is replaced entirely by secondary cell wall, and radial walls are thickened as well. (E) In mature seeds, the deposited mucilage desiccates under the primary cell wall, resulting in a trough around the columella. (F) Upon hydration, the hydrophilic mucilage swells, leading to breakage between the distal and radial cell walls (G), allowing the release of mucilage (North et al. 2014).

Figure 1.1

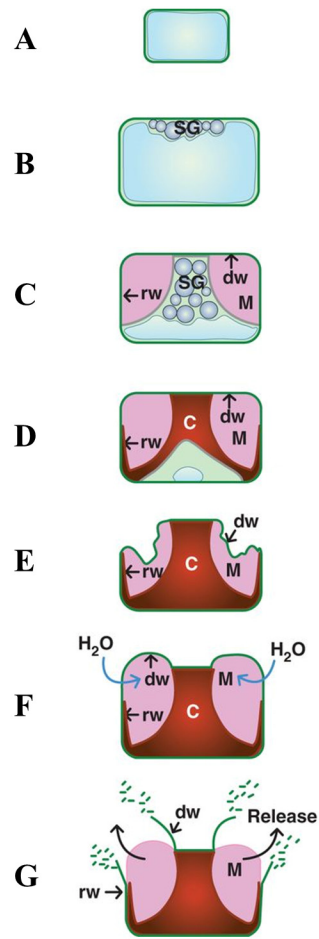
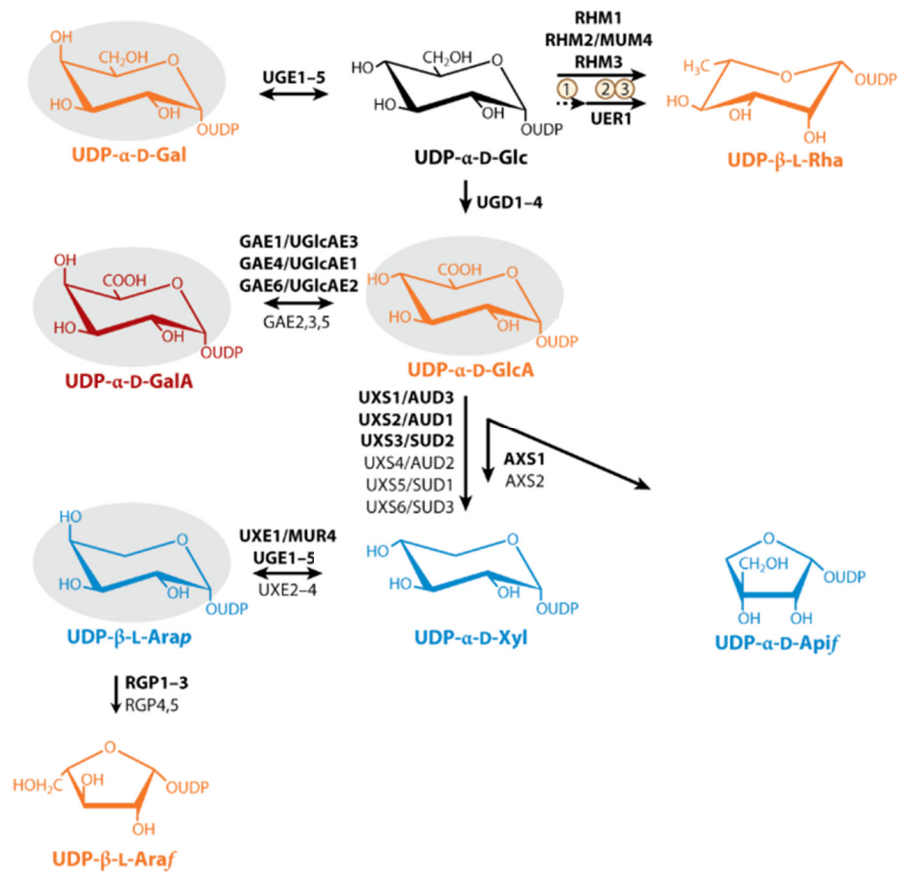


Figure 1.2 Selection of nucleotide sugar interconversion reactions catalyzed by NSEs

Illustration showing NSE reactions involving precursor UDP-D-Glc (shown in black). Enzymes in bold are those that have been proven biochemically in Arabidopsis. UDP-D-GalA (red) is present in all pectins, sugars in orange are present in RG I or RG II (i.e. GlcA), and those in blue are found in RG II and other galacturonans. UDP-D-Xyl, UDP-L-Araf, and UDP-D-GlcA are all found in xylans. UGE=UDP-Glc 4-epimerase / UDP-Gal 4-epimerase; RHM=trifunctional enzyme with UDP-Glc 4,6-dehydratase, UDP-4-keto-6-deoxy-D-Glc 3,5-epimerase, and UDP-4-keto-L-Rha 4-keto-reductase activity (intermediates not shown); UER=bi-functional UDP-4-keto-6-deoxy-D-Glc 3,5-epimerase, and UDP-4-keto-L-Rha 4-keto-reductase activity; UGD=UDP-Glc dehydrogenase; GAE=UDP-GlcA 4-epimerase; UXS=UDP-GlcA decarboxylase / UDP-Xyl synthase (note Xyl can also be synthesized by AXS, a dual-role UDP-D-Araf / UDP-D-Xyl synthase); UXE=UDP-Xyl 4-epimerase / UDP-Ara 4-epimerase; RGP=UDP-L-Araf mutase (Atmodjo et al. 2014).

Figure 1.2



Link between Chapter 1 and 2

Chapter 1 introduced the widespread trait known as myxospermy, whereby specialized seed coat epidermal cells produce large quantities of mucilage, which can vary greatly in terms of composition across species. This trait has been characterized extensively at the cell biological and genetic level in *Arabidopsis*, where the MSCs provide a model system to study mucilage production as well as other aspects of cell wall component biosynthesis, modification, secretion, regulation, and structure. Mucilage production is found across many plant species in a wide range of environments, including a number of economically valuable crop species. As mucilage itself is used as a commodity with roles in nutrition, agriculture, and pharmaceuticals, considerable work has gone into the biochemical and physical characterization of mucilages in certain species. Despite this, relatively little is known about the cell biology and regulation of mucilage production in these crop species. **Chapter 2** presents a detailed study of flax MSC differentiation at both the gross morphological and cytological level. This work also investigates putative mucilage biosynthetic genes that are substantially upregulated in flax seed coats during mucilage production, suggesting a potential role in mucilage regulation at the nucleotide sugar substrate level. Finally, the targeting of exogenous proteins to flax mucilage is investigated as a potential agricultural co-product.

CHAPTER 2

The cell biology, patterning, and regulation of mucilage production in the seed coat mucilage secretory cells of *Linum usitatissimum* L. (linseed flax)

ABSTRACT

Linseed flax (*Linum usitatissimum* L.) has long been valued as an agricultural commodity. Strong fibres in the stem provide material for textiles, while linseed oil is derived from embryos in the seeds. In addition, the mucilage secretory cells (MSCs) surrounding the seed coat of flax produces a viscous, matrix polysaccharide-rich mucilage that is used commercially as a soluble dietary fibre, an emulsifier and texturizing agent in food and cosmetics, and as a substitute for animal products in food. Flax mucilage is primarily composed of the hemicellulose arabinoxylan and the pectin rhamnogalacturonan I. In order to understand the regulation of mucilage production in flax, this study correlates the expression of genes that may be involved in polysaccharide biosynthesis with both cytological changes of the flax seed coat MSCs, and the patterned deposition of neutral and acidic regions within the secreted mucilage over the course of MSC differentiation. These results have identified key time points in flax mucilage production, as well as putative UDP-L-Rha and UDP-D-Xyl biosynthetic genes that are specifically upregulated in flax seed coats during mucilage production, which may serve as control points for regulating mucilage production through nucleotide sugar substrate availability. In addition, the isoform heterogeneity of the *RHAMNOSE SYNTHASE* gene family in flax was investigated. Finally, flax MSCs were manipulated through the expression of a promoter-reporter gene construct, which targeted exogenous protein expression into flax mucilage.

2.1 INTRODUCTION

A trait known as myxospermy is seen across a wide array of plant species including the Linaceae, Solanaceae, Brassicaceae, and Plantaginaceae, whereby the seed epidermis has a specialized layer of cells that synthesizes pectinaceous mucilage. Upon seed hydration, these hydrophilic polysaccharides swell rapidly and the cells rupture, creating a gelatinous capsule around the seed. Studies have supported a role for seed mucilage as an aid in seed hydration under water/salt stress, a water and nutrient reserve to support germination, seed priming (DNA repair) in the embryo, seed adherence to a substrate such as soil or an animal vector, and germination inhibition through preventing oxygen from reaching the embryo (Wilson 1960; Gutterman and Shem-Tov 1997; Yang et al. 2010; reviewed in Western 2012; Yang et al. 2012). As seed coat mucilage is found across many plant species and habitats, this feature is likely advantageous on various accounts specific to their environments.

While a number of myxospermous species have been investigated in terms of their ability to synthesize mucilage, the developmental timing of mucilage secretory cell (MSC) differentiation and mucilage composition have been studied most extensively in the genetic model plant *Arabidopsis*. Mutations in over 50 genes leading to phenotypic deviations in MSC differentiation, mucilage production, structural organization of mucilage polymers, and cell wall composition have been characterized thus far using the *Arabidopsis* MSC model system (reviewed in Western 2012; North et al. 2014; Voiniciuc, Yang, et al. 2015). Its largely pectinaceous mucilage is synthesized in the Golgi apparatus and secreted to the apoplast via secretory vesicles (McFarlane et al. 2008; Young et al. 2008). The mucilage is deposited underneath the primary cell wall at the apical domain in a ring-shaped zone of secretion, leading to the restriction the cytoplasm to a volcano-

shaped column. Lining the plasma membrane of this apical secretion domain are cortical microtubule arrays (McFarlane et al. 2008), which are thought to guide cellulose synthase complexes as they contribute cellulose into the accumulating mucilage (Griffiths et al. 2015). Once mucilage production is complete, a primarily cellulosic secondary cell wall is deposited interior to the mucilage, displacing the cytoplasm. This results in a volcano-shaped secondary cell wall protrusion or ‘columella’ interior to a donut-shaped mucilage pocket. The radial cell walls of the MSCs are also reinforced with secondary cell wall components, forming a trough on either side of the columella. When *Arabidopsis* seeds are exposed to water, the mucilage is released due to weakening of the outer primary cell wall and the rapid expansion of the hydrophilic pectin (Frey-Wyssling 1976; Beeckman et al. 2000; Western 2000).

Mucilage extrusion upon seed hydration in *Arabidopsis* results in two distinct mucilage layers: an outer, water-soluble layer, which can be removed upon agitation, and an adherent inner layer that remains tightly associated with the seed coat (Western et al. 2000). In both layers, the most abundant pectic polysaccharide is rhamnogalacturonan I (RG I), a repeat of the disaccharide 1,2-L-Rhamnose and 1,4-D-Galacturonic acid, which forms long polymers that often contain Rha-linked, neutral sidechains of arabinans, galactans, arabino-galactans, and terminal galactose. RG I, however, remains largely unbranched in the outer mucilage layer (Penfield et al. 2001; A. Macquet et al. 2007). Homogalacturonan (HG), a linear, unbranched polymer of α -linked 1,4-D-galacturonic acid that can be methylesterified and acetylated, is also present (Willats et al. 2001; Macquet et al. 2007; Caffall and Mohnen 2009). Cellulose microfibrils line the inner domain, and along with interacting branched RG I, tightly adhere mucilage to the seed coat in this region (Macquet et al. 2007; Haughn and Western 2012). Small amounts of the hemicelluloses xyloglucan (XG), a β 1,4-linked glucan backbone decorated with xylose residues (Young et al. 2008),

galactoglucomannan, a 1,4-linked glucose/mannose backbone with galactose sidechains (Voiniciuc, Schmidt, et al. 2015), and a highly branched xylan composed of a 1,4-linked xylose backbone decorated with single xylose residues are also present in the inner mucilage (Naran et al. 2008; Voiniciuc et al. 2015; Hu et al. 2016). These hemicelluloses play a structural role, aiding in mucilage adherence to the seed (Wu et al. 2010; Voiniciuc et al. 2015; Hu et al. 2016; Ralet et al. 2016).

The copious seed mucilage from cultivated flax (*Linum utitatisimum L.*) is an important commodity in a number of human applications. These roles include its various implications in human dietary nutrition (Ganorkar and Jain 2013) and as a useful texturizing agent/emulsifier in the food industry (Anttila et al. 2008). It can be used as a thickening agent and stabilizer in oil/water emulsions, foams, and moisturizers, as well as in medical adhesives, due to its high viscosity, hypo-allergenicity and water-holding capabilities (Mazza and Biliaderis 1989; Fedeniuk and Biliaderis 1994; Khalloufi et al. 2009; Kaewmanee et al. 2014). Due to its importance as a commodity, considerable work has gone into characterizing its chemical composition and physical properties. Flax mucilage contains both neutral and acidic polysaccharide components, and is considered a ‘true slime,’ as it does not contain cellulose (Muralikrishna et al. 1987; Mazza and Biliaderis 1989; Naran et al. 2008; Kaewmanee et al. 2014; Pavlov et al. 2014). The most abundant neutral polymer in flax mucilage is a highly branched arabinoxylan (AX), with primarily double branched L-arabinosyl subunits at the O-2 and O-3 positions of the xylan backbone. The acidic pectin RG I is the second most abundant polymer in flax mucilage and has unusual side chain substitutions such as single, terminal D- and L-galactose and L-fucose residues attached at the O-3 position rather than the usual O-4 branch point (Warrand et al. 2003; Naran et al. 2008). Much smaller amounts of HG are also present in flax mucilage (Naran et al. 2008). The relative

proportions of the different mucilage polysaccharides tend to vary across cultivars derived from different environments and breeding programs. For example, proportions can range from ~75% AX : 25% RG I to ~50% AX : 50% RG I (Oomah et al. 1995; Pavlov et al. 2014).

Despite the utility of flax mucilage and interest in its chemical and physical properties, there has been limited study of flax MSC structure, development, and cell biology. Early developmental observations of general seed coat morphology indicated that flax MSCs lack columellae, but accumulate large amounts of mucilage in striated layers (Kraemer 1898; Boesewinkel 1980). Ruthenium red, which stains acidic polysaccharides, is taken up most intensely in the outermost layer of mucilage within cells, while more diffuse staining is observed in the inner layer (Boesewinkel 1980). Once released, flax mucilage has been proposed to be similar to that of *Arabidopsis* in its distribution into a diffuse outer region and an inner adherent region that clings to the seed (Naran et al. 2008), although these regions are not as distinct as they are in *Arabidopsis* and can both be easily removed by agitation.

In *Arabidopsis*, the availability of the nucleotide sugar synthase RHAMNOSE SYNTHASE 2 (RHM2) / MUCILAGE-MODIFIED 4 (MUM4) serves as a key control point in mucilage production, and *mum4* mutant seeds produce around one tenth the amount of mucilage as wild-type seeds (Western et al. 2001; Usadel et al. 2004; Western et al. 2004). *MUM4/RHM2* encodes one of three rhamnose synthases found in *Arabidopsis*, and is the only isoform upregulated in MSCs during mucilage synthesis (Western et al. 2004). This upregulation of *MUM4* during MSC differentiation is tightly regulated by several transcription factors including the outer integument differentiation factor APETALA2 (AP2), the homeobox transcription factor GLABRA2 (GL2) (Rerie et al. 1994; Western et al. 2004), the R2R3 MYB proteins MYB5 and

TRANSPARENT TESTA2 (TT2), the basic helix-loop-helix proteins TT8 and ENHANCER OF GLABRA3 (EGL3), and the WD40 repeat protein TRANSPARENT TESTA GLABRA1 (TTG1) (Walker et al. 1999; Debeaujon 2000; Zhang et al. 2003; Gonzalez et al. 2009; Li et al. 2009). Plant *RHM* genes encode a tri-functional enzyme, where the first domain acts as a UDP-glucose 4, 6-dehydratase, while the second domain has the combined properties of a UDP-4-keto-6-deoxy-D-glucose 3, 5-epimerase and a UDP-4-keto-L-rhamnose 4-keto-reductase. The first domain converts UDP-D-glucose to UDP-4-keto-6-deoxy-glucose, while the second domain converts this intermediate to UDP-L-rhamnose, an essential nucleotide sugar to make the RG I backbone (Western et al. 2004; Oka et al. 2007). A related protein, UDP-4-keto-6-deoxy-D-glucose-3,5-epimerase-4-reductase (UER1/NRS-ER), is capable of carrying out the latter two functions of RHMs (Reiter and Vanzin 2001; Watt et al. 2004), but is not required for mucilage synthesis in Arabidopsis. The two domains of the RHM proteins each contain a GxxGxxA/G Rossmann-fold motif required for NAD(P)(H) co-factor binding, and two catalytic YxxxK motifs. Both wild-type and recombinant versions of RHM2 were expressed in yeast for enzymatic assays, which determined the relative importance of these six conserved motifs in terms of their impact on enzyme activity (Oka et al. 2007). Rossmann-fold one and two are essential for both enzymatic activity and protein stability. The second catalytic site (YxxxK) of the first domain is essential for enzyme activity but does not affect protein stability. The first and fourth catalytic sites are required for robust conversion of UDP-D-Glc to UDP-L-Rha, but their losses do not inhibit enzyme activity completely. Deletion of the third catalytic site has no effect on enzyme activity, and is not conserved in UER1, which is still a functional enzyme for the latter two reactions in Rha synthesis (Watt et al. 2004; Oka et al. 2007).

Production of the β -1,4-xylose backbone of xylans requires the significant availability of UDP-D-Xyl, whose synthesis is catalyzed by the decarboxylation of UDP-D-GlcA by the UDP-D-XYLOSE SYNTHASE (UXS) enzymes (Harper and Bar-Peled 2002a). *UXS* genes have been well characterized both bioinformatically and enzymatically in poplar, barley, and Arabidopsis (Harper and Bar-Peled 2002b; Zhang et al. 2005; Pattathil et al. 2005; Pan et al. 2010; Du et al. 2013). Six *UXS* genes have been identified in Arabidopsis, and encode both transmembrane (*UXS1*, 2, 4) and cytosolic (*UXS3*, 5, 6) isoforms. The cytosolic transcription of *AtUXS3* is regulated by several MYB transcription factors in vascular tissue where it is involved in secondary cell wall production, suggesting a role for this cytoplasmic UXS protein in hemicellulose/xylan biosynthesis (Harper and Bar-Peled, 2002; Zhong and Ye, 2011).

EST gene expression libraries have been produced for flax seed coats, endosperm, and embryos at several stages relatively early in flax seed development (Venglat et al. 2011). Using homology to Arabidopsis mucilage-related genes, the authors noted the enrichment of transcripts for an *RHM* gene, several putative galacturonic acid transferases, and homologs of the pectin modifying enzymes BXL1 and BXL2 (Venglat et al. 2011). No genes involved in AX synthesis were mentioned in this study, despite AX comprising up to 75% of mucilage polysaccharides found in flax mucilage. While these results indicate some degree of conservation between Arabidopsis and flax mucilage biosynthetic pathways, they also suggest that further investigation of cell wall-related genes expressed throughout more stages of flax mucilage synthesis is necessary to gain a more complete understanding of mucilage production in flax.

In this study, we characterize the gross and subcellular morphology of the flax seed coat epidermal cells during differentiation and mucilage deposition. To determine if flax mucilage

production is regulated at the level of UDP-sugar substrate availability, we identify candidate *RHM* and *UXS* genes in flax. A switch from high *RHM* transcript expression to *UXS* enrichment in the seed coat is observed over the course of mucilage production. This coincides with a change in the morphology of the Golgi apparatus in MSCs, along with the appearance of compositionally different layers of deposited mucilage. Finally, we express an exogenous protein in flax MCS to investigate the potential for co-secretion of novel products to the extractable mucilage.

2.2 MATERIALS AND METHODS

2.2.1 Plant materials and growth conditions

The Hanley flax cultivar used in microscopy, developmental dot blots, and quantitative RT-PCR, and the Prairie Grand cultivar used in the GUS assay were supplied by Dr. Mark Jordan of Agriculture and Agri-Food Canada, Winnipeg. A non-breeder Hanley stock used for bulk mucilage extraction for mucilage fractionation was supplied by SeCan, Kanata, Ontario. Seeds were stratified prior to transplanting on minimal media as described in Western et al. (2001). Plants were grown using a photoperiod of 16 hours of continuous light (90-120 $\mu\text{E m}^{-2} \text{s}^{-1}$ photosynthetically active radiation) at 17 °C, and 8 hours at 15°C on Sunshine Mix #5, SunGro Horticulture soil that was fertilized with Plant-Prod Smartcote Controlled Release Fertilizer (Hanging Basket 14-14-14).

2.2.2 Staging of flower age

Flowers were marked as 0 days after flowering (DAF) upon the first emergence of the open flower. Marking was performed using non-toxic, water-soluble paint of different colors on flower pedicels. Seeds were harvested from the marked seed bolls at the various times noted.

2.2.3 Microscopy

Flax seeds were dissected to isolate a small fragment of the seed coat prior to fixation to allow proper infiltration of fixation buffers. Flax seed coats from 0-36 DAF staged for every other day were fixed with 0.5% (v/v) glutaraldehyde and 1.5% (v/v) formaldehyde in PIPES buffer (pH 7.0). Samples were also post-fixed for one hour using 1% osmium tetroxide in PIPES buffer, rinsed, and dehydrated in an acetone series before being embedded in Spurr's resin (Spurr 1969), sectioned at 500nm with a Leica EM UC7 , and stained with toluidine blue as described in Western et al. (2001).

For immunofluorescence microscopy, flax seed coats were dissected, fixed in 0.5% (v/v) glutaraldehyde and 1.5% (v/v) formaldehyde, dehydrated using an ethanol series, and embedded in LR White resin (Sigma-Aldrich). 500nm-thick sections were fixed to Teflon-coated slides with poly-L-lysine and blocked in TBST buffer + 1% (v/v) normal goat serum (Invitrogen). Slides were incubated with a 1:10 dilution of primary antibody in PBS buffer for 1hour followed by a 1:100 dilution of secondary antibody in PBS buffer (Invitrogen Alexa Fluor 488 goat anti-mouse IgG) for 45 minutes. Sections were visualized using a FITC filter on a Leica DM600 B and captured using a Qimaging Retiga CCD camera operated through Openlab imaging software (Agilent Technologies).

For transmission electron microscopy, dissected flax seed coats at 5, 10, 13, and 16 DAF were prepared using high-pressure freezing and freeze substitution as described in Young et al. (2008). Samples were loaded into gold hats (Leica) filled with 1-hexadecene, and high-pressure frozen with a Leica Microsystems EM PACT HPF System. Hats were then immediately transferred to frozen cryovials containing 2% (w/v) osmium tetroxide in acetone with 8% (v/v) dimethoxypropane, and freeze-substituted for 5 days at -20°C in a slush of acetone and dry ice. Samples were then gradually brought to 4°C in metal chucks, and finally brought to room temperature over the course of 3 days, after which they were embedded in Spurr's resin (EMS) (Spurr 1969). Ultrathin straw-coloured sections (50-60nm) were transferred to copper grids (EMS) and stained with Reynolds lead citrate and 2% (w/v) uranyl acetate as described in Young et al. (2008) and imaged using a FEI Tecnai 12 120 kV TEM.

2.2.4 Dot blots

For immunoblotting of mature mucilage, 100 mg of seeds (approximately 6 seeds) were shaken in 1.5 ml of distilled water for 90 min at 37°C. For the water-soluble cell wall preparations of flax seed coats, 5 seed coats at each stage (5, 10, 13, 16, and 20 DAF) were separated from their embryos, ground into powder in liquid nitrogen, rinsed into tubes with distilled water, and centrifuged to remove insoluble material. Both mucilage and water-soluble cell wall extracts were dried by evaporation under a stream of air and resuspended in 200 µl of PBS pH 7.4. Four µl of concentrated mucilage and 1/10 dilutions of soluble cell wall extracts were spotted on nitrocellulose membranes as 2 x 2 µl aliquots. Membranes were blocked in 5% BSA in PBS solution for 1 hour, followed by incubation in primary antibody (1:10 [v/v] dilution) for 90 minutes. Alkaline phosphatase conjugated secondary antibodies (anti-mouse for CCRC antibodies

and anti-rat for LM antibodies; Invitrogen) were diluted 1:1000 (v/v) and detected using the BCIP/NBT-Purple liquid substrate (Sigma-Aldrich), with the reaction stopped by rinsing with water. CCRC antibodies (listed in Table 2.1) were obtained from CarboSource (University of Georgia, Athens; http://cell.crc.uga.edu/carbosource/CSS_home.html), while the two LM antibodies tested were obtained from PlantProbes (University of Leeds, Leeds; <http://www.plantprobes.net>).

2.2.5 Separation of flax mucilage

For separation on an anion exchange column, 100g of Hanley seeds were added to 800ml of distilled water and stirred for 24 hours. The supernatant was filtered through nylon mesh, and dialyzed under running distilled water for 36 hours, followed by dialysis in reverse-osmicated water for an additional 12 hours. Dialyzed mucilage was frozen to -20°C, and freeze dried for approximately 72 hours. Ten mg of freeze-dried mucilage was resuspended in 100ml of 30mM ammonium acetate pH 5.2, centrifuged briefly and filtered to remove any remaining insoluble material. The sample was loaded onto a Hi-Prep™ DEAE Sepharose Fast Flow 16/10 prepacked column (GE Life Sciences), and separated into fractions on a smooth or step-wise gradient from 30mM to 2M ammonium acetate pH 5.2 using an ÄKTA Chromatography System and fraction collector. Each of the 1.5 ml fractions was determined for total sugar content using a colourimetric phenol-sulphuric acid assay (DuBois et al., 1956).

2.2.6 Sequence alignments and bioinformatics

All RHM and UXS amino acid sequences were obtained from the publicly available genomes found at Phytozome v11.0 (<https://phytozome.jgi.doe.gov/pz/portal.html>), including the

Linum usitatissimum v1.0 and Arabidopsis thaliana TAIR10 annotated genomes. Multiple sequence alignments and phylogenetic tree assembly was carried out using the MUSCLE alignment feature of the Geneious® V9.0.5 software (<http://www.geneious.com>, Kearse et al., 2012). Transmembrane domains in the flax UXS amino acid sequences were predicted using the TMHMM Server v.2.0 (<http://www.cbs.dtu.dk/services/TMHMM-2.0/>; Sonnhammer et al., 1998).

2.2.7 Quantitative RT-PCR

Whole flax seeds at 5 DAF and dissected seed coats and embryos from 10, 13, 16, and 20 DAF flax seeds were used for quantitative RT-PCR analysis. RNA extraction was performed using a modified RNeasy plant mini protocol where a maximum of 100mg of tissue was ground in liquid nitrogen, resuspended in 600 μ l RLT-PVP40 (540 μ l RLT + 60 μ l 10% (w/v) polyvinylpyrrolidone) plus 10 μ l β -mercaptoethanol per ml buffer, and processed according to the manufacturer's instructions (Qiagen). 500 ng of extracted RNA was used to perform the reverse transcriptase reaction using the QuantiTect Reverse Transcription kit (Qiagen), which included a DNase treatment step, and this was used as a template in the PCR reaction using SYBR Green reagent (Thermo Scientific) in a Bio-Rad iCycler using an annealing temperature of 60°C (gene-specific primers listed in Supplemental Table 2.1). All primers were designed to flank intron regions, with predicted amplicon sizes between 150 and 200 bp. Melt curves were analyzed to confirm product specificity, and all amplified products shown in Figure 2.9 were sequenced. All values were normalized against the *LuACTIN* housekeeping gene using forward primer 5'-ACACTGGTGTCATGGTTGGGA-3' and reverse primer 5'-CCTGTGGACGATGGATGGACC-3' described in Hano et al. (2006). Gene expression analysis was carried out using the $2^{-\Delta\Delta CT}$ method as described by Livak & Schmittgen (2001). A one-way

ANOVA analysis was performed to identify significant differences, followed by a Student-Neuman-Keuls post-hoc analysis to identify homogenous subsets of results between seed coats and embryos at the different developmental stages (Software: IBM SPSS Statistics 23.0).

2.2.8 BETA-GLUCURONIDASE (GUS) assay

Transgenic GUS lines were created in the Prairie Grand cultivar by Dr. Mark Jordan, Agriculture and Agri-food Canada, Winnipeg, using a GL2promoter::GUS construct provided by Drs. A. Abdeen and T. Western. Wild-type and transgenic seed bolls and seeds were harvested at different stages of development and dissected prior to staining. All tissues were incubated in GUS staining buffer (containing 5-bromo-4-chloro-3-indolyl glucuronide) for 16 hours at 37°C, rinsed and cleared with 70% ethanol and briefly fixed as described in (Wiegel and Glazebrook 2002). Several GUS stained seeds per stage were further fixed in with 4% glutaraldehyde and embedded in Spurr's resin for thick sectioning. For staining of extracted mucilage, mature seeds were shaken at 37°C in GUS staining buffer for 16 hours, the supernatant was removed, and the mucilage was precipitated by adding three volumes of 70% ethanol.

2.3 RESULTS

2.3.1 Mucilage secretory cell differentiation in flax

In order to establish a developmental time course of mucilage production in the seed coat of flax, seeds were collected every other day from 0 to 36 days after flowering (DAF), glutaraldehyde-fixed, and resin-embedded for bright field microscopy. Sections were stained with

the metachromatic dye toluidine blue, which stains cellular components differently based on their composition (O'Brien et al. 1964). Unlignified cell walls stain purple, while more acidic substances (e.g. pectins) stain magenta-pink. Early in their differentiation, prior to the onset of mucilage production, flax MSCs expand in size and are filled almost entirely by a large central vacuole, with the cytoplasm and enlarging starch granules restricted to the cell margins (Figure 2.1, A, B, C). At 8 DAF, cytoplasm and included starch granules are apparent in the apical region of the cells and the vacuole is restricted to the basal region (Figure 2.1, C). Mucilage accumulation becomes apparent by 10 DAF, along with a decrease in the size of the vacuole (Figure 2.1, D). At this stage, a thin layer of mucilage staining slightly pink relative to surrounding cell components is seen at the most apical region of the MSCs, in the apoplast between the plasma membrane and the outer primary cell wall. Mucilage continues to accumulate while the vacuole shrinks, and the starch granules gradually decrease in size, resulting in mucilage taking up much of the cells' volume, with a small layer of cytoplasm restricted to the basal end of the MSCs (Figure 2.1, E, F, G). By 20 DAF, mucilage synthesis is largely complete, and the cytoplasm is barely visible along the bottom of the cell. This detailed time course of flax MSC development allowed for the selection of key stages for further study of mucilage production. A notable feature of the later stages of MSC development is the appearance of differently stained regions of mucilage in the apoplast. The outermost region appears to stain more pink-magenta than the inner region of deposited mucilage that has a more purple appearance (Figure 2.1, F, G, H). Based on the metachromatic properties of toluidine blue as a histochemical stain, this suggests that the outer, earlier-deposited mucilage contains more acidic polysaccharides (e.g. pectins) than the inner layer. Non-lignified cell walls tend to stain purple, which suggests that the inner layer is composed of less acidic polysaccharides.

2.3.2 Cell biology and ultrastructural features of mucilage production in flax MSCs

In order to study the secretory apparatus and the cell biology of mucilage production, high pressure frozen and freeze-substituted flax seed coats at 5 (pre-mucilage production), 10, 13, and 16 (early, mid, and late mucilage production) DAF were observed using transmission electron microscopy (TEM). At 5 DAF, the relatively undifferentiated cells have not begun to produce mucilage. A large central vacuole is present, and starch granules appear throughout the cytoplasmic regions (Figure 2.1 B (6 DAF similar to 5 DAF), Figure 2.2 A). Golgi stacks appear relatively inactive, with long, thin cisternae and a small trans-Golgi network (TGN), with cisternae often curved toward the TGN (Figure 2.2 B, C). At 10 DAF, the vacuole is still present, but decreased in size, and starch granules remain in the cytoplasmic region (Figure 2.1 D). More Golgi stacks are seen throughout the cytoplasm at this stage relative to 5 DAF (data not shown), and a thin layer of mucilage is deposited atop the plasma membrane (Figure 2.1 D, Figure 2.2, E, H). At this stage, a morphological change is seen in the Golgi stacks, where stacks appear shorter in diameter with swollen lumenal margins (Figure 2.2, F, G). The cis- and trans-Golgi regions are more distinct at this stage, where cis regions appear lighter compared to the electron dense trans-Golgi region and secretory vesicles presumably full of mucilage. Secretory vesicles are larger and more abundant relative to 5 DAF, and can be observed fusing with the plasma membrane, where their contents are released into the apoplast (Figure 2.2, H). This closely resembles the swollen Golgi stack morphology seen in *Arabidopsis* MSCs at 7 days post anthesis (DPA), when copious amounts of RG I are synthesized and secreted to the mucilage pocket (Figure 2.2, D) (McFarlane et al. 2008; Young et al. 2008). During the later stages of mucilage production, 13 and 16 DAF, the cytoplasm and starch granules are compressed against the basal region of the MSCs (Figure 2.1 F, G; Supplemental Figure 2.1, A, C) and Golgi morphology undergoes further change. Golgi

stacks at these later stages appear relatively thin with lengthened, flattened cisternae, and a less pronounced cis-trans polarity (Figure 2.2, J, K, N, O). While this flattened appearance is somewhat similar to that seen at 5 DAF, the curved, cup-shaped trans-Golgi seen at 5 DPA is not seen at these later stages, and vesicles are still prominent near the Golgi stacks and throughout the cytoplasm. Further, localization of darkly stained vesicles to the plasma membrane is still seen at 13 and 16 DAF (Supplemental Figure 2.1, B, D). As seen in Arabidopsis, Golgi stacks appear to localize randomly throughout the cytoplasm at all observed stages and do not accumulate in any sort of pattern adjacent to the apical face of the cytosol (data not shown). Finally, the apical plasma membrane secretion domain was examined for an accumulation of cortical microtubules, as seen in Arabidopsis, and none were observed at any point during MSC development.

2.3.3 Patterned deposition of polymers in flax MSCs

The striped appearance of the deposited mucilage in flax MSCs observed with toluidine blue staining suggests there could also be compositional differences as the mucilage is deposited (Figure 2.1 F—H, Figure 2.3, C). To investigate this further, a combination of dot blots on mature mucilage and cell wall extracts from developing seeds, and immunofluorescence on MSC sections was performed. A selection of antibodies raised against various polysaccharide epitopes including RG I, xylans, XG, and flax mucilage were assayed on water-soluble cell wall extracts from 5, 10, 13, 16, and 20 DAF flax seed coats, as well as mature flax mucilage (listed in Table 2.1). Of the anti-RG I antibodies tested, only the unbranched RG I antibodies CCRC-M36 (Young et al. 2008; Arsovski et al. 2009; Pattathil et al. 2010) and CCRC-M14 (Young et al. 2008; Hao et al. 2014; Hu et al. 2016) bound to mature flax mucilage as well as developmental seed coat extracts (Table

2.1; Supplemental Figure 2.2) An interesting feature of the CCRC-M36/-M14-bound RG I was that, once mucilage production had started, its mobility and spread on the nitrocellulose membrane, which is not seen for the polymers detected by other antibodies. This may be due to the greater solubility of unbranched RG I, and has also been observed for Arabidopsis mucilage RG I on dot blots (Arsovski et al. 2009). The anti-HG antibody CCRC-M38 did not bind. Four anti-xyylan antibodies were tested, including CCRC-M118, CCRC-M139, LM10 and LM11 (McCartney et al. 2005; Pattathil et al. 2010; Voiniciuc et al. 2015; Hu et al. 2016). Of these, only CCRC-M118, proposed to bind to monocot arabinoxyylan (Pattathil et al. 2010), gave faint binding to mature mucilage, while none bound otherwise. CCRC-M141 binds exclusively to flax mucilage, though its epitope specificity has not been determined, and the dot blot shows binding to mature mucilage and soluble preparations only late in mucilage production, at 16 and 20 DAF. Finally, two antibodies that potentially bind to non-fucosylated xyloglucan sidechains CCRC-M58 and CCRC-M89 (Cavalier et al. 2008; Pattathil et al. 2010; Zabortina et al. 2012) were tested. While both CCRC-M58 and CCRC-M89 bound to developmental seed coat extracts after 10 DAF, indicating they are detecting unique epitopes deposited later than unbranched RG I, only CCRC-M89 bound to mature mucilage. CCRC-M58 binds at stages 13, 16, and 20 DAF, but not in mature mucilage, which likely indicates that it binds an epitope found in some other soluble cell wall component of the seed coat cells which is not present in the mucilage, or that it binds an epitope in the mucilage that is lost through modification. These dot blots determine that different epitopes are present in the water soluble seed coat preparations at different stages of mucilage deposition.

To visualize the pattern of mucilage deposition in the MSCs, 5, 10, and 16 DAF seed coats were glutaraldehyde-fixed, embedded in LR White, and labelled with antibodies that were positive in developmental dot blots (Table 2.1). Data is shown for those antibodies that bound to sectioned

MSCs (Figure 2.3). Corresponding sections were also stained with toluidine blue for comparison with the differently stained layers of mucilage observed with this dye (Figure 2.3, A, B, C). Note that, at 16 DPA (Figure 2.3, C), mucilage stains pink/acidic in the outer region, and more purple/neutral in the inner region of deposited mucilage. Of the two unbranched RG I antibodies, CCRC-M14 gave the strongest signal in immunofluorescence staining of flax MSC sections. CCRC-M14 bound to all regions of flax mucilage at 10 and 16 DAF (Figure 2.3, D, E, F), with a higher signal in the outer region, indicating that, while all deposited mucilage contains unbranched RG I, high levels are found at the outer face. The flax mucilage-specific antibody CCRC-M141 also stains the outermost layer of mucilage, with much weaker signal observed in the inner mucilage layer (Figure 2.3, G, H, I). Interestingly, CCRC-M141 bound in the cytoplasm at 16 DAF (Figure 2.3, I), which may indicate that the recognized epitope is being synthesized during this stage of mucilage production. While CCRC-M89 is predicted to bind non-fucosylated XG, it stains flax MSC sections in a pattern somewhat reciprocal to CCRC-M141 (Figure 2.3, J, K, L). At 10 DAF, CCRC-M89 stains the outer mucilage layer that has begun to emerge (Figure 2.3, K), but this layer does not stain in later stages. After 10 DAF, CCRC-M89 binds solely to the inner layer (Figure 2.3, L), supporting the idea that the layers contain different polymers. CCRC-M118, defined as an antibody to AX, did not give detectable signal when used in immunofluorescence staining.

In an attempt to define the epitope is bound by CCRC-M141 in flax mucilage, as well as to confirm that for CCRC-M89, which is predicted to bind non-fucosylated sidechains bound of xyloglucan, we separated flax mucilage using anion-exchange chromatography and tested the antibodies for binding in fractions using dot blots. Water-extracted mucilage from mature seeds was dialyzed, freeze-dried, and separated according to charge on a Hi-prep DEAE anion exchange

column. This resulted in the elution of three overlapping peaks, with a large neutral fraction eluting first and more acidic fractions eluting after (Supplemental Figure 2.3, A). This closely resembles what was seen in the study by Naran et al., where the three peaks were defined as primarily AX, inseparable AX-RG I, and RG I, respectively (Naran et al. 2008). Fractions corresponding to these three peaks were assayed in dot blots to see if the antibodies would bind specifically to any one of the three peaks, but all antibodies tested (CCRC-M14, -M36, -M141, -M89) bound to all three fractions (data not shown). The three eluted peaks had overlapping shoulders, so, in order to achieve greater separation of these products, a stepwise gradient at both low and high salt concentrations was used to repeat the elution. This resulted not only in a greater resolution of separation between peaks, but an increase in the number of separated compounds (Supplemental Figure 2.3, B), with peaks eluting at approximately 0.28M, 0.33M, 0.38, 0.42M in which two small peaks eluted together, 0.62M, and 2M. While it is not possible without chemical analysis to precisely define the compositional identity of the peaks, it is possible that the double-peaked fraction eluting at 0.42M (Supplemental Figure 2.3, B) represents the AX-RG I peak in Supplemental Figure 2.3, A, where AX and RG I could not be separated into discrete products. This may explain the presence of these two overlapping peaks persistent in Supplemental Figure 2.3, B. If this is the case, products eluting prior to the double peak are likely primarily composed of AX, as these are more neutral polymers easily released from the column, while the fractions following the double peak are likely some form of RG I, as pectins are acidic and bind very strongly to the column.

Dot blots of peaks one through seven (Supplemental Figure 2.3, C) revealed that CCRC-M36 and M14 both bound fractions corresponding to all separated peaks except for peak 1, indicating that this is the only fraction that does not contain unbranched RG I. CCRC-M36 and –

M14 also do not bind the column flow through, indicating that these antibodies bind exclusively to more charged, acidic polymers that bind strongly to the column. CCRC-M89 bound all fractions to some extent, although very weakly to the later eluted peaks. This suggests it binds more neutral products such as XG or AX. This is also supported by its strong binding to the flow-through, which contains the very neutral polymers that do not bind the column, and void in the initial column wash. CCRC-M141 strongly binds all fractions tested, and so it remains unknown whether it is recognizing hemicellulose, pectin, or some unique sidechain component specific to flax mucilage. Despite achieving greater separation of specific products in the mucilage, we were not able to conclusively identify specific epitopes bound by the antibodies.

2.3.4 UDP-L-RHAMNOSE SYNTHASE homologs in flax

Due to the requirement for UDP-L-Rha to form the backbone of RG I, a key component of flax mucilage, the amino acid sequences of the RHM proteins from Arabidopsis were used as a query to identify putative *LuRHM* and *LuUER* gene family members. Seven putative *RHM* and two *UER1* homologs were identified, with amino acid similarities between 93.9% and 82.3% to their Arabidopsis orthologs (Supplemental Table 2.1). In Arabidopsis, the *RHM* gene family contains a number of characteristic amino acid motifs (Figure 2.4, A; Figure 2.5, A). Both the C-terminal 4, 6-dehydratase and N-terminal 3, 5-epimerase/4-reductase domains of *RHM2/MUM4* contain a Rossmann-fold motif (GxxGxx(A/G)) and two catalytic sites (YxxxK), whereas *UER1* contains only the last three motifs (Usadel et al. 2004; Watt et al. 2004; Western et al. 2004; Oka et al. 2007; Han et al. 2015). An alignment of both Arabidopsis and flax RHM orthologs reveals that, while the amino acid sequences are highly homologous between all RHM and UER orthologs

(Figure 2.4, A), some key differences occur within the flax *RHM* gene family, indicating greater divergence among this family compared to the strong sequence conservation seen within the Arabidopsis genes (Figure 2.4, B). A comparison of the conserved motifs between Arabidopsis and the predicted protein sequences of flax RHM and UER proteins further illustrates the high level of variation seen in flax RHMs, which is not observed in Arabidopsis (Figure 2.5, A). None of the seven flax RHM homologs exhibit conservation of all six motifs found in the Arabidopsis versions, but can be grouped based on which domains are affected. When compared to the AtRHM1/2/3 protein model, Lus10033846 and Lus10042497 contain the co-factor binding domain (R-fold 1) and both catalytic sites (CS 1 and CS 2) characteristic of the 4, 6-dehydratase domain of RHM. These also contain the essential R-fold 2 and CS 4 of the C-terminal 3, 5-epimerase/4-reductase domain, but contain substitutions disrupting CS3. Lus10010942 contains all characteristic domains except for CS 1 of the 4, 6-dehydratase domain, which contains substitutions. Lus10020776 and Lus10007355 are the most unique family members (Figure 2.4, B), as they are substituted in CS 1, but are still predicted to contain the N-terminal dehydratase domain, according to both PFAM and PANTHER databases. Conversely, their amino acid sequences are predicted to lack a NAD-dependent epimerase/reductase domain. Their C-terminal co-factor binding motif (R-fold 2) is conserved, but has the motif GxxGxxA, whereas all other RHMs in flax and Arabidopsis contains a GxxGxxG at this location. Furthermore, these two flax RHM homologs lack the highly conserved CS 4 completely. Lus10005560 and Lus10013695 appear to be missing the first Rossmann-fold (R-fold 1) and CS 1 due to a truncation in the 4, 6-dehydratase domain. Based on the publicly available genomic and upstream sequence information for these two isoforms, these deletions appear to be true truncations as opposed to an artefact caused by misannotation of this fairly recently established genome. The two flax UER homologs

are conserved at both motifs exhibited by the Arabidopsis sequence (Watt et al. 2004), with both a GxxGxxG co-factor binding site and C-terminal catalytic site (CS 4), while CS3 is not conserved in either Arabidopsis or flax UER sequences.

Since great divergence is seen between the flax RHM homologs and the well-characterized Arabidopsis *RHM* gene family, our analysis was broadened to determine the divergence of RHMs across all 52 available plant genomes currently annotated at Phytozome (v11.0). It is currently thought that plants contain a combination of full length, bi-functional *RHM* genes and the partially redundant *UER/NRS* genes capable of carrying out the same C-terminal function as the *RHM* genes (Yin et al. 2011). Since Lus10007355 and Lus10020776 were the most divergent, with a substitution in CS 1, a sequence gap resulting in the deletion of CS 4, and a G to A substitution in R-fold 2, Lus10007355 was chosen as a query to see if there were similar potential RHMs predicted to only contain the 4, 6-dehydratases in other species. The resulting alignment of 69 sequences (Figure 2.6, Figure 2.7, A) includes the seven putative flax RHMs, Arabidopsis RHM2, and the 61 best hits to Lus10007355 with representatives from 32 other species. These sequences sharing amino acid similarity with Lus10007355 were used to create a multiple sequence alignment (MUSCLE in Geneious v.9.0.5) and create a neighbor-joining tree (Figure 2.6). Highlighted in red, Lus10020776 and Lus10007355 are both positioned further out on the phylogenetic tree, indicating higher sequence divergence of these *RHM* homologs with respect to the most similar homologs in 33 other species. Also highlighted in blue are the N-terminally truncated versions Lus10013695 and Lus10005560, which are also highly diverged from the other *RHM* homologs. A closer view of the alignments (Figure 2.7, A) illustrates how these sequences diverge structurally. While it is apparent that these genes are highly conserved even across species, there are fairly large deletions seen in the four aforementioned flax sequences, which are not seen

in orthologs in other species. The gap deleting the second YxxK catalytic site (CS 4) of the second domain of *RHM* in Lus1000735 and Lus10020776, and the truncated N-terminus removing the first co-factor binding and catalytic site of Lus10013695 and Lus10005560 appear to be unique changes specific to the flax *RHM* gene family. A breakdown of motif conservation across the genes selected from all 34 species (including flax and Arabidopsis) for the RHM phylogeny is shown in Figure 2.7, B. All selected *RHMs* except for the two N-terminal truncated flax homologs (Lus10005560 and Lus10013695) are conserved at the first co-factor binding site, GxxGxxA. In fact, all proteins aligned had the sequence GAAGFIA at this location, which may confer co-factor specificity in these proteins. Catalytic site 1 is fairly conserved as well, being maintained in 83% of selected *RHMs* in this alignment. Catalytic site 2, which is required for rhamnose synthesis (Oka et al. 2007), is conserved among all 69 proteins in the alignment. Furthermore, all 69 proteins contained the CS 2 sequence YSATK, except for one protein from *Panicum virgatum*, which had the sequence YAATK at this location. The co-factor binding site of the second RHM protein domain (R-fold 2) was also conserved among all species in the alignment. Interestingly they all contained the motif GxxGxxG at this location except for the two flax homologs Lus10007355 and Lus10020776 described previously, which instead had another GxxGxxA motif in this location. Unsurprisingly, CS 3 was the least conserved catalytic motif (57%) as it is not required for catalytic activity of RHM (Oka et al. 2007) and is not found in Arabidopsis UER1, while catalytic site 4 was conserved among all proteins in the alignment with the sequence YSKTK, except for the two flax homologs (Lus10007355 and Lus10020776), which contain a sequence gap in this position.

2.3.5 UDP-D-XYLOSE SYNTHASE homologs in flax

Thirteen putative *UXS* orthologs were predicted within the flax genome, with amino acid similarities between 74.3% and 96% to their closest *Arabidopsis* ortholog (Supplemental Table 2.1). A protein alignment of the 13 flax *UXS* homologs with the six *Arabidopsis* genes demonstrated the high sequence homology of this family, and the presence of characteristic conserved features including the N-terminal Rossmann-fold motif (GxxGxxG) needed for NAD(P)-dependent binding of sugar substrates (Harper and Bar-Peled 2002), and the highly conserved Ser, Tyr, and Lys triad, of which Lys and Tyr are in the C-terminal YxxxK motif (Figure 2.8, A). As seen in *Arabidopsis*, the flax *UXS* family contains both cytoplasmic and transmembrane isoforms (Figure 2.8, A, B). Flax homologs Lus10015038, Lus10025293, Lus10024436, Lus10003605, Lus10037499, Lus10006510, and Lus10030368 all contain the N-terminal transmembrane domain, which was predicted using TMHMM Server v. 2.0 (<http://www.cbs.dtu.dk/services/TMHMM-2.0/>) (Sonnhammer et al. 1998). All 13 predicted flax *UXS* orthologs contain the conserved regions of their corresponding *Arabidopsis* orthologs, except for Lus10001705, which lacks the N-terminal Rossmann-fold motif required for NAD(P)-dependent binding of UDP-GlcA (Figure 2.8, A; Figure 2.5, B). Publicly available genomic and upstream sequence information suggests this is a true truncation, and likely results in a non-functional protein/pseudogene.

2.3.6 Expression of flax *RHM* homologs

In *Arabidopsis*, the onset of mucilage production is correlated with transcriptional upregulation of the UDP-L-Rha synthase gene *MUM4/RHM2*, which is required to supply sufficient UDP-L-Rha levels for RG I backbone synthesis (Usadel et al. 2004; Western et al. 2004;

Oka et al. 2007). To see if a similar regulation of substrate genes occurs during flax mucilage production, we tested their mRNA levels via qRT-PCR using gene-specific primers (Supplemental Table 2.1) at stages prior to (5 DAF whole seed), during (10 DAF, 13 DAF, 16 DAF seed coat versus embryo) and after (20 DAF seed coat versus embryo) mucilage synthesis. Expression data was normalized against *LuACTIN* as a housekeeping gene. The fold-change values reported in 10, 13, 16, and 20 DAF are compared to transcript expression for 5 DAF whole seed, and these values were subject to one-way ANOVA followed by a Student-Neuman-Keuls post hoc test, which allowed for comparison of these values between seed coat and embryos at different developmental stages.

All putative members of the *RHM* family were tested. Two of the seven putative rhamnose synthase genes, Lus10020776 and Lus10007355, were identified as having the largest fold-change in transcript levels versus 5 DAF whole seeds in flax seed coats at the time of mucilage production (Figure 2.9, A, B). Lus10007355 (Figure 2.9, A) has increased expression in the seed coat at both 10 and 13 DAF, with highest expression seen at 13 DAF, while its expression at 16 and 20 DAF is low. Lus10020776 (Figure 2.9, B) also has increased transcript levels at both 10 and 13 DAF, while seed coat expression at 16 and 20 DAF is not significantly increased. Interestingly, these two upregulated transcripts encode the two most peculiar flax *RHM* family members previously identified in this study, which are predicted to carry out the first RHM enzymatic function as a 4, 6-dehydratase, but may not be capable of efficiently carrying out the latter function as a combined 3, 5-epimerase/4-reductase. Flax *UERS* Lus10006719 and Lus10014147 are found to have increased transcript levels in seed coats at 10, 13, and 16 DAF (Figure 2.9, C, D), with highest expression observed at 10 and 13 DAF. Their stages of peak expression, while potentially more subtle in terms of fold-change magnitude, do coincide with patterns of upregulation seen in the

RHM genes Lus10007355 and Lus10020776 at 10 and 13 DAF (Figure 2.9, A, B). Other *RHM* homologs such as Lus10038146, 10042497, and Lus10005560 have little to no upregulation in seed coat tissues (Supplemental Figure 2.4, A, B, C, D, respectively). Lus10013695 (Supplemental Figure 2.4, C) has increased transcript levels in the 10 DAF seed coat, with lower expression seen at 16 DAF.

2.3.7 Expression of flax *UXS* homologs

In order to determine if any of the flax 13 flax *UXS* homologs are upregulated at the time of mucilage synthesis, we tested their mRNA via qRT-PCR using gene-specific primers (Supplemental Table 2.1) as described previously for the flax *RHM* homologs. A selection of the 13 *UXS* genes assayed for expression pattern in the seed coat and are shown in Figure 2.9, E and Supplemental Figure 2.4 (E—H). Of the 13 *UXS* genes tested, Lus10006510 was the only gene that exhibited increased expression in seed coat tissue versus the embryo (Figure 2.9, E). Unlike the *RHM* and *UER* homologs, this *UXS* homolog is expressed most highly at 16 DAF. Lus10025293 and Lus10003605 (Supplemental Figure 2.4, E, F) are upregulated at most 2-fold during some stages of seed coat development, while upregulation in seed coats of Lus10001707 are barely detectable (Supplemental Figure 2.4, G). Lus10030368 (Supplemental Figure 2.4, H) is upregulated in the embryo rather than seed coats, indicating the necessity in dissecting seed coats from embryos and testing expression in these tissues separately. Note that all 13 *UXS* homologs were tested, and those not shown did not exceed more than a 2-fold upregulation compared to 5 DAF at any stage of development.

2.3.8 Exogenous protein expression in flax mucilage

In addition to examining mucilage production in flax MSCs, we investigated the potential for expression of exogenous co-products into flax mucilage. The Arabidopsis gene *GLABRA2* (*GL2*) is expressed highly in the seed coat at key stages of mucilage production in Arabidopsis (Rerie et al. 1994; Western et al. 2001; Western et al. 2004). The *AtGL2* promoter was cloned upstream of *GUSplus*, a form of the *BETA-GLUCURONIDASE* (*GUS*) reporter gene that is optimized for secretion (Broothaerts et al. 2005). This promoter-reporter gene construct was further optimized for secretion to the apoplast through the addition of the MUM2 signal peptide (Dean et al. 2007) and the omega translational enhancer element from the tobacco mosaic virus (Gallie and Kado 1989) (Figure 2.10, A).

Flax bolls harvested at 14 DAF expressing the *GL2::MUM2sp::GUS+* construct, and exposed to the GUS substrate, exhibit deep staining in both the seed coat and embryo tissues (Figure 2.10, B, i). Staining is also seen in the seed coat at 18 DAF, but is largely absent from the embryo (Figure 2.10, B, ii). When mature transgenic flax seeds were incubated in the aqueous GUS substrate buffer, the released mucilage stained blue along the fissures of the seed coat (Figure 2.10, B, iii). Staining was not observed in mature embryos (Figure 2.10, B, iv), which were cut prior to staining to allow proper buffer infiltration. To further confirm that the exogenous GUS expression was targeted to the secreted mucilage, seeds from the transgenic lines were resin embedded and sectioned. Staining is largely absent in the thin mucilage layer at seeds staged at approximately 10 DAF (Figure 2.10, C, i). However, at 15 DAF, thick deposited mucilage layers are present and GUS staining is observed in both outer and inner layers (Figure 2.10, C, ii). At this stage, GUS expression appears strongest in the outer deposited mucilage layer, with weaker

staining in the inner layer, which may be the result of mucilage compression differences between the layers. Finally, to determine if exogenous protein expressed in the mucilage could be extracted, mature transgenic seeds from were shaken in water and soluble mucilage was removed and incubated with GUS substrate, followed by ethanol precipitation (Figure 2.10, D). This resulted in the presence of GUS staining in the extracted mucilage, which was precipitated for easier viewing of the stained substance. This confirmed that exogenous co-products can indeed be expressed, secreted to the mucilage, and collected easily via water extraction. These results also suggest that cis-regulatory elements involved in seed coat expression in Arabidopsis are conserved in flax.

2.4 DISCUSSION

2.4.1 Flax MSCs are specialized seed coat epidermal cells that fill entirely with mucilage

This study presents the first detailed analysis of flax MSC morphology, cell biology, and differentiation. Flax MSCs begin to synthesize copious amounts of mucilage around the time when the developing embryo reaches the torpedo stage (data not shown), and continue to produce mucilage over a span of approximately ten days. Over the course of MSC differentiation, this results in the gradual accumulation of mucilage at the apical face of the cells, where differentially staining striations or regions are observed within the deposited mucilage. Mucilage production in flax MSCs is associated with the appearance of large starch granules, which are depleted over time until they become very small at the end of MSC development, when the cells primarily contain mucilage, suggesting that these provide sugar reserves for the synthesis of mucilage. Polar secretion of this mucilage is coordinated by an active endomembrane system where an increased

abundance of Golgi stacks produces many secretory vesicles that fuse to the plasma membrane at the apical face of the cell. Golgi stacks were distributed randomly throughout the cytoplasm rather than concentrated near the site of secretion (data not shown). This is in contrast to reports in other tissue types where polar secretion is accompanied by Golgi stack positioning near the site of deposition, which occurs in tips of growing cells and during the production of the cell plate (Jürgens 2005; Cole and Fowler 2006; Campanoni and Blatt 2007), but is typical of MSCs (Hyde 1970; Van Caesele et al. 1981; Young et al. 2008). The process of MSC development in flax resembles what has been observed in other species, including *Plantago ovata* and *Brassica campestris*, which lack columella or other secondary cell wall inclusions, and rather create a thick apical layer of mucilage driven by polar secretion of mucilage and shrinkage of the central vacuole (Hyde 1970; Van Caesele et al. 1981). This is also similar to the polar secretion of mucilage in *Arabidopsis*, except that the secretion domain includes the entire runs apical face of the cell in flax MSCs, creating an unstructured interface between the cytoplasm and mucilage, rather than forming a ring-shaped domain of secretion (Western et al. 2000). In addition, the cortical microtubules lining the mucilage pocket suggested to guide cellulose synthases in *Arabidopsis* (McFarlane et al. 2008; Griffiths et al. 2015) are not observed in flax MSCs, which is in agreement with its non-cellulosic mucilage.

2.4.2 Changes in Golgi stack morphology during mucilage production

A change in Golgi stack morphology is observed concurrent with the onset of mucilage production between 5 and 10 DAF, whereby thin curved stacks that are not undergoing significant amounts of secretion become shorter in diameter with widened lumens, swelled margins, and have

many mucilage-rich vesicles surrounding the TGN. This obvious increase in the activity of the secretory apparatus is also observed during mucilage production in *Arabidopsis*, where a strikingly similar change in Golgi stack morphology occurs between 4 and 7 DPA (Young et al. 2008). In *Arabidopsis*, it has been shown that this morphology is associated with the production of a massive amount of pectin, and more specifically RG I, as immunogold labelling with anti-RG I antibody CCRC-M36 bound to Golgi lumens and vesicles. Furthermore, this highly active Golgi stack morphology is disrupted in the *mum4* rhamnose synthase mutant, indicating that swollen cisternae and large numbers of secretory vesicles are associated with copious amounts of RG I production (Western et al. 2004; Young et al. 2008). By 13 DAF, flax Golgi stacks no longer exhibit the swollen appearance seen at 10 DAF, and rather appear to have longer, thinner, and straight cisternae, but still have an active TGN with lots of secretory vesicles present. Their appearance at later stages of flax MSC development is similar to Golgi stacks observed in the high-pressure frozen cells of other actively secreting tissues such as the mucilage-producing root cap cells of tobacco and *Arabidopsis* (Kiss et al. 1990; Staehelin et al. 1990). Since the root cap mucilage of *Arabidopsis* is of a different composition (primarily HG and arabinogalactan proteins) (Vicré et al. 2005; Durand et al. 2009) than seed coat mucilage (primarily RG I), this suggests that the altered morphology of flax Golgi stacks observed at later stages of mucilage production could be associated with a change in the product being synthesized.

2.4.3 Deposited mucilage has striped regions of different polysaccharide compositions

While the composition of extracted flax mucilage is fairly well characterized, this is the first study to suggest a patterned deposition of compositionally distinct domains of mucilage

during MSC development. When flax seed coats were stained with toluidine blue, two to three distinct domains of mucilage were observed. The pink staining in the outer region suggests that a higher proportion of acidic polymers are present, compared to the more purple colour observed in the inner layers, which stain in a way that is characteristic of more neutral polymers. Early work describing flax MSCs corroborates with this observation, where the outer mucilage region in MSC sections was reported to stain more intensely with acidic pectin stain ruthenium red (Boesewinkel 1980). While compression of the deposited mucilage could be argued to explain the greater intensity of ruthenium red staining in the outer region, it does not explain the change in colour seen with the metachromatic dye toluidine blue. Rather, it suggests an increased concentration or proportion of acidic polymers in the apical layer, and more neutral polymers in the regions below (O'Brien et al. 1964; Sterling 1970).

This layered pattern of acidic and neutral polymers was also supported by immunostaining of seed coat sections, which revealed differential binding to these mucilage domains by antibodies predicted to bind different polysaccharide epitopes. Immunostaining with the anti- unbranched RG I antibody CCRC-M14 on 16 DAF seed coat sections suggests that there is a higher concentration of unbranched RG I in the apical region of the deposited mucilage, and lower levels throughout the middle and lower mucilage regions. This is consistent with the toluidine blue and ruthenium red results, as the presence of large amounts of the pectin RG I in the apical region would indeed lead to greater overall acidity in this location. Conversely, the anti-non-fucosylated XG antibody CCRC-M89 bound most strongly to the mid to lower region of the deposited mucilage at 16 DAF. This also corroborates with our results suggesting the presence of greater amounts of neutral polysaccharides in the inner mucilage regions. CCRC-M141 has been defined as an antibody specific to flax mucilage. Its binding to seed coat sections overlaps to some degree with that of

anti-RG I antibody CCRC-M14, such that it binds strongly to the apical mucilage zone, and also to the middle region of deposited mucilage to some extent. Interestingly, CCRC-M141 binding is also observed in the cytoplasm, which could reflect its ongoing synthesis even at later stages (16 DAF). Cytoplasmic binding is also seen in Arabidopsis, where anti-RG I antibody CCRC-M36 is seen in the cytoplasm at the time of mucilage production in addition to binding in the mucilage pocket (Young et al. 2008). The exact epitope recognized by flax mucilage antibody CCRC-M141 has yet to be defined, but our data is consistent with it being the unusually branched RG I that is characteristic flax mucilage, whereby many L-galactose residues are attached at the O-3 rather than the typical O-4 position of rhamnose subunits (Naran et al. 2008). Particularly, CCRC-M141 binds both to seed coat sections and in fractionated mucilage in a similar pattern to the two unbranched RG I antibodies CCRC-M36 and CCRC-M14, which suggests that its recognized epitope is likely acidic in nature. Overall, these results are consistent with the existence of different compositional zones with different proportions of neutral and acidic polysaccharides along the vertical axis of deposited mucilage in flax MSCs.

Flax mucilage has been well characterized and has generally been reported as being primarily composed of AX and RG I (Muralikrishna et al. 1987; Warrand et al. 2003; Naran et al. 2008). While xyloglucan is not a well known polysaccharide present in flax mucilage, our dot blot analysis on isolated mature mucilage, as well as linkage analysis by Naran et al. 2008 where relatively small amounts of 4-Glc and terminal-Xyl residues were detected, suggest that xyloglucan could be present as a minor component. Alternatively, CCRC-M89 could be binding to side chains of the non-fucosylated xyloglucan that are shared with a component of flax mucilage, as this antibody has been demonstrated to bind to more than just xyloglucan by ELISA analysis (Pattathil et al. 2010) and bound to the neutral polysaccharides found in the flow-through in our

fractionation of flax mucilage. Arabinoxylans comprise the majority of flax mucilage polymers (Muralikrishna et al. 1987; Warrand et al. 2003; Naran et al. 2008). However, only one of the four anti-xylan antibodies we tested bound to our isolated flax mucilage. The anti-xylan antibodies that did not bind flax mucilage may have failed to bind due to structural differences in flax AXs compared to their raised antigens. The anti-monocot arabinoxylan antibody CCRC-M118 weakly bound to isolated mucilage in dot blots, but it did not give sufficient signal with immunostaining, possibly due to polymer epitope masking in the sections, which may make AX inaccessible. However, the toluidine blue staining of a purple region in the lower mucilage region suggests that the predominant polymer in the mid to lower zones is not strongly acidic, and could reflect the primary location of these xylans that make up the majority of flax mucilage.

2.4.4 Upregulation of nucleotide sugar synthase genes potentially involved in the production of substrates for mucilage production

Based on their sequence homology to Arabidopsis genes and those from other publicly available genomes, we identified flax homologs of both the *UXS* UDP-D-Xyl synthase gene family and the *RHM* and *UER* UDP-L-Rha synthase gene families. Transcriptional analysis of the expression of these gene family members at different stages of flax seed coat differentiation identified increases in the expression of certain *RHM* and *UXS* family members at particular developmental time points (Figure 2.11). Two *RHM* homologs were found to have substantially increased transcription at the time of mucilage production. In the case of both of the upregulated *RHM* genes, the most significant increases in expression were observed earlier in mucilage production, at 10 and 13 DAF. Both of the obvious *UER* homologs were also increased in fold-

expression levels at the time of mucilage production, but to a lesser extent. This dramatic increase of *RHM* transcription and, presumably, the encoded RHM proteins, is similar to what has been found in *Arabidopsis* mucilage production, whereby *MUM4/RHM2* has been demonstrated to be specifically upregulated through its activation by several transcription factors that regulate mucilage production and seed coat differentiation (Usadel et al. 2004; Western et al. 2004; Oka et al. 2007). Furthermore, in *Arabidopsis*, the significant loss of mucilage in *mum4/rhm2* mutants demonstrate that this is likely a control point in the regulation of mucilage production through the modulation of sugar substrate availability for the production of RG I (Usadel et al. 2004; Western et al. 2004; Oka et al. 2007; Young et al. 2008).

Similarly, a single transmembrane *UXS* gene, Lus10006510, demonstrated an increase in transcript expression during mucilage production, with significant expression seen most prominently in 16 DAF seed coats, with little to no expression seen at 20 DAF. The gradually increased expression pattern of this particular *UXS* homolog could provide an increased quantity of UDP-D-Xyl for the purpose of its channelling into xylan backbone synthesis. In *Arabidopsis*, the putative cytosolic *UXS3* gene is thought to be directly involved in the supply of UDP-D-Xyl for xylan synthesis, and is upregulated in vascular tissues by several MYB transcription factors involved in the regulation of secondary cell wall synthesis (Harper and Bar-Peled 2002b; Zhong and Ye 2012). The potential increase in xylan synthesis later in MSC differentiation also corroborates with the higher proportion of neutral polysaccharides in the mid and inner region of flax mucilage, as assessed with toluidine blue staining. While a correlation is seen between the timing of mucilage synthesis and the expression of putative mucilage biosynthetic genes, we cannot rule out the possibility that these genes may be involved in other processes occurring in different cell layers of the seed coat, such as the formation of the thickened sclerenchymous tissue

in the inner endothelium (Boesewinkel 1980). However, the abrupt loss of gene upregulation between 16 and 20 DAF for most of these genes suggest that their decrease in expression coincides with the end of mucilage production. Finally, these results also represent regulation of these synthases at the transcript level, but does not account for post-transcriptional regulation, including feedback inhibition of nucleotide sugar synthases by monosaccharide substrates. For example, UDP-D-Xyl inhibits the enzymatic activity of RHM2/MUM4 (Oka et al. 2007), which may provide a tighter, more discrete regulation of RHM and UXS activity in the cell.

2.4.5 *RHM* genes in flax have undergone unique divergence compared to orthologs in other genomes

The putative flax *RHM* gene family contains members with deletions and changes in the characteristic conserved motifs seen not only in the three Arabidopsis *RHMs*, but also those we could predict in other species. A previous study of the enzymatic functions of Arabidopsis RHM2/MUM4 determined, through site-directed mutagenesis of conserved domains, which motifs were essential for proper enzymatic function in the conversion of UDP-D-Glucose to UDP-L-Rhamnose (Oka et al. 2007). Lus10038146 and Lus10042497 are the closest to the Arabidopsis *RHMs*, as these homologs only lack CS 3. This motif is not conserved in Arabidopsis or flax *UERS* (Watt et al. 2004), is the least conserved motif in the *RHM* alignment across species, and therefore is expected to have little effect on protein stability or enzyme function. Thus, these are likely to be normally functioning *RHM* proteins (Oka et al. 2007). Lus10010942 lacks CS 1, which, based on enzyme assays in Arabidopsis, should decrease enzymatic activity of the first step in UDP-L-Rhamnose synthesis, leading to less robust synthesis overall (Oka et al. 2007). Lus10005560 and

Lus10013695 both have an N-terminal truncation that removes both R-fold 1 and CS 1. Despite the observed upregulation of one of these RHMs, these homologs likely do not produce a functional protein, as it is expected that the Rossmann-fold is required for both enzyme activity and protein stability, and R-fold 1 deletion in Arabidopsis assays ablated protein function completely (Oka et al. 2007). Alternatively, if this first Rossmann-fold is not required for protein stability in flax RHMs, it is possible these may be UER-like, in that these act as a partial version of full-length RHMs and carry out the second two activities of the three-step reaction (Watt et al. 2004; Oka et al. 2007).

The two most highly expressed *RHM* genes in the seed coat, *Lus10007355* and *Lus10020776*, are substituted in the fairly well conserved CS 1, completely lack the essential CS 4, and have a different Rossmann fold sequence in the second domain, differentiating them from Arabidopsis *RHMs*, as well as all *RHM* homologs that were compared across 33 other species, making these peculiar *RHM* versions unique to flax. One possibility is that *Lus10007355* and *Lus10020776* are functionally capable of synthesizing rhamnose. When Arabidopsis RHM2/MUM4 was studied in the yeast heterologous system, mutations in CS 1 or CS 4 did not ablate rhamnose synthesis completely (Oka et al. 2007), but instead substantially decreased enzyme efficiency. Also, the change in the second Rossmann-fold sequence could cause a change in enzymatic co-factor specificity (Kallberg and Persson 2006). Considering there is a mutation/deletion in two domains necessary for robust enzymatic activity, it is likely that these enzymes are not producing rhamnose as efficiently as other, more characteristic *RHMs*. However, their upregulation suggests that they are involved in an important cellular process at this time (i.e. RG I synthesis), and therefore may need to be expressed at high levels during mucilage synthesis as a means to compensate for the low enzyme efficiency of the proteins. These two *RHMs* are also

complementary to the expression of the upregulated *UXS* gene, as all three of these genes increase in expression to a similar magnitude. However, it is also possible that these *RHMs* can perform the first step of the rhamnose synthase reaction and only lack the second function of rhamnose synthesis, and require the co-expression of the *UER* or other full-length *RHM* genes to efficiently carry out the 3, 5-epimerase/4-reductase reaction for robust rhamnose synthesis, which is supported by the upregulation of the *UER* genes at similar stages. In order to confirm the exact functional capabilities of these enzymes, enzymatic assays and/or molecular complementation of functional mutants is required.

This finding that the flax *RHM* gene family contains various mutations and/or deletions of conserved amino acid motifs is peculiar, in that none of the *RHM* family members share all of the same conserved motifs that are seen in *Arabidopsis* and many other putative *RHMs* in other species. This great divergence could merely be a result of genomic aberrations. Chromosomal rearrangements and whole-genome duplication events, at least one of which is known to have occurred in flax even prior to its domestication (Sveinsson et al. 2014), are extremely common among crop plants and often lead to the creation of large, redundant gene families, and pseudogenes that are able to persist in the population as a result of preferential breeding for other unrelated traits (reviewed in Michael and VanBuren 2015). However, the precedent set by the upregulation of *RHM* during mucilage synthesis in *Arabidopsis* (Usadel et al. 2004; Western et al. 2004), and the increased expression of two flax *RHM* homologs strongly suggests a functional role for at least some members of this gene family.

2.4.6 *RHM*, *UER* and *UXS* expression are correlated with both differential polysaccharide deposition and changes in Golgi stack morphology

The presence of distinct mucilage regions with compositional differences in terms of the proportions of different polysaccharides suggests that there could be regulation of specific polysaccharide synthases in order to produce these components in a sequential or overlapping manner during mucilage production. Figure 2.11 illustrates the correlation between the differential peaks of expression of *RHM*, *UER*, and *UXS* homologs in flax seed coats over the course of mucilage secretion. When viewed in terms of their relative expression (as a percent of their stage of maximum expression) a reciprocal pattern is observed whereby both *RHM* homologs Lus10007355 and Lus10020776 are maximally expressed at 10 and 13 DAF. The *UERs* homologs Lus 10006719 and Lus10014147 have increased expression at 10, 13, and 16 DAF, but exhibit highest expression at 10 and 13 DAF, similar to the *RHM* genes. The expression of these genes in the early to mid stages of mucilage production coincide with the production of the acidic, pink-staining outer region of mucilage, as well as the shortened, swollen Golgi stack morphology observed at 10 DAF. Conversely, the *UXS* homolog (Lus10006510) is expressed most highly at 16 DAF, which coincides with the expected timing of the production of the inner purple-staining neutral region of mucilage deposition and the elongated, flattened morphology of the Golgi stacks observed in the later stages of mucilage deposition.

The changes in Golgi apparatus morphology seen in differentiating flax MSCs may reflect differences in the enzyme content and/or polysaccharide cargo of Golgi lumens as the relative proportions of different polymers being synthesized changes over time. Interestingly, Golgi stacks in the early stage of mucilage production in flax resemble the primarily RG I-producing Golgi stacks of *Arabidopsis* MSCs (Young et al. 2008; McFarlane et al. 2013). This earliest stage in flax mucilage production is presumably when cells are depositing the apical-most region of mucilage, which is also the region in which anti-RG I antibodies bound most strongly. In terms of

ecological function for the layering of flax mucilage to have a higher proportion of acidic RG I in the outer region of the mucilage, it could be postulated that the more hydrophilic properties of RG I aid in the quick hydration of the mucilage upon water imbibition, allowing the mucilage to swell quickly and break the primary cell wall. This is supported by an earlier study that looked at mucilage release over time and found that RG I is released earlier in greater quantities than AX (Paynel et al. 2013). It would be interesting to follow flax mucilage production using immunogold labelling of MSC Golgi stacks with antibodies against the various polysaccharides, which would confirm these findings, particularly if an appropriate anti-xylan antibody could be identified.

2.4.6 Functional protein co-products can be secreted into flax mucilage

Our results demonstrate that the production and secretion of a functional *BETA-GLUCURONIDASE* (GUSPlus) enzyme into flax mucilage is possible, and this co-product can be extracted together with the soluble mucilage. The ability to secrete exogenous products to the mucilage has multiple agricultural applications, including the creation of value-added oilseed crops. A product that accumulates in the mucilage could be easily water-extracted, while the remaining intact seed could be processed further, i.e. for flax oil collection. Flax has already been well established as a health food, both for its embryo-derived oil and its seed husk/mucilage, and there is potential for nutritional enrichment of the seed via expression of proteins implicated in health. One caveat of secretion to the apoplast, however, is the challenge of separating proteins from the mucilage, particularly if the protein forms interactions with the polysaccharide network through glycosylation of the proteins, which would need to be determined for the potential proteins employed for this purpose. This study demonstrates the use of the *Arabidopsis GL2* promoter,

which targets products not only to the seed coat in flax, but other tissues including root hairs and root tips (data not shown), in accordance with its expression pattern in *Arabidopsis*, where strong expression of *GL2* is also observed in roots (Rerie et al. 1994; Johnson et al. 2002; Lin et al. 2012). This suggests that cis-regulatory elements driving seed coat expression may be evolutionarily conserved.

FIGURES

Figure 2.1. Gross morphological features of flax MSC differentiation

Bright field microscopy of glutaraldehyde/osmium-fixed flax seed coat sections stained with toluidine blue over the course of MSC differentiation. (A) 0 DAF MSCs are small and undergoing vacuole-driven cell expansion. (B) At 6 DAF, the cells are larger and starch granules are visible in the cytoplasm. (C) 8 DAF MSCs have further increased in size, with large central vacuoles at the basal region of the cell, and cytoplasm and starch granules observed at the apical face of the cells. (D) 10 DAF MSCs show enlarged starch granules, and an observable layer of pink-stained mucilage beginning to accumulate between the apical primary cell wall and the cytoplasm. (E) At 12 DAF, pink-stained mucilage continues to accumulate, starch granules begin to shrink, and the vacuole retreats towards the basal face of the cells. (F) 14 DAF MSCs appear to have no vacuole remaining at the basal region of the cells, and mucilage continues to accumulate. Note the presence of differently staining regions within the deposited mucilage, where the outer region appears pink relative to the purple-stained inner region. (G) 16 DAF cells continue to accumulate mucilage while cytoplasm and reduced starch granules continue to retreat and shrink to the basal region of the cells. (H) at 20 DAF, prominent regions of differentially stained mucilage regions are observed and secretion is largely complete. Cytoplasm is compressed to the bottom of the cells, as the starch granules become barely visible at this stage. Scale bar = 50 μ m.

Figure 2.1

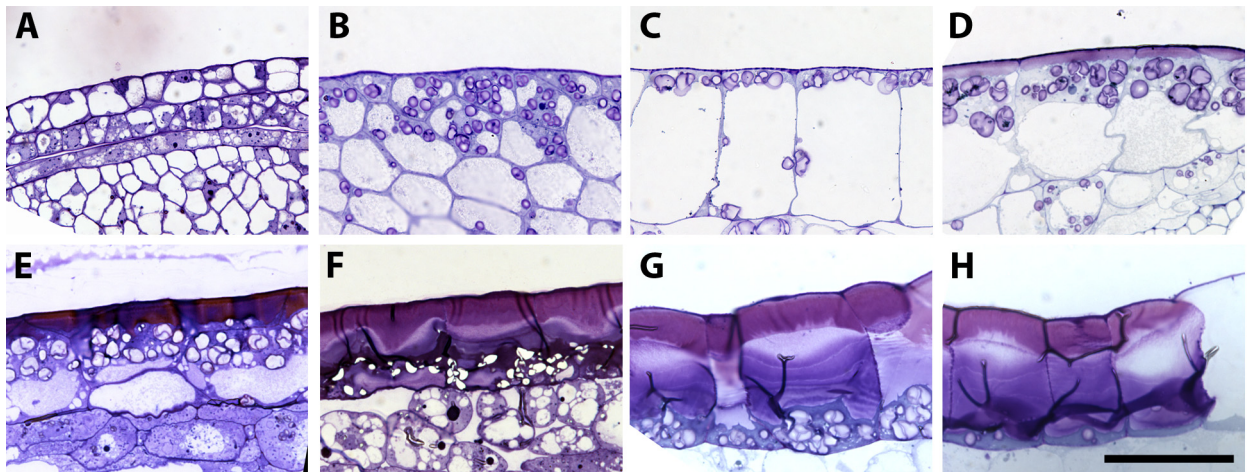


Figure 2.2. TEM of high-pressure frozen flax MSCs to observe features of the secretory apparatus during mucilage production

(A-C) 5 DAF (A) Low-magnification image shows cells have not begun mucilage synthesis. Arrow indicates the presence of large starch granules. (B-C) Golgi are long, thin, with cup-shaped trans-Golgi region. Arrows show TGN face of Golgi stacks. (D) 7 DPA Arabidopsis MSC showing enlarged cisternae with swollen termini (arrow) indicating active synthesis of large amounts of RG I. (E-H) 10 DAF (E) Low-magnification image shows mucilage has begun to accumulate across the outer face of the MSC (arrow). Note some folding of the section. (F-G) Golgi are swollen with prominent cis-trans polarity (C=cis, T=trans), and many secretory vesicles (V) are present. (H) Vesicles (arrows) are seen along the plasma membrane for secretion of mucilage (M) to apoplast. (I-J) 13 DAF Golgi are straightened, flat with difficult to discern cis-trans polarity. (K-L) 16 DAF Golgi remain flattened, similar to 13 DAF. Arrow indicates swollen termini still observed at this stage. (A, E) Scale bar = 2 μ m. (B, C, F, G, I, J, K, L) Scale bar = 100nm. (D, H) Scale bar = 500nm.

Figure 2.2

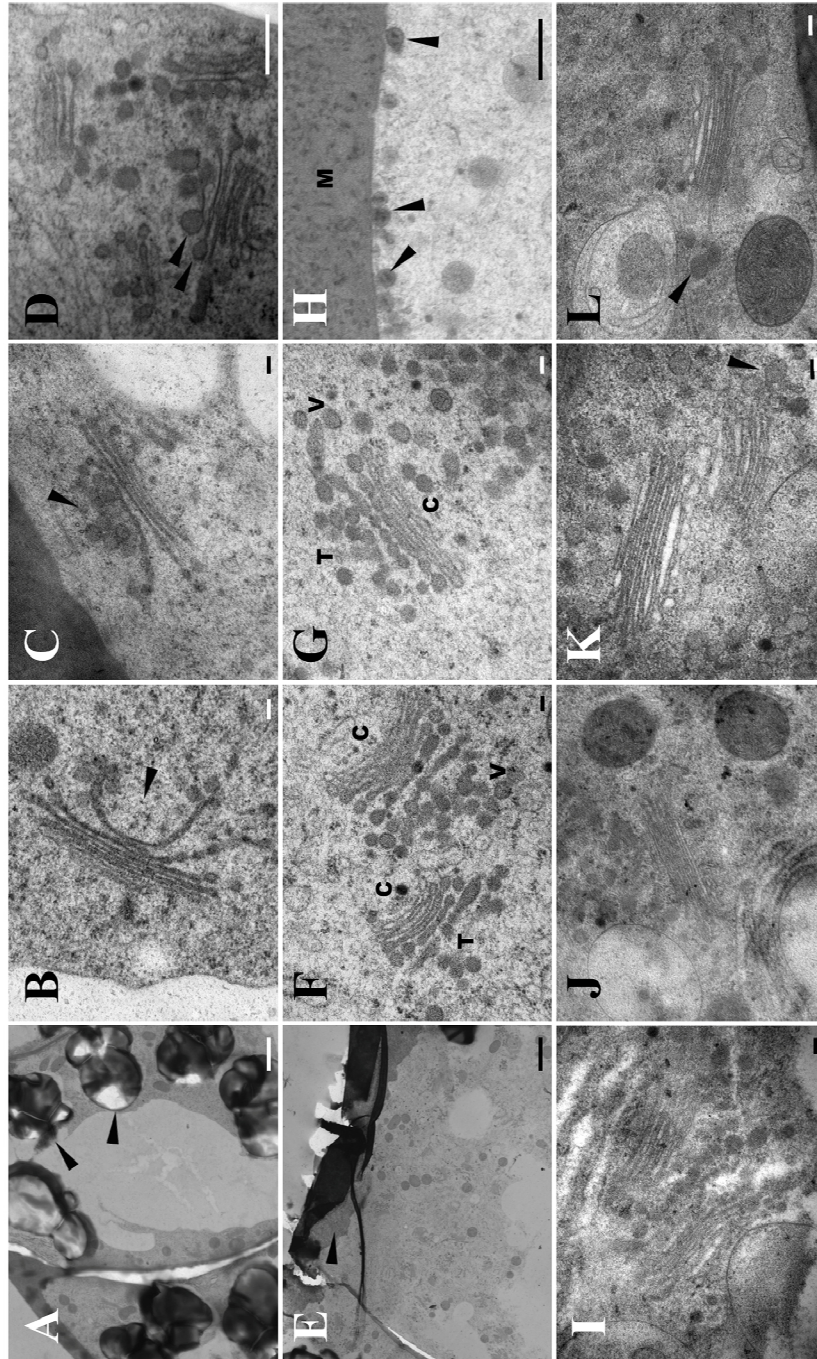


Table 2.1. Polysaccharide antibodies tested on flax mucilage

Shown is a list of monoclonal antibodies against a variety of cell wall polysaccharide epitopes, which were tested on mucilage fractions and used for immunofluorescence. Positive and negative results are noted.

Table 2.1

Antibody Name	Predicted Antigen	Mucilage^a	Sections^b	References
CCRC-M36	Unbranched rhamnogalacturonan I backbone	+	+/-	1, 2
CCRC-M14	Rhamnogalacturonan I backbone	+	+	1, 3, 4
CCRC-M7	Rhamnogalacturonan I (β -1,6-Gal with >1 Ara residues)	-	nd	1, 5, 6, 7
CCRC-M15	Rhamnogalacturonan I (structure unknown)	-	nd	1, 7
CCRC-M38	De-esterified homogalacturonan	-	nd	1, 8
CCRC-M118	Xylan (monocot)	+	-	1
CCRC-M139	Xylan (monocot & dicot)	-	-	1, 4, 9
LM10	Unsubstituted xylan	-	nd	1, 10
LM11	Xylan, arabinoxylan	-	-	1, 10
CCRC-M141	Linseed mucilage specific	+	+	1
CCRC-M100	Xyloglucan	-	nd	1
CCRC-M89	Non-fucosylated xyloglucan + pectic polysaccharides	+	+	1, 11
CCRC-M58	Xyloglucan	-	-	1, 12

^aResult of dot blot with mature flax mucilage; '+' = antibody binding; '-' = no antibody binding

^bAntibody binding to flax seed coat sections; '+' = antibody binding; '-' = no antibody binding; nd = not determined

(1) Pattathil et al. 2010 (2) Young et al. 2008 (3) Hao et al. 2014 (4) Hu et al. 2016 (5) Puhlmann et al. 1994 (6) Steffan et al. 1995 (7) Hall et al. 2013 (8) Gritsch et al. 2015 (9) Voiniciuc et al. 2015 (10) McCartney et al. 2005 (11) Cavalier et al. 2008 (12) Zabolina et al. 2012

Figure 2.3. Antibodies for different cell wall polysaccharides bind to distinct domains of deposited flax mucilage

(A-D) Toluidine blue staining on chemically fixed flax seed coats. (A) 5 DAF with large central vacuole. (B) 10 DAF with mucilage accumulating in apoplast in apical region of the cell. (C) 16 DAF with cytoplasm greatly reduced to the lower region of MSCs. Two to three layers of mucilage are apparent through differential staining with toluidine blue. (D-F) 5, 10, and 16 DAF seed coat immunostained with anti-RG I antibody CCRC-M14. (D) Signal is seen in emerging mucilage at 10 DAF (E), and in all mucilage at 16 DAF (F), with greater signal in the outer region. (G-I) CCRC-M141 binds to the thin stripe of mucilage at (H) 10 DAF, the outer region at (I) 16 DAF, and also binds in the cytoplasm at 16 DAF (I). (J-L) CCRC-M89 appears to bind the emerging mucilage layer at 10 DAF (K), but only stains the inner region later in development at 16 DAF (L). Scale bar = 50 μ m.

Figure 2.3

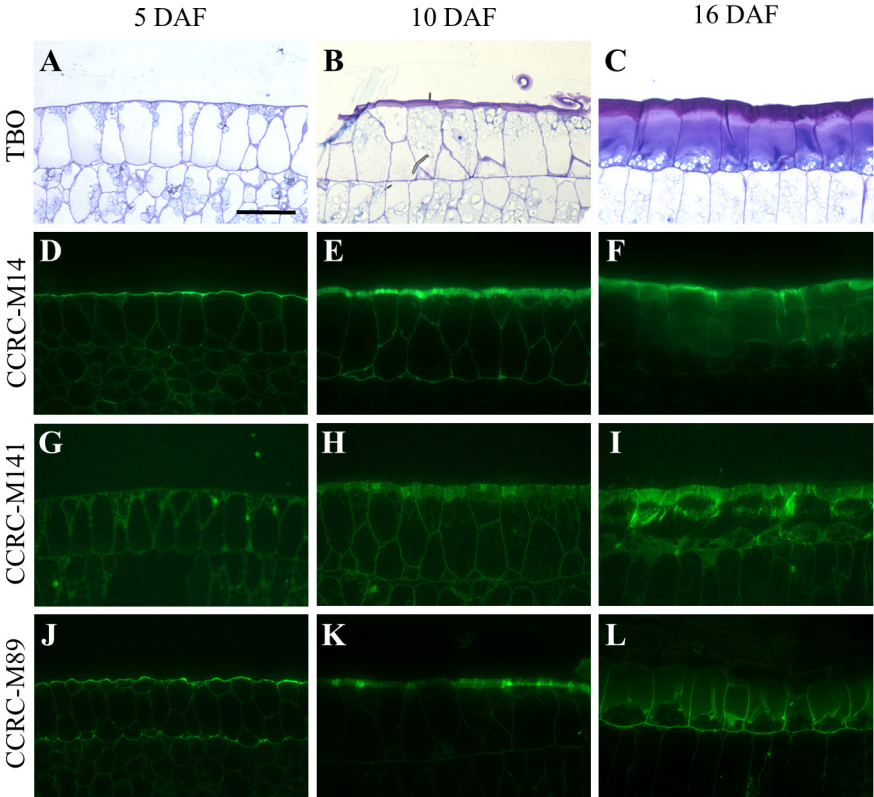


Figure 2.4. Protein alignment of Arabidopsis and seven putative RHM & UER homologs in flax

(A) Amino acid alignment of Arabidopsis and flax RHM homologs. Full length RHM proteins in Arabidopsis have two domains, each containing a Rossmann-fold motif (GxxGxx(G/A)) (R-fold 1, 2), and two YxxxK catalytic sites (CS 1, 2, 3, 4). UER proteins contain only the second domain of RHM, starting at the second R-fold. Note that flax RHM homolog Lus1000560 is truncated at the N-terminus, losing R-fold 1. Lus10020776 and Lus10007355 contain Ala instead of Gly in the last position of the GxxGxxG motif of R-fold 2, and are missing CS 4. (B) Flax and Arabidopsis RHM and UER proteins represented in a neighbor-joining tree, where Lus10020776 and Lus10007355 are more divergent relative to the other RHM isoforms.

Figure 2.4

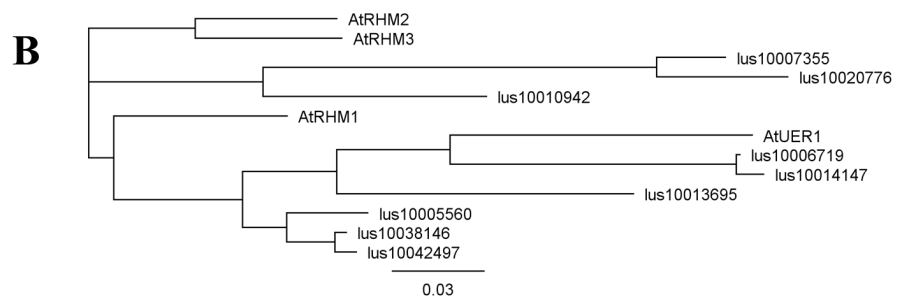


Figure 2.5. Protein motif structure of UXS, RHM, and UER orthologs in Arabidopsis and flax

Diagrams showing predicted functional motifs for (A) RHM and UER, and (B) UXS enzymes in Arabidopsis and flax. (A) Flax RHM enzymes have an N-terminal 4, 6-dehydratase domain (shown in orange) and a C-terminal 3, 5-epimerase / 4-reductase domain (shown in green). Both domains have an R-fold (red) and two CS motifs, where CS1 and 3 (blue) are less frequently conserved across species than the highly conserved CS 2 and 4 (yellow). Missing/mutated motifs are shown in black. UER proteins only contain the second domain of full length RHMs. Flax UER homologs are highly conserved, while RHM isoforms are more divergent. Lus10007355 and Lus10020776 lack CS 1 and CS 4, and have an Ala residue instead of Gly at the last position of R-fold 2 (denoted by *). Lus10005560 and Lus10013695 are truncated at the N-terminus, losing R-fold 1 and CS 1, possibly making these inactive pseudogenes or UER-like, having only the latter RHM functional domain. (B) Arabidopsis UXS proteins have a conserved Rossmann fold (R-fold, shown in red) and YxxxK catalytic motif (CS; shown in yellow). AtUXS1, 2, and 4 contain an N-terminal transmembrane domain (TMD, shown in blue). All putative flax homologs share these features, except for the possible pseudogene/inactive form Lus1000175, which is truncated at its N-terminus.

Figure 2.5

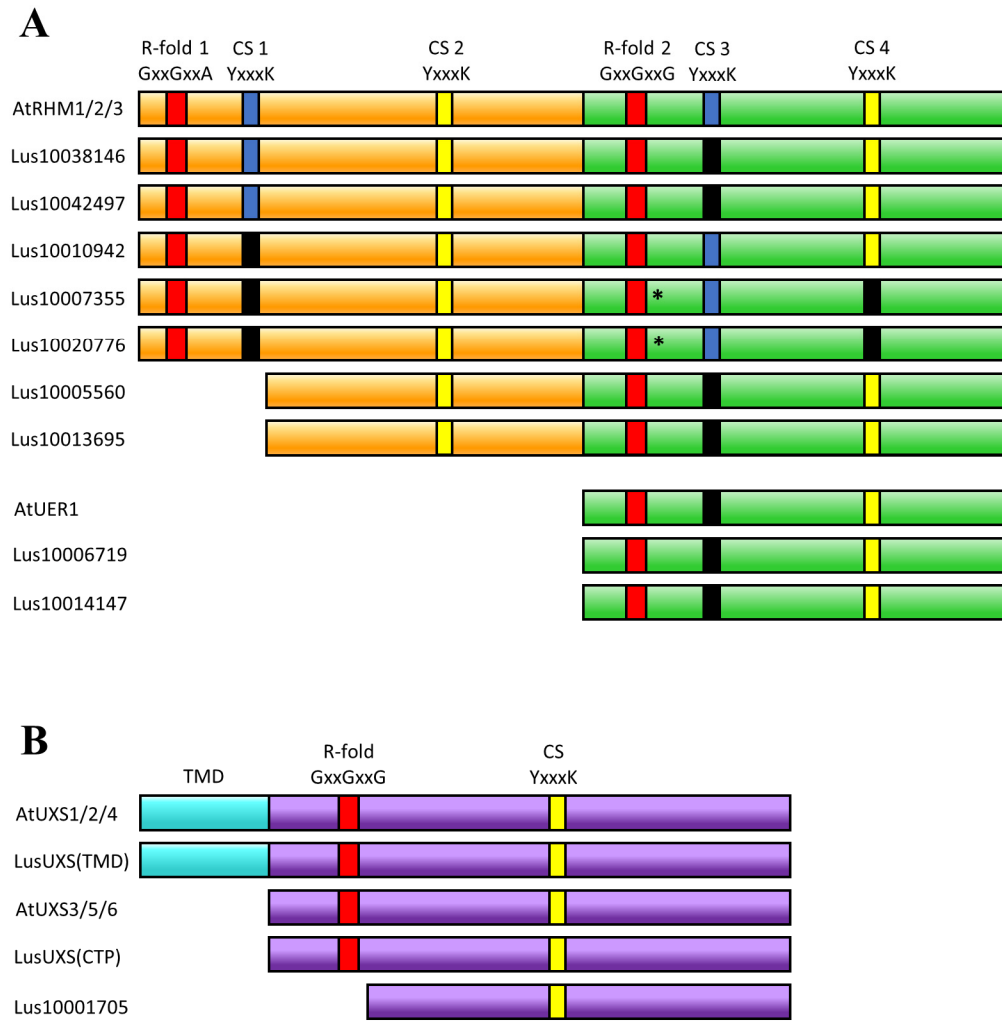


Figure 2.6. Neighbor-joining tree of putative RHM genes across 34 species

An alignment of 69 sequences across 34 species represented as neighbor-joining tree shows high conservation overall. Branches shown in red (Lus10020776 and Lus10007355) and blue (Lus10013695 and Lus10005560) extend further out from the majority of tree branches, indicating these are more divergent, partly due to their deletions in key motifs of the characteristic RHM proteins.

Figure 2.6

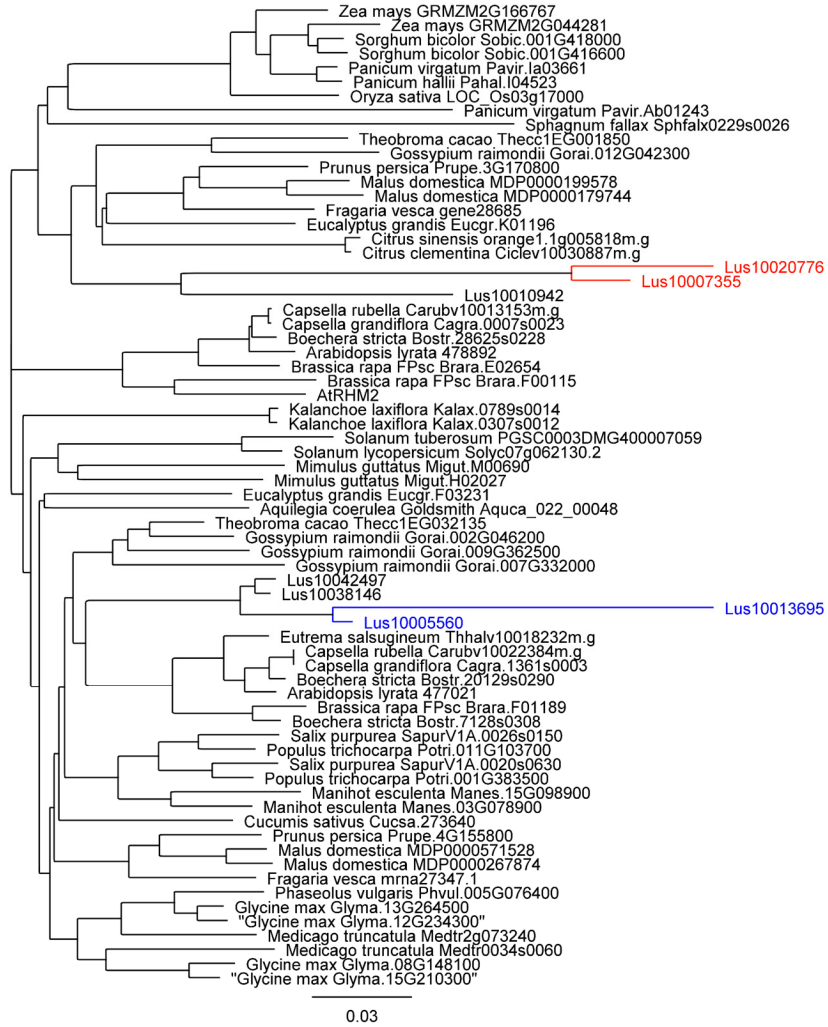
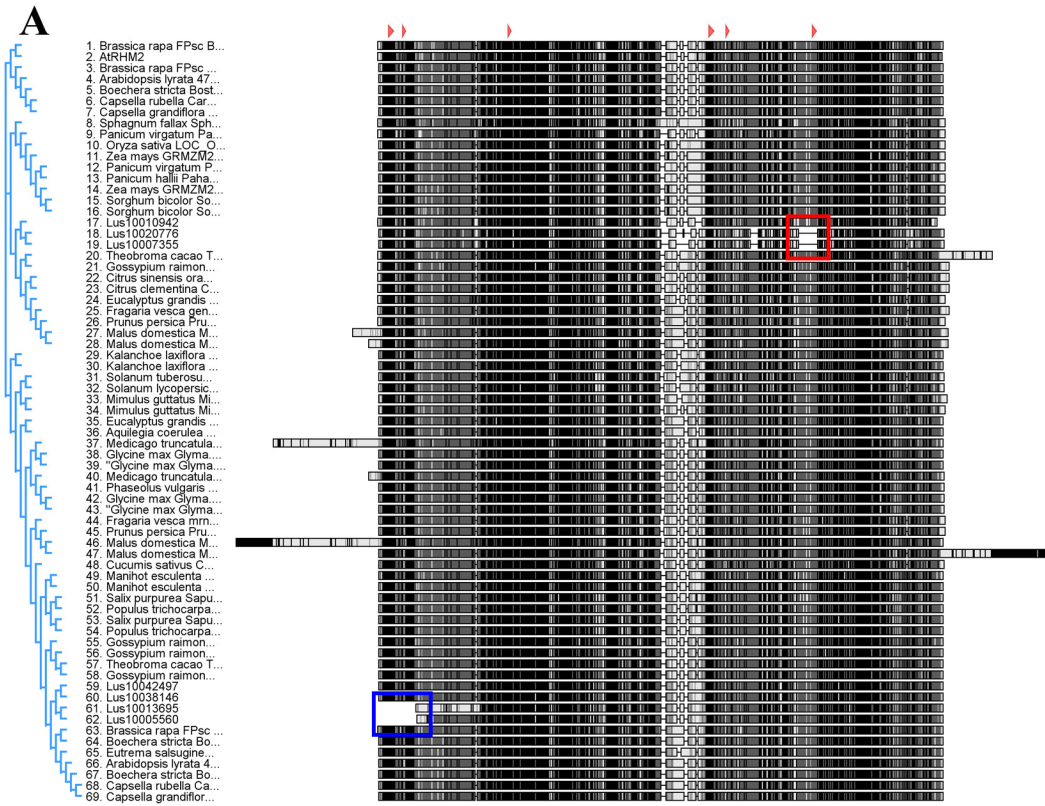


Figure 2.7. Protein alignment of putative rhamnose synthases across 34 species

(A) An alignment view of a neighbor joining tree created using the best matches to flax RHM Lus10007355. Red arrows at the top of the alignment indicate the positions of R-fold 1, CS 1, CS 2, R-fold 2, CS 3, and CS 4, respectively. The box shown in red indicates the gaps in the two flax homologs spanning the conserved CS 4 (YxxxK) motifs, which are not seen in any of the other homologs in the alignment. The blue box indicates the position of the N-terminal truncation in flax homologs Lus10013695 and Lus10005560. Shading indicates level of similarity at a given residue. Identical or highly similar residues are shown in black, while residues of moderate similarity are shown in grey. (B) A table summarizing the number of sequences from the above alignment which are conserved at each R-fold and CS motif. The two proteins lacking R-fold 1 are flax RHMs Lus10013695 and Lus10005560, while the two proteins lacking CS 4 are Lus10020776 and Lus10007355.

Figure 2.7



B

Motif	R-fold 1	CS 1	CS 2	R-fold 2	CS 3	CS 4
# conserved/total # genes	67/69	57/69	69/69	69/69	39/69	67/69

Figure 2.8. Protein alignment of Arabidopsis and thirteen putative UXS homologs in flax

(A) Amino acid alignment of Arabidopsis and flax UXS homologs. A selection of flax UXS proteins contain the transmembrane domain (TMD) seen in Arabidopsis UXS1, 2, and 4. Flax UXS homologs also contain the N-terminal Rossmann-fold motif (GxxGxxG) for NAD(P)-dependent binding (R-fold), and the C-terminal YxxxK catalytic site (CS). Note that flax homolog Lus10001705 (*) is truncated and does not contain the essential R-fold motif, indicating that this UXS isoform may be a non-functional pseudogene. (B) Flax and Arabidopsis UXS proteins represented in a neighbor-joining tree. Transmembrane and cytosolic isoforms are indicated. Possible pseudogene Lus10001705 is indicated by (*).

Figure 2.8

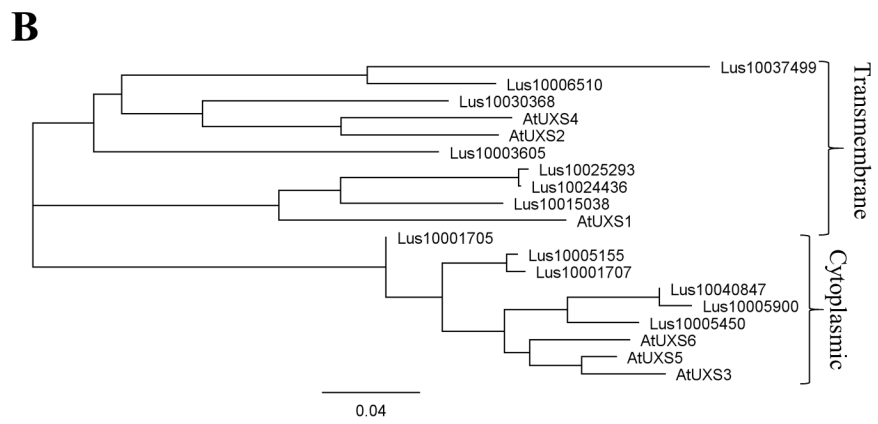


Figure 2.9. Transcript expression of highly upregulated *UXS*, *RHM*, and *UER* orthologs in flax seed coat tissue

Expression was determined via qRT-PCR and is given as fold-change relative to 5 DAF whole seed values, which allows a comparison with the tissue that has not begun mucilage synthesis. Stages tested were 5 DAF (whole seed), 10, 13, 16, and 20 DAF embryo versus seed coat. Embryo expression appears as solid color bars; seed coat expression appears as striped bars. (A) Putative RHM Lus10007355 is expressed at 10 DAF and 13 DAF, and decreases at 16 DAF. (B) Similar RHM isoform Lus10020776 is also expressed at 10 DAF and 13 DAF, and decreases at 16 DAF. (C) UER homolog Lus10006719 is expressed at 10 DAF, 13 DAF, and 16 DAF, with highest expression at 10 and 13 DAF. (D) Nearly identical UER homolog Lus10014147 is expressed in a similar pattern seen with Lus10006719. (E) Flax UXS Lus10006510 is significantly expressed in the seed coat at 16 DAF. All values were normalized to *LuACTIN* as a housekeeping gene. Comparisons of 5 DAF expression with embryo and seed coat samples at all developmental stages were subject to ANOVA analysis followed by a Student-Neuman-Keuls post-hoc test to create homogenous subsets that are noted in the figure as a, b, c, and d. Note that axes vary significantly in range. Biological replicate values are (B) n=4 (A, C, D) n=6 (E) n=8.

Figure 2.9

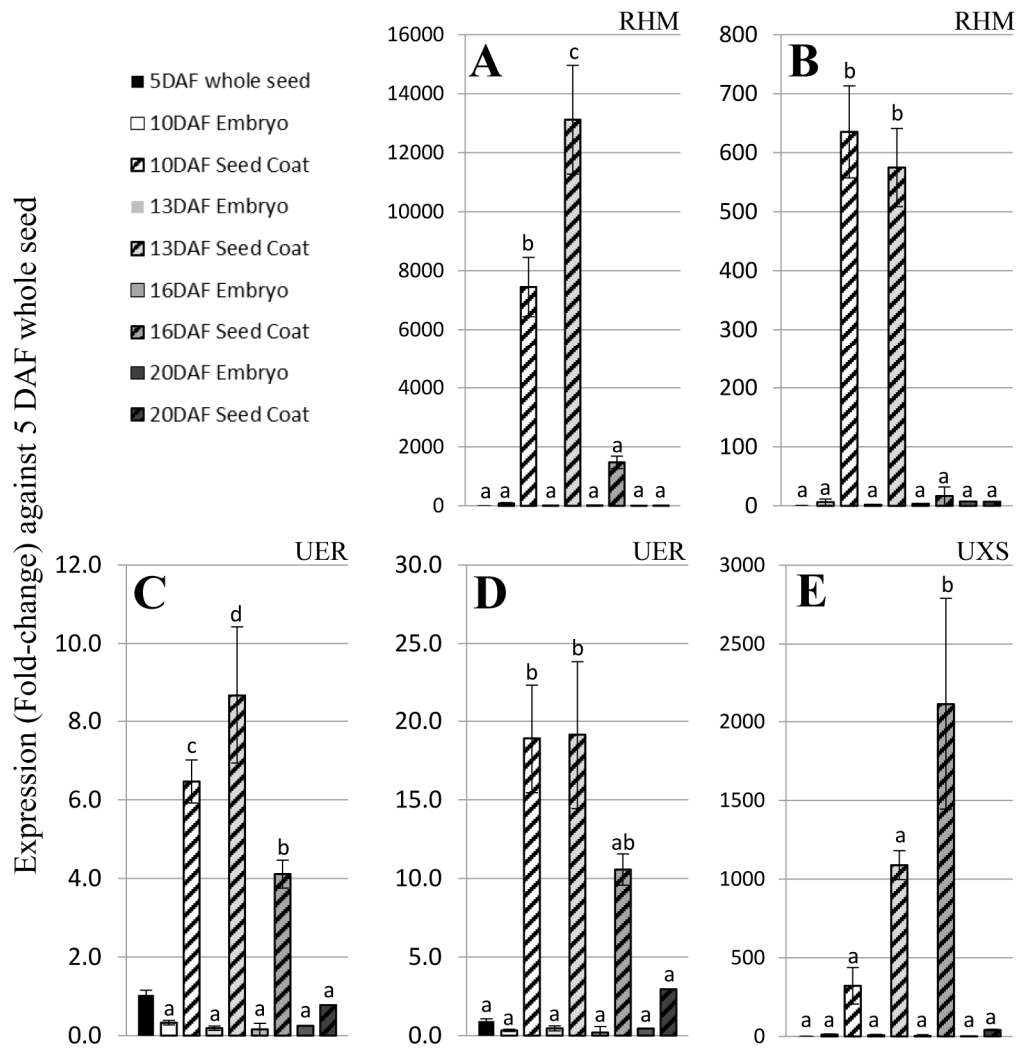


Figure 2.10. The Arabidopsis *GL2* promoter drives exogenous protein expression in the flax seed coat for secretion to the mucilage

(A) The *GL2* promoter followed by an omega enhancer element from the tobacco mosaic virus was cloned upstream of a modified secretable reporter gene, GUSPlus. The MUM2 signal peptide was fused to GUSPlus to target reporter gene secretion to the apoplast. A FLAG epitope tag was also included, followed by the NOS terminator sequence. (B, i-iv) GUSPlus expression in flax seed and mucilage. i) 14 DAF seeds in cross sections of seed bolls exhibit dark GUS staining in both seed coat and embryo. Later, at 18 DPA ii) GUS expression is seen in the seed coat, but much less so in the embryo tissue. In mature seeds with extruded mucilage iii), the mucilage appears to have a blue color, indicating GUS secretion to mucilage. iv) Dissected seeds show no GUS staining in the mature embryo, indicating specificity of secretion. (C) Embedded flax seed coats expressing GUS construct sectioned at 1 μ m. i) 10 DAF MSCs appear to have background GUSPlus staining in the cytoplasm. ii) 15 DAF MSCs stain strongly in MSC, and both mucilage layers also contain GUS, with strongest staining in the outer mucilage layer. Scale bar = 50 μ m. (D) Extracted mucilage stained with GUS buffer and precipitated in ethanol. GUS stains mucilage, indicating protein secretion into the mucilage.

Figure 2.10

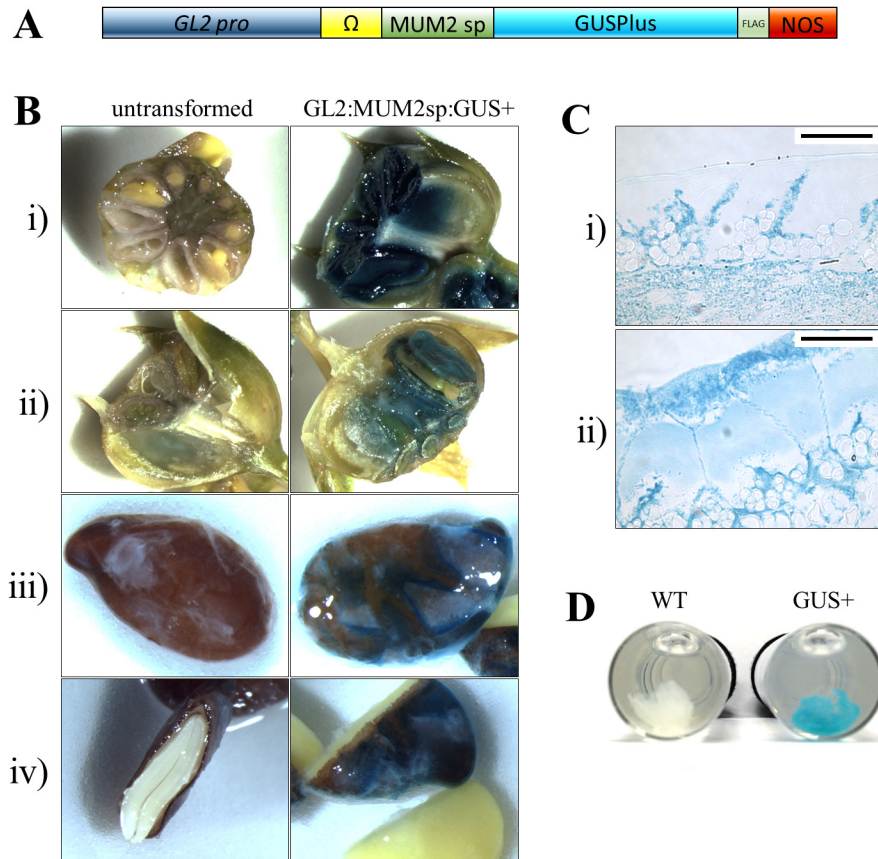
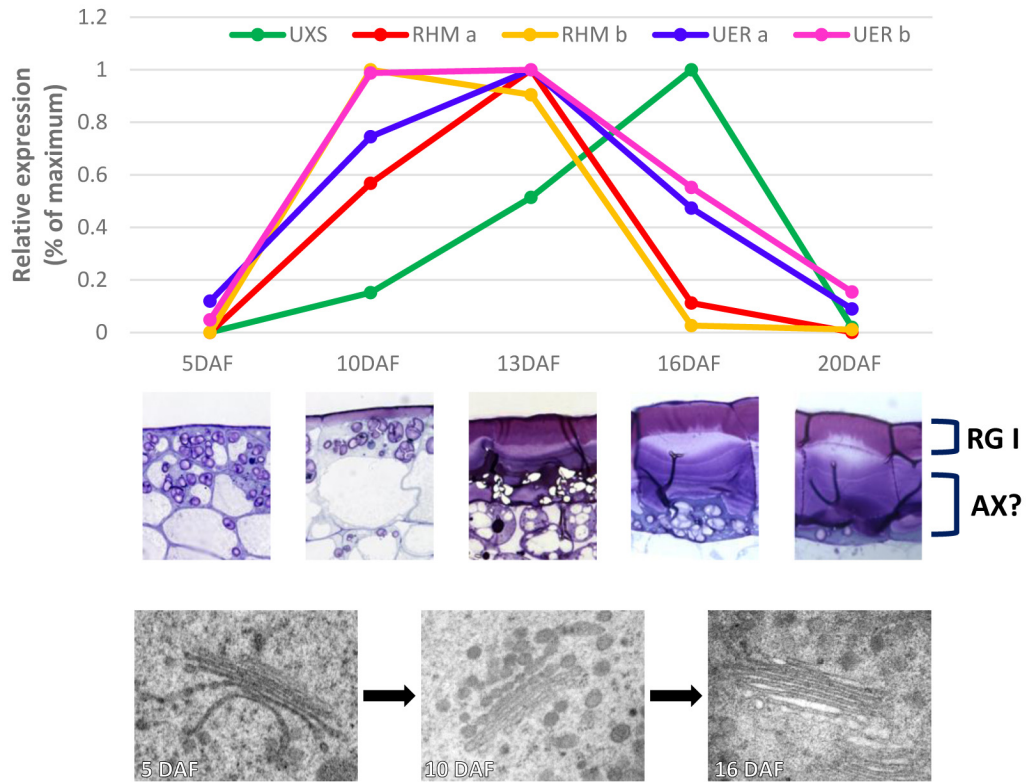


Figure 2.11. Flax RHM and UXS homolog expression is correlated with the deposition of compositionally distinct mucilage regions and changes in Golgi stack morphology

The graph indicates the pattern of peaks of transcript expression for the flax *RHM*, *UER* and *UXS* homologs found to be upregulated during mucilage synthesis. Values are shown as percent of maximum expression, whereby the peak expression of a given gene is set at 1. Peak expression of the RHM homologs (RHM a = Lus10007355; RHM b = Lus10020776; UER a =Lus10006719; UER b = Lus10014147) occurs earlier during mucilage synthesis at 10 and 13 DAF, correlating with the greater proportion of acidic polysaccharides, including RG I, in the outer regions of the deposited mucilage. The peak expression of the UXS homolog (Lus10006510) later in mucilage production (16 DAF) correlates with the production of an inner, neutral region of mucilage, which may be the site of AX deposition. The change in Golgi stack morphology at early and later stages of mucilage secretion may indicate the production of different polysaccharide cargo over time.

Figure 2.11

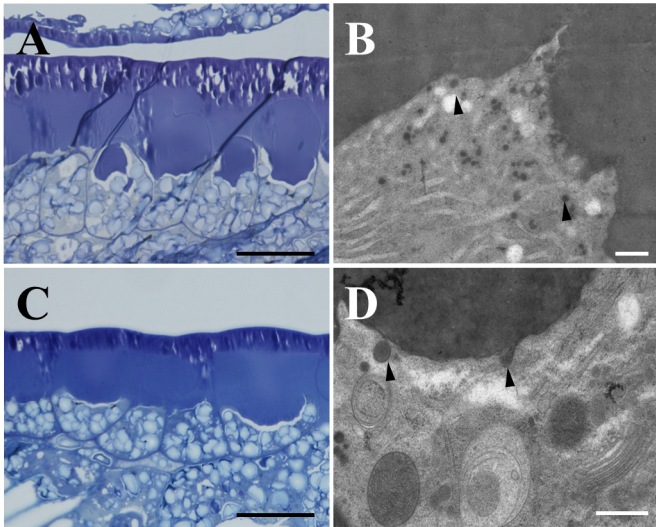


SUPPLEMENTAL MATERIAL

Supplemental Figure 2.1. TEM on 13 and 16 DAF seed coats shows vesicles fusing with the plasma membrane

(A-B) 13 DAF (A) Toluidine blue stained section shows starch granules and cytoplasm are restricted to basal region of the cell. (B) Some secretory vesicles are still present and can be seen along the plasma membrane, where mucilage will be secreted (arrows). (C-D) 16 DAF (C) Mucilage synthesis continues while cytoplasm is further compressed to the basal face of the MSCs and starch granules continue to shrink, (D) while some vesicles are still seen bringing mucilage to apoplast (arrows). (A, C) Scale bar = 2 μ m. (B, D) Scale bar = 500nm.

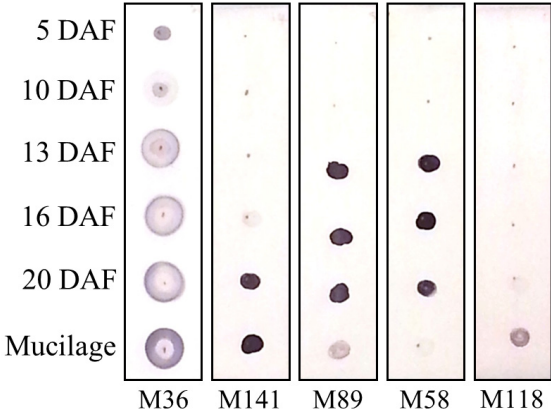
Supplemental Figure 2.1



Supplemental Figure 2.2. Selected dot blots of flax mucilage and water soluble cell wall extracts from developing seed coats

Antibodies were tested on water soluble fractions of cell wall extracts from flax seed coats at stages prior to (5 DAF), during (10, 13, 16 DAF), and after (20 DAF) mucilage production. Water-extracted mucilage from mature seeds was also included. Antibodies tested include anti-unbranched RG I CCRC-M36, anti-flax mucilage CCRC-M141, anti-non-fucosylated xyloglucan CCRC-M89, anti-non-fucosylated xyloglucan CCRC-M58, and anti-monocot AX CCRC-M118. Note the greater mobility of RGI on the membrane, causing antibody staining in a larger diameter compared to other polysaccharides.

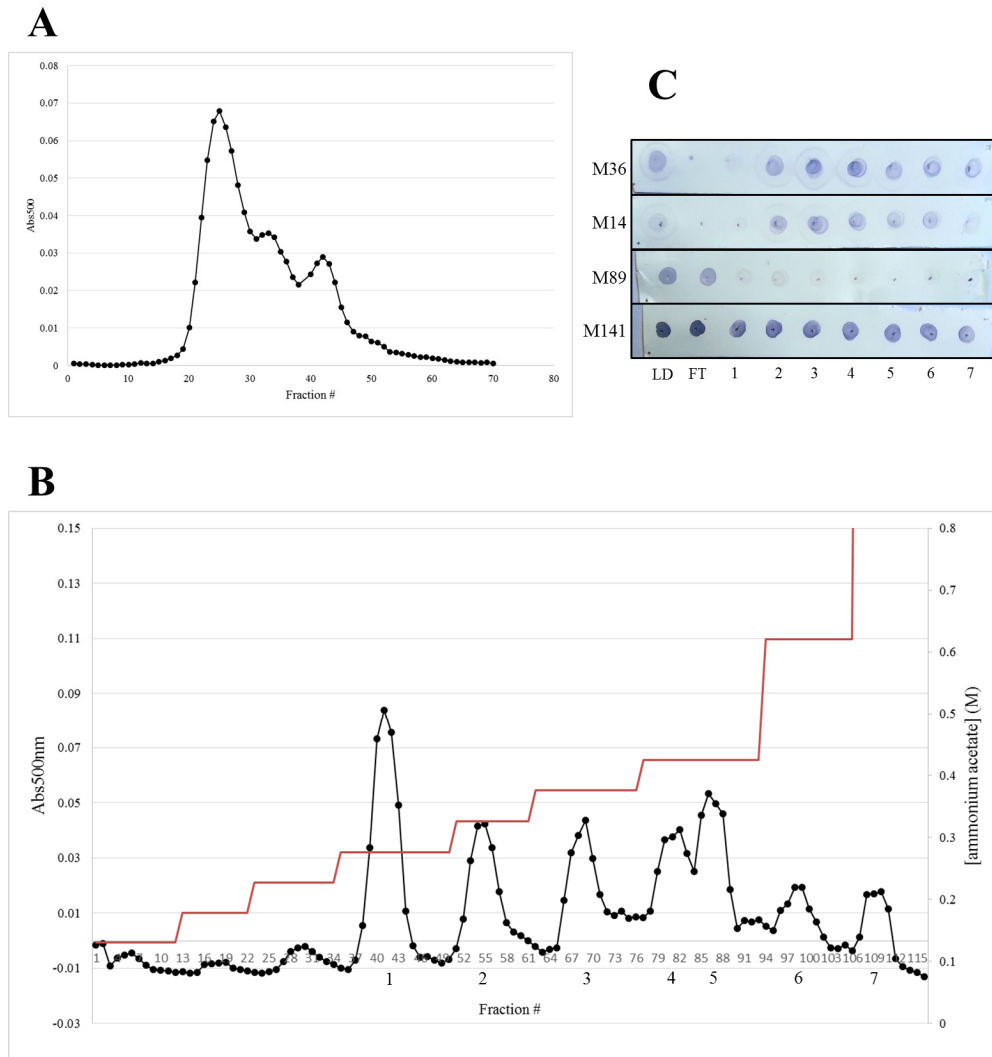
Supplemental Figure 2.2



Supplemental Figure 2.3. Separation of flax mucilage on an anion exchange column into fractions containing polymers of increasing acidity

When run through a Hi-Prep Anion exchange column on an ammonium acetate pH5.2 gradient from 0.03M to 2M and collected over 70 fractions (A), mucilage separates into three peaks with overlapping shoulders. The first peak is expected to contain primarily AX, the second a mixture of unresolved AX and RG I, while the third contains the most acidic mucilage component RG I (Naran et al. 2008). (B) A stepwise gradient is shown in which each elution step yields the release of separate mucilage fractions from the column. Peaks elute from the column in order of increasing acidity, using salt concentrations of 0.28M (Fraction 1), 0.33M (Fraction 2), 0.38M (Fraction 3), 0.42M (Fraction 4 & 5), 0.62M (Fraction 6), and 2M (Fraction 7), respectively. (C) Dot blots on fractions from the seven peaks eluted from the column in (B). LD = Loaded mucilage pre-separation; FT = flow-through containing product(s) that do not bind the resin and void the column prior to elution steps. Antibodies tested include anti-unbranched RG I CCRC-M36 and CCRC-M14, anti-non-fucosylated xyloglucan CCRC-M89, and anti-flax mucilage CCRC-M141. Note the greater mobility of RGI on the membrane, causing antibody staining in a larger diameter compared to other polysaccharides.

Supplemental Figure 2.3



Supplemental Table 2.1. Flax homologs of *UXS*, *RHM*, and *UER* tested for expression levels by qRT-PCR

Listed are all flax genes tested in at least one replicate for high expression in the seed coat. Indicated are the flax gene locus, its closest predicated Arabidopsis homolog (At) according to the % amino acid similarity of their protein sequences, and gene-specific primers used in quantitative RT-PCR analysis.

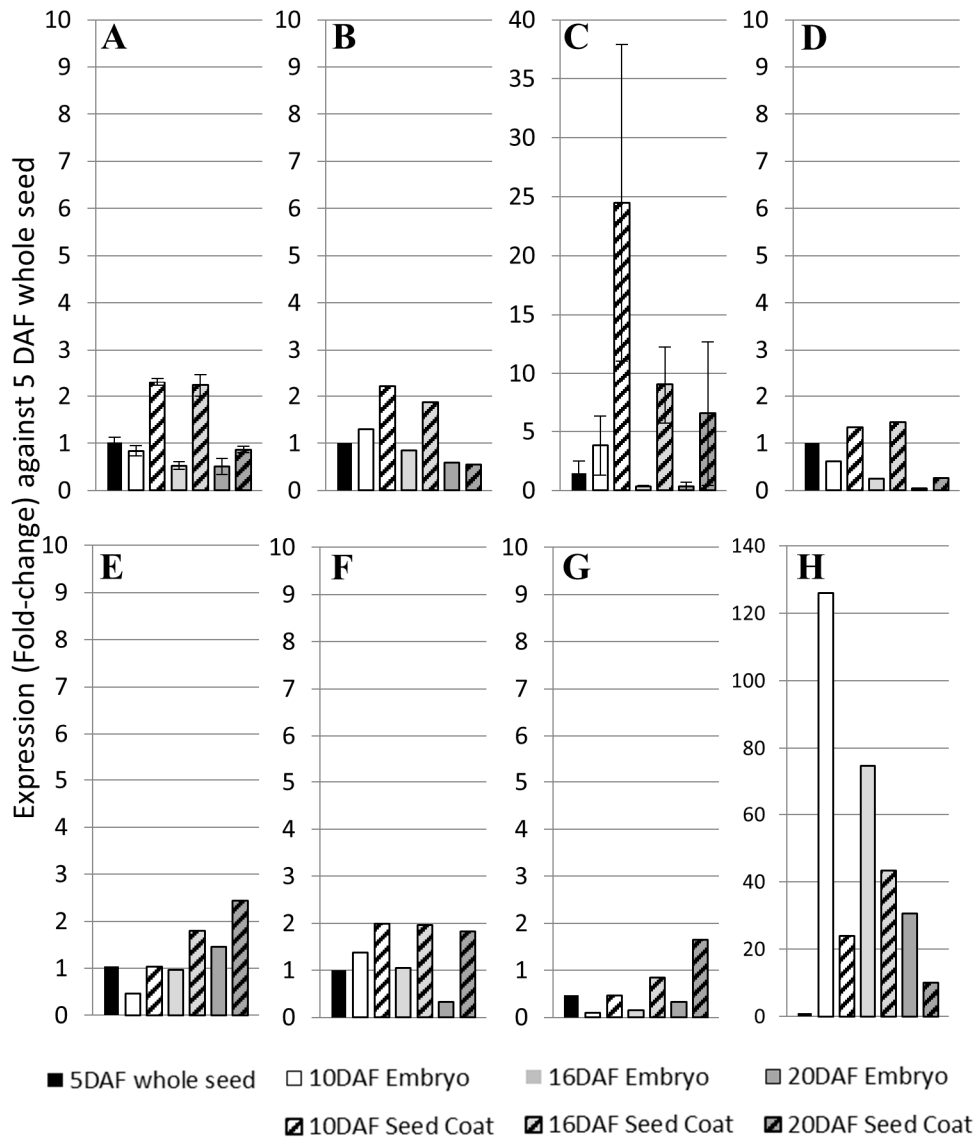
Supplemental Table 2.1

Flax gene ID	Predicted At ortholog	% similarity	qRT-PCR primers
Lus10024436	UXS1	88.6	F-CAGCGGAAACGTTGGCCATG R-TAAATCCCTTTGCCTTCGTCTT
Lus10025293	UXS1	88.4	F-CGGATTCCAAAGGAGGACAGTCTC R-CATGGCCAACGTTTCTGCTGTTCG
Lus10015038	UXS1	91.5	F-GAGCTTATTCGTACGACGTTG R-GCTCAAGAGGGTCTCCGTAG
Lus10006510	UXS2	81.4	F-GCACCATTTTCGGTAATCACAAGTTTGAG R-GGCGCCTCTGTGATAGTCCATCG
Lus10003605	UXS2	79.8	F-GGAGAGGGGACGGTGGAGTC R-CTCCCCGTGAAGAAATTGTCCACC
Lus10030368	UXS2	85.7	F-CCCGGTTCTGCTCACCAG R-GCACATCCTAGGTCCATAAGTGTTG
Lus10037499	UXS2	74.3	F-GAGCTCATCCGGCAGCAGC R-GCCGTAGACCTCGCTGGTGC
Lus10001707	UXS3	95.1	F-CAGACCAATGGAGATCACAAC R-TGTCCTTCGACCCAGTGAAGTA
Lus10005155	UXS3	95.1	F-CAGACGAATGTAGATCACAAC R-TGTCCTTTGACCCAGTGAATA
Lus10040847	UXS3	90.4	F-TGGATTGGCCACCCGAGATTG R-TCTCGGGTTGAGGGTGGATAA
Lus10005450	UXS3	94.4	F-AACCTGGTACACAACTCGCAGC R-TTTCTCTGCTTTGGATCGTCGGGC
Lus10001705	UXS6	95	F-ATGTCCTGTTTAGATGTGACGG R-CCTAGCTCCAACCTCTTTGGCAA
Lus10005900	UXS6	96	F-CCAAGATTCGAGCTCATCCGTC R-GTTCATGCGCGGTCCATATGTGT
Lus10042497	RHM1	93.7	F-CTGCTCACAAGGAAGGTTCTGGC R-GATCTTCGTGATGAAGTTGCGTGGG
Lus10038146	RHM1	93.9	F-GGTTCTGGCATAGGGTTAAGGAGG R-CCGTGAGATCTTTGTGATGAAGTTGCG
Lus10005560	RHM1	92.3	F-CACAAGGAAGGTTCTGGCATAGGG R-GACAACCTTGCTGTAACGAGAGATC
Lus10010942	RHM1	90.3	F-CCCCGTGTACTCTGGAATCGG R-CCACTTTGTTGTACCGCGAAATTTTGG
Lus10013695	RHM1	82.3	F-CGTTTCTTCTCCTTCTG R-CGAATACGGATTTGTAGGAAGAAGC
Lus10007355	RHM1	84.9	F-GAGGCTTCCCAGTTGCTGCC R-CCCATCTCCGTGAATCGGTAAAG
Lus10020776	RHM1	85.4	F-CCTGAGAGGTGTGTGGGACTTC R-GCCACCGCCGAGATCTTGCTC
Lus10006719	UER1	91.3	F-TAATGGTTAATTACGCCACCGGTTG R-GTTACGTGGATTGTTCAAGTCTGATGA
Lus10014147	UER1	93	F-TGATGGTTAATTACGCCACTGGCTG R-GTTACGTGGGTTGCTCAAATCTGATGA

Supplemental Figure 2.4. Transcript expression of a selection of *RHM* and *UXS* genes tested for upregulation in seed coat

Expression was determined via qRT-PCR and is given as fold-change relative to 5 DAF whole seed values, which allows a comparison of tissue that has not begun mucilage synthesis. Stages tested in first-pass screen of candidates were 5 DAF (whole seed), 10, 16, and 20 DAF embryo versus seed coat. Embryo expression appears as solid color bars; seed coat expression appears as striped bars. (A-D) A selection of putative RHM genes tested in first-pass screen. (A) Lus10038146, (B) Lus10042497 and (D) Lus10005560 show little increase in expression in seed coat tissue. (C) Lus10013695 expression is increased in 10 DAF seed coats, however this transcript is unlikely to code for a stable protein product. (E-H) Several putative UXS homologs tested in first-pass qRT-PCR screen. (E) Lus10025293 and (F) Lus10003605 show expression of transcript in seed coats, while (G) Lus10001707 exhibits little to no discernible upregulation. (H) Lus10030368 shows considerable upregulation in the embryo rather than seed coat based on the one replicate tested. All values were normalized to *LuACTIN* as a housekeeping gene. Note that all scales have a maximum value of 10 except (C) and (H). Error bars are only shown for those with replicates ≥ 3 .

Supplemental Figure 2.4



Link between Chapter 2 and 3

Chapter 2 investigated MSC differentiation, cell biology, and potential genes involved in mucilage biosynthesis in the commercially valuable crop plant, flax. This was facilitated through the application of the genetic model system provided by the MSCs of Arabidopsis. The specific isoforms of the putative nucleotide sugar interconversion enzymes required for both UDP-L-Rha and UDP-D-Xyl production appear to have specific upregulation in the seed coat during mucilage production. This resembles the increase in *MUM4/RHM2* transcript expression in Arabidopsis, where it plays an essential role in mucilage production by supplying the RG I substrate UDP-L-Rha. In addition to identifying potential mucilage related genes in crop species, we are also interested in the further investigation of mucilage production in Arabidopsis, as it is estimated that many pectin biosynthetic genes, secretion factors, and regulators have yet to be identified. In **Chapter 3**, we return to the genetic model Arabidopsis to further investigate the role of *MUM4 ENHANCER 4 (MEN4)*, which was identified previously in an enhancer screen of the *mum4* mutant phenotype. This study provides a detailed analysis of the *men4* mutant phenotype, including the cell biology and chemical analysis. The cloning of *MEN4* identifies this gene as a novel putative transcription factor required in the regulation of mucilage production, and we investigate its potential molecular roles as a putative regulator of transcription.

CHAPTER 3

The identification and characterization of *MUCILAGE-MODIFIED 4 ENHANCER 4 (MEN4)*, a putative transcription factor involved in the regulation of mucilage production

ABSTRACT

The seed coat mucilage secretory cells (MSCs) of *Arabidopsis thaliana* provide a model system to study cell wall biosynthesis, secretion, and modification, and how these processes affect cell morphology and cell wall properties. One of the best characterized genes required for mucilage production is *MUCILAGE-MODIFIED4 /RHAMNOSE SYNTHASE 2 (MUM4/RHM2)*, a UDP-L-rhamnose synthase that is developmentally upregulated to provide rhamnose for the synthesis of the mucilage pectin RG I. *mum4* mutants produce a reduced amount of mucilage with proportional decreases in rhamnose and galacturonic acid, which comprise the alternating backbone of RG I. A screen for enhancers of the *mum4* phenotype identified *MUM4 ENHANCER 4 (MEN4)* as an enhancer of the *mum4* reduced mucilage phenotype that also exhibited a less severe single mutant phenotype. *mum4 men4* double mutants display an additive phenotype whereby seeds show significant reductions in mucilage compared to *mum4* or *men4* alone. *men4* single mutant exhibit a 30% mucilage reduction compared to wild type seeds, and altered MSC morphology. A combination of chemical and immunohistochemical analyses confirm a reduction in rhamnogalacturonan I and possibly homogalacturonan, while no changes in Golgi morphology were obvious when observed at the cytological level. Whole genome sequencing followed by Next-Generation Mapping identified *MEN4* as a putative novel transcriptional regulator, and its sequence analysis suggests it is a homolog of the TATA-Binding Protein-Associated Factor 8, a component of the general transcription machinery that recruits RNA Pol II to transcriptional start sites prior to the onset of basal transcription. While the specific regulatory scope of *MEN4* is unclear based on our current transcriptional analyses, the tissue-specific expression of *MEN4*, its nuclear localization, and the associated *men4* mutant phenotypes suggest a potentially diverse array of downstream targets. Furthermore, the additive phenotype of the *mum4 men4* double

mutant indicates that MEN4 regulates mucilage gene targets other than, and possibly in addition to the regulation of, *MUM4*.

3.1 INTRODUCTION

In flowering plants, pollination initiates the process of ovule integument differentiation to form the seed coat, in addition to embryogenesis and formation of the endosperm. *Arabidopsis thaliana* (*Arabidopsis*) seeds exhibit a trait known as myxospermy, whereby the mucilage secretory cells (MSCs) forming the outermost cell layer of the seed coat produce copious amounts of pectinaceous mucilage, which is released from these cells when the seed is exposed to water. Seed coat mucilage composition varies extensively across species (Western 2012; North et al. 2014), and has a number of proposed roles in the seed, where it may promote seed hydration and germination, prevent gas exchange leading to premature germination in unfavourable conditions, and aid in the attachment of seeds to substrates such as soil or animal vectors to prevent or aid dispersal (Esau 1977; Grubert 1981; Fahn 1982b). Mucilage is found across a diverse range of environments in plant families including the Brassicaceae, Linaceae, Solanaceae, and Plantaginaceae, and has been proposed to play a versatile role in seed adaptation depending on the environmental context (reviewed in Grubert 1974; Mott 1974; Western 2012; Yang et al. 2012).

The complex process of MSC differentiation and mucilage production has been studied extensively in *Arabidopsis* (Beeckman et al. 2000; Western 2000; Windsor et al. 2000). Mucilage accumulates in the apoplast via secretory vesicles from the Golgi apparatus, where pectins and hemicelluloses are synthesized (Young et al. 2008). The mucilage is deposited underneath the original primary cell wall by targeted polar secretion to the outer corners of the cell, which simultaneously alters the cytoplasmic shape by restricting the cytoplasm to a tapered column in the centre of the cell. After this period of mucilage production, a cellulosic secondary cell wall is deposited over this column, eventually displacing the cytoplasm. This results in a prominent

volcano-shaped cell wall protrusion called a columella. The radial cell walls are also reinforced with secondary cell wall components, forming a trough on either side of the columella. This tightly regulated process results in a donut-shaped pocket of mucilage under the primary cell wall, sitting around and on top of the columella. When mature *Arabidopsis* seeds are exposed to water, the mucilage is released through both weakening of the radial primary (outer) cell wall and the rapid expansion of the hydrophilic pectins that comprise most of the mucilage (Beeckman et al. 2000; Western 2000; Windsor et al. 2000).

Arabidopsis mucilage is primarily composed of the pectin rhamnogalacturonan I (RG I), which is comprised of an alternating backbone of 1,2-linked L-rhamnose (Rha) and 1,4-linked D-galacturonic acid (GalA). RG I can form long polymers that often contain Rha-linked, neutral sidechains of arabinans, galactans, arabino-galactans, and terminal galactose. A smaller amount of the pectin homogalacturonan (HG) is also present, and consists of a linear, unbranched polymer of α -linked D-GalA that can be methylesterified and acetylated, which influences its cross-linkage potential (Willats, McCartney, et al. 2001; Caffall and Mohnen 2009; Atmodjo et al. 2013). Mucilage extrusion results in the formation of two distinct mucilage layers: an outer, water-soluble layer, which can be largely removed upon agitation, and an adherent inner layer, which remains tightly associated with the seed coat (Western 2000; A. Macquet et al. 2007). These layers can be easily visualized using the stain ruthenium red, which strongly stains pectic polysaccharides and acidic polymers (Sterling 1970). In both layers, the most abundant pectic polysaccharide is RG I, which is largely unbranched in the outer mucilage layer (Penfield et al. 2001; A. Macquet et al. 2007). Cellulose microfibrils characterize the innermost domain, where they are thought to make direct interactions (Dick-Pérez et al. 2011) with pectins like RG I, tightly adhering mucilage to the seed coat in this region (A. Macquet et al. 2007; Sullivan et al. 2011; Haughn and Western 2012).

Small amounts of the hemicelluloses xyloglucan (Young et al. 2008), galactoglucomannan (Voiniciuc, Schmidt, et al. 2015) and arabinoxylan (Voiniciuc et al. 2015; Hu et al. 2016; Ralet et al. 2016) are also present in the inner mucilage, and play a structural role, aiding in mucilage adherence to the seed (Wu et al. 2010; Voiniciuc et al. 2015).

Mutations in genes required for the synthesis, secretion and modification of mucilage, and for other secondary cell wall components involved in columella formation, can result in MSC defects. Mucilage production and extrusion are not essential for seed viability or germination under laboratory conditions, making genetic study of even severe mucilage and MSC differentiation phenotypes possible (Western et al. 2000; Western et al. 2001). This makes *Arabidopsis* MSCs a powerful model system in which to study cell wall polysaccharides and regulation of their production and modification, and how these polymers affect cell wall properties. Presently, over 50 genes involved in mucilage production, mucilage release, and other aspects of MSC differentiation have been identified using this model (Haughn and Western 2012; Western 2012; North et al. 2014; Francoz et al. 2015; Cătălin Voiniciuc, Yang, et al. 2015). Of these, a number have been confirmed to be enzymes involved in mucilage biosynthesis.

Despite the importance of pectin production in the synthesis of copious amounts of mucilage in *Arabidopsis* MSCs, relatively few genes for pectin biosynthetic enzymes have been identified to date. The best characterized is *MUCILAGE-MODIFIED4 (MUM4)*. *MUM4* is one of three *RHAMNOSE SYNTHASE (RHM)* genes, all of which encode tri-functional proteins that catalyze the conversion of UDP-D-glucose into UDP-L-Rha (Oka et al. 2007). All three *RHM* genes are expressed ubiquitously, however *MUM4/RHM2* is upregulated in the seed coat at the time of mucilage production (Western et al. 2004). *mum4* mutants produce approximately 10% of the

mucilage amount seen in wild type, as quantified by Rha and GalA levels, which indicates that the MUM4/RHM2 enzyme is a key limiting factor in mucilage production at the RG I substrate level (Usadel et al. 2004; Western et al. 2004; Arsovski et al. 2009). As RHM enzymes are cytoplasmic and presumably produce a supply of UDP-L-Rha in the cytosol, nucleotide sugar transporters (NSTs) are required to import this substrate to the Golgi apparatus to be incorporated into the RG I backbone. A recently discovered bi-functional UDP-L-Rha / UDP-D-Gal transporter URGT2 is able to transport UDP-L-Rha in reconstituted liposomes, and *urgt2* mutants also produce a decreased amount of RG I, as evidenced by both monosaccharide analysis and immunolabelling with an anti-RG I antibody (Rautengarten et al. 2014). One *urgt2* mutant allele also exhibited decreased UDP-D-Gal in extracted mucilage, suggesting that this NST is able to transport both substrates (Rautengarten et al. 2014). Two putative GTs GALACTURONOSYL-TRANSFERASE-LIKE 5 (GATL5) and GALACTURONOSYL-TRANSFERASE 11 (GAUT11) were also identified, and may be involved in pectin synthesis (Caffall et al. 2009; Kong et al. 2013). *gat15* mutants, although subtle compared to what is seen in *mum4/rhm2* mutants, have reduced mucilage (Kong *et al.*, 2011), and a reduction in both Rha and GalA (Kong *et al.*, 2013). The RG I present in *gat15* mutants is approximately 60% higher in molecular weight than that of wild-type, suggesting that the role of GATL5 in RG I production involves more than GalAT activity, and may regulate RG I molecular size (Kong et al. 2013). One *gaut11* mutant allele produces somewhat reduced mucilage, with a decrease in GalA levels exclusively, suggesting this has an effect on HG rather than RG I synthesis (Caffall *et al.*, 2009).

The majority of the known genes affecting overall mucilage production have been identified as TFs, indicating the existence of complex regulatory networks exerting tight control over this energetically expensive process. There are currently an estimated three regulatory

pathways controlling mucilage production through upstream regulation of pectin biosynthetic genes, and these have been identified by their reduced mucilage phenotypes. *GLABRA 2 (GL2)* and *TRANSPARENT TESTA GLABRA 1 (TTG1)* have been demonstrated via transcriptional analysis to regulate *MUM4/RHM2*, and are required for the specific upregulation of *MUM4/RHM2* in MSCs during mucilage production (Western et al. 2004). In MSCs, the regulation of *GL2* requires the outer integument differentiation factor *APETALA2 (AP2)*, along with a complex of pleiotropic epidermal cell differentiation factor *TTG1* and several bHLH and MYB TFs. *TTG1*, a WD40 repeat protein, complexes with bHLHs *EGL3* and *TT8*, and the R2R3 MYBs *TT2* and *MYB5* (Koornneef 1981; Rerie et al. 1994; Walker et al. 1999; Debeaujon 2000; Zhang et al. 2003; Western et al. 2004; Gonzalez et al. 2009; Li et al. 2009; Ranocha et al. 2014). This *TTG1*-bHLH-MYB complex, along with *AP2*, also regulates *TRANSPARENT TESTA GLABRA 2 (TTG2)*, which encodes a WRKY TF that is required for mucilage production in a pathway independent of *GL2* and *MUM4* (Western et al. 2004). Another R2R3 MYB, *MYB61*, regulates mucilage production through a third distinct pathway (Penfield et al. 2001; Western et al. 2004). Interestingly, *GATL5* appears to be regulated by all three transcriptional pathways, as its expression decreases in *gl2*, *ttg2*, and *myb61* mutants, indicating that some degree of crosstalk likely exists between these regulatory networks (Kong et al. 2013). This model continues to expand with the identification of novel players, and more regulators continue to be incorporated, such as tri-helix factor *DEI BINDING FACTOR 1 (DF1)*, whose network connections have yet to be determined (Vasilevski et al. 2012).

The *mum enhancer 4 (men4)* mutant was isolated in an enhancer/suppressor screen of EMS mutagenized lines created in a *mum4* mutant background (Arsovski et al. 2009). This screen was used to identify novel genes involved in MSC development and mucilage production in a

sensitized mutant background, where more subtle phenotypes masked by compensation might be identified, as mucilage production was already compromised. This uncovered eight *mum* enhancers (*men*), two of which were found to be novel mutant alleles of the previously identified mucilage-related genes *MUM2* and *MYB61*, validating the efficacy of the screen. Of the six novel enhancer genes identified, *MEN4* was of particular interest as it was the only enhancer gene that displayed a single mutant phenotype. *men4* seeds have a mucilage phenotype similar to *mum4*, but less severe. Mucilage quantity was estimated using Rha monosaccharide quantity, and soluble mucilage extracted from *men4* seeds contained approximately 65% less Rha than for wild type extracts (Arsovski et al. 2009).

In this study, we perform a more detailed phenotypic characterization of the *men4* mutant, revealing its putative role in seed size in addition to its effect on mucilage production. We also identify *MEN4* as a nuclear protein bearing closest resemblance to a TATA-Binding Protein (TPB)-Associated Factor (TAF). *MEN4* is expressed in a variety of tissues, with highest expression in seeds and meristematic tissue, however its potential cis-targets in regulation of mucilage production are still to be determined.

3.2 MATERIALS AND METHODS

3.2.1 Plant lines, mutagenesis and growth conditions

Lines of *Arabidopsis thaliana* used were Col-2, Col-0, *mum4-1* (Col-2 ecotype) (Western et al., 2004), T-DNA insertion line Salk_091380C (*men4-2*) (Col-0 ecotype) (ABRC, Ohio State University), *men4-1* and *men4-1 mum4-1* (A. a. Arsovski et al. 2009). Seeds were planted on AT

minimal medium plates (Haughn and Somerville 1986) or directly on soil (Sunshine Mix #5, SunGro Horticulture), stratified for 3-4 days at 4°C and then transferred to growth chambers at 22°C under continuous light (90-120 $\mu\text{E m}^{-2} \text{s}^{-1}$ photosynthetically active radiation). Flower staging for days post anthesis (DPA) was performed as in Western *et al.* (2001).

3.2.2 Microscopy

Developing seeds were prepared for brightfield microscopy, sectioned and stained with toluidine blue O as described in Western *et al.* (2001). Samples were examined using a Leica DM 6000B compound microscope and images captured with a Qimaging Retiga CCD camera operated through Openlab software (Agilent Technologies, Santa Clara, California).

For transmission electron microscopy, developing seeds were fixed using high-pressure freezing and freeze substitution as described in Young *et al.* (2008). Briefly, samples were loaded into gold hats (Leica) filled with 1-hexadecene, and high-pressure frozen with Leica Microsystems EM PACT HPF System. Hats were then immediately transferred to frozen cryovials containing 2% (w/v) osmium tetroxide in acetone with 8% (v/v) dimethoxypropane, and freeze-substituted for 5 days at -20°C in a slush of acetone and dry ice. Samples were then gradually brought to 4°C in metal chucks, and finally brought to room temperature over the course of 3 days, after which they were embedded in Spurr's Resin (EMS) (Spurr 1969). Ultrathin straw-coloured sections (50-60nm) were transferred to copper grids (EMS) and stained with Reynolds lead citrate and 2% (w/v) uranyl acetate as described in Young *et al.* (2008) and imaged using a FEI Tecnai 12 120 kV TEM.

3.2.3 Seed Size Measurements

100 seeds of each line were observed on a Leica MZ-16F stereomicroscope and imaged with a Micropublisher 3.3 camera (Qimaging) operated via Openlab 5 (Perkin Elmer). Seed size was measured using Image J software (Rasband, W.S., ImageJ, U. S. National Institutes of Health, Bethesda, Maryland, USA, <http://rsb.info.nih.gov/ij/>, 1997-2009). A one-way ANOVA followed by a Student-Newman-Keuls post hoc test was used to compare seed sizes to wild type (Software: IBM SPSS Statistics 23.0).

3.2.4 Chemical Analysis

To quantify neutral sugars in crude mucilage extracts, 50 mg of intact seeds were incubated in 0.2% (w/v) ammonium oxalate with vigorous shaking for 2 h at 30 °C. 1 μ mole of myo-inositol was added to the supernatant and samples were precipitated with 5 volumes ethanol, directly hydrolyzed with 2M trifluoroacetic acid and derivatized to alditol acetates. Derivatization to alditol acetates and gas chromatography were performed as in Gibeault and Carpita (1991), but with an HP-23 glass capillary column (30 m x 0.25 mm i.d.; Agilent Technologies). Seeds used for chemical analyses were collected from mutant and control plants cultivated together.

To identify acid sugars as well as neutral monosaccharides, carbodiimide reduction using sodium borodeuteride was performed prior to hydrolysis and alditol acetate derivatization. 200 mg of seeds were extracted sequentially with 0.2% ammonium oxalate for 1 h each with vigorous shaking at 37°C. The supernatant for the extractions were filtered through a glass fibre filter, dialyzed, freeze-dried, and carboxyl reduced as performed by Kim and Carpita (1992), and modified in Carpita and McCann (1996). Samples were then re-dialyzed and subjected to TFA hydrolysis and derivatized to alditol acetates as in Gibeault and Carpita (1991).

3.2.5 Immunofluorescence

For immunofluorescence on developing seeds, seeds were dissected from 7 and 10 dpa siliques and fixed for 2 hr in 4% (v/v) formaldehyde (freshly prepared from paraformaldehyde) in 50 mM PIPES (pH 7.0). Samples were rinsed, dehydrated through an ethanol series and embedded in LR White resin. Embedded samples were sectioned to 0.5 μm , affixed to slides with poly-L-lysine, and subjected to antibody detection as described in Young et al. (2008), except primary antibodies were used full strength and secondary antibodies were diluted as described below for whole seed samples.

Whole seed immunofluorescence was performed as in Young et al. (2008). Primary antibodies (1:20 [v/v]) were detected with a 1:100 (v/v) dilution of Alexfluor 488 conjugated goat anti-mouse (CCRC-M36), goat anti-rat (LM18, JIM5) secondary antibodies (Molecular Probes, Invitrogen). Seeds were counterstained with 0.2 $\mu\text{g}/\text{ml}$ propidium iodide in 50 mM phosphate buffer pH 7.4 to visualize the outer cell wall. Treatments without primary antibody were included to test for non-specific staining, and all seeds were mounted in 1:100 (v/v) India ink in 90% (v/v) glycerol in water to confirm the presence of released mucilage. Immunofluorescence samples were observed with a Zeiss Meta 510 LSM confocal microscope.

3.2.6 *MEN4* mapping and bioinformatics

To identify the point mutation in the *men4-1* mutant, DNA was extracted from the leaves of 48 *men4-1* F2 homozygous mutants as described in (Dellaporta et al. 1983), and pooled. Next-Generation Sequencing was performed using the Illumina HiSeq platform at the McGill University

and Genome Quebec Innovation Centre (Montreal, Quebec). Next-Generation Mapping was also performed at Genome Quebec through SNP library analysis as described by Austin et al. (2011).

Arabidopsis sequences were obtained from Arabidopsis thaliana TAIR10 (<https://phytozome.jgi.doe.gov/pz/portal.html>). Amino acid alignments and predicted percent identities / percent similarities were performed using the MUSCLE alignment feature of the Geneious® V9.0.5 software (<http://www.geneious.com>, Kearse et al., 2012). The databases used to predict conserved protein motifs were the Conserved Domains Database (CDD) (<http://www.ncbi.nlm.nih.gov/cdd/>) as described by Marchler-Bauer et al. (2015), and the Pfam Database (EMBL-EBI, <http://pfam.xfam.org/>) (Finn et al. 2016). The web-based cNLS-Mapper (http://nls-mapper.iab.keio.ac.jp/cgi-bin/NLS_Mapper_form.cgi) was used to predict nuclear localization sequences (Kosugi, Hasebe, Matsumura, et al. 2009).

3.2.7 *MEN4* cloning and fusion constructs

For molecular complementation of the *men4* mutant, a 3810 bp genomic fragment was amplified from wild-type (Col-2) DNA (Forward primer with *Bam*HI site: 5'-CGCGGGAT CCTCAAAGTGTATCATATAG-3' Reverse primer with *Sma*I site: 5'-ATATCCCGGGGGA TGAGGACG ATG-3'), which included 1485 bp upstream of the transcriptional start site, the 1825 genomic sequence of *MEN4* (*At5g15570*), and 500 bp downstream of the *MEN4* locus, and cloned in the pGREEN0029 binary vector (Hellens et al. 2000). *men4* plants were transformed with the *MEN4* construct or the empty vector as in (Clough and Bent 1998). Transformants were selected by germinating seeds on plates containing 50µg/ml kanamycin, and putative transformants were verified by PCR.

The *MEN4* promoter region used in the GUS reporter construct was cloned from wild-type (Col-2) genomic DNA (Forward Primer: 5'-CTGTATCATATAGTTTGAATCTTTTTG-3' Reverse primer: 5'-ATTCAAACCTTTATTACAACTTTACACACC-3') and included 1485 bp upstream of the *MEN4* transcriptional start site and the 5'UTR, including the 243 bp intron present within the 5'UTR, which was cloned into the Gateway cloning vector pMDC162 (Curtis and Grossniklaus 2003) and transformed into both wild-type and *men4* plants. The MEN4::GFP construct included the 1485 bp upstream region and the genomic *MEN4* sequence spanning to, but not including, the *MEN4* stop codon (Forward primer: 5'-CTGTATCATATAGTTTGAATCTTTTTG-3' Reverse primer: 5'-TTTTACATCTGCGTCAATACTTTCGCTC). This fragment was cloned into the Gateway cloning vector pMDC45, which contained the C-terminal *GFP6his* sequence (Curtis and Grossniklaus 2003). The 35Spromoter::HA::MEN4 construct included the wild-type CDS sequence of *MEN4* (Forward primer: 5'-ATGATCAATGGAGGTGGAGAGGG-3' Reverse primer: 5'-CTATTTTACATCTGCGTCAATACTTTCGC-3') with its stop codon, and was cloned into the pEarleyGate 201 vector (Earley et al. 2006). Constructs were transformed into *Agrobacterium tumefaciens* and transfected via floral dip (Clough and Bent 1998) into both wild-type plants and *men4* mutants to ensure proper function of the MEN4 translational fusions.

3.2.8 GUS expression assay

Developing tissue from seedlings, rosette leaves, inflorescences, and seeds were harvested at different stages of development. All tissues were incubated in GUS staining buffer (containing 5-bromo-4-chloro-3-indolyl glucuronide) for 16 hours, rinsed and cleared with 70% ethanol and briefly fixed as described in (Weigel and Glazebrook 2002). Samples were cleared in 70% ethanol

and observed on a Leica MZ-16F stereomicroscope and imaged with a Micropublisher 3.3 camera (Qimaging) operated via Openlab 5 (Perkin Elmer).

3.2.9 GFP imaging

Developing seeds (approximately 7 DPA) from wild-type plants and from plants expressing the MEN4::GFP constructs were harvested from live siliques and incubated with 1µg/ml DAPI in PBS for 15 minutes, before being mounted in 70% glycerol. Whole seeds were observed using a Leica SP8 point-scanning confocal system on a Leica DMI 6000 B inverted microscope with a PMT fluorescent light detector. DAPI was detected with a 405nm laser, and GFP was detected with a 488nm laser. Images were captured using the Leica Application Suite X Software.

3.2.10 Qualitative and quantitative (real-time) RT-PCR

RNA extraction was performed using a modified RNeasy plant mini protocol where a maximum of 100mg of tissue was ground in liquid nitrogen, resuspended in 600 µl RLT-PVP40 (540 µl RLT + 60 µl 10% (w/v) polyvinylpyrrolidone) plus 10 µl β- mercaptoethanol per ml buffer, and processed according to the manufacturer's instructions (Qiagen). 500 ng of extracted RNA was used to perform the reverse transcriptase reaction using the QuantiTect Reverse Transcription kit (Qiagen), and this was used as a template in the PCR reaction (30 cycles) to determine transcription levels in *men4-1* and *men4-2* mutant seeds. *MEN4* primers used were Fwd 5'-AAGTACCTGGGAGTTTGTCT-3' Rev 5'-ACAACGTAAAGTGCATTCCTTGA CAC-3.' For quantitative RT-PCR analysis, SYBR Green reaction mix was used according to manufacturer's instructions (Thermo Scientific), in a Bio-Rad iCycler (*MUM4*: Fwd 5'-

AAGTTACAGGACAGATCAGG-3' Rev 5'-TAGGCCCATAAACATTGTTCC-3;' *GATL5*:
Fwd 5'-GCATTCTGGTCCTGTGAGTTTGC-3' Rev 5'-CTCTGCTATCTTC
GGTTTAGTCCCC-3;' *GL2* Fwd 5'-GGAAGAGGAGGACGGCGCAG-3' Rev 5'-
CCAGAACTTGACCTGGCGAGGG-3;' *CESA5*: Fwd 5'-CTGGTGGTCGGCTCATCGCTG-3'
Rev 5'-CAAGGTCTACAGACAGGGAAAGCAC-3;' *URGT2*: Fwd 5'-GGGCTATGAA
CGTAACGAGCTCC-3' Rev 5'-GTCGCATTCGACACCATAACCAACG-3'). All values were
normalized against the GAPC housekeeping gene using Fwd 5'-TCAGAC
TCGAGAAAGCTGCTAC-3' and 5'-GATCAAGTCGACCACACGG-3.' Gene expression and
statistical analysis were carried out using the $2^{-\Delta\Delta CT}$ method as described by Livak & Schmittgen
(2001), with 4 DPA wild-type seeds set as the reference stage.

3.3 RESULTS

3.3.1 *men4* mutants produce less mucilage

The *men4* mutant was isolated from an genetic enhancer screen of the reduced mucilage mutant *mum4-1* (Arsovski et al. 2009). When wild-type seeds are directly stained with the pectin dye ruthenium red with shaking, a thick adherent layer of mucilage is observed. Conversely, *men4-1* seeds fail to release mucilage (Figure 3.1 A, B; Arsovski et al. 2009). When treated with a chelator such as EDTA prior to ruthenium red staining, a thin capsule of ragged mucilage is observed surrounding *men4-1* seeds, suggesting that a reduced amount of mucilage is produced by these mutants (Figure 3.1 C, D; Arsovski et al. 2009).

To determine what developmental defects may be occurring during seed coat epidermal cell differentiation, developing *men4-1* seeds were sectioned and stained with the metachromatic dye toluidine blue O (Figure 3.1 E—L). The epidermal cells of wild-type seed coats at 4 days post anthesis (DPA) are characterized by a large vacuole occupying most of the cell (Figure 3.1 E). Cells then switch to a phase of pectin biosynthesis and secretion such that, by 7 DPA, there is a central cytoplasmic column marked by large starch granules and surrounded by apoplastic pockets containing the accumulated mucilage, which stains a pink-purple colour (Figure 3.1 F). Following mucilage production, at 10 DPA, cellulosic secondary cell wall material is being laid down around the cytoplasmic column to form the columella. Mucilage is restricted to a donut-shaped pocket above the columella cell wall, while the remaining cytoplasm is found underneath it (Figure 3.1 G). By 13 DPA, mucilage secretory cell differentiation is largely complete, and the columella secondary cell wall fills the entire cytoplasmic column. Under aqueous fixation conditions at this stage, mucilage can be released through breakage of the primary cell wall, leaving the bare columellae with remnants of broken cell wall attached (Figure 3.1 H). The differentiation of *men4-1* seed coat epidermal cells resembles that of wild-type seeds until 13 DPA (compare Figure 3.1 E-H with Figure 3.1 I—L). At this stage, though both mucilage pockets and columellae are present, the mucilage pockets are smaller and shallower. As for reduced mucilage mutants such as *mum4*, decreased mucilage pocket size is accompanied by a broader and flatter cytoplasmic column and resulting columella (Figure 3.1 L) (Western et al. 2004). Further, unlike for wild type seeds, the mucilage is retained in the cell upon hydration in aqueous fixative (Figure 3.1 L). Together, the lack of mucilage release upon hydration, the reduced mucilage pocket size and flattened columellae are consistent with reduced mucilage production by *men4-1* mutants.

Mucilage was extracted from whole wild-type and *men4-1* seeds using the mild chelator ammonium oxalate and subjected to hydrolysis, derivitization and gas chromatography to determine its quantity and neutral monosaccharide composition (Table 3.1). One-way analysis of variance (ANOVA) followed by post-hoc analysis with the Student-Newman-Keuls test determined a significant (~60%) decrease in the total mucilage extracted from *men4-1* (174.5 ± 20.2 $\mu\text{g}/50$ mg seed) versus wild-type seeds (407.1 ± 11.6 $\mu\text{g}/50$ mg seed). This was largely accounted for by a 65% decrease in Rha (119.1 ± 13.0 μg for *men4-1* versus 339.6 ± 9.7 μg for wild type/50 mg seed), and to a lesser extent by a decrease in Xyl (Table 3.1). Together these confirm that *men4-1* mutant seeds produce significantly less mucilage than wild-type seeds. Mucilage extraction followed by carbodiimide reduction was also performed to allow detection of acidic together with neutral monosaccharides, and similar results were obtained (Table 3.2). Namely, there were large and significant decreases in total mucilage (49% decrease) and Rha (52% decrease), plus a 43% decrease in GalA and a smaller decrease in Xyl (31%). Since RG I, with a repeating backbone of 1,2-Rha-1,4-GalA, is the primary component of Arabidopsis mucilage, these data suggest that *men4-1* mutants are deficient either in RG I or overall mucilage production.

To further pursue a reduction in RG I and mucilage production in *men4-1* mutants, both developing and mature seeds were investigated via immunostaining with the antibody CCRC-M36. CCRC-M36 was raised to Arabidopsis mucilage and has been shown to be specific to the unbranched RG I that makes up much of easily extractable mucilage (McFarlane et al. 2008; Young et al. 2008; Pattathil et al. 2010). Under the conditions used for embedding in LR White resin and immunostaining, wild-type seed coat epidermal cells at 10 DPA burst open. However, a significant quantity of CCRC-M36-staining material is seen radiating from these cells surrounding a columella-shaped area with no stain (Figure 3.2 A). Conversely, *men4-1* cells remain intact, with

moderately staining material in the mucilage pockets surrounding the columellae. Some faint stain is also seen within the cytoplasm (Figure 3.2 B), as also has been observed in developing wild-type seed coat cells (Young et al. 2008). When whole, mature wild-type seeds are stained with CCRC-M36, the seed is surrounded by a thick layer of strongly staining mucilage (Figure 3.2 E). This staining is restricted to occasional ‘puffs’ of material apparently emerging from individual cells when *men4-1* seeds are stained, suggesting both that less mucilage is present and that mucilage release is impaired for *men4-1* mutants during whole seed immunostaining. Together, these CCRC-M36 staining results are consistent with a reduction in unbranched RG I in *men4-1* mutant seed coat epidermal cells.

The production of HG was also investigated in *men4-1* mutants using anti-HG antibodies, including JIM7, LM20 (recognizing highly methyl-esterified HG), and JIM5, LM18 and LM19 (specific to low or partially esterified HG) (Willats et al. 2000; Verhertbruggen et al. 2009). Under our conditions, only JIM5 and LM18 bound, and showed similar patterns of immunostaining (Figure 3.2 I—P). Wild-type seeds stained with both antibodies demonstrated a thin but very strongly staining layer of HG close to the seed (Figure 3.2 I,M). In contrast, *men4-1* seeds had only very faint staining of the released mucilage ‘puffs’ and more strong staining of cell wall outlines (Figure 3.2 J,N). Together these suggest that the quantity of HG could also be reduced in *men4-1* seeds.

3.3.2 Additive phenotype of *men4 mum4* mutants

A role for *MEN4* in mucilage production was first suggested by the enhancement of the rhamnose synthase *mum4-1* reduced mucilage phenotype in *men4-1 mum4-1* double mutants (Arsovski et al. 2009). To further characterize this enhancement, both chemical analysis and immunofluorescence of *mum4-1* and *men4-1 mum4-1* mutants was performed along with those of *men4-1* single mutants (Figure 3.2, Tables 3.1, 2). When neutral monosaccharides of extracted mucilage are quantified, significant stepwise reductions in the quantities of both total sugar and Rha are seen going from wild type to *men4-1* to *mum4-1* (compared to wild type, a 65% reduction in *men4-1* and an 89% reduction in *mum4-1* for Rha) (Table 3.1). *men4-1 mum4-1* double mutants have a 95% reduction in Rha, though it groups with *mum4-1* with the conservative post-hoc test chosen to complement the ANOVA analyses (Table 3.1). In this analysis, *men4-1 mum4-1* double mutants have a similar amount of total extracted sugar to *mum4-1* single mutants. However, since *men4-1 mum4-1* have no obvious mucilage release in the presence of chelator (Arsovski et al. 2009), this is likely due to extraction of primary cell wall materials in addition to any mucilage, as suggested by the significant increase in the quantity of Glc for this genotype alone (Table 3.1). When carbodiimide reduced extracted mucilage is considered to determine acidic as well as neutral monosaccharides, similar results were seen (Table 3.2). Namely, there were strong decreases in Rha, GalA and total mucilage quantities going from wild type to *men4-1* to *mum4-1*, with some further decreases also seen for the double mutant.

Immunostaining with the anti-unbranched RG I antibody CCRC-M36 on developing (10 DPA) seed coat cells of *mum4-1* mutants reveals intact cells with small, RG I containing mucilage pockets over a low, broad columella. As for *men4-1* seeds, some faint staining is seen in the cytoplasm (Figure 3.2 B,C). *men4-1 mum4-1* epidermal cells have an even more compressed and faintly staining mucilage pocket, suggesting a further decrease in RG I and mucilage in the double

mutant (Figure 3.2 D). When whole seed immunostaining is performed on mature *mum4-1* and *men4-1 mum4-1* seeds with CCRC-M36, no stained mucilage appears to be released, though some staining appears to occur at the cell surface (Figure 3.2 G,H). Staining of whole seeds with the anti-partially methylesterified HG antibodies JIM5 and LM18 shows little staining for *mum4-1* seeds beyond some cell walls that appear to be lifted above the seed surface, perhaps due to some swelling of seed coat epidermal cells without their bursting to release mucilage (Figure 3.2 K,O). *men4-1 mum4-1* seeds stained with both JIM5 and LM18 exhibit a small amount of sporadic staining on the seed surface (Figure 3.2 L,P). Together with the chemical analysis, these results are consistent with a further decrease in Rha and RG I, if not total mucilage, when both *MEN4* and *MUM4* are defective.

3.3.3 *men4* mutants have no gross defects in Golgi stack morphology

Since a reduction in mucilage production can result from reduced sugar production or secretion of these substances (Western et al. 2004; Young et al. 2008; Kulich et al. 2010), we investigated whether *men4* mutants had any obvious defects in secretory apparatus morphology. Seeds at 7 DPA, which are actively secreting mucilage, were fixed by high-pressure freezing and freeze substitution, as this method is superior to standard chemical fixation in its preservation of the endomembrane system (Kiss et al. 1990; Staehelin et al. 1990; Moore et al. 1991). Samples were resin-embedded, and observed using transmission electron microscopy (Figure 3.3). 7 DPA Golgi stacks in Col-2 MSCs have the characteristic darkly-staining, swollen cisternae with many secretory vesicles present (Figure 3.3 A). The *men4-1* single mutant (Figure 3.3 B) shows no apparent change in Golgi apparatus morphology, and largely resembles wild-type Golgi stacks at

this stage, indicating that the secretory apparatus is not grossly affected by the *men4* mutation. Golgi stacks in the *mum4-1* mutant, as reported previously (Young et al. 2008) are much thinner, stain lighter in Golgi lumens, exhibit fenestration of the cisternae, and lack the many secretory vesicles normally associated with the Golgi at this stage of active secretion (Figure 3.3 C). The *men4-1 mum4-1* double mutant (Figure 3.3 D) resembles the *mum4-1* single mutant.

3.3.4 *men4* mutants have smaller seeds

Observations during seed staining suggested that *men4-1* seeds may be smaller than those of wild-type plants. To test this, wild-type, *men4-1*, *mum4-1* and *men4-1 mum4-1* seeds were photographed and their cross-sectional surface areas determined as number of pixels using Image J software (Figure 3.4). Comparisons across 100 seeds of each genotype were analyzed using one-way ANOVA followed by a Student-Newman-Keuls post hoc test. The results demonstrate that *men4-1* seeds at 1300.8 ± 15.4 pixels are significantly smaller than both wild-type (21% smaller) and *mum4-1* seeds (16% smaller), and that *mum4-1* seeds (1549.9 ± 19.2 pixels) are also a little smaller (6% reduction) than wild-type seeds (1643.1 ± 20.0 pixels). Interestingly, *men4-1 mum4-1* seeds are the same size as *men4-1* seeds, suggesting that, while *men4-1* and *mum4-1* act additively in terms of mucilage production, *men4-1* is epistatic in terms of seed size.

3.3.5 *MEN4* encodes a novel putative transcription factor with homology to a TATA-Binding Protein-Associated Factor

Next generation mapping was performed by creating a mapping population of *men4-1* x *Ler* plants. DNA pooled from forty-eight homozygous mutant plants from the F2 generation were

used for whole genome sequencing followed by Next-Generation Mapping (Austin et al. 2011). A comparison of single nucleotide polymorphisms identified a point mutation in the gene at locus *At5g15570*, referred to as “Bromodomain transcription factor,” a yet uncharacterized protein-coding gene of unknown function. To confirm that the *At5g15570* locus was responsible for the *men4-1* mutant phenotype, the wild-type genomic copy of this gene was cloned downstream of its endogenous promoter region, which included the 5' UTR, the small 243 bp intron within the 5' UTR, and 1485 bp upstream of the transcriptional start site (Figure 3.5 A). A 500 bp region downstream of the *MEN4* locus was also included in the rescue construct. Molecular complementation of *men4-1* with the wild-type genomic clone of this gene confirmed that the mutation at this locus was responsible for the reduced mucilage phenotype (Figure 3.5 C, vi, vii). Rescue of *men4* mutants was also achieved using an N-terminally HA epitope-tagged genomic construct under the constitutively active 35S promoter (Supplemental figure 3.1 A). Further, a T-DNA insertional mutant in the same locus was identified (*men4-2*), and both mutant alleles result in similar reduced mucilage phenotypes when seeds are stained directly with ruthenium red or pre-treated with the calcium chelator EDTA prior to staining (Figure 3.5 C, i-vi). The EMS point mutation in *men4-1* creates a premature stop codon within the so-called BTP domain (Figure 3.5; Figure 3.6) (see below), while the T-DNA allele *men4-2* has a T-DNA insertion just prior to the BTP domain (Figure 3.5 A), and is a transcriptional knock-out (Figure 3.5 B).

When queried against the Conserved Domains Database (CDD) (www.ncbi.nlm.nih.gov) (Marchler-Bauer et al. 2015), two domains are predicted within the 381 amino acid MEN4 protein (Figure 3.6). At the N-terminal region of MEN4, a so-called BTP domain ‘found in eukaryotic Bromodomain transcription factors and PHD domain-containing proteins; a subdomain of archaeal histone-like TFs’ (accession: smart00576) is predicted to span residues 25-116 with an e-value of

2.13e⁻²⁷. The Pfam database predicts the similar Bromo_TP domain (accession: pfam07524) between residues 27-111 with an e-value of 3.73e⁻¹⁴, and likewise notes that this domain is predicted to bind DNA through a histone-like fold (InterPro accession: IPR006565). While the BTP domain tends to be associated with bromodomain proteins, MEN4 does not contain a bromodomain according to its predicted amino acid sequence. At the C-terminal region of MEN4, there is fairly weak but significant homology at residues 176-221 to the ‘Transcription factor IID complex subunit 8 C-terminus’ (TAF8) domain (accession: pfam10406), with an e-value of 8.76e⁻⁰⁴. This domain is described as being the C-terminal, ‘Delta’ portion of the TATA Binding Protein (TPB) - Associated Factor 8 (TAF8) superfamily (accession: cd08049), where the N-terminal domain of proteins containing this Delta C-terminal domain is generally the histone-fold domain Bromo_TP (accession: pfam07524) seen in MEN4. The small TAF8 Delta C-terminal domain is also referred to as the TAF65-PDS domain (TAPD), which was originally found in the yeast TAF8/TAF65 ortholog, and exhibits partial functional redundancy with the histone-fold domain in its N-terminus (Gangloff et al. 2001). While the precise function of this small C-terminal domain is not known, it appears to be unique to putative TAF8 proteins and can therefore be used to predict TAF8 orthologs in other species including Arabidopsis (Lago et al. 2004). The closest homolog to AtTAF8 in the Arabidopsis genome is MEN4. An alignment of MEN4 and AtTAF8 protein sequences (Figure 3.6) reveals that, while these two proteins have a fairly low 26.9% identity (with 43.8% amino acid similarity) overall, there is much higher sequence identity within the limited BTP and TAPD domains predicted in both proteins, at 38% and 40% identity, respectively.

3.3.6 *MEN4* is expressed in multiple tissues including the developing seed coat

Based on publicly available microarray data (Arabidopsis eFP Browser: bar.utoronto.ca), the *MEN4* transcript is predicted to be expressed at low to mid- levels across all tissues, with highest expression in vegetative, transition, and inflorescence meristem tissue, early buds of the inflorescence, and throughout development of seeds and seed coats (Supplemental Figure 3.2 A) (Schmid et al. 2005; Winter et al. 2007; Dean et al. 2011).

In order to confirm the expression pattern of *MEN4*, the 1961 bp promoter sequence that was used for molecular complementation of *men4* mutants was fused to the *BETA-GLUCURONIDASE (GUS)* reporter gene. To assess whether *MEN4* undergoes any gross self-regulation, the *MEN4promoter::GUS* construct was expressed in both wild-type (Col-2) and *men4-1* mutant plant lines in order to compare their expression patterns for any obvious differences. Figure 3.7 shows a summary of the tissues in which substantial GUS expression was detected. GUS expression in seedlings was seen fairly ubiquitously, with deepest staining taking place in the youngest leaves closest to the vegetative meristem, as predicted from the microarray data (Figure 3.7 A, B, C). Expression was also observed through the length of seedling roots. The cotyledon leaves and oldest true leaves of seedlings exhibited less staining, but low levels of GUS staining were sometimes observed primarily in the vasculature tissue in these older leaves (Figure 3.7 A, B, C). In the rosette leaves (Figure 3.7 D, E, F), some GUS expression was observed to varying degrees in the vasculature of the younger leaves, with very little expression in the more mature rosette leaves, which stained faintly in the vasculature, if at all. High expression in young buds and meristem of the inflorescence was also confirmed (Figure 3.7 G, H, I), with darkest staining in the inner unopened flower buds, and lighter staining in mature opened inflorescences, with little to no staining in the attached pedicels, although this was variable with this assay. Seeds were also assayed for GUS expression under the *MEN4* promoter at 4, 7, and 9 DPA (Figure 3.7

J—R), as these represent stages before, during, and after mucilage synthesis, respectively. All three stages of seed development appear to have expression in, but not exclusive to the seed coat, as embryo staining is visible at all three stages, where the stained embryo can be seen through the still transparent testa. To confirm these observations that GUS expression occurred in both seed coat and embryo tissue, embryos between 7 and 9 DPA were dissected from the seed coat before GUS buffer incubation as well (data not shown), and staining was apparent in both seed coat and embryo tissues. No major differences in GUS expression were observed between wild-type (Col-2) tissues and *men4-1* mutant tissues, indicating that the MEN4 protein does not likely regulate its own promoter. Overall, these results support the expression pattern predicted for *MEN4* via microarray, and corroborate with the phenotypes described previously. Expression in the seed coat supports the observed role of *MEN4* in mucilage production.

3.3.7 MEN4 localizes to the nucleus in Arabidopsis MSCs

The MEN4 protein is a putative homolog of the general transcription factor TAF8. TAF8 proteins, including AtTAF8, often contain a small nuclear localization sequence (NLS) at the C-terminus. MEN4 does not contain any obvious predicted importin α -dependent nuclear localization sequence at its N- or C-terminal regions when its sequence is analyzed using the cNLS-Mapper program (http://nls-mapper.iab.keio.ac.jp/cgi-bin/NLS_Mapper_form.cgi) (Kosugi, Hasebe, Tomita, et al. 2009; Kosugi, Hasebe, Matsumura, et al. 2009).

In order to determine the subcellular localization of the MEN4 protein, a *MEN4promoter::MEN4::GFP6his* fusion construct was stably expressed in Arabidopsis. This

GFP fusion construct was able to rescue the phenotype of both *men4* mutant alleles, suggesting that it is a functional protein (Figure 3.5 C, ix). Expression of the construct at the transcript level was confirmed in a number of transgenic lines, a selection of which is shown in Supplemental Figure 3.3 B, where a line of highest expression was selected for fluorescence microscopy and live seeds were collected at 7 DPA. The fluorescent DNA stain DAPI was used to stain live MSC nuclei, seen as large round structures on the outer edges of the cells (Figure 3.8 A, B). Some background GFP fluorescence is seen in the starch granules in WT cells, but no signal is detected in the nucleus (Figure 3.8 C). When both DAPI and GFP channels are merged, there is no co-localization observed in the non-transgenic line (Figure 3.8 E). In the transgenic MSCs containing the MEN4::GFP fusion, however, GFP signal was detected in large round structures, as well as the adjacent areas around the starch granules (Figure 3.8 D), likely indicating MEN4 is localized to some degree in the cytoplasm as well as the nucleus. Figure 3.8 F indicates that there is strong co-localization of the MEN4 translational fusion and DAPI, indicating that the large round structures where MEN4 localizes are nuclei. Unlabelled areas within nuclei are likely nucleoli, and do not appear to contain GFP signal. These results confirm the localization of the MEN4 protein to the nucleus, further supporting its putative role as a transcriptional regulator.

3.3.8 MEN4 may regulate mucilage production via transcriptional regulation of currently unknown targets

Since *MEN4* encodes a putative transcription factor that is essential for the production of the wild-type amount of mucilage, we predicted that its target(s) could include one or more of the currently known genes involved in mucilage synthesis, or the regulation thereof. To investigate

potential targets of MEN4, quantitative RT-PCR was performed using gene-specific primers on the UDP-L-Rha synthase gene *MUM4/RHM2*, the UDP-L-Rha transporter *URGT2*, the putative galacturonosyltransferase *GATL5*, the cellulose synthase gene *CESA5*, as well as the mucilage regulator *GL2* (Rerie et al. 1994; Usadel et al. 2004; Western et al. 2004; Oka et al. 2007; Sullivan et al. 2011; Kong et al. 2013; Rautengarten et al. 2014). The expression levels of these genes were tested in whole seeds at 4, 7, and 9 DPA in both *men4-1* and *men4-2* mutants, as well as their corresponding wild-types, Col-2 and Col-0. Based on preliminary first-pass results (data not shown), the transcript levels of *GL2*, *MUM4*, and *GATL5* were selected as candidates for more detailed analysis.

The expression of *MUM4*, *GATL5*, and *GL2* in both wild-type backgrounds (Col-2 and Col-0) (Figure 3.9 A, B, C; white bars) exhibit expression patterns that are consistent with previous transcriptional analyses reported for these genes. As these genes are required in mucilage production, their expression is upregulated at 7 DPA relative to 4 DPA, when mucilage production is underway (Western et al. 2004; Kong et al. 2013). *MUM4* expression (Figure 3.9 A) in the *men4-1* mutant background is slightly lower than in Col-2 at 7 DPA, but this result is not significant. In the *men4-2* mutant seeds, *MUM4* expression is slightly higher, but this value is also not significant, thus it appears that *MUM4* is not regulated to an observable extent in whole seeds by *MEN4* at the time of mucilage production. *GATL5* expression (Figure 3.9 B) was also tested with multiple biological replicates, and its expression decreases insignificantly at 7 DPA in the *men4-1* mutant, while it increases to a slightly higher level in the *men4-2* mutant, but this is also not statistically significant. *GL2*, which regulates mucilage production through the upregulation of *MUM4* (Western et al. 2004), was also tested, and its increase in the seed is relatively small at 7 DPA in both wild-types where it is up approximately 2-fold compared to wild-type expression at 4 DPA

(Figure 3.9 C). In the *men4-1* mutant, *GL2* appears to be decreased approximately 2-fold at 7 DPA, and this is statistically significant ($t = 0.0052$). However, this is not the case in the second mutant allele *men4-2*, where *GL2* expression remains similar to that seen in wild-type.

This analysis suggests possible changes in the regulation of these three genes in whole seeds at 9 DPA, although their role at 9 DPA may or may not be mucilage-related. *MUM4* expression increases at 9 DPA in both *men4-1* and *men4-2*, with statistically significant upregulation in *men4-1* mutants ($p = 0.012$). *GATL5* expression in *men4-1* is significantly down at 9 DPA ($p = 0.0035$), but this is not confirmed in the *men4-2* mutant background. *GL2* is significantly increased in the *men4-1* mutant ($p = 0.049$). This increasing trend is also seen in the *men4-2* background, but this is not statistically significant, as the variation in *GL2* expression was quite large in this group. Overall, these results suggest that subtle changes in *GL2* expression may be occurring in the *men4* mutant backgrounds, however, a clear determination of *MEN4* targets remains inconclusive. A caveat of this analysis is that expression was tested on RNA extracted from whole seeds, rather than isolated seed coats. As both *GL2* and *MUM4* are expressed in the embryo in addition to the seed coat (Usadel et al. 2004; Esfandiari et al. 2012), background expression of these genes in the embryo may be interfering with our ability to detect subtle expression changes in the seed coats of *men4* mutants.

3.4 DISCUSSION

3.4.1 *MEN4* affects mucilage production

Seeds of *men4* mutants exhibit a reduction in the amount of mucilage produced by the MSCs. This phenotype is confirmed by ruthenium red staining of its smaller capsule of released mucilage, toluidine blue staining on cross sections showing a reduced mucilage pocket, and through chemical analysis, which revealed a proportional reduction of Rha. These results indicate a decrease specifically in pectin, that is supported through immunofluorescence staining with anti-RG I antibodies. While the overall reduction in GalA reduction seen with chemical analysis is consistent with a decrease in RG I, it cannot definitively establish a general effect on both RG I and HG. However, immunostaining with anti-HG antibodies suggests that both may be affected in the *men4* mutant. Simultaneous reductions observed in RG I, and smaller effects on xylose and HG levels are seen in other RG I reduced mutants, and may be a result of crosstalk between the regulatory pathways (Orfila et al. 2005; Bernal et al. 2007; Brown et al. 2007; Persson et al. 2007; Atmodjo et al. 2013; Kong et al. 2013; Ebert et al. 2015).

In general, the *men4* mutant phenotype is similar to those seen in other pectin synthesis mutants with a clear reduction in RG I. For example, the *men4* mutant resembles a less severe allele of both *mum4* and *urgt2* mutants, which are reduced in RG I synthesis through UDP-L-Rha availability (Usadel et al. 2004; Western et al. 2004; Oka et al. 2007; Rautengarten et al. 2014). Another mucilage production-related gene *GATL5*, which is thought to affect RG I production and size, have mutants that exhibit reduced RG I as well as a reduction in staining with anti-HG antibodies (Kong et al. 2013), but to a lesser extent than the *men4* mutant. Qualitatively, *men4* mutants also resemble mutants that are affected in exocyst secretory complex components SEC8 and EXO708A (Kulich et al. 2010). While the *men4-1* mutant was examined at the ultrastructural level and revealed no gross changes in the secretory apparatus or obvious mis-targeting of mucilage, we cannot rule out a potential role of *MEN4* in regulating secretion. The shape of the

Golgi stacks has been shown to be affected by severe reductions in pectin production, as seen in the *mum4* mutant, where Golgi lumens are thin, flat, and fenestrated, with a reduced amount of vesicle production in the trans-Golgi network (Young et al. 2008). This suggests that the reduction in mucilage produced in the *men4* mutant is not substantial enough to have an effect on the shape of the Golgi stacks (Usadel et al. 2004; Western et al. 2004; Kulich et al. 2010; Rautengarten et al. 2014). Also, in this class of reduced mucilage mutants are a number of transcriptional regulators including TTG1, TTG2, GL2, and MYB61, some of which have been shown to affect the expression of downstream RG I biosynthetic targets (Koornneef 1981; Rerie et al. 1994; Western et al. 2004; Francoz et al. 2015). Based on the putative identity of MEN4 as a general transcription factor, it likely functions similarly to these regulators through the regulation of one or more pectin biosynthesis or secretion genes. Interestingly, when compared to the *mum4* mutant, the enhanced phenotype of the *mum4 men4* double mutant suggests that *men4* mutants are affected through additional mechanisms independent of and potentially in addition to *MUM4*.

3.4.2 MEN4 is a putative transcription factor and may be a paralog of a TATA-binding Protein Associated Factor (TAF)

Based on its sequence homology with TAF8 in Arabidopsis, yeast, and a number of animal genomes, MEN4 is predicted to be a somewhat divergent paralog of AtTAF8, with which it shares a similar size and domain structure. More specifically, MEN4 is predicted to contain the C-terminal TAPD domain, which is unique to TAF8 proteins, and may exhibit functional redundancy with the N-terminal BTP domain (Gangloff et al. 2001; Lago et al. 2004). Relatively low percent identities in the full length TAF8 protein sequences, with higher sequence conservation observed

within the limited regions of the N-terminal BTP domain and the C-terminal TAPD domain tends to be the case when comparing TAF8 across species (Lago et al. 2004; Lawit et al. 2007). This is also seen with the comparison of MEN4 and the previously annotated AtTAF8 (At4g34340), which revealed low overall sequence conservation, but much higher conservation of the BTP and TAPD domains at 38% and 40% identity, respectively. While the BTP domain is characterized as a member of the TAF9 domain superfamily, this histone fold domain is a feature of many TAFs. AtTAF9 could not be successfully aligned with TAF8 or MEN4 (data not shown), further suggesting that MEN4 is a homolog of TAF8. While most of the 12-14 distinct TAF proteins present in eukaryotic genomes have at least one paralog, as seen in Arabidopsis, and a number of other models investigated (Lago et al. 2004; reviewed in Thomas and Chiang 2006), TAF8 has not been reported to have paralogs in any of the genomes that have been mined thus far, making the discovery of MEN4 as a putative TAF8 paralog somewhat unexpected. AtTAF8 has been previously verified as a true member of the TAF family due to its interaction with other TAFs including TAF12b/EER4 (Robles et al. 2007), as well as TAF4, TAF4b, TAF5, TAF8, TAF10, TAF13, and TAF14 (Lawit et al. 2007).

Lending support to the role of MEN4 as a potential TAF8-like transcription factor is its localization to the nucleus in seed coat epidermal cells. Interestingly, MEN4 achieves nuclear localization despite lacking an obvious nuclear localization sequence (NLS) predicted within its amino acid sequence. This is in contrast to AtTAF8 as well as TAF8 homologs in other species, which are all found to contain a NLS (Lago et al. 2004; Soutoglou et al. 2005; Thomas and Chiang 2006; Demény et al. 2007; Tamada et al. 2007). In humans, the nuclear import of TAF10, which lacks a NLS, may be dependent on heterodimerization with TAF8 and/or other NLS-containing TAFs to recruit it to its proper subcellular location (Soutoglou et al. 2005). As MEN4 is not

predicted to contain a NLS in its N- or C-terminus, it may therefore require other NLS-containing proteins to recruit it to the nucleus. This is supported by the detection of cytoplasmic MEN4::GFP signal in addition to that seen accumulated in the nucleus. Interestingly, when this MEN4::GFP construct was expressed transiently in tobacco leaves, little to no signal was detected in most cells, with very low levels of diffuse GFP signal seen throughout the cytoplasm, but not detected in the nucleus (data not shown). These results may also suggest that MEN4 requires other co-factors in order to be recruited to its proper sub-cellular location. These potential NLS-containing co-factors may not be present in tobacco leaves, as it is a heterologous tissue and system, and the members of the potential complex may not be present or conserved.

In a study where Arabidopsis TAF proteins were predicted bioinformatically by sequence-based homology, eight of the 14 predicted TAFs were found to have related paralogs (Lago et al. 2004). The precise number of TAFs and their specific associations with TFIID are still undetermined, and it is therefore reasonable to suspect that there may be other yet unidentified TAF proteins in Arabidopsis. There are several possibilities regarding the molecular role of MEN4, given its putative identity as a tissue-specific paralog of AtTAF8. TAFs are best known for their role within the general transcription machinery. TAF8 proteins across species have been found to interact with other TAFs in the TFIID complex, which assembles with the TATA-Binding Protein (TBP) and other general transcription factor complexes (e.g. TFIIA, B, E, F, and H). This amalgamation of transcription factors aids in the recognition of the core promoter and recruits RNA-polymerase II to its proper location within the pre-initiation complex just prior to the onset of basal transcription (reviewed in Thomas and Chiang 2006; Hiller et al. 2001; Pointud et al. 2003; Falender et al. 2005).

TAFs and TAF-like paralogs can also affect transcription activation through the formation of TAF-containing complexes that are unrelated to the TBP or the recruitment of RNA polymerase II (Wieczorek et al. 1998; reviewed in Thomas and Chiang 2006; Demény et al. 2007). TAFs and TAF-like homologs are constituents of the TBP-free TAF-containing complex (TFTC) (Wieczorek et al. 1998), the TFTC-related PCAF/GCN5 complex (Ogryzko et al. 1998), the Spt-Ada-GNC5 acetyltransferase (SAGA) and SAGA-like complexes (Grant et al. 1998), the Spt3-TAF9-GCN5L acetyltransferase (STAGA) complex (Martinez et al. 1998; Martinez et al. 2001), the Small TAF-containing (SMAT) complex, (Demény et al. 2007) and the Polycomb Repressive complex (PRC) (Saurin et al. 2001). The TFTC, TFTC-related, SAGA, and STAGA complexes all lack TBPs, contain histone acetyltransferases, and activate transcription via histone acetyltransferase (HAT) activity, which promotes an open chromatin conformation (Grant et al. 1998; Martinez et al. 2001; Thomas and Chiang 2006; Demény et al. 2007). These are thought to enhance TBP and/or TFIID binding to the promoter and increase transcription factor accessibility via GNC5-mediated acetylation of histones in the promoter region (Thomas and Chiang 2006). SMATs do not have inherent acetyltransferase activity, but have a role in organizing or nucleating both TFTC and SAGA/STAGA assembly (Demény et al. 2007; Lindner et al. 2013). Interestingly, human TAF8 plays a critical role in SMATs, where it is predicted to heterodimerize with other histone fold-containing proteins at both its N- and C- termini (Demény et al. 2007). Although fewer studies of these complexes have been performed in plants, there is some evidence on conservation of TAF-containing complexes in Arabidopsis. AtTAF13 interacts with PCR1 components, where it has a role in transcriptional repression of subsets of genes affecting seed development (Lindner et al. 2013). More recently, an Arabidopsis SAGA complex has been implicated in controlling juvenile to adult transition via regulation activity in the meristem (Kim et al. 2015).

According to the gross morphological expression pattern seen with GUS staining, preliminary qRT-PCR analysis of leaves and developing seeds (data not shown), and publicly available microarray data, *MEN4* expression at the transcript level appears fairly ubiquitous, with highest expression in developing seeds, young leaves, and meristematic tissues of both seedlings/rosettes and inflorescences. *MEN4* and *AtTAF8* seem to have specialized subsets of tissues having highest expression (See Supplemental Figure 3.2 for comparison), with some overlap in the seeds. TAF proteins are often expressed ubiquitously at relatively even levels across tissue types (Lago et al. 2004; Lago et al. 2005; Robles et al. 2007). There is evidence however, in both plant and animal systems, of instances of tissue-specific TAFs and TAF-related proteins, which suggests that variations in the subunit composition of TFIID exist and are likely another means to regulate gene expression during specific developmental processes (Freiman et al. 2001; Hiller et al. 2001; Guermah et al. 2003; Lago et al. 2005; Gao et al. 2006; Robles et al. 2007). In some cases, there is a substoichiometric ratio of some components of the TFIID complex where particular TAFs are enriched in the complex in a tissue specific-manner, where they likely confer unique properties to TFIID in a particular cellular context. For example, in mouse, TAF8 is implicated in adipogenesis, and is upregulated in adipocyte precursor cells in the embryo (Guermah et al. 2003). While TAFs have been more extensively studied in animals, evidence of differential *TAF* expression and their role in regulating particular subsets of genes has been confirmed in Arabidopsis. For example, Arabidopsis regulator of pollen tube formation *TAF6* and its paralog are expressed in all tissues. A *taf6* knockout is lethal, while the *TAF6b* paralog is not, (Lago et al. 2005). *TAF10* controls leaf and meristem development, and osmotic regulation (Gao et al. 2006; Tamada et al. 2007), while *EER4*, otherwise known as *AtTAF12*, has an ethylene-dependent phenotype, where it controls a subset of genes specifically involved in the ethylene

response (Robles et al. 2007). *taf1* mutants have decreased acetylation levels of histone H3 in light-responsive promoters, leading to decreased expression of light-induced mRNAs (Bertrand et al. 2005). This further lends evidence to the view that TAFs can act in tissue-specific manners, with particular isoforms affecting a selection of processes rather than being universally required for transcription of all RNA polymerase II dependent genes.

Finally, MEN4 could simply be a divergent relative of TAF8 that performs a different function in gene regulation than TAF proteins or their paralogs. The BTP domain found in MEN4 and a number of TAFs contains a histone-like fold that is predicted to allow the protein to bind DNA, however this histone-like fold is thought to be required for heterodimerization in TAFs via protein-protein interactions (Ogryzko et al. 1998; Soutoglou et al. 2005; Thomas and Chiang 2006; Demény et al. 2007). It remains unclear if TAFs bind only to other TAFs, DNA, or both. It is possible that MEN4 binds DNA and stabilizes the general transcription machinery as a co-factor or activator rather than a substituent of TFIID or other TAF-related complexes. Sequence homology alone cannot determine whether MEN4 acts as a bona fide TAF8 paralog, and therefore protein-protein interaction assays such as co-immunoprecipitation would be interesting to perform with the MEN4 protein in order to determine its interaction partners, which may allow MEN4 to be more clearly categorized into any of the previously discussed complexes.

3.4.3 Overview of the potential roles of MEN4

Both the GUS reporter gene assay and preliminary RT-PCR analysis (data not shown) indicate that *MEN4* is expressed in the developing seed, which provides a context for the observed

reduced mucilage phenotype. Due to the additive phenotype exhibited by the *men4 mum4* double mutant, we know that MEN4 has some effect on gene targets other than *MUM4*. Of the genes we tested, only *GL2* showed significant, albeit slight, downregulation at 7 DPA in *men4-1* seeds. However, this result was not replicable in the second knockout allele *men4-2*, and thus our results currently remain inconclusive. It is possible that MEN4 does exhibit a regulatory effect on one or more of the known pectin biosynthetic genes, but we are unable to detect subtle changes in their expression in MSCs over the ‘noise’ produced by background expression levels in the embryo. GUS expression shows that both *MUM4* and *GL2* are present in the embryo in addition to the seed coat (data not shown). In order to conclusively determine or rule out *GL2* and *MUM4* as potential MEN4 targets, this expression analysis should be repeated on dissected seeds to separate the seed coat from the embryo. Another possibility is that MEN4 regulates mucilage production through one or more currently unknown pectin biosynthetic genes. Relatively few of the pectin biosynthetic enzymes have been determined in the MSC system compared to the estimated number of specific nucleotide sugar synthases, glycosyltransferases, nucleotide sugar transporters, and secretion factors that are likely involved in mucilage production (reviewed in Mohnen 2008; Atmodjo et al. 2013), and therefore it is possible that one or more of these are regulated by MEN4, resulting in its reduced mucilage phenotype.

MEN4 expression in the seed also correlated with a significant reduction in seed size in the *men4* mutant. Seed size has not been correlated with mucilage production, and therefore we may expect MEN4 to have different downstream targets in this process. Seed size aberrations have primarily been found as a result of mutations in genes encoding factors of integument cell elongation and endosperm growth (Garcia et al. 2003; Garcia et al. 2005; Luo et al. 2005; Schruff et al. 2005; Riefler et al. 2006; Ohto et al. 2009; Wang et al. 2010). Interestingly, the endosperm

growth controlled by the *HAIKU* (*IKU*) genetic pathway and the integument cell elongation factor TTG2 have been found to show more drastic effects on seed size in double mutants (Garcia et al. 2003; Garcia et al. 2005). TTG2 also regulates mucilage production, possibly through subtle regulation of *GATL5* (Kong et al. 2013), and therefore would be of interest to investigate for potential genetic interactions with *MEN4*.

MEN4 expression in the meristematic tissue, particularly in the vegetative meristem in the centre of the growing seedling, may also provide context for the preliminary results in two independent tests suggesting decreased apical dominance seen in *men4* mutant plants, whereby the number of lateral branches is slightly increased and plants appear to be “bushier” than their wild-type counterparts (J. Palozzi, B. Forward, & T. Western, unpublished data). These results are currently being confirmed with a larger sample size. *MEN4* targets of transcriptional regulation in meristem tissue may include genes involved in hormone signalling and auxin response that may work to suppress lateral branching in wild-type plants (Cline 1994; Leyser 2005; Tanaka et al. 2006; Yin et al. 2007).

Our phenotypic and expression results, along with its potential role as a component of the general transcriptional machinery, suggest that *MEN4* likely has a diverse array of targets, which likely differs depending on the tissue type. As the identity of *MEN4* targets remains inconclusive, it may be clearer to pursue the role of *MEN4* using a more global approach to expression analysis. It would also be interesting to determine whether *MEN4* has different targets in the seed coat versus the meristem, for example, using ChIP-Seq, which would identify cis-regulatory elements bound to *MEN4* in different tissues. RNA-Seq would also allow us to determine changes in expression levels of potential *MEN4* targets by comparing both *men4* mutants, as well as

overexpression lines. This approach may also reveal novel players in mucilage production, as MEN4 may regulate currently unknown biosynthetic enzymes, secretion factors, modifying enzymes, or regulators.

FIGURES

Figure 3.1. Ruthenium red staining and seed coat structure of *men4-1* versus wild-type Col-2 seeds

A and B, Wild-type (A) and *men4-1* (B) seeds stained with 0.01% ruthenium red with shaking. Note absence of thick mucilage capsule for *men4-1* seeds. C and D, Wild-type (C) and *men4-1* (D) seeds pretreated with 0.5M EDTA followed by staining with ruthenium red. *men4-1* seeds have smaller mucilage capsules. E to L, Cross sections of developing seed coat epidermal cells stained with toluidine blue. E to H, wild type. (E) 4 DPA with central vacuole filling most of the cell. (F) 7 DPA, purple-staining mucilage is accumulating. (G) 10 DPA, dark-purple staining mucilage is found in the outer tangential regions of the cell surrounding the purple-blue staining secondary cell wall forming around the cytoplasm. (H) 13 DPA, secondary cell wall has filled the central region of the cell and the cell has burst under the aqueous fixation conditions to release the mucilage. I to L, *men4-1* mutant sections. Note the similarity of 4 DPA (I) 7 DPA (J) and 10 DPA (K) to wild-type seed epidermal cells at the same stage. (L) 13 DPA, *men4-1* cells have flattened columellae secondary cell walls, smaller mucilage pocket areas and retain faint-staining pink mucilage. Bars = 500 μm in (A to D) and 50 μm in (E to L).

Figure 3.1

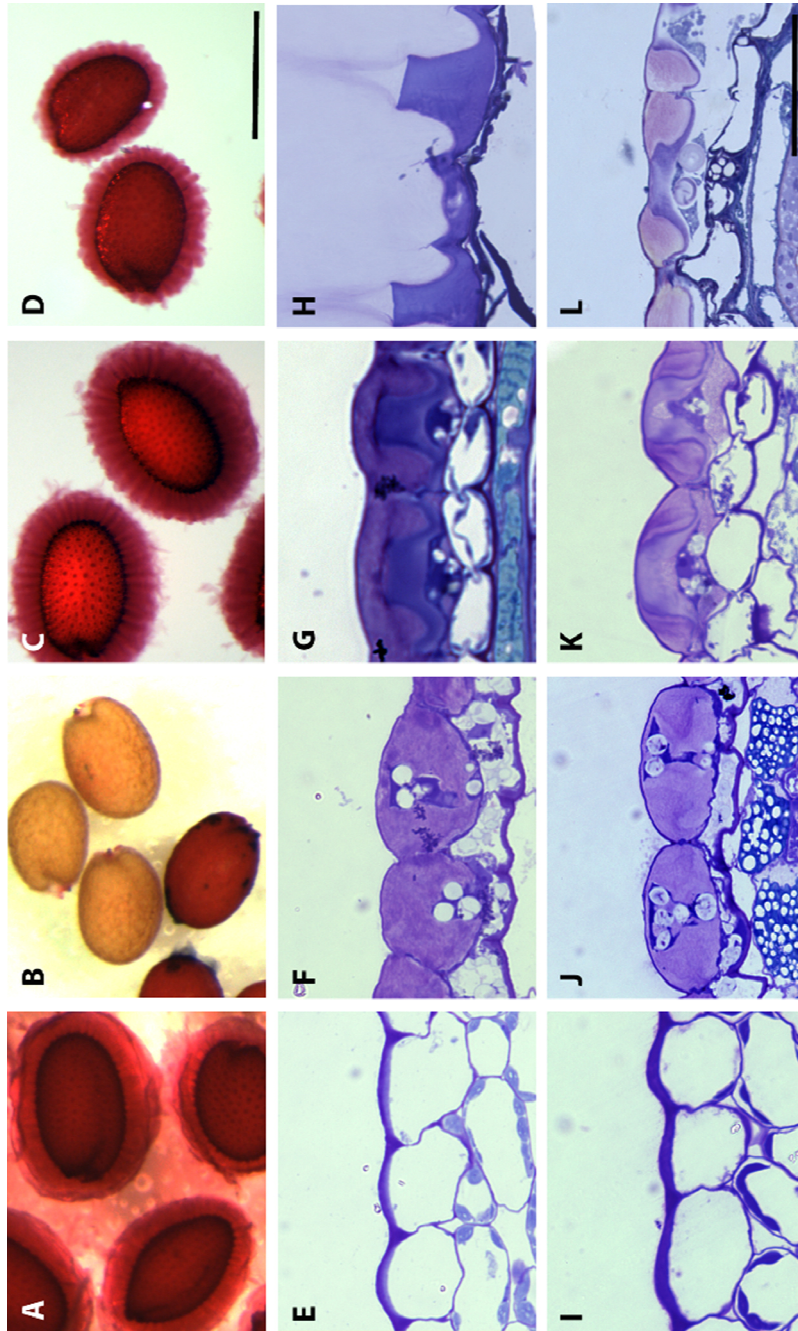


Table 3.1. Neutral monosaccharide quantification of mucilage extracted from *men4-1*, *mum4-1* and *men4-1 mum4-1* versus wild-type seeds

Soluble polysaccharides from intact seeds were isolated by shaking in ammonium oxalate. Samples were ethanol precipitated and directly hydrolyzed with trifluoroacetic acid followed by derivitization to alditol acetates. Results are given as average μg sugar per 50 mg seed and SE calculated from three independent samples. All genotypes were grown, harvested and stored together.

Table 3.1

Genotype	Monosaccharide (μg)							
	Rha	Fuc	Ara	Xyl	Man	Gal	Glc	Total
WT	339.6 ± 9.7^a	n.d. ^a	6.3 ± 0.2^a	25.5 ± 0.9^a	6.6 ± 0.6^a	13.1 ± 1.0^a	16.0 ± 1.0^a	407.1 ± 11.6^a
<i>men4-1</i>	119.1 ± 13.0^b	0.5 ± 0.5^a	5.5 ± 0.7^a	11.7 ± 1.3^b	5.6 ± 0.7^a	8.6 ± 1.1^a	23.5 ± 3.2^a	174.5 ± 20.2^b
<i>mum4-1</i>	38.9 ± 3.5^c	n.d. ^a	5.4 ± 0.5^a	8.7 ± 0.5^b	5.8 ± 0.3^a	8.1 ± 0.5^a	22.2 ± 1.4^a	89.2 ± 6.3^c
<i>men4-1 mum4-1</i>	15.9 ± 3.4^c	3.79 ± 3.79^a	7.9 ± 3.4^a	10.6 ± 4.3^b	13.1 ± 3.8^a	12.1 ± 2.8^a	35.8 ± 2.0^b	99.2 ± 23.3^c

Differences among genotypes were tested using one-way ANOVA (analysis of variance) with a cut-off of $P = 0.05$ (critical F-value of 4.07). Grouping of genotypes into homogeneous subsets for each individual sugar was performed with a post-hoc analysis using the Student-Newman-Keuls test, whereby ^{a-c} represent groupings.
n.d. = not detected

Table 3.2. Monosaccharide quantification of mucilage extracted from *men4-1*, *mum4-1* and *men4-1 mum4-1* versus wild-type seeds using carbodiimide reduction to identify uronic acids

Soluble polysaccharides from intact seeds were isolated by shaking in ammonium oxalate. Following dialysis, samples were subjected to carbodiimide reduction with sodium borodeuteride to identify acid sugars, hydrolyzed with trifluoroacetic acid and derivitized to alditol acetates. Results are given as average μg sugar per 200 mg seed and SE calculated from three independent samples, except for *men4-1 mum4-1*, which was done in duplicate. All genotypes were grown, harvested and stored together.

Table 3.2

Genotype	Monosaccharide								Total
	Rha	Fuc	Ara	Xyl	Man	Gal	GalA	Glc	
WT	542.0 ± 50.4 ^a	n.d.	5.5 ± 1.5 ^a	23.9 ± 2.2 ^a	22.3 ± 1.7 ^a	17.9 ± 2.9 ^a	349.5 ± 21.1 ^a	12.1 ± 1.7 ^a	623.8 ± 59.6 ^a
<i>men4-1</i>	261.9 ± 17.8 ^b	n.d.	4.7 ± 0.5 ^a	16.6 ± 1.0 ^b	18.2 ± 1.5 ^{ab}	10.7 ± 0.4 ^b	198.0 ± 11.3 ^b	8.5 ± 0.9 ^{ab}	320.7 ± 21.6 ^b
<i>mum4-1</i>	47.2 ± 3.3 ^c	n.d.	2.5 ± 1.3 ^a	3.9 ± 0.4 ^c	14.2 ± 1.1 ^b	5.7 ± 0.7 ^b	67.4 ± 6.3 ^c	6.2 ± 0.7 ^b	79.7 ± 5.3 ^c
<i>men4-1 mum4-1</i>	30.0 ± 4.3	n.d.	3.8 ± 0.5	7.9 ± 0.6	16.0 ± 0.8	5.0 ± 0.6	63.4 ± 10.0	5.5 ± 0.3	68.3 ± 5.4

Differences among genotypes were tested using one-way ANOVA (analysis of variance) with a cut-off of $P = 0.05$ (critical F-value of 5.14). Grouping of genotypes into homogeneous subsets for each individual sugar was performed with a post-hoc analysis using the Student-Newman-Keuls test, whereby ^{a-c} indicate groupings (*men4-1 mum4-1* not included in statistical analyses).
n.d. = not detected

Figure 3.2. Immunofluorescence of developing Col-2 (WT), *men4-1*, *mum4-1* and *men4-1 mum4-1* seed coats, and of mature whole seeds

A to D, confocal sections of 10 DPA Col-2 (A) *men4-1* (B), *mum4-1* (C) and *men4-1 mum4-1* (D) seed coats stained with the anti-branched rhamnogalacturonan I antibody CCRC-M36. Note that, under staining conditions, Col-2 epidermal cells burst open to release antibody staining material, while seed coat cells of the three mutants do not. Further, increasingly flatter unstained columellae and unstained cytoplasm plus smaller stained mucilage pockets are seen comparing *men4-1* (B), *mum4-1* (C) and *men4-1 mum4-1* cells. E to P, Confocal images of whole seed immunofluorescence shown as Z-stack projections. Note that seed coat cells were counterstained with propidium iodide (red channel) prior to immunostaining. E to H, CCRC-M36. E, Col-2, the seed is surrounded by a thick capsule of stained mucilage. F, *men4-1*, note small amount of mucilage released during staining treatments that stains in discrete puffs around the seed. G, H, *mum4-1* and *men4-1 mum4-1*, respectively, some staining of the seed coat with nothing radiating from the seed. I to L, Anti-homogalacturonan antibody JIM5. I, Col-2, the seed is surrounded by a moderate capsule of stained mucilage. F, *men4-1*, note faint staining of puffs of mucilage and outlines of certain cells. G, *mum4-1*, some staining of cell wall outlines. H, *men4-1 mum4-1*, minimal staining of seed coat. M to P, Anti-homogalacturonan antibody LM18. Note similar staining pattern to JIM5. M, Col-2. N, *men4-1*. O, *mum4-1*. P, *men4-1 mum4-1*. Bars = 50 μ m in A to D and 250 μ m in E to P.

Figure 3.2

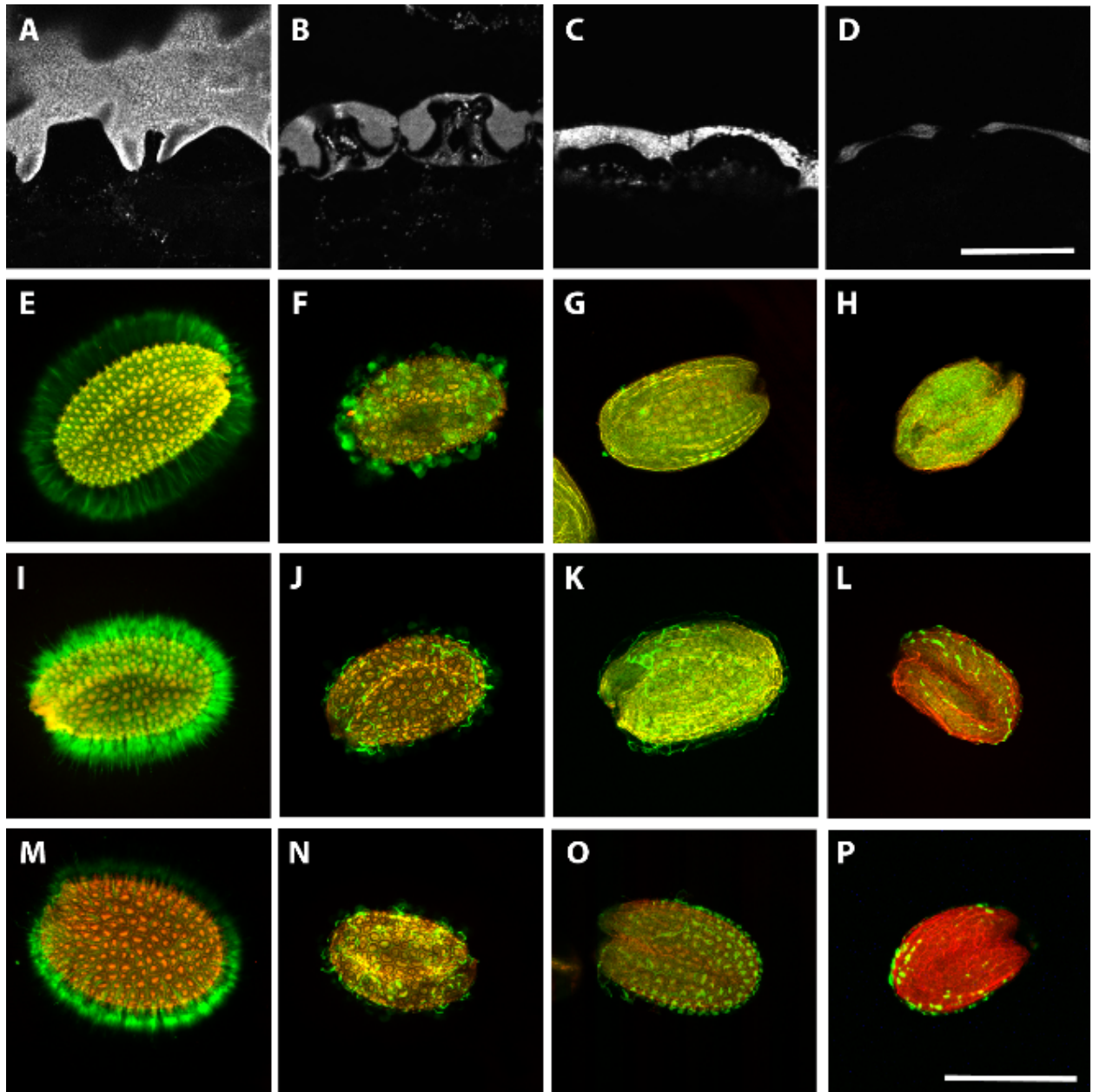


Figure 3.3. Transmission electron micrographs of high-pressure frozen and freeze-substituted developing epidermal cells of Col-2 (WT), *men4-1*, *mum4-1* and *men4-1 mum4-1* seed coats

A to D, typical Golgi stacks of 7 DPA cells. A, Col-2. B, *men4-1*. C, *mum4-1*. D, *men4-1 mum4-1*. Col-2 and *men4-1* (A, B) appear similar, with swollen, darkly stained cisternae and many associated secretory vesicles. Note thinner and more elongated cisternae in *mum4-1* (C) and *men4-1 mum4-1* (D) cells, with light staining in cisternae and few associated vesicles. Bar = 200 nm, all images are at the same magnification.

Figure 3.3

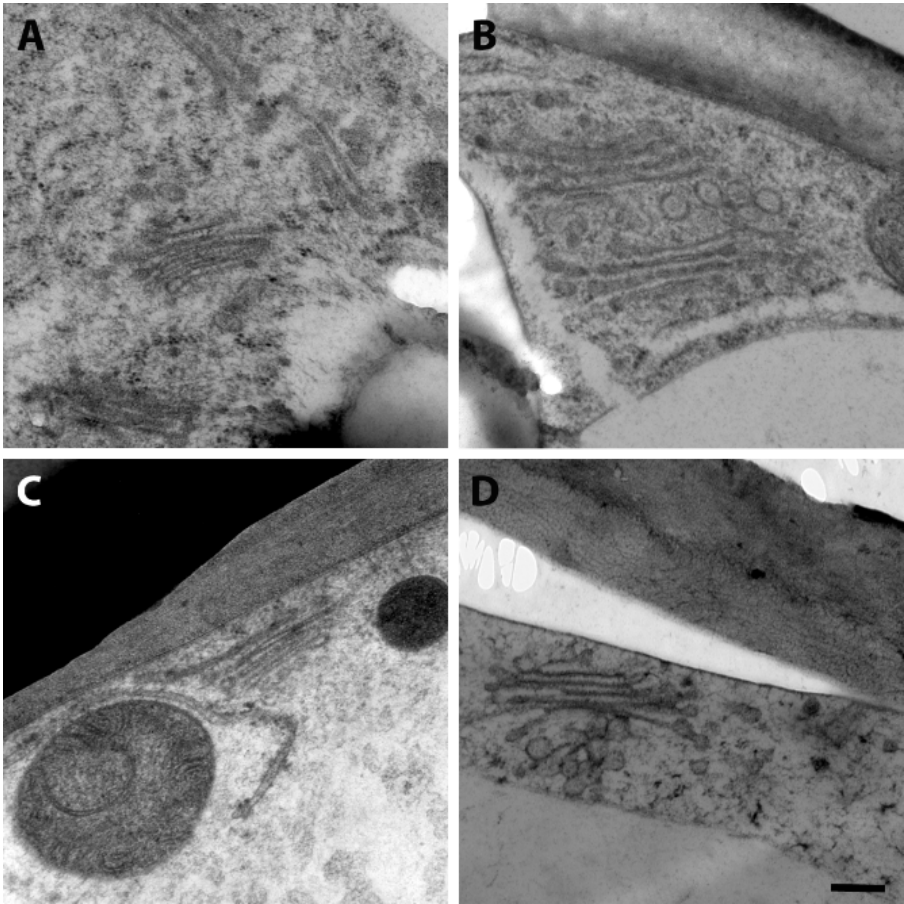


Figure 3.4. Comparison of seed size for Col-2 (WT) *men4-1*, *mum4-1* and *men4-1 mum4-1* seeds

100 seeds from each line were photographed and their areas measured using Image J. Seed size is given in pixels. Error bars represent SE. Differences among genotypes were tested using one-way ANOVA (analysis of variance) with a cut-off of $P = 0.05$ (critical F-value of 2.70). Grouping of genotypes into homogeneous subsets was performed with a post-hoc analysis using the Student-Newman-Keuls test, whereby 'a' to 'c' represent groupings.

Figure 3.4

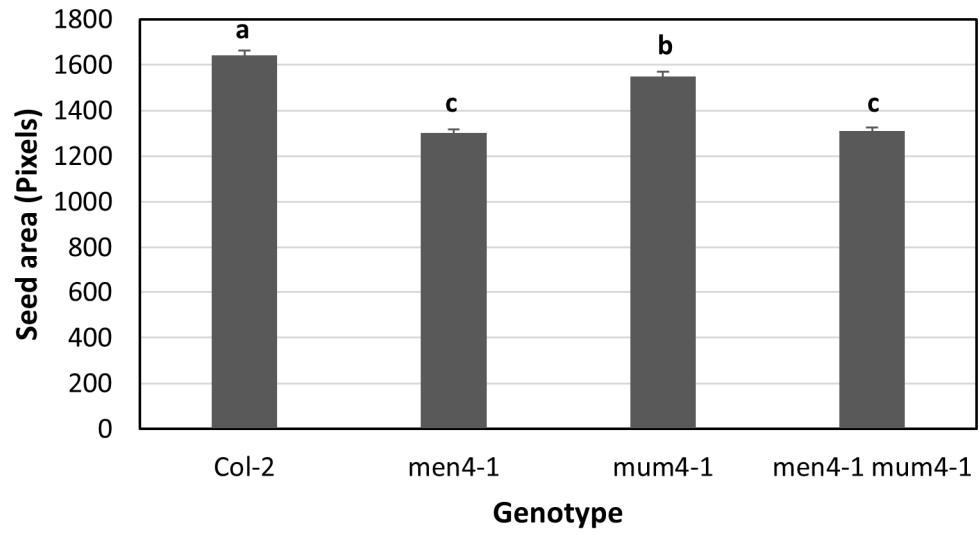


Figure 3.5. *MEN4* encodes a novel putative transcription factor that contains domains similar to those of TATA-Binding Protein Associated Factors (TAFs)

(A) Gene model of *MEN4* (*At5g15570*). UTRs shown in grey; within coding region (green) are the “bromodomain transcription factor” BTP domain (blue), and TAPD domain unique to TAF8 proteins (purple). The point mutation (*) creating a premature stop codon is located within the BTP, while the T-DNA insertion (triangle) occurs prior to the BTP domain. (B) RT-PCR of *MEN4* in seeds of WT versus *men4* mutants. *GLYCERALDEHYDE-3-PHOSPHATE DEHYDROGENASE* (*GAPC*) was used as a housekeeping control gene. The point mutant *men4-1* is unaffected at the transcriptional level, while *men4-2* results in a transcriptional knockout. (C, i-vi) Mucilage capsule staining comparison of Col-2 (WT) and both *men4* mutant alleles. When seeds were shaken in distilled water prior to staining with ruthenium red, *men4-1* (ii) and *men4-2* (iii) mutant seeds release little to no mucilage compared to Col-2 (i). Seeds pre-treated with EDTA prior to ruthenium red release all mucilage, and both *men4-1* (v) and *men4-2* (vi) release a decreased amount of mucilage compared to Col-2 (iv) under these conditions. (vii-ix) Molecular complementation of the *men4* mutant. (vii) Empty vector control. (viii) The wild-type genomic clone of *At5g15570* under its native promoter is able to rescue the *men4-1* mutant phenotype. (ix) Molecular complementation of the *men4-2* mutant with a *MEN4::GFP* translational fusion expressed under the native promoter.

Figure 3.5

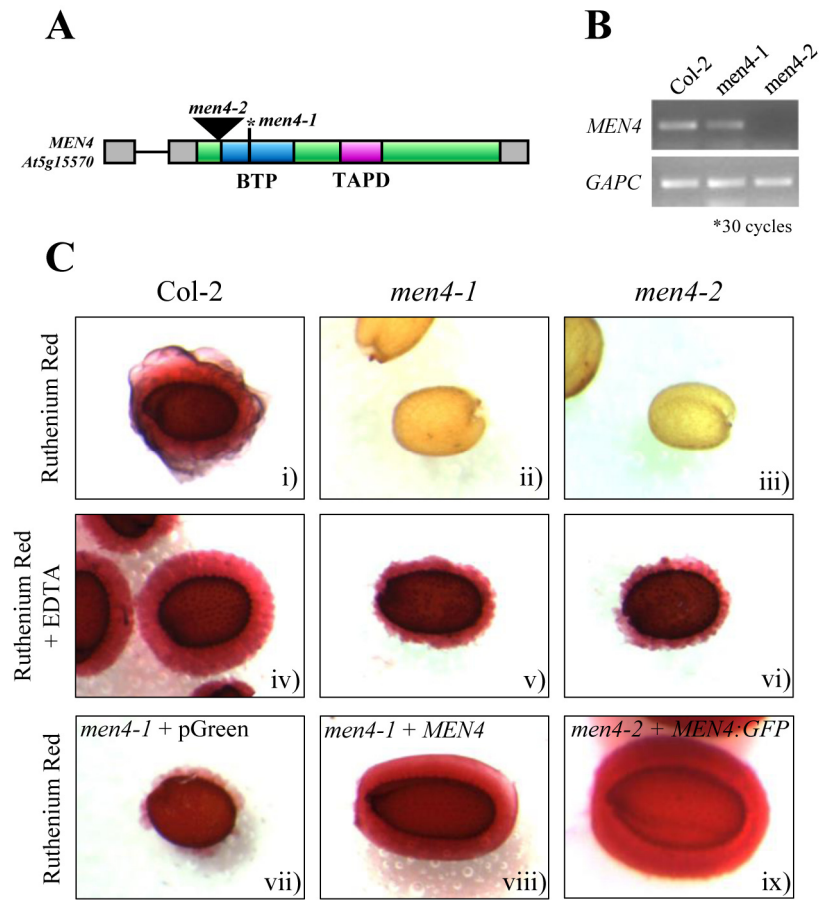


Figure 3.6. Alignment of MEN4 and AtTAF8 amino acid sequences

An alignment of AtTAF8 and its closest homolog MEN4 share 27% identity (43.8% similarity) overall. Higher homology between the two exists within the N-terminal BTP and C-terminal TAPD domains (underlined in red), where they share 38% and 40% identity, respectively. Mutation sites are shown for *men4-1* (*) and *men4-2* (triangle) alleles.

Figure 3.6

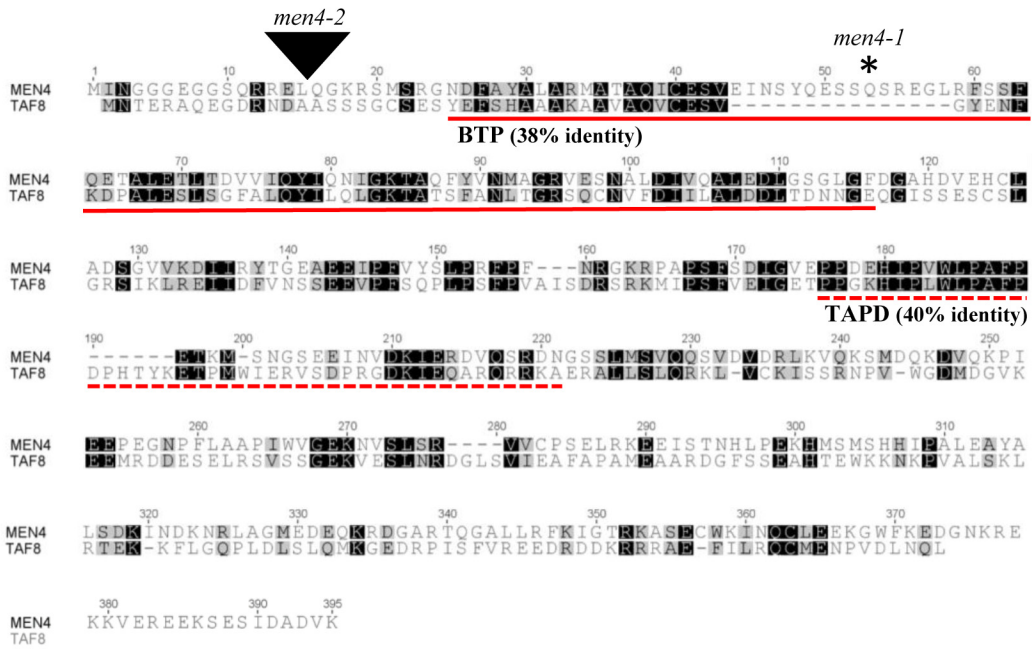


Figure 3.7. The MEN4 promoter drives GUS expression in seedlings, inflorescence, leaves, and seeds

The first column (A, D, G, J, M, P) shows lack of GUS staining in the wild-type control tissues. The second and third columns show GUS protein expression driven by the *MEN4* promoter in wild-type and *men4-1* backgrounds. Highest expression is observed in meristem and youngest leaves of seedlings (B, C, H, I), and youngest buds of the inflorescence (H, I), and seed coat and embryo tissue of seeds at each stage (K, L, N, O, Q, R). No obvious differences were observed in the GUS staining pattern between wild-type and *men4-1* plant tissues.

Figure 3.7

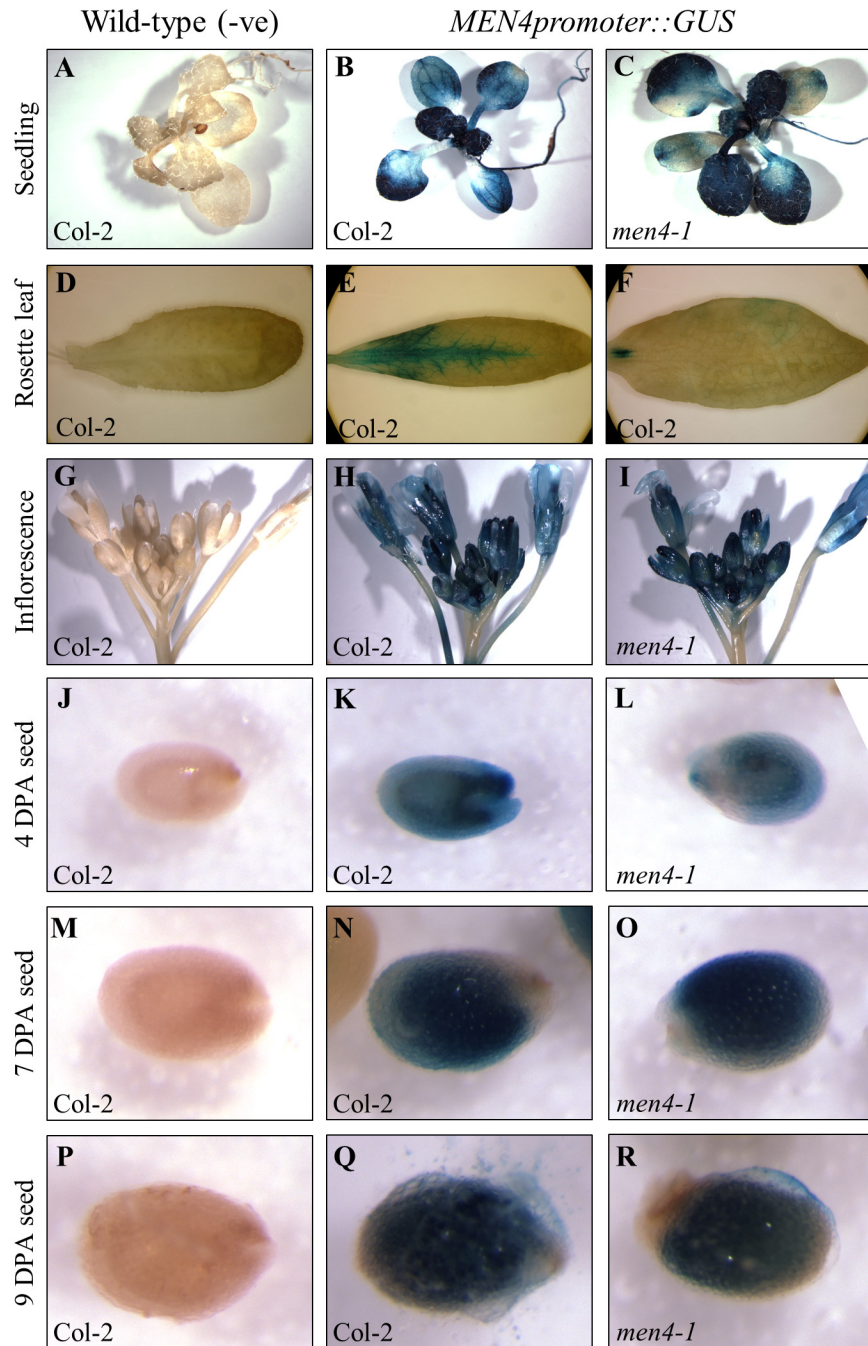


Figure 3.8. MEN4 localizes primarily to the nucleus in MSCs

(A, B) DAPI stained nuclei in developing MSCs are seen as large round structures. (C, D) Cells observed for GFP signal. Some autofluorescence is seen in starch granules in wild-type (C). In transgenic line expressing *MEN4promoter::MEN4::GFP* (D), GFP signal is seen mainly in large round inclusions that resemble the size and shape of DAPI stained nuclei, as well as more faintly throughout the surrounding cytoplasm. (E, F) Merged images of DAPI stained DNA and GFP signal do not colocalize the signals in the WT negative control (E), while strong colocalization is seen in transgenic lines (F), indicating that the MEN4 protein localizes primarily to the nucleus. Scale bar = 25 μ m.

Figure 3.8

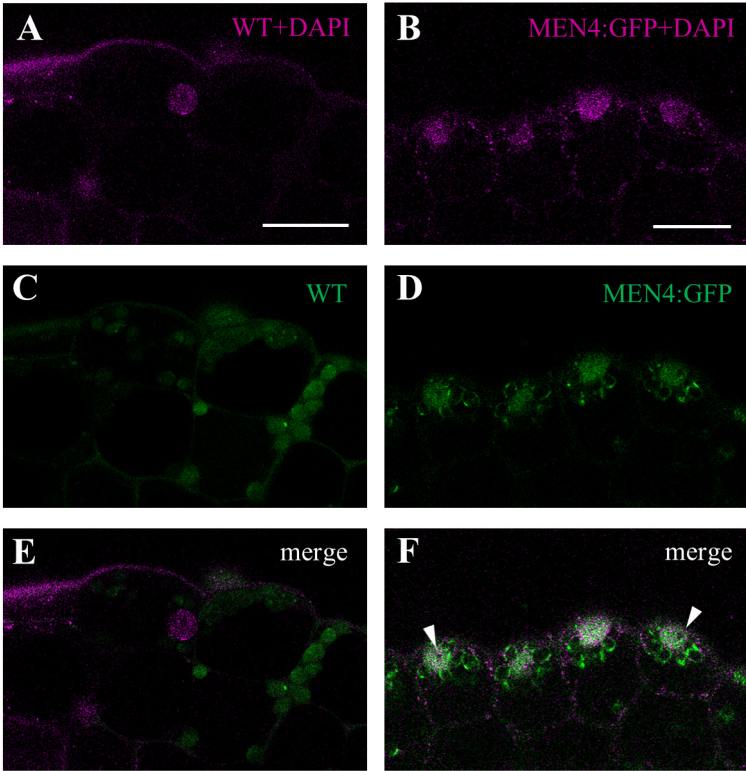
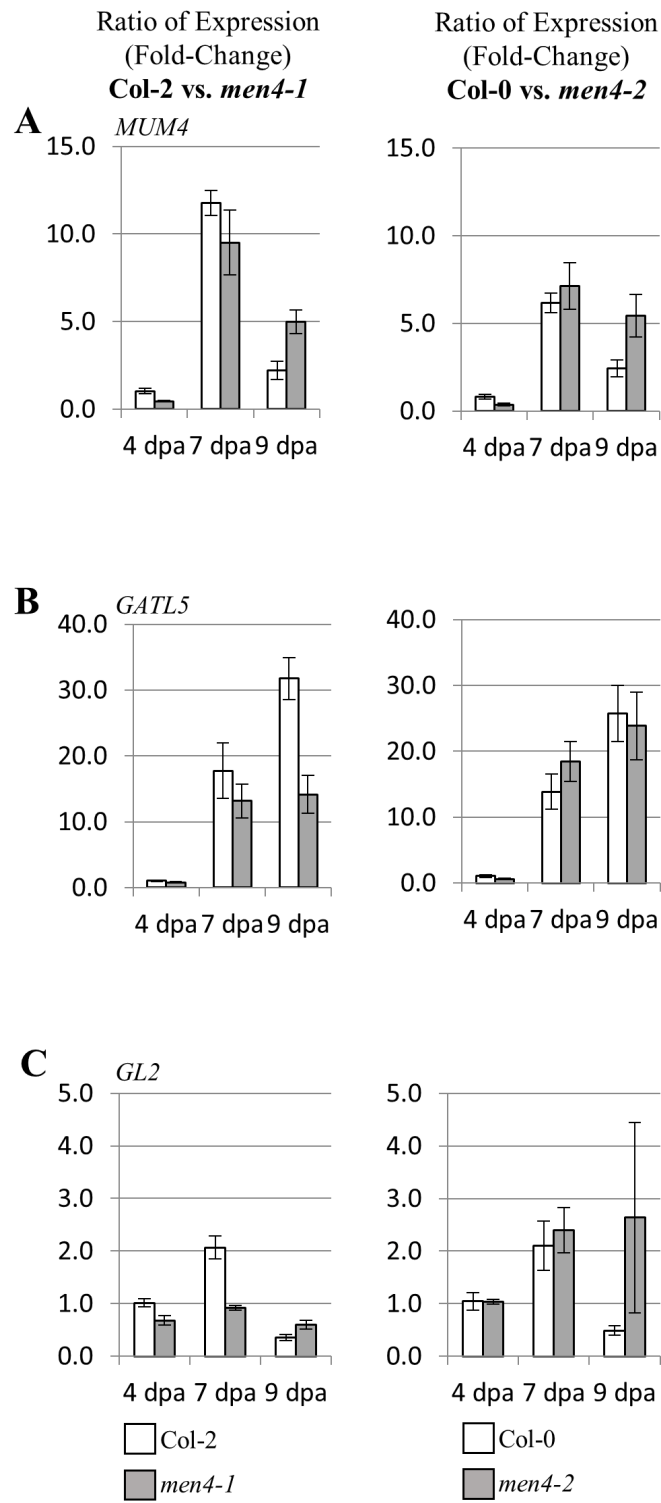


Figure 3.9. Quantitative RT-PCR of mucilage-related genes in WT and *men4* mutant backgrounds

Quantitative RT-PCR of *MUM4* (A), *GATL5* (B), and *GL2* (C) in developing seeds. Expression values are given as a fold-change ratio where 4 DPA WT = 1. All expression was normalized against the *GLYCERALDEHYDE-3-PHOSPHATE DEHYDROGENASE* (*GAPC*) housekeeping gene. (A) Changes in *MUM4* expression in *men4-1* and *men4-2* backgrounds are not significant at 7 DPA. Slightly higher expression is seen at 9 DPA in *men4-1* (p=0.012). This trend is seen in *men4-2*, but is not significant. (B) *GATL5* expression is the same at 7 DPA in WT and mutant backgrounds. *GATL5* expression in *men4-1* is decreased at 9 DPA, but this is not replicated in the *men4-2* background. (C) *GL2* expression is approximately 2-fold lower at 7 DPA in *men4-1* (p=0.005), but this is not replicated in *men4-2*. Replicates were performed (n=6) for all genes and the $2^{-\Delta\Delta CT}$ method was used for all data (Livak and Schmittgen 2001).

Figure 3.9

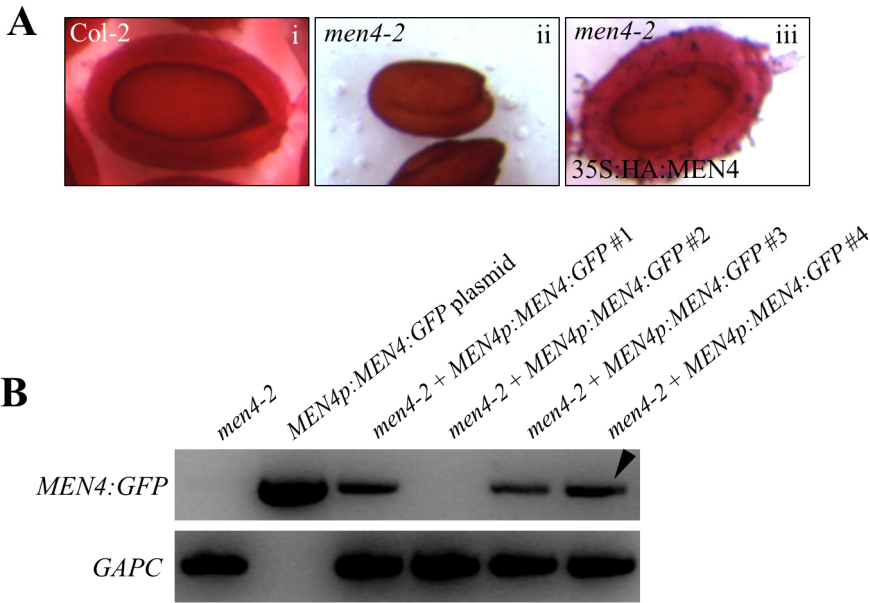


SUPPLEMENTAL MATERIAL

Supplemental Figure 3.1. Molecular complementation with HA epitope-tagged MEN4 and RT-PCR of *MEN4::GFP* expression lines

(A) The HA::MEN4 fusion protein under the constitutive 35S promoter rescues the *men4-2* mutant seed coat phenotype. Wild-type seeds release normal amounts of mucilage (i) compared to *men4-2* seeds (ii), which fail to release any mucilage when shaken in water. When the 35S::HA::MEN4 construct is expressed in the *men4-2* mutant, the mucilage phenotype is rescued (iii). (B) A selection of lines in which MEN4::GFP is driven by the endogenous *MEN4* promoter was tested with RT-PCR on the *MEN4::GFP* transcript in ~10 DPA siliques. Arrow shows line with strong expression of the fusion protein that was used for MEN4 localization. Housekeeping control *GLYCERALDEHYDE-3-PHOSPHATE DEHYDROGENASE (GAPC)* is shown for comparison.

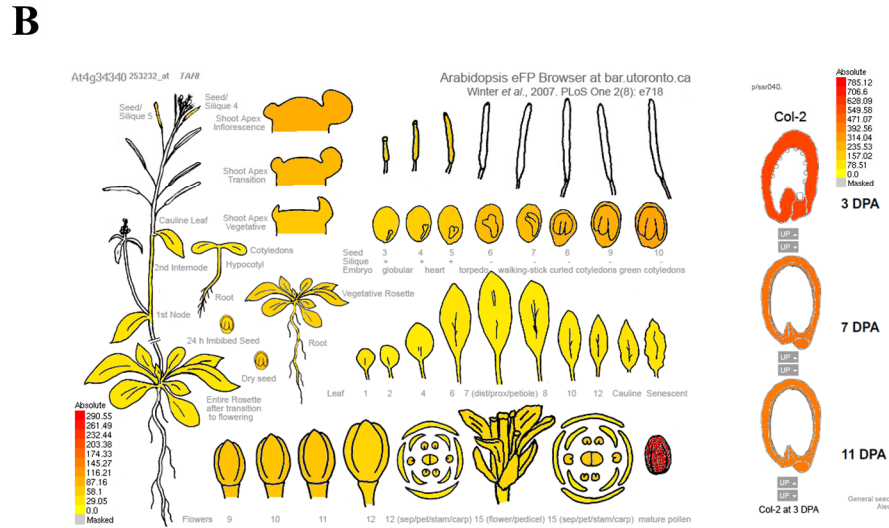
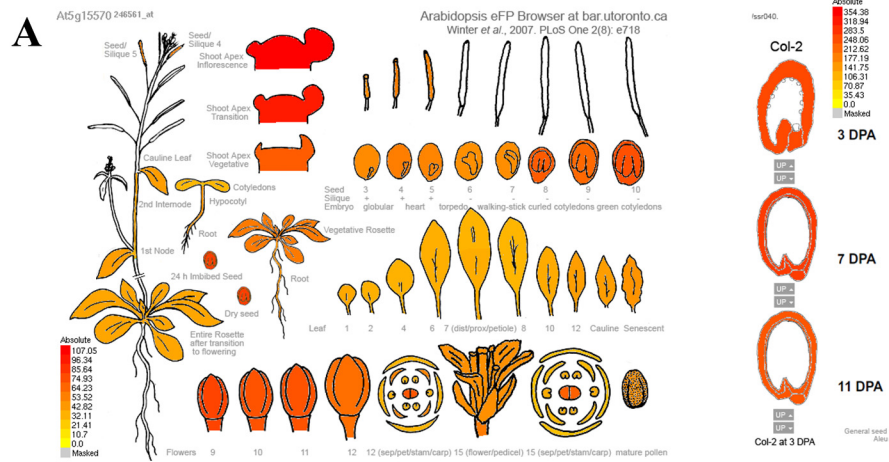
Supplemental Figure 3.1



Supplemental Figure 3.2. *MEN4* and *AtTAF8* expression based on publicly available microarray data

Publicly available microarray data shows expression patterns of *MEN4* (A) and *AtTAF8* (B) in the developing plant and seed coat throughout development. *MEN4* expression is predicted throughout all plant tissues, with highest expression in meristems, young inflorescence buds, and seeds. *AtTAF8* is expressed throughout the plant fairly ubiquitously, with highest levels observed in mature pollen. Note that both *MEN4* and *AtTAF8* expression are found in the developing seed coat. Data was mined using the BAR eFP Browser and Seed eFP Browser (bar.utoronto.ca) (Schmid et al. 2005; Winter et al. 2007; Dean et al. 2011).

Supplemental Figure 3.2



CONCLUSIONS AND FUTURE WORK

The production of mucilage and other cell wall components requires an abundance of transcriptional regulators, biosynthetic enzymes, secretion factors, and cell wall modification enzymes that are under tight regulation in order to give rise to a large diversity of glycosidic cell wall polymers. Seed coat MSCs are not only an ecologically adaptive feature of the seed in the context of its environment, but provide a powerful model system for the study of cell wall production in a developmental context, as is the case with the MSCs of *Arabidopsis*. In addition, the mucilage produced by the MSCs in a number of myxospermous species serve as a valuable product with a number of nutritional, agricultural, medicinal and pharmaceutical applications. While mucilage properties and MSC differentiation of the genetic model *Arabidopsis* have been by far the most extensively studied, MSC structure and mucilage composition varies extensively across species, and the seed coats of valuable myxospermous crop species have yet to be characterized. This study contributes to our understanding of the regulation of mucilage biosynthesis through the detailed characterization of mucilage production in the crop plant, flax, and through using the *Arabidopsis* model to identify a novel putative TF involved in the regulation of mucilage production.

Chapter Two establishes the process of MSC differentiation in flax, whereby the epidermal cell layer of the seed synthesizes large amounts of mucilage in compositionally distinct regions. The deposition of these acidic and neutral staining regions correlates with a change in Golgi stack morphology over the course of mucilage deposition. Ultimately, while immunostaining of the deposited mucilage suggests that the Golgi apparatus may be synthesizing different amounts of different polymers at particular developmental time points, it would be interesting to confirm these

results with immunogold labeling using the polysaccharide antibodies detailed in this study. Specifically, anti-unbranched RG I and anti-non-fucosylated xyloglucan antibodies CCRC-M14 and CCRC-M89 could be used to determine if binding is stronger with either of these in Golgi stacks at distinct or overlapping stages of mucilage deposition to see whether the shape of the Golgi stacks truly reflects the production of different cargo over time. Moreover, the determination of a strongly binding anti-xylan/arabinoxylan antibody for flax mucilage would be further useful in understanding the patterned deposition of flax mucilage.

The discovery of putative nucleotide sugar synthases that may be involved in producing these layers of mucilage in flax also serves as a starting point from which we can determine the specific genes required for mucilage production in flax, and how nucleotide sugar synthases may be regulating flax mucilage at the substrate level. While the identification of several enormously upregulated sugar synthases suggests they are involved in mucilage production, we cannot definitively conclude that these have a role in flax mucilage production without flax transformants to create knockdowns, or the analysis of mucilage mutants and the ability to complement their phenotypes. However, flax mutant lines are not yet available to perform mutant screens. In the meantime, in order to address whether the *UXS* and *RHM* genes identified in this study are functional as UDP-L-Rha and UDP-D-Xyl synthases, several of these genes have been cloned for exogenous expression in *Arabidopsis* backgrounds. All of the gene constructs were cloned under both the constitutive *35S* promoter and the *MUM4* promoter, as these are useful for overexpression and seed coat expression, respectively (Odell et al. 1985; Usadel et al. 2004; Western et al. 2004). Lus10038146 contains all characteristic motifs necessary in a Rha synthase enzyme, and shares 84% identity with *Arabidopsis* RHM2/MUM4, and will therefore be used as a positive control for molecular complementation in *Arabidopsis* *mum4* mutants. We will additionally test one of the

two highly upregulated flax *RHM* isoforms, *Lus10007355*, to see if this divergent RHM isoform able to rescue the *mum4* phenotype, or if this requires the co-expression of *Lus10014147* (*UER*) to carry out this function. We have also cloned the putative flax *UXS* gene, *Lus10006510*. While none of the *Arabidopsis uxs* mutants have a discernible phenotype which we can rescue, it is now known that *Arabidopsis* mucilage contains arabinoxylan, and levels can be detected using the CCRC-M139 antibody (Voiniciuc et al. 2015). While xylosyltransferase *muci21* mutants show alterations to mucilage adherence, it is possible that by overexpressing the flax *UXS* in wild-type *Arabidopsis*, we might be able to drive an increased amount of arabinoxylan in seed mucilage, which may be observed via increased adherence to the seeds, or stronger antibody staining in these lines. This work is currently underway, with rescue lines being grown and putative transformants being selected via antibiotic resistance and PCR verification. The results of these molecular complementation assays in *Arabidopsis* mutants may clarify the potential involvement of these upregulated flax homologs in mucilage production.

In Chapter Three, *MEN4* was studied for its role in mucilage production, and was identified as a nuclear-localized putative transcription factor that may be involved in the general transcription of mucilage-related gene targets. Sequence analysis of the *MEN4* protein suggests it is similar to *TAF8*, a component of a several complexes that regulate transcription through associations with *TFIID*, as well as smaller TBP-free complexes that regulate transcription through mechanisms separate from the general transcription machinery. The similarity of *MEN4* to *TAF8* proteins, as well as its localization to the nucleus independent of a NLS, suggest that *MEN4* complexes with other proteins *in vivo*, which may recruit it to the nucleus. In order to gain a better understanding of how *MEN4* regulates transcription, co-immunoprecipitation is required to determine what other proteins may form a complex with *MEN4*. TAF proteins purify with other TAFs as components

of TFIID and other TAF-containing complexes, and so if MEN4 co-purified with other TAFs, we could conclude that MEN4 is in fact a bona fide TAF. Depending on the combination of interaction partners, MEN4 may be more clearly categorized into any of the previously discussed complexes. This has been initiated, as MEN4 has been tagged with GFP and HA, which will be used to purify MEN4 and the members of any bound complex.

The quantitative RT-PCR assays performed in Chapter Three were inconclusive in terms of identifying potential downstream gene targets of the MEN4 protein. However, the variation in expression levels may be a result of the presence of the embryo in which both *MUM4* and *GL2* at least are strongly expressed, which was included in the RNA preparations for these experiments. These RT-PCR assays are currently being repeated using only dissected seed coat tissue for RNA preparations to confirm whether any of the previously described mucilage-related genes are under regulation of MEN4. Chromatin-immunoprecipitation (ChIP) and ChIP-sequencing could also be performed in different tissues such as seed coats and meristems in order to identify specific cis-elements recognized by MEN4 and/or any complexes in which it is found. Alternatively, RNA-sequencing would also identify changes in overall gene expression in WT versus *men4* mutants in various tissues. Because *MEN4* appears to regulate targets in a subtle manner, it would also be interesting to investigate expression levels of targets in a MEN4 overexpression line. The HA epitope tagged line is driven by the 35S constitutive promoter, and could be used for this purpose, and these lines will be confirmed for their degree of *MEN4* overexpression.

Finally, in addition to the reduced mucilage phenotype and smaller seed size of the *men4* mutant, a preliminary investigation of other gross morphological plant features revealed a potential reduction of apical dominance in the *men4* mutant. Apical dominance occurs whereby the primary inflorescence promotes its own growth and inhibits the growth of lateral axillary buds (reviewed

in Dun et al., 2006; Leyser, 2005). This process appears to be disrupted in *men4* mutants, where there is a small but clear increase in the number of axillary shoots, according to our preliminary data. While sample sizes for these observations is currently small, more plants are being grown currently in order to confirm these findings statistically. Based on the high expression of *MEN4* in meristematic tissue, and its putative effect on apical growth and branching, it is possible that *MEN4* could be regulating downstream target genes involved in signalling pathways of the plant hormone auxin, as this is of primary influence in maintaining apical dominance (Dun et al. 2006). To investigate the potential relationship between *MEN4* and auxin signalling, we will carry out plant growth assays whereby wild-type and *men4* mutant seedlings will be grown on auxin-treated media and observe whether plant growth differs in response to the presence of the hormone. This, in addition to RNA-sequencing or ChIP in meristem tissue, may provide insight into the downstream targets of *MEN4*, which are not necessarily the same in meristem tissue as those that affect mucilage production.

LITERATURE CITED

- Abdel-Massih RM, Baydoun EAH, Brett CT. 2003. In vitro biosynthesis of 1,4-beta-galactan attached to a pectin-xyloglucan complex in pea. *Planta* 216:502–11.
- Abeysekera R, Willinson J. 1988. Development of helicoidal texture in the prerelease mucilage of quince (*Cydonia oblonga*) seed epidermis. *Can. J. Bot.* 66:460–467.
- Anders N, Wilkinson MD, Lovegrove A, Freeman J, Tryfona T, Pellny TK, Weimar T, Mortimer JC, Stott K, Baker JM, et al. 2012. Glycosyl transferases in family 61 mediate arabinofuranosyl transfer onto xylan in grasses. *Proc. Natl. Acad. Sci. U. S. A.* 109:989–93.
- Anderson CT. 2015. We be jammin': an update on pectin biosynthesis, trafficking and dynamics. *J. Exp. Bot.*:erv501.
- Anttila M., Kankaanpä-Anttila B., Sepponen M., Timonen H. AK. 2008. Improving of texture of dairy products. Patent WO/2008/000913. *Int. Appl. N.*
- Arsovski A a., Villota MM, Rowland O, Subramaniam R, Western TL. 2009. MUM Enhancers are important for seed coat mucilage production and mucilage secretory cell differentiation in *Arabidopsis thaliana*. *J. Exp. Bot.* 60:2601–2612.
- Arsovski A, Popma TM, Haughn GW, Carpita NC, McCann MC, Western TL. 2009. AtBXL1 Encodes a Bifunctional -D-Xylosidase/ -L-Arabinofuranosidase Required for Pectic Arabinan Modification in *Arabidopsis* Mucilage Secretory Cells. *Plant Physiol.* 150:1219–1234.
- Atmodjo M a., Hao Z, Mohnen D. 2013. Evolving Views of Pectin Biosynthesis. *Annu. Rev. Plant Biol.* 64:747–779.
- Atmodjo MA, Sakuragi Y, Zhu X, Burrell AJ, Mohanty SS, Atwood JA, Orlando R, Scheller H V, Mohnen D. 2011. Galacturonosyltransferase (GAUT)1 and GAUT7 are the core of a plant cell wall pectin biosynthetic homogalacturonan:galacturonosyltransferase complex. *Proc. Natl. Acad. Sci. U. S. A.* 108:20225–30.
- Austin RS, Vidaurre D, Stamatiou G, Breit R, Provart NJ, Bonetta D, Zhang J, Fung P, Gong Y, Wang PW, et al. 2011. Next-generation mapping of *Arabidopsis* genes. *Plant J.* 67:715–725.
- Barber C, Rösti J, Rawat A, Findlay K, Roberts K, Seifert GJ. 2006. Distinct properties of the five UDP-D-glucose/UDP-D-galactose 4-epimerase isoforms of *Arabidopsis thaliana*. *J. Biol. Chem.* 281:17276–85.
- Bar-peled M, Neill MAO. 2011. Plant Nucleotide Sugar Formation , Interconversion , and Salvage by Sugar. *Annu. Rev. Plant Biol.* 67:127–155.
- Basu D, Tian L, DeBrosse T, Poirier E, Emch K, Herock H, Travers A, Showalter AM. 2016. Glycosylation of a Fasciclin-Like Arabinogalactan-Protein (SOS5) mediates root growth and seed mucilage adherence via a cell wall receptor-like kinase (FEI1/ FEI2) Pathway in *Arabidopsis*. *PLoS One* 11.
- Baydoun EA-H, Abdel-Massih RM, Dani D, Rizk SE, Brett CT. 2001. Galactosyl- and fucosyltransferases in etiolated pea epicotyls: product identification and sub-cellular localisation. *J. Plant Physiol.* 158:145–150.
- Beeckman T, De Rycke R, Viane R, Inzé D. 2000. Histological Study of Seed Coat Development in *Arabidopsis thaliana*. *J. Plant Res.* 113:139–148.

- Ben-Tov D, Abraham Y, Stav S, Thompson K, Loraine A, Elbaum R, De Souza A, Pauly M, Kieber JJ, Harpaz-Saad S. 2015. COBRA-LIKE 2, a member of the GPI-anchored COBRA-LIKE family, plays a role in cellulose deposition in Arabidopsis seed coat mucilage secretory cells. *Plant Physiol.* 167:104-114.
- Bernal AJ, Jensen JK, Harholt J, Sørensen S, Moller I, Blaukopf C, Johansen B, de Lotto R, Pauly M, Scheller HV, et al. 2007. Disruption of ATCSLD5 results in reduced growth, reduced xylan and homogalacturonan synthase activity and altered xylan occurrence in Arabidopsis. *Plant J.* 52:791-802.
- Bertrand C, Benhamed M, Li Y-F, Ayadi M, Lemonnier G, Renou J-P, Delarue M, Zhou D-X. 2005. Arabidopsis HAF2 gene encoding TATA-binding protein (TBP)-associated factor TAF1, is required to integrate light signals to regulate gene expression and growth. *J. Biol. Chem.* 280:1465-73.
- Bhargava A, Ahad A, Wang S, Mansfield SD, Haughn GW, Douglas CJ, Ellis BE. 2013. The interacting MYB75 and KNAT7 transcription factors modulate secondary cell wall deposition both in stems and seed coat in Arabidopsis. *Planta* 237:1199-1211.
- Bidhendi AJ, Geitmann A. 2015. Relating the mechanics of the primary plant cell wall to morphogenesis. *J. Exp. Bot.*:erv535.
- Bindschedler L V., Tuerck J, Maunders M, Ruel K, Petit-Conil M, Danoun S, Boudet AM, Joseleau JP, Bolwell GP. 2007. Modification of hemicellulose content by antisense down-regulation of UDP-glucuronate decarboxylase in tobacco and its consequences for cellulose extractability. *Phytochemistry* 68:2635-2648.
- Boesewinkel, F D and Bouman F. 1984. The seed: structure. In: Johri, B.M. Embryology of angiosperms. New York, NY: Springer-Verlag. p. 567-610.
- Boesewinkel FD. 1980. Development of ovule and testa of *Linum usitatissimum* L. *Acta Bot. Neerl.* 29:17-32.
- Bouman F. 1975. Integument initiation and testa development in some Cruciferae. *Bot. J. Linn. Soc.* 70:213-229.
- Bouton S, Leboeuf E, Mouille G, Leydecker M-T, Talbotec J, Granier F, Lahaye M, Höfte H, Truong H-N. 2002. QUASIMODO1 encodes a putative membrane-bound glycosyltransferase required for normal pectin synthesis and cell adhesion in Arabidopsis. *Plant Cell* 14:2577-2590.
- Bowman, J.L. and Koornneef M. 1994. Seed morphology. In: Arabidopsis: an atlas of morphology and development. New York, NY: Springer-Verlag. p. 398-401.
- Broothaerts W, Mitchell HJ, Weir B, Kaines S, Smith LM, Yang W, Mayer JE, Roa-Rodriguez C, Jefferson RA. 2005. Gene transfer to plants by diverse species of bacteria. *Nature* 433:629-633.
- Brown DM, Goubet F, Wong VW, Goodacre R, Stephens E, Dupree P, Turner SR. 2007. Comparison of five xylan synthesis mutants reveals new insight into the mechanisms of xylan synthesis. *Plant J.* 52:1154-1168.
- Brown DM, Zhang Z, Stephens E, Dupree P, Turner SR. 2009. Characterization of IRX10 and IRX10-like reveals an essential role in glucuronoxylan biosynthesis in Arabidopsis. *Plant J.* 57:732-746.
- Buanafina MMDO, Fescemyer HW, Sharma M, Shearer EA. 2015. Functional testing of a

- PF02458 homologue of putative rice arabinoxylan feruloyl transferase genes in *Brachypodium distachyon*. *Planta* 243:1–16.
- Bui M, Lim N, Sijacic P, Liu Z. 2011. LEUNIG-HOMOLOG and LEUNIG Regulate Seed Mucilage Extrusion in *Arabidopsis*. *J. Integr. Plant Biol.* 53:399–408.
- Burn JE, Hurley UA, Birch RJ, Arioli T, Cork A, Williamson RE. 2002. The cellulose-deficient *Arabidopsis* mutant *rsw3* is defective in a gene encoding a putative glucosidase II, an enzyme processing N-glycans during ER quality control. *Plant J.* 32:949–960.
- Burton RA, Gidley MJ, Fincher GB. 2010. Heterogeneity in the chemistry, structure and function of plant cell walls. *Nat. Chem. Biol.* 6:724–732.
- Bushway A, Belyea P, Bushway R. 1981. Chia seed as a source of oil, polysaccharide, and protein. *J. Food Sci.*:1349–1356.
- Busse-Wicher M, Gomes TCF, Tryfona T, Nikolovski N, Stott K, Grantham NJ, Bolam DN, Skaf MS, Dupree P. 2014. The pattern of xylan acetylation suggests xylan may interact with cellulose microfibrils as a twofold helical screw in the secondary plant cell wall of *Arabidopsis thaliana*. *Plant J.* 79:492–506.
- Van Caesele L, Mills JT, Sumner M, Gillespie R. 1981. Cytology of mucilage production in the seed coat of Candle canola (*Brassica campestris*). *Can. J. Bot.* 59:292–300.
- Caffall KH, Mohnen D. 2009. The structure, function, and biosynthesis of plant cell wall pectic polysaccharides. *Carbohydr. Res.* 344:1879–1900.
- Caffall KH, Pattathil S, Phillips SE, Hahn MG, Mohnen D. 2009. *Arabidopsis thaliana* T-DNA mutants implicate GAUT genes in the biosynthesis of pectin and xylan in cell walls and seed testa. *Mol. Plant* 2:1000–14.
- Campanoni P, Blatt MR. 2007. Membrane trafficking and polar growth in root hairs and pollen tubes. *J. Exp. Bot.* 58:65–74.
- Cavalier DM, Lerouxel O, Neumetzler L, Yamauchi K, Reinecke A, Freshour G, Zabolina OA, Hahn MG, Burgert I, Pauly M, et al. 2008. Disrupting two *Arabidopsis thaliana* xylosyltransferase genes results in plants deficient in xyloglucan, a major primary cell wall component. *Plant Cell* 20:1519–37.
- Chiniquy D, Sharma V, Schultink A, Baidoo EE, Rautengarten C, Cheng K, Carroll A, Ulvskov P, Harholt J, Keasling JD, et al. 2012. XAX1 from glycosyltransferase family 61 mediates xylosyltransfer to rice xylan. *Proc. Natl. Acad. Sci.* 109 :17117–17122.
- Chiniquy D, Varanasi P, Oh T, Harholt J, Katnelson J, Singh S, Auer M, Simmons B, Adams PD, Scheller H V, et al. 2013. Three Novel Rice Genes Closely Related to the *Arabidopsis* IRX9, IRX9L, and IRX14 Genes and Their Roles in Xylan Biosynthesis. *Front. Plant Sci.* 4:83.
- Chou Y-H, Pogorelko G, Zabolina O a. 2012. Xyloglucan Xylosyltransferases XXT1, XXT2, and XXT5 and the Glucan Synthase CSLC4 Form Golgi-Localized Multiprotein Complexes. *Plant Physiol.* 159:1355–1366.
- Cline MG. 1994. The role of hormones in apical dominance. New approaches to an old problem in plant development. *Physiol. Plant.* 90:230–237.
- Clough SJ, Bent AF. 1998. Floral dip: a simplified method for *Agrobacterium*-mediated transformation of *Arabidopsis thaliana*. *Plant J.* 16:735–743.
- Cole RA, Fowler JE. 2006. Polarized growth: maintaining focus on the tip. *Curr. Opin. Plant Biol.* 9:579–588.

- Curtis MD, Grossniklaus U. 2003. A gateway cloning vector set for high-throughput functional analysis of genes in planta. *Plant Physiol.* 133:462–9.
- Dean G, Cao Y, Xiang D, Provart NJ, Ramsay L, Ahad A, White R, Selvaraj G, Datla R, Haughn G. 2011. Analysis of Gene Expression Patterns during Seed Coat Development in *Arabidopsis*. *Mol. Plant* 4:1074–1091.
- Dean GH, Zheng H, Tewari J, Huang J, Young DS, Hwang YT, Western TL, Carpita NC, McCann MC, Mansfield SD, et al. 2007. The *Arabidopsis* MUM2 Gene Encodes a β -Galactosidase Required for the Production of Seed Coat Mucilage with Correct Hydration Properties. *Plant Cell Online* 19:4007–4021.
- Debeaujon I. 2000. Influence of the Testa on Seed Dormancy, Germination, and Longevity in *Arabidopsis*. *PLANT Physiol.* 122:403–414.
- Dellaporta SL, Wood J, Hicks JB. 1983. A plant DNA miniprep: Version II. *Plant Mol. Biol. Report.* 1:19–21.
- Demény MA, Soutoglou E, Nagy Z, Scheer E, Jánoshazi A, Richardot M, Argentini M, Kessler P, Tora L. 2007. Identification of a small TAF complex and its role in the assembly of TAF-containing complexes. *PLoS One* 2:e316.
- Detlef W, Glazebrook J. 2002. *Arabidopsis: A Laboratory Manual*. CSHL Press.
- Dick-Pérez M, Zhang Y, Hayes J, Salazar A, Zabolina OA, Hong M. 2011. Structure and Interactions of Plant Cell-Wall Polysaccharides by Two- and Three-Dimensional Magic-Angle-Spinning Solid-State NMR. *Biochemistry* 50:989–1000.
- Diederichsen A, Raney JP, Duguid SD. 2006. Variation of Mucilage in Flax Seed and Its Relationship with Other Seed Characters. *Crop Sci.* 46:365.
- Diet A, Link B, Seifert GJ, Schellenberg B, Wagner U, Pauly M, Reiter W, Ringli C. 2006. The *Arabidopsis* Root Hair Cell Wall Formation Mutant *lrx1* Is Suppressed by Mutations in the *RHM1* Gene Encoding a UDP- L -Rhamnose Synthase. *Plant Cell* 18:1630–1641.
- Driouich A, Follet-Gueye M-L, Bernard S, Kousar S, Chevalier L, Vicré-Gibouin M, Lerouxel O. 2012. Golgi-mediated synthesis and secretion of matrix polysaccharides of the primary cell wall of higher plants. *Front. Plant Sci.* 3:79.
- Du Q, Pan W, Tian J, Li B, Zhang D. 2013. The UDP-glucuronate decarboxylase gene family in *Populus*: structure, expression, and association genetics. *PLoS One* 8:e60880.
- DuBois M, Gilles K a., Hamilton JK, Rebers P a., Smith F. 1956. Colorimetric method for determination of sugars and related substances. *Anal. Chem.* 28:350–356.
- Duletia-Lauševia S, Marin PD. 1999. Pericarp structure and myxocarpy in selected genera of *Nepetoideae* (Lamiaceae). *Nord. J. Bot.* 19:435–446.
- Dun EA, Ferguson BJ, Beveridge CA. 2006. Apical Dominance and Shoot Branching. Divergent Opinions or Divergent Mechanisms? *PLANT Physiol.* 142:812–819.
- Dupree P, Sherrier DJ. 1998. The plant Golgi apparatus. *Biochim. Biophys. Acta - Mol. Cell Res.* 1404:259–270.
- Durand C, Vicre-Gibouin M, Follet-Gueye ML, Duponchel L, Moreau M, Lerouge P, Driouich A. 2009. The Organization Pattern of Root Border-Like Cells of *Arabidopsis* Is Dependent on Cell Wall Homogalacturonan. *Plant Physiol.* 150:1411–1421.
- Earley KW, Haag JR, Pontes O, Opper K, Juehne T, Song K, Pikaard CS. 2006. Gateway-compatible vectors for plant functional genomics and proteomics. *Plant J.* 45:616–29.

- Ebert B, Rautengarten C, Guo X, Xiong G, Stonebloom S, Smith-Moritz AM, Herter T, Chan LJ, Adams PD, Petzold CJ, et al. 2015. Identification and Characterization of a Golgi-Localized UDP-Xylose Transporter Family from Arabidopsis. *Plant Cell* 27:1218–1227.
- Egelund J, Damager I, Faber K, Olsen C-E, Ulvskov P, Petersen BL. 2008. Functional characterisation of a putative rhamnogalacturonan II specific xylosyltransferase. *FEBS Lett.* 582:3217–22.
- Egelund J, Petersen BL, Motawia MS, Damager I, Faik A, Olsen CE, Ishii T, Clausen H, Ulvskov P, Geshi N. 2006. Arabidopsis thaliana RGXT1 and RGXT2 encode Golgi-localized (1,3)-alpha-D-xylosyltransferases involved in the synthesis of pectic rhamnogalacturonan-II. *Plant Cell* 18:2593–607.
- Ellner S, Shmida A. 1981. Why are adaptations for long-range seed dispersal rare in desert annual plants? *Oecologia* 51:133–144.
- Esau K. 1977. Anatomy of Seed Plants, 2nd Edition. In: *Anatomy of Seed Plants, 2nd Edition.* Toronto: Wiley. p. 455–473.
- Eskin NAM. 1992. Effect of variety and geographical location on the incidence of mucilage in canola seeds. *Can. J. Plant Sci.*:1223–125.
- Fahn A. 1979. Secretory tissues in plants. New York, NY: Academic Press.
- Fahn A. 1982a. *Plant Anatomy* (3rd edition). Press P, editor. New York, NY.
- Fahn A. 1982b. *Plant Anatomy, 3rd Edition.* Toronto: Pergamon Press. p. 479–496.
- Faik A. 2010. Xylan Biosynthesis: News from the Grass. *Plant Physiol.* 153 :396–402.
- Falender AE, Freiman RN, Geles KG, Lo KC, Hwang K, Lamb DJ, Morris PL, Tjian R, Richards JS. 2005. Maintenance of spermatogenesis requires TAF4b, a gonad-specific subunit of TFIID. *Genes Dev.* 19:794–803.
- Fedeniuk RW, Biliaderis CG. 1994. Composition and physicochemical properties of linseed (*Linum usitatissimum* L.) mucilage. *J. Agric. Food ...* 42:240–247.
- Finn RD, Coghill P, Eberhardt RY, Eddy SR, Mistry J, Mitchell AL, Potter SC, Punta M, Qureshi M, Sangrador-Vegas A, et al. 2016. The Pfam protein families database: towards a more sustainable future. *Nucleic Acids Res.* 44:D279–85.
- Fitch EA, Walck JL, Hidayati SN. 2007. Germinating seeds of *Lesquerella perforata* and *stonensis*: substrate effects and mucilage production. *Nativ. Plants J.* 8:4–10.
- Francoz E, Ranocha P, Burlat V, Dunand C. 2015. Arabidopsis seed mucilage secretory cells: regulation and dynamics. *Trends Plant Sci.* 20:515–524.
- Freiman RN, Albright SR, Zheng S, Sha WC, Hammer RE, Tjian R. 2001. Requirement of tissue-selective TBP-associated factor TAFIII105 in ovarian development. *Science* 293:2084–2087.
- Frey-Wyssling A. 1976. *The Plant Cell Wall.* Berlin: Borntraeger.
- Fuller PJ, Hay ME. 1983. Is glue production by seeds of *Salvia columbariae* a deterrent to desert granivores? *Ecology* 64:960–963.
- Gallie DR, Kado CI. 1989. A translational enhancer derived from tobacco mosaic virus is functionally equivalent to a Shine-Dalgarno sequence. *Proc. Natl. Acad. Sci. U. S. A.* 86:129–32.
- Gangloff Y, Pointud J, Carré L, Romier C, Muratoglu S, Brand M, Tora L, Couderc J, Gangloff

- L, Thuault S, et al. 2001. The TFIID Components Human TAF II 140 and Drosophila BIP2 (TAF II 155) Are Novel Metazoan Homologues of Yeast TAF II 47 Containing a Histone Fold and a PHD The TFIID Components Human TAF II 140 and Drosophila BIP2 (TAF II 155) Are Novel Metazoan Homol. *Mol. Cell. Biol.* 2:5109–5121.
- Ganorkar PM, Jain RK. 2013. Flaxseed - A nutritional punch. *Int. Food Res. J.* 20:519–525.
- Gao X, Ren F, Lu YT. 2006. The Arabidopsis mutant stg1 identifies a function for TBP-associated factor 10 in plant osmotic stress adaptation. *Plant Cell Physiol.* 47:1285–1294.
- Garcia D, Gerald JNF, Berger F. 2005. Maternal Control of Integument Cell Elongation and Zygotic Control of Endosperm Growth Are Coordinated to Determine Seed Size in Arabidopsis. *Plant Cell Online* 17:52–60.
- Garcia D, Saingery V, Chambrier P, Mayer U, Jürgens G, Berger F. 2003. Arabidopsis haiku Mutants Reveal New Controls of Seed Size by Endosperm. *PLANT Physiol.* 131:1661–1670.
- Gendre D, McFarlane HE, Johnson E, Mouille G, Sjödin A, Oh J, Levesque-Tremblay G, Watanabe Y, Samuels L, Bhalerao RP. 2013. Trans-Golgi network localized ECHIDNA/Ypt interacting protein complex is required for the secretion of cell wall polysaccharides in Arabidopsis. *Plant Cell* 25:2633–46.
- Geshi N, Jørgensen B, Scheller H V, Ulvskov P. 2000. In vitro biosynthesis of 1,4-beta-galactan attached to rhamnogalacturonan I. *Planta* 210:622–9.
- Geshi N, Jørgensen B, Ulvskov P. 2004. Subcellular localization and topology of beta(1,4)galactosyltransferase that elongates beta(1,4)galactan side chains in rhamnogalacturonan I in potato. *Planta* 218:862–8.
- Geshi N, Pauly M, Ulvskov P. 2002. Solubilization of galactosyltransferase that synthesizes 1,4-beta-galactan side chains in pectic rhamnogalacturonan I. *Physiol. Plant.* 114:540–548.
- Gibeaut D. 2000. Nucleotide sugars and glycosyltransferases for synthesis of cell wall matrix polysaccharides. *Plant Physiol. Biochem.* 38:69–80.
- Gonzalez A, Mendenhall J, Huo Y, Lloyd A. 2009. TTG1 complex MYBs, MYB5 and TT2, control outer seed coat differentiation. *Dev. Biol.* 325:412–21.
- Gorshkova T, Brutch N, Chabbert B, Deyholos M, Hayashi T, Lev-Yadun S, Mellerowicz EJ, Morvan C, Neutelings G, Pilate G. 2012. Plant Fiber Formation: State of the Art, Recent and Expected Progress, and Open Questions. *CRC. Crit. Rev. Plant Sci.* 31:201–228.
- Goto N. 1985. A mucilage polysaccharide secreted from testa of Arabidopsis thaliana. *Arab. Inf. Serv.:*143–145.
- Goubet F, Morvan C. 1993. Evidence for Several Galactan Synthases in Flax (*Linum usitatissimum* L.) Suspension-Cultured Cells. *Plant Cell Physiol.* 34:1297–1303.
- Gowda DC. 1984. Polysaccharide components of the seed- coat mucilage from *Hyptis suaveolens*. *Phytochemistry* 23:337–338.
- Grabber JH. 2005. How do lignin composition, structure, and cross-linking affect degradability? A review of cell wall model studies. *Crop Sci.* 45:820–831.
- Grant PA, Schieltz D, Pray-Grant MG, Steger DJ, Reese JC, Yates JR, Workman JL. 1998. A subset of TAF(II)s are integral components of the SAGA complex required for nucleosome acetylation and transcriptional stimulation. *Cell* 94:45–53.
- Griffiths JS, Šola K, Kushwaha R, Lam P, Tateno M, Young R, Voiniciuc C, Dean G, Mansfield

- SD, DeBolt S, et al. 2015. Unidirectional movement of cellulose synthase complexes in Arabidopsis seed coat epidermal cells deposit cellulose involved in mucilage extrusion, adherence, and ray formation. *Plant Physiol.* 168:502–20.
- Griffiths JS, Tsai AY-L, Xue H, Voiniciuc C, Sola K, Seifert GJ, Mansfield SD, Haughn GW. 2014. SALT-OVERLY SENSITIVE5 Mediates Arabidopsis Seed Coat Mucilage Adherence and Organization through Pectins. *Plant Physiol.* 165:991–1004.
- Grubert M. 1974. Studies on the distribution of myxospermy among seeds and fruits of Angiospermae and its ecological importance. *Acta Biol. Venez.*:315–551.
- Grubert M. 1981. *Mucilage or Gum in Seeds and Fruits of Angiosperms: A Review.* Munich: Minerva Press.
- Gu X, Bar-Peled M. 2004. The Biosynthesis of UDP-Galacturonic Acid in Plants. Functional Cloning and Characterization of Arabidopsis UDP-d-Glucuronic Acid 4-Epimerase. *Plant Physiol.* 136:4256–4264.
- Guermah M, Ge K, Chiang CM, Roeder RG. 2003. The TBN protein, which is essential for early embryonic mouse development, is an inducible TAFII implicated in adipogenesis. *Mol. Cell* 12:991–1001.
- Gutterman Y, Shem-Tov S. 1997. Mucilaginous seed coat structure of *Carrichtera annua* and *Anastatica hierochuntica* from the Negev Desert highlands of Israel, and its adhesion to the soil crust. *J. Arid Environ.* 35:695–705.
- Han X, Qian L, Zhang L, Liu X. 2015. Structural and biochemical insights into nucleotide-rhamnose synthase/epimerase-reductase from Arabidopsis thaliana. *Biochim. Biophys. Acta* 1854:1476–86.
- Hao Z, Avci U, Tan L, Zhu X, Glushka J, Pattathil S, Eberhard S, Sholes T, Rothstein GE, Lukowitz W, et al. 2014. Loss of Arabidopsis GAUT12/IRX8 causes anther indehiscence and leads to reduced G lignin associated with altered matrix polysaccharide deposition. *Front. Plant Sci.* 5:357.
- Hao Z, Mohnen D. 2014. A review of xylan and lignin biosynthesis: Foundation for studying Arabidopsis irregular xylem mutants with pleiotropic phenotypes. *Crit. Rev. Biochem. Mol. Biol.* 49:212–241.
- Harholt J, Jensen JK. 2006. ARABINAN DEFICIENT 1 Is a Putative Arabinosyltransferase Involved in Biosynthesis of Pectic Arabinan in Arabidopsis. *Plant Physiol.* 140:49–58.
- Harholt J, Jensen JK, Verhertbruggen Y, Søgaard C, Bernard S, Nafisi M, Poulsen CP, Geshi N, Sakuragi Y, Driouich A, et al. 2012. ARAD proteins associated with pectic Arabinan biosynthesis form complexes when transiently overexpressed in planta. *Planta* 236:115–128.
- Harholt J, Suttangkakul A, Vibe Scheller H. 2010. Biosynthesis of Pectin. *Plant Physiol.* 153:384–395.
- Harpaz-Saad S, McFarlane HE, Xu S, Divi UK, Forward B, Western TL, Kieber JJ. 2011. Cellulose synthesis via the FEI2 RLK/SOS5 pathway and CELLULOSE SYNTHASE 5 is required for the structure of seed coat mucilage in Arabidopsis. *Plant J.* 68:941–953.
- Harpaz-Saad S, McFarlane HE, Xu S, Divi UK, Forward B, Western TL, Kieber JJ. 2011. Cellulose synthesis via the FEI2 RLK/SOS5 pathway and cellulose synthase 5 is required for the structure of seed coat mucilage in Arabidopsis. *Plant J.* 68:941–53.

- Harpaz-Saad S, Western TL, Kieber JJ. 2012 Feb 1. The FEI2-SOS5 pathway and CELLULOSE SYNTHASE 5 are required for cellulose biosynthesis in the Arabidopsis seed coat and affect pectin mucilage structure. *Plant Signal. Behav.* 48:112-118
- Harper AD, Bar-Peled M. 2002a. Biosynthesis of UDP-Xylose. Cloning and Characterization of a Novel Arabidopsis Gene Family. *Plant Physiol.* 130:2188–2198.
- Harper AD, Bar-Peled M. 2002b. Biosynthesis of UDP-xylose. Cloning and characterization of a novel Arabidopsis gene family, UXS, encoding soluble and putative membrane-bound UDP-glucuronic acid decarboxylase isoforms. *Plant Physiol.* 130:2188–98.
- Harper J, Benton R. 1966. The behaviour of seeds in soil. II. The germination of seeds on the surface of a water supplying substrate. *J. Ecol.* 54:151–166.
- Haughn GW, Somerville C. 1986. Sulfonylurea-resistant mutants of Arabidopsis thaliana. *MGG Mol. Gen. Genet.* 204:430–434.
- Haughn GW, Western TL. 2012. Arabidopsis Seed Coat Mucilage is a Specialized Cell Wall that Can be Used as a Model for Genetic Analysis of Plant Cell Wall Structure and Function. *Front. Plant Sci.* 3:1–5.
- Hellens RP, Edwards EA, Leyland NR, Bean S, Mullineaux PM. 2000. pGreen: a versatile and flexible binary Ti vector for Agrobacterium-mediated plant transformation. *Plant Mol. Biol.* 42:819–832.
- Heydecker W, Orphanos P. 1968. The effect of excess moisture on the germination of Spinacia oleracea L. *Planta* 83:237–247.
- Hiller MA, Lin TY, Wood C, Fuller MT. 2001. Developmental regulation of transcription by a tissue-specific TAF homolog. *Genes Dev.* 15:1021–1030.
- Hinterberg B, Klos C, Tenhaken R. 2002. Recombinant UDP-glucose dehydrogenase from soybean. *Plant Physiol. Biochem.* 40:1011–1017.
- Hsiao Y, Chuang TI. 1981. Seed-Coat Morphology and Anatomy in Collomia (Polemoniaceae). *Bot. Soc. Am.* 68:1155–1164.
- Hu R, Li J, Wang X, Zhao X, Wang Z, Yang X, Tang Q, He G, Zhou G, Kong Y. 2016. Xylan synthesized by Irregular Xylem 14 (IRX14) maintains the structure of seed coat mucilage in Arabidopsis. *J. Exp. Bot.*:erv510.
- Huang J, DeBowles D, Esfandiari E, Dean G, Carpita NC, Haughn GW. 2011. The Arabidopsis transcription factor LUH/MUM1 is required for extrusion of seed coat mucilage. *Plant Physiol.* 156:491–502.
- Huang Z, Boubriak I, Osborne DJ, Dong M, Gutterman Y. 2008. Possible role of pectin-containing mucilage and dew in repairing embryo DNA of seeds adapted to desert conditions. *Ann. Bot.* 101:277–283.
- Hyde BB. 1970. Mucilage-Producing Cells in the Seed Coat of Plantago ovata: Developmental Fine Structure. *Am. J. Bot.* 57:1197.
- Ibar C, Orellana A. 2007. The import of S-adenosylmethionine into the Golgi apparatus is required for the methylation of homogalacturonan. *Plant Physiol.* 145:504–12.
- Inceer H. 2011. Achene slime content in some taxa of Matricaria L. (Asteraceae). *Acta Bot. Croat.* 70:109–114.
- Ishii T, Konishi T, Ito Y, Ono H, Ohnishi-Kameyama M, Maeda I. 2005. A beta-(1,3)-arabinopyranosyltransferase that transfers a single arabinopyranose onto arabino-

- oligosaccharides in mung bean (*Vigna radiata*) hypocotyls. *Phytochemistry* 66:2418–25.
- Ishii T, Ohnishi-Kameyama M, Ono H. 2004. Identification of elongating beta-1,4-galactosyltransferase activity in mung bean (*Vigna radiata*) hypocotyls using 2-aminobenzaminated 1,4-linked beta-D-galactooligosaccharides as acceptor substrates. *Planta* 219:310–8.
- Ishii T, Ono H, Ohnishi-Kameyama M, Maeda I. 2005. Enzymic transfer of alpha-L-arabinopyranosyl residues to exogenous 1,4-linked beta-D-galacto-oligosaccharides using solubilized mung bean (*Vigna radiata*) hypocotyl microsomes and UDP-beta-L-arabinopyranose. *Planta* 221:953–63.
- Jensen JK, Johnson N, Wilkerson CG. 2013. Discovery of diversity in xylan biosynthetic genes by transcriptional profiling of a heteroxylan containing mucilaginous tissue. *Front. Plant Sci.* 4:183.
- Jensen JK, Johnson NR, Wilkerson CG. 2014. *Arabidopsis thaliana* IRX10 and two related proteins from psyllium and *Physcomitrella patens* are xylan xylosyltransferases. *Plant J.* 80:207–215.
- Jensen JK, Sørensen SO, Harholt J, Geshi N, Sakuragi Y, Møller I, Zandleven J, Bernal AJ, Jensen NB, Sørensen C, et al. 2008. Identification of a xylogalacturonan xylosyltransferase involved in pectin biosynthesis in *Arabidopsis*. *Plant Cell* 20:1289–302.
- Jofuku KD, den Boer BG, Van Montagu M, Okamoto JK. 1994. Control of *Arabidopsis* flower and seed development by the homeotic gene APETALA2. *Plant Cell* 6:1211–1225.
- Johnson CS, Kolevski B, Smyth DR. 2002. TRANSPARENT TESTA GLABRA2, a trichome and seed coat development gene of *Arabidopsis*, encodes a WRKY transcription factor. *Plant Cell* 14:1359–75.
- Jürgens G. 2005. Cytokinesis in Higher Plants. *Annu. Rev. Plant Biol.* 56:281–299.
- Kaewmanee T, Bagnasco L, Benjakul S, Lanteri S, Morelli CF, Speranza G, Cosulich ME. 2014. Characterisation of mucilages extracted from seven Italian cultivars of flax. *Food Chem.* 148:60–69.
- Kallberg Y, Persson B. 2006. Prediction of coenzyme specificity in dehydrogenases/reductases. A hidden Markov model-based method and its application on complete genomes. *FEBS J.* 273:1177–84.
- Kearse M, Moir R, Wilson A, Stones-Havas S, Cheung M, Sturrock S, Buxton S, Cooper A, Markowitz S, Duran C, et al. 2012. Geneious Basic: an integrated and extendable desktop software platform for the organization and analysis of sequence data. *Bioinformatics* 28:1647–9.
- Kelley DR, Skinner DJ, Gasser CS. 2009. Roles of polarity determinants in ovule development. *Plant J.* 57:1054–64.
- Khalloufi S, Corredig M, Goff HD, Alexander M. 2009. Flaxseed gums and their adsorption on whey protein-stabilized oil-in-water emulsions. *Food Hydrocoll.* 23:611–618.
- Kim B-G, Jung WD, Ahn J-H. 2013. Cloning and characterization of a putative UDP-rhamnose synthase 1 from *Populus euramericana* Guinier. *J. Plant Biol.* 56:7–12.
- Kim J-Y, Oh JE, Noh Y-S, Noh B. 2015. Epigenetic control of juvenile-to-adult phase transition by the *Arabidopsis* SAGA-like complex. *Plant J.* 83:537–45.
- Kiss JZ, Giddings TH, Staehelin L a, Sack FD. 1990. Comparison Of The Ultrastructure Of

- Conventionally Fixed And High-Pressure Frozen Freeze Substituted Root-Tips Of Nicotiana And Arabidopsis. *Protoplasma* 157:64–74.
- Kong Y, Zhou G, Abdeen AA, Schafhauser J, Richardson B, Atmodjo MA, Jung J, Wicker L, Mohnen D, Western T, et al. 2013. GALACTURONOSYLTRANSFERASE-LIKE5 is involved in the production of Arabidopsis seed coat mucilage. *Plant Physiol.* 163:1203–17.
- Kong Y, Zhou G, Yin Y, Xu Y, Pattathil S, Hahn MG. 2011. Molecular analysis of a family of Arabidopsis genes related to galacturonosyltransferases. *Plant Physiol.* 155:1791–1805.
- Konishi T, Kotake T, Tsumuraya Y. 2007. Chain elongation of pectic beta-(1,4)-galactan by a partially purified galactosyltransferase from soybean (*Glycine max* Merr.) hypocotyls. *Planta* 226:571–9.
- Konishi T, Ono H, Ohnishi-Kameyama M, Kaneko S, Ishii T. 2006. Identification of a Mung Bean Arabinofuranosyltransferase That Transfers Arabinofuranosyl Residues onto (1, 5)-Linked α -l-Arabino-Oligosaccharides. *Plant Physiol.* 141:1098–1105.
- Koornneef M. 1981. The complex syndrome of ttg mutants. *Arab. Inf. Serv.:*45–51.
- Kosugi S, Hasebe M, Matsumura N, Takashima H, Miyamoto-Sato E, Tomita M, Yanagawa H. 2009. Six classes of nuclear localization signals specific to different binding grooves of importin?? *J. Biol. Chem.* 284:478–485.
- Kosugi S, Hasebe M, Tomita M, Yanagawa H. 2009. Systematic identification of cell cycle-dependent yeast nucleocytoplasmic shuttling proteins by prediction of composite motifs. *Proc. Natl. Acad. Sci. U. S. A.* 106:10171–10176.
- Kotwal S, Kaul S, Sharma P, Gupta M, Shankar R, Jain M, Dhar MK. 2016. De Novo Transcriptome Analysis of Medicinally Important *Plantago ovata* Using RNA-Seq. *PLoS One* 11:e0150273.
- Kraemer BH. 1898. Botanical Medicine Monographs and Sundry ORIGIN AND DETECTION OF MUCILAGE IN PLANTS . *Am. J. Pharm.* 70.
- Kreitschitz A. 2009. Functional Surfaces in Biology: Little Structures with Big Effects Volume 1. In: Gorb SN, editor. Dordrecht: Springer Netherlands. p. 11–30.
- Kreitschitz A, Kovalev A, Gorb SN. 2015. Slipping vs sticking: water-dependent adhesive and frictional properties of *Linum usitatissimum* L. seed mucilaginous envelope and its biological significance. *Acta Biomater.* 17:152–9.
- Kreitschitz A, Tadele Z, Gola EM. 2009. Slime cells on the surface of *Eragrostis* seeds maintain a level of moisture around the grain to enhance germination. *Seed Sci. Res.* 19:27.
- Kreitschitz A, Vallès J. 2007. Achene morphology and slime structure in some taxa of *Artemisia* L. and *Neopallasia* L. (Asteraceae). *Flora - Morphol. Distrib. Funct. Ecol. Plants* 202:570–580.
- Krupková E, Immerzeel P, Pauly M, Schmülling T. 2007. The TUMOROUS SHOOT DEVELOPMENT2 gene of Arabidopsis encoding a putative methyltransferase is required for cell adhesion and co-ordinated plant development. *Plant J.* 50:735–50.
- Kulich I, Cole R, Drdová E, Cvrčková F, Soukup A, Fowler J, Žárský V. 2010. Arabidopsis exocyst subunits SEC8 and EXO70A1 and exocyst interactor ROH1 are involved in the localized deposition of seed coat pectin. *New Phytol.* 188:615–625.
- Kulkarni AR, Peña MJ, Avci U, Mazumder K, Urbanowicz BR, Pattathil S, Yin Y, O'Neill MA, Roberts AW, Hahn MG, et al. 2012. The ability of land plants to synthesize glucuronoxylans

- predates the evolution of tracheophytes. *Glycobiology* 22:439–51.
- Kunieda T, Mitsuda N, Ohme-Takagi M, Takeda S, Aida M, Tasaka M, Kondo M, Nishimura M, Hara-Nishimura I. 2008. NAC family proteins NARS1/NAC2 and NARS2/NAM in the outer integument regulate embryogenesis in *Arabidopsis*. *Plant Cell* 20:2631–42.
- Kunieda T, Shimada T, Kondo M, Nishimura M, Nishitani K, Hara-Nishimura I. 2013. Spatiotemporal secretion of PEROXIDASE36 is required for seed coat mucilage extrusion in *Arabidopsis*. *Plant Cell* 25:1355–67.
- Lago C, Clerici E, Dreni L, Horlow C, Caporali E, Colombo L, Kater MM. 2005. The *Arabidopsis* TFIID factor AtTAF6 controls pollen tube growth. *Dev. Biol.* 285:91–100.
- Lago C, Clerici E, Mizzi L, Colombo L, Kater MM. 2004. TBP-associated factors in *Arabidopsis*. *Gene* 342:231–241.
- Lawit SJ, O’Grady K, Gurley WB, Czarnecka-Verner E. 2007. Yeast two-hybrid map of *Arabidopsis* TFIID. *Plant Mol. Biol.* 64:73–87.
- Lee C, O’Neill MA, Tsumuraya Y, Darvill AG, Ye ZH. 2007. The irregular xylem9 mutant is deficient in Xylan xylosyltransferase activity. *Plant Cell Physiol.* 48:1624–1634.
- Lee C, Teng Q, Huang W, Zhong R, Ye Z-H. 2010. The *Arabidopsis* family GT43 glycosyltransferases form two functionally nonredundant groups essential for the elongation of glucuronoxylan backbone. *Plant Physiol.* 153:526–41.
- Lee C, Teng Q, Zhong R, Ye Z-H. 2011. The four *Arabidopsis* reduced wall acetylation genes are expressed in secondary wall-containing cells and required for the acetylation of xylan. *Plant Cell Physiol.* 52:1289–301.
- Lee C, Zhong R, Ye Z-H. 2012. *Arabidopsis* family GT43 members are xylan xylosyltransferases required for the elongation of the xylan backbone. *Plant Cell Physiol.* 53:135–43.
- Lerouxel O, Cavalier DM, Liepman AH, Keegstra K. 2006. Biosynthesis of plant cell wall polysaccharides - a complex process. *Curr. Opin. Plant Biol.* 9:621–630.
- Levesque-Tremblay G, Pelloux J, Braybrook SA, Müller K. 2015. Tuning of pectin methylesterification: consequences for cell wall biomechanics and development. *Planta* 242:791–811.
- Leyser O. 2005. The fall and rise of apical dominance. *Curr. Opin. Genet. Dev.* 15:468–471.
- Li S, Bashline L, Lei L, Gu Y. 2014. Cellulose Synthesis and its Regulation. In: *The Arabidopsis Book*. 12th ed. p. e0169.
- Li SF, Milliken ON, Pham H, Seyit R, Napoli R, Preston J, Koltunow AM, Parish RW. 2009. The *Arabidopsis* MYB5 Transcription Factor Regulates Mucilage Synthesis, Seed Coat Development, and Trichome Morphogenesis. *Plant Cell Online* 21:72–89.
- Lin Q, Qing L, Aoyama T. 2012. Pathways for epidermal cell differentiation via the homeobox gene *GLABRA2*: update on the roles of the classic regulator. *J. Integr. Plant Biol.* 54:729–37.
- Lindner M, Simonini S, Kooiker M, Gagliardini V, Somssich M, Hohenstatt M, Simon R, Grossniklaus U, Kater MM. 2013. TAF13 interacts with PRC2 members and is essential for *Arabidopsis* seed development. *Dev. Biol.* 379:28–37.
- Liu X-L, Liu L, Niu Q-K, Xia C, Yang K-Z, Li R, Chen L-Q, Zhang X-Q, Zhou Y, Ye D. 2011. Male gametophyte defective 4 encodes a rhamnogalacturonan II xylosyltransferase and is important for growth of pollen tubes and roots in *Arabidopsis*. *Plant J.* 65:647–60.

- Liu Y, Douglas CJ. 2015. A role for OVATE FAMILY PROTEIN1 (OFP1) and OFP4 in a BLH6-KNAT7 multi-protein complex regulating secondary cell wall formation in *Arabidopsis thaliana*. *Plant Signal. Behav.* 2324:00–00.
- Livak KJ, Schmittgen TD. 2001. Analysis of Relative Gene Expression Data Using Real-Time Quantitative PCR and the $\Delta\Delta C_T$ Method. *METHODS* 25:402–408.
- Liwanag AJM, Ebert B, Verhertbruggen Y, Rennie EA, Rautengarten C, Oikawa A, Andersen MCF, Clausen MH, Scheller HV. 2012. Pectin biosynthesis: GAL51 in *Arabidopsis thaliana* is a β -1,4-galactan β -1,4-galactosyltransferase. *Plant Cell* 24:5024–36.
- Lobova TA, Mori SA, Blanchard F, Peckham H, Charles-Dominique P. 2003. Cecropia as a food resource for bats in French Guiana and the significance of fruit structure in seed dispersal and longevity. *Am. J. Bot.* 90:388–403.
- Lund CH, Bromley JR, Stenbæk A, Rasmussen RE, Scheller H V, Sakuragi Y. 2015. A reversible Renilla luciferase protein complementation assay for rapid identification of protein-protein interactions reveals the existence of an interaction network involved in xyloglucan biosynthesis in the plant Golgi apparatus. *J. Exp. Bot.* 66:85–97.
- Luo M, Dennis ES, Berger F, Peacock WJ, Chaudhury A. 2005. MINISEED3 (MINI3), a WRKY family gene, and HAIKU2 (IKU2), a leucine-rich repeat (LRR) KINASE gene, are regulators of seed size in *Arabidopsis*. *Proc. Natl. Acad. Sci.* 102:17531–17536.
- Macquet A, Ralet MC, Kronenberger J, Marion-Poll A, North HM. 2007. In situ, chemical and macromolecular study of the composition of *Arabidopsis thaliana* seed coat mucilage. *Plant Cell Physiol.* 48:984–999.
- Macquet A, Ralet M-C, Kronenberger J, Marion-Poll A, North HM. 2007. In situ, Chemical and Macromolecular Study of the Composition of *Arabidopsis thaliana* Seed Coat Mucilage. *Plant Cell Physiol.* 48:984–999.
- Macquet A, Ralet M-C, Loudet O, Kronenberger J, Mouille G, Marion-Poll A, North HM. 2007. A naturally occurring mutation in an *Arabidopsis* accession affects a beta-D-galactosidase that increases the hydrophilic potential of rhamnogalacturonan I in seed mucilage. *Plant Cell* 19:3990–4006.
- Manabe Y, Nafisi M, Verhertbruggen Y, Orfila C, Gille S, Rautengarten C, Cherk C, Marcus SE, Somerville S, Pauly M, et al. 2011. Loss-of-function mutation of REDUCED WALL ACETYLATION2 in *Arabidopsis* leads to reduced cell wall acetylation and increased resistance to *Botrytis cinerea*. *Plant Physiol.* 155:1068–78.
- Marchler-Bauer A, Derbyshire MK, Gonzales NR, Lu S, Chitsaz F, Geer LY, Geer RC, He J, Gwadz M, Hurwitz DI, et al. 2015. CDD: NCBI's conserved domain database. *Nucleic Acids Res.* 43:D222–D226.
- Martinez E, Kundu TK, Fu J, Roeder RG. 1998. A human SPT3-TAFII31-GCN5-L acetylase complex distinct from transcription factor IID. *J. Biol. Chem.* 273:23781–5.
- Martinez E, Palhan VB, Tjernberg a, Lyman ES, Gamper a M, Kundu TK, Chait BT, Roeder RG. 2001. Human STAGA complex is a chromatin-acetylating transcription coactivator that interacts with pre-mRNA splicing and DNA damage-binding factors in vivo. *Mol. Cell. Biol.* 21:6782–6795.
- Mazza G, Biliaderis CG. 1989. Functional Properties of Flax Seed Mucilage. *J. Food Sci.* 54:1302–1305.

- McAbee JM, Hill TA, Skinner DJ, Izhaki A, Hauser BA, Meister RJ, Venugopala Reddy G, Meyerowitz EM, Bowman JL, Gasser CS. 2006. Aberrant testa shape encodes a KANADI family member, linking polarity determination to separation and growth of Arabidopsis ovule integuments. *Plant J.* 46:522–531.
- McCartney L, Marcus SE, Knox JP. 2005. Monoclonal antibodies to plant cell wall xylans and arabinoxylans. *J. Histochem. Cytochem.* 53:543–6.
- McFarlane HE, Döring A, Persson S. 2014. The cell biology of cellulose synthesis. *Annu. Rev. Plant Biol.* 65:69–94.
- McFarlane HE, Watanabe Y, Gendre D, Carruthers K, Levesque-Tremblay G, Haughn GW, Bhalerao RP, Samuels L. 2013. Cell wall polysaccharides are mislocalized to the vacuole in echidna Mutants. *Plant Cell Physiol.* 54:1867–1880.
- McFarlane HE, Young RE, Wasteneys GO, Samuels a. L. 2008. Cortical microtubules mark the mucilage secretion domain of the plasma membrane in Arabidopsis seed coat cells. *Planta* 227:1363–1375.
- Mendu V, Griffiths JS, Persson S, Stork J, Downie AB, Voiniciuc C, Haughn GW, DeBolt S. 2011. Subfunctionalization of Cellulose Synthases in Seed Coat Epidermal Cells Mediates Secondary Radial Wall Synthesis and Mucilage Attachment. *Plant Physiol.* 157:441–453.
- Miao Y, Li H, Shen J, Wang J, Jiang L. 2011. QUASIMODO 3 (QUA3) is a putative homogalacturonan methyltransferase regulating cell wall biosynthesis in Arabidopsis suspension-cultured cells. 00740:1–16.
- Michael TP, VanBuren R. 2015. Progress, challenges and the future of crop genomes. *Curr. Opin. Plant Biol.* 24:71–81.
- Moffatt BA, Stevens YY, Allen MS, Snider JD, Pereira LA, Todorova MI, Summers PS, Weretilnyk EA, Martin-mccaffrey L, Wagner C. 2002. Adenosine Kinase Deficiency Is Associated with Developmental Abnormalities and Reduced Transmethylation. *Plant Physiol.* 128:812–821.
- Mohnen D. 2008. Pectin structure and biosynthesis. *Curr. Opin. Plant Biol.* 11:266–277.
- Mølhøj M, Verma R, Reiter W-D. 2004. The Biosynthesis of d-Galacturonate in Plants. Functional Cloning and Characterization of a Membrane-Anchored UDP-d-Glucuronate 4-Epimerase from Arabidopsis. *Plant Physiol.* 135:1221–1230.
- Moore PJ, Swords KMM, Lynch MA, Staehelin LA. 1991. Spatial organization of the assembly pathways of glycoproteins and complex polysaccharides in the Golgi apparatus of plants. *J. Cell Biol.* 112:589–602.
- Mott J. 1974. Factors affecting seed germination in three annual species from an arid region of Western Australia. *J. Ecol.* 62:699–709.
- Mouille G, Ralet M-C, Cavelier C, Eland C, Effroy D, Hématy K, McCartney L, Truong HN, Gaudon V, Thibault J-F, et al. 2007. Homogalacturonan synthesis in Arabidopsis thaliana requires a Golgi-localized protein with a putative methyltransferase domain. *Plant J.* 50:605–14.
- Muñoz LA, Cobos A, Diaz O, Aguilera JM. 2012. Chia seeds: Microstructure, mucilage extraction and hydration. *J. Food Eng.* 108:216–224.
- Munoz P, Norambuena L, Orellana a. 1996. Evidence for a UDP-Glucose Transporter in Golgi Apparatus-Derived Vesicles from Pea and Its Possible Role in Polysaccharide Biosynthesis.

- Plant Physiol. 112:1585–1594.
- Muralikrishna G, Salimath P V., Tharanathan RN. 1987. Structural features of an arabinoxylan and a rhamno-galacturonan derived from linseed mucilage.pdf. Carbohydr. Res. 161:265–271.
- Naran R, Chen G, Carpita NC. 2008. Novel rhamnogalacturonan I and arabinoxylan polysaccharides of flax seed mucilage. Plant Physiol. 148:132–41.
- North HM, Berger A, Saez-Aguayo S, Ralet MC. 2014. Understanding polysaccharide production and properties using seed coat mutants: Future perspectives for the exploitation of natural variants. Ann. Bot. 114:1251–1263.
- O'Brien TP, Feder N, McCully ME. 1964. Polychromatic staining of plant cell walls by toluidine blue O. Protoplasma 59:368–373.
- O'Neill MA, Ishii T, Albersheim P, Darvill AG. 2004. Rhamnogalacturonan II: structure and function of a borate cross-linked cell wall pectic polysaccharide. Annu. Rev. Plant Biol. 55:109–39.
- ØBro J, Harholt J, Scheller HV, Orfila C. 2004. Rhamnogalacturonan I in *Solanum tuberosum* tubers contains complex arabinogalactan structures. Phytochemistry 65:1429–38.
- Odell JT, Nagy F, Chua N-H. 1985. Identification of DNA sequences required for activity of the cauliflower mosaic virus 35S promoter. Nature 313:810–812.
- Ogryzko V V, Kotani T, Zhang X, Schiltz RL, Howard T, Yang X-J, Howard BH, Qin J, Nakatani Y. 1998. Histone-like TAFs within the PCAF Histone Acetylase Complex. Cell 94:35–44.
- Ohto M, Floyd SK, Fischer RL, Goldberg RB, Harada JJ. 2009. Effects of APETALA2 on embryo, endosperm, and seed coat development determine seed size in *Arabidopsis*. Sex. Plant Reprod. 22:277–289.
- Oikawa A, Lund CH, Sakuragi Y, Scheller H V. 2013. Golgi-localized enzyme complexes for plant cell wall biosynthesis. Trends Plant Sci. 18:49–58.
- Oka T, Nemoto T, Jigami Y. 2007. Functional Analysis of *Arabidopsis thaliana* RHM2/MUM4, a Multidomain Protein Involved in UDP-D-glucose to UDP-L-rhamnose Conversion. J. Biol. Chem. 282:5389–5403.
- Oomah BD, Kenaschuk E, Cui W, Mazza G. 1995. Variation in the Composition of Water-Soluble Polysaccharides in Flaxseed. J. Agric. Food Chem. 43:1484–1488.
- Orfila C, Sørensen SO, Harholt J, Geshi N, Crombie H, Truong H-N, Reid JSG, Knox JP, Scheller HV. 2005. QUASIMODO1 is expressed in vascular tissue of *Arabidopsis thaliana* inflorescence stems, and affects homogalacturonan and xylan biosynthesis. Planta 222:613–22.
- Pan Y, Wang X, Liu H, Zhang G, Ma Z. 2010. Molecular Cloning of Three UDP-Glucuronate Decarboxylase Genes That Are Preferentially Expressed In *Gossypium* Fibers From Elongation to Secondary Cell Wall Synthesis. J. Plant Biol. 53:367–373.
- Park YB, Cosgrove DJ. 2015. Xyloglucan and its interactions with other components of the growing cell wall. Plant Cell Physiol. 56:180–194.
- Pattathil S, Avci U, Baldwin D, Swennes AG, McGill JA, Popper Z, Bootten T, Albert A, Davis RH, Chennareddy C, et al. 2010. A comprehensive toolkit of plant cell wall glycan-directed monoclonal antibodies. Plant Physiol. 153:514–25.
- Pattathil S, Harper AD, Bar-Peled M. 2005. Biosynthesis of UDP-xylose: Characterization of

- membrane-bound At Uxs2. *Planta* 221:538–548.
- Pavlov A, Paynel F, Rihouey C, Porokhvinova E, Brutch N, Morvan C. 2014. Variability of seed traits and properties of soluble mucilages in lines of the flax genetic collection of Vavilov Institute. *Plant Physiol Biochem* 80:348–361.
- Paynel F, Pavlov A, Ancelin G, Rihouey C, Picton L, Lebrun L, Morvan C. 2013. Polysaccharide hydrolases are released with mucilages after water hydration of flax seeds. *Plant Physiol. Biochem.* 62:54–62.
- Penfield S, Meissner RC, Shoue DA, Carpita NC, Bevan MW. 2001. MYB61 is required for mucilage deposition and extrusion in the Arabidopsis seed coat. *Plant Cell* 13:2777–91.
- Persson S, Caffall KH, Freshour G, Hilley MT, Bauer S, Poindexter P, Hahn MG, Mohnen D, Somerville C. 2007. The Arabidopsis irregular xylem8 mutant is deficient in glucuronoxylan and homogalacturonan, which are essential for secondary cell wall integrity. *Plant Cell* 19:237–55.
- Petersen BL, Egelund J, Damager I, Faber K, Jensen JK, Yang Z, Bennett EP, Scheller HV, Ulvskov P. 2009. Assay and heterologous expression in *Pichia pastoris* of plant cell wall type-II membrane anchored glycosyltransferases. *Glycoconj. J.* 26:1235–46.
- Peugnet I, Goubet F, Bruyant-Vannier MP, Thoiron B, Morvan C, Schols HA, Voragen AG. 2001. Solubilization of rhamnogalacturonan I galactosyltransferases from membranes of a flax cell suspension. *Planta* 213:435–45.
- Pointud J-C, Mengus G, Brancorsini S, Monaco L, Parvinen M, Sassone-Corsi P, Davidson I. 2003. The intracellular localisation of TAF7L, a paralogue of transcription factor TFIID subunit TAF7, is developmentally regulated during male germ-cell differentiation. *J. Cell Sci.* 116:1847–1858.
- Ralet M-C, Crépeau M-J, Vigouroux J, Tran J, Berger A, Sallé C, Granier F, Botran L, North HM. 2016. The affinity of xylan branches on rhamnogalacturonan I for cellulose provides the structural driving force for mucilage adhesion to the Arabidopsis seed coat. *Plant Physiol.*:pp.00211.2016.
- Ranocha P, Francoz E, Burlat V, Dunand C. 2014. Expression of PRX36, PME16 and SBT1.7 is controlled by complex transcription factor regulatory networks for proper seed coat mucilage extrusion. *Plant Signal. Behav.*
- Rautengarten C, Ebert B, Moreno I, Temple H, Herter T, Link B, Doñas-Cofré D, Moreno A, Saéz-Aguayo S, Blanco F, et al. 2014. The Golgi localized bifunctional UDP-rhamnose/UDP-galactose transporter family of Arabidopsis. *Proc. Natl. Acad. Sci. U. S. A.* 111:11563–8.
- Rautengarten C, Usadel B, Neumetzler L, Hartmann J, Büssis D, Altmann T. 2008. A subtilisin-like serine protease essential for mucilage release from Arabidopsis seed coats. *Plant J.* 54:466–480.
- Reiter W-D. 2008. Biochemical genetics of nucleotide sugar interconversion reactions. *Curr. Opin. Plant Biol.* 11:236–43.
- Reiter WD, Vanzin GF. 2001. Molecular genetics of nucleotide sugar interconversion pathways in plants. *Plant Mol. Biol.* 47:95–113.
- Ren Y, Hansen SF, Ebert B, Lau J, Scheller HV. 2014. Site-Directed Mutagenesis of IRX9, IRX9L and IRX14 Proteins Involved in Xylan Biosynthesis: Glycosyltransferase Activity Is Not Required for IRX9 Function in Arabidopsis. *PLoS One* 9:e105014.

- Rennie EA, Scheller HV. 2014. Xylan biosynthesis. *Curr. Opin. Biotechnol.* 26:100–107.
- Rerie WG, Feldmann KA, Marks MD. 1994. The GLABRA2 gene encodes a homeo domain protein required for normal trichome development in *Arabidopsis*. *Genes Dev.* 8:1388–99.
- Reyes F, Orellana A. 2008. Golgi transporters: opening the gate to cell wall polysaccharide biosynthesis. *Curr. Opin. Plant Biol.* 11:244–251.
- Riefler M, Novak O, Strnad M, Schmülling T. 2006. *Arabidopsis* Cytokinin Receptor Mutants Reveal Functions in Shoot Growth, Leaf Senescence, Seed Size, Germination, Root Development, and Cytokinin Metabolism. *PLANT CELL ONLINE* 18:40–54.
- Robles LM, Wampole JS, Christians MJ, Larsen PB. 2007. *Arabidopsis* enhanced ethylene response 4 encodes an EIN3-interacting TFIID transcription factor required for proper ethylene response, including ERF1 induction. *J. Exp. Bot.* 58:2627–2639.
- Romano JM, Dubos C, Prouse MB, Wilkins O, Hong H, Poole M, Kang KY, Li E, Douglas CJ, Western TL, et al. 2012. AtMYB61, an R2R3-MYB transcription factor, functions as a pleiotropic regulator via a small gene network. *New Phytol.* 195:774–786.
- Rösti J, Barton CJ, Albrecht S, Dupree P, Pauly M, Findlay K, Roberts K, Seifert GJ. 2007. UDP-glucose 4-epimerase isoforms UGE2 and UGE4 cooperate in providing UDP-galactose for cell wall biosynthesis and growth of *Arabidopsis thaliana*. *Plant Cell* 19:1565–79.
- Ryding O. 2001. Myxocarpy in the Nepetoideae (Lamiaceae) with notes on mxyodiaspory in general. *Syst. Geogr. Plants*:502–514.
- Saeedi M, Morteza-Semnani K, Ansoroudi F, Fallah S, Amin G. 2010. Evaluation of binding properties of *Plantago psyllium* seed mucilage. *Acta Pharm.* 60:339–48.
- Saez-Aguayo S, Ralet M-C, Berger A, Botran L, Ropartz D, Marion-Poll A, North HM. 2013. PECTIN METHYLESTERASE INHIBITOR6 promotes *Arabidopsis* mucilage release by limiting methylesterification of homogalacturonan in seed coat epidermal cells. *Plant Cell* 25:308–23.
- Saurin AJ, Shao Z, Erdjument-Bromage H, Tempst P, Kingston RE. 2001. A *Drosophila* Polycomb group complex includes Zeste and dTAFII proteins. *Nature* 412:655–60. Scheible WR, Pauly M. 2004. Glycosyltransferases and cell wall biosynthesis: Novel players and insights. *Curr. Opin. Plant Biol.* 7:285–295.
- Schmid M, Davison TS, Henz SR, Pape UJ, Demar M, Vingron M, Schölkopf B, Weigel D, Lohmann JU. 2005. A gene expression map of *Arabidopsis thaliana* development. *Nat. Genet.* 37:501–6.
- Schnepf E, Deichgraber G. 1983a. Structure and Formation of Fibrillar Mucilages in Seed Epidermis Cells II. *Ruellia* (Acanthaceae). *Protoplasma* 234:222–234.
- Schnepf E, Deichgraber G. 1983b. Structure and formation of fibrillar mucilage in seed epidermis cells. *Protoplasma* 114:210–221.
- Schruff MC, Spielman M, Tiwari S, Adams S, Fenby N, Scott RJ. 2005. The AUXIN RESPONSE FACTOR 2 gene of *Arabidopsis* links auxin signalling, cell division, and the size of seeds and other organs. *Development* 133: 531–541.
- Schultink A, Naylor D, Dama M, Pauly M. 2015. The role of the plant-specific ALTERED XYLOGLUCAN9 protein in *Arabidopsis* cell wall polysaccharide O-acetylation. *Plant Physiol.* 167:1271–83.
- Seifert GJ. 2004. Nucleotide sugar interconversions and cell wall biosynthesis: how to bring the

- inside to the outside. *Curr. Opin. Plant Biol.* 7:277–84.
- Sharma P, Koul A. 1986. Mucilage in seeds of *Plantago ovata* and its wild allies. *J. Ethnopharmacol.* 17:289–295.
- Sonnhammer EL, von Heijne G, Krogh A. 1998. A hidden Markov model for predicting transmembrane helices in protein sequences. *Proc. Int. Conf. Intell. Syst. Mol. Biol.* 6:175–82.
- Soutoglou E, Demeny MA, Scheer E, Fienga G, Sassone-Corsi P, Tora L. 2005. The Nuclear Import of TAF10 Is Regulated by One of Its Three Histone Fold Domain-Containing Interaction Partners. *Mol. Cell. Biol.* 25:4092–4104.
- Spurr AR. 1969. A low-viscosity epoxy resin embedding medium for electron microscopy. *J. Ultrastruct. Res.* 26:31–43.
- Srinivas M, Joshi S, Krishnan R. 1998. Ontogeny of solasodine-containing mucilage layer in *Solanum viarum* Dunal, ploidy types. *J. Biosci.* 23:155–162.
- Staehelin LA, Giddings TH, Kiss JZ, Sack FD. 1990. Macromolecular differentiation of Golgi stacks in root tips of *Arabidopsis* and *Nicotiana* seedlings as visualized in high pressure frozen and freeze-substituted samples. *Protoplasma* 157:75–91.
- Sterling C. 1970. Crystal-Structure of Ruthenium Red and Stereochemistry of its Pectic Stain Author (s): Clarence Sterling Published by : Botanical Society of America
- Sterling JD, Quigley HF, Orellana A, Mohnen D. 2001. The catalytic site of the pectin biosynthetic enzyme alpha-1,4-galacturonosyltransferase is located in the lumen of the Golgi. *Plant Physiol.* 127:360–71.
- Stork J, Harris D, Griffiths J, Williams B, Beisson F, Li-Beisson Y, Mendu V, Haughn G, Debolt S. 2010. CELLULOSE SYNTHASE9 serves a nonredundant role in secondary cell wall synthesis in *Arabidopsis* epidermal testa cells. *Plant Physiol.* 153:580–9.
- Sullivan S, Ralet M-C, Berger A, Diatloff E, Bischoff V, Gonneau M, Marion-Poll A, North HM. 2011. CESA5 is required for the synthesis of cellulose with a role in structuring the adherent mucilage of *Arabidopsis* seeds. *Plant Physiol.* 156:1725–39.
- Sun Y, Tan DY, Baskin CC, Baskin JM. 2012. Role of mucilage in seed dispersal and germination of the annual ephemeral *Alyssum minus* (Brassicaceae). *Aust. J. Bot.* 60 :439–449.
- Sveinsson S, McDill J, Wong GKS, Li J, Li X, Deyholos MK, Cronk QCB. 2014. Phylogenetic pinpointing of a paleopolyploidy event within the flax genus (*Linum*) using transcriptomics. *Ann. Bot.* 113:753–761.
- Swarbrick J. 1971. External mucilage production by seeds of British plants. *J. Linn. Soc.* 64:157–162.
- Tamada Y, Nakamori K, Nakatani H, Matsuda K, Hata S, Furumoto T, Izui K. 2007. Temporary expression of the TAF10 gene and its requirement for normal development of *Arabidopsis thaliana*. *Plant Cell Physiol.* 48:134–46.
- Tan L, Eberhard S, Pattathil S, Warder C, Glushka J, Yuan C, Hao Z, Zhu X, Avci U, Miller JS, et al. 2013. An *Arabidopsis* cell wall proteoglycan consists of pectin and arabinoxylan covalently linked to an arabinogalactan protein. *Plant Cell* 25:270–87.
- Tanaka M, Takei K, Kojima M, Sakakibara H, Mori H. 2006. Auxin controls local cytokinin biosynthesis in the nodal stem in apical dominance. *Plant J.* 45:1028–1036.
- Thomas MC, Chiang C-M. 2006. The general transcription machinery and general cofactors. *Crit.*

- Rev. Biochem. Mol. Biol. 41:105–178.
- Turbant A, Fournet F, Lequart M, Zabijak L, Pageau K, Bouton S, Van Wuytswinkel O. 2016. PME58 plays a role in pectin distribution during seed coat mucilage extrusion through homogalacturonan modification. *J. Exp. Bot.* 67:2177–90.
- Turner W, Botha FC. 2002. Purification and kinetic properties of UDP-glucose dehydrogenase from sugarcane. *Arch. Biochem. Biophys.* 407:209–216.
- Urbanowicz BR, Pena MJ, Moniz HA, Moremen KW, York WS. 2014. Two Arabidopsis proteins synthesize acetylated xylan in vitro. *Plant J.* 80:197–206.
- Usadel B, Kuschinsky AM, Rosso MG, Eckermann N, Pauly M. 2004. RHM2 is involved in mucilage pectin synthesis and is required for the development of the seed coat in Arabidopsis. *Plant Physiol.* 134:286–295.
- Vasilevski A, Giorgi FM, Bertinetti L, Usadel B. 2012. LASSO modeling of the Arabidopsis thaliana seed/seedling transcriptome: a model case for detection of novel mucilage and pectin metabolism genes. *Mol. Biosyst.* 8:2566–74.
- Vaughan JG, Whitehouse JM. 1971. Seed structure and the taxonomy of the Cruciferae. *Bot. J. Linn. Soc.* 64:383–409.
- Venglat P, Xiang D, Qiu S, Stone SL, Tibiche C, Cram D, Alting-Mees M, Nowak J, Cloutier S, Deyholos M, et al. 2011. Gene expression analysis of flax seed development. *BMC Plant Biol.* 11:74.
- Verherbruggen Y, Marcus SE, Haeger A, Ordaz-Ortiz JJ, Knox JP. 2009. An extended set of monoclonal antibodies to pectic homogalacturonan. *Carbohydr. Res.* 344:1858–62. Vicré M, Santaella C, Blanchet S, Gateau A. 2005. Root Border-Like Cells of Arabidopsis . *Microscopical Characterization and Rol.* 138:998–1008.
- Voiniciuc C, Dean GH, Griffiths JS, Kirchsteiger K, Hwang YT, Gillett A, Dow G, Western TL, Estelle M, Haughn GW. 2013. FLYING SAUCER1 Is a Transmembrane RING E3 Ubiquitin Ligase That Regulates the Degree of Pectin Methylesterification in Arabidopsis Seed Mucilage. *Plant Cell* 25 :944–959.
- Voiniciuc C, Guenl M, Schmidt MH-W, Usadel B. 2015. Highly Branched Xylan Made by IRX14 and MUCI21 Links Mucilage to Arabidopsis Seeds. *Plant Physiol.* 49:pp.01441.2015.
- Voiniciuc C, Schmidt MH-W, Berger A, Yang B, Ebert B, Scheller H V., North HM, Usadel B, Günl M. 2015. MUCILAGE-RELATED10 Produces Galactoglucomannan That Maintains Pectin and Cellulose Architecture in Arabidopsis Seed Mucilage. *Plant Physiol.* 169:403–420.
- Voiniciuc C, Yang B, Schmidt M, Günl M, Usadel B. 2015. Starting to Gel: How Arabidopsis Seed Coat Epidermal Cells Produce Specialized Secondary Cell Walls. *Int. J. Mol. Sci.* 16:3452–3473.
- Walker AR, Davison PA, Bolognesi-Winfield AC, James CM, Srinivasan N, Blundell TL, Esch JJ, Marks MD, Gray JC. 1999. The TRANSPARENT TESTA GLABRA1 locus, which regulates trichome differentiation and anthocyanin biosynthesis in Arabidopsis, encodes a WD40 repeat protein. *Plant Cell* 11:1337–50.
- Walker M, Tehseen M, Doblin MS, Pettolino FA, Wilson SM, Bacic A, Golz JF. 2011. The transcriptional regulator LEUNIG_HOMOLOG regulates mucilage release from the Arabidopsis testa. *Plant Physiol.* 156:46–60.

- Wang A, Garcia D, Zhang H, Feng K, Chaudhury A, Berger F, Peacock WJ, Dennis ES, Luo M. 2010. The VQ motif protein IKU1 regulates endosperm growth and seed size in *Arabidopsis*. *Plant J.* 63:670–679.
- Wang J, Ji Q, Jiang L, Shen S, Fan Y, Zhang C. 2009. Overexpression of a cytosol-localized rhamnose biosynthesis protein encoded by *Arabidopsis* RHM1 gene increases rhamnose content in cell wall. *Plant Physiol. Biochem.* 47:86–93.
- Wang T, Park YB, Cosgrove DJ, Hong M. 2015. Cellulose-Pectin Spatial Contacts Are Inherent to Never-Dried *Arabidopsis* Primary Cell Walls: Evidence from Solid-State Nuclear Magnetic Resonance. *Plant Physiol.* 168:871–884.
- Warrand J, Michaud P, Picton L, Muller G, Courtois B, Ralainirina R, Courtois J. 2003. Large-scale purification of water-soluble polysaccharides from flaxseed mucilage, and isolation of a new anionic polymer. *Chromatographia* 58:331–335.
- Watt G, Leoff C, Harper AD, Bar-Peled M. 2004. A bifunctional 3,5-epimerase/4-keto reductase for nucleotide-rhamnose synthesis in *Arabidopsis*. *Plant Physiol.* 134:1337–46.
- Western TL. 2000. Differentiation of Mucilage Secretory Cells of the *Arabidopsis* Seed Coat. *Plant Physiol.* 122:345–356.
- Western TL. 2012. The sticky tale of seed coat mucilages: production, genetics, and role in seed germination and dispersal. *Seed Sci. Res.* 23:1–25.
- Western TL, Burn J, Tan WL, Skinner DJ, Martin-McCaffrey L, Moffatt BA, Haughn GW. 2001. Isolation and characterization of mutants defective in seed coat mucilage secretory cell development in *Arabidopsis*. *Plant Physiol.* 127:998–1011.
- Western TL, Skinner DJ, Haughn GW. 2000. Differentiation of Mucilage Secretory Cells of the *Arabidopsis* Seed Coat. *Plant Physiol.* 122:345–356.
- Western TL, Young DS, Dean GH, Tan WL, Samuels a L, Haughn GW. 2004. MUCILAGE-MODIFIED4 encodes a putative pectin biosynthetic enzyme developmentally regulated by APETALA2, TRANSPARENT TESTA GLABRA1, and GLABRA2 in the *Arabidopsis* seed coat. *Plant Physiol.* 134:296–306.
- Wieczorek E, Brand M, Jacq X, Tora L. 1998. Function of TAF(II)-containing complex without TBP in transcription by RNA polymerase II. *Nature* 393:187–91.
- Wightman R, Turner S. 2010. Trafficking of the Plant Cellulose Synthase Complex. *Plant Physiol.* 153 :427–432.
- Willats WG, Limberg G, Buchholt HC, van Alebeek GJ, Benen J, Christensen TM, Visser J, Voragen A, Mikkelsen JD, Knox JP. 2000. Analysis of pectic epitopes recognised by hybridoma and phage display monoclonal antibodies using defined oligosaccharides, polysaccharides, and enzymatic degradation. *Carbohydr. Res.* 327:309–20.
- Willats WGT, McCartney L, Knox JP. 2001. In-situ analysis of pectic polysaccharides in seed mucilage and at the root surface of *Arabidopsis thaliana*. *Planta* 213:37–44.
- Willats WGT, Orfila C, Limberg G, Buchholt HC, Van Alebeek GJWM, Voragen AGJ, Marcus SE, Christensen TMIE, Mikkelsen JD, Murray BS, et al. 2001. Modulation of the degree and pattern of methyl-esterification of pectic homogalacturonan in plant cell walls: Implications for pectin methyl esterase action, matrix properties, and cell adhesion. *J. Biol. Chem.* 276:19404–19413.
- Wilson CL. 1960. *Anatomy of Seed Plants*. Katherine Esau. Wiley, New York, 1960. viii + 376

- pp. Illus. \$6.95. *Science* (80-.). 131:1727–1728.
- Windsor JB, Symonds VV, Mendenhall J, Lloyd AM. 2000. Arabidopsis seed coat development: Morphological differentiation of the outer integument. *Plant J.* 22:483–493.
- Winter D, Vinegar B, Nahal H, Ammar R, Wilson G V., Provart NJ. 2007. An “Electronic Fluorescent Pictograph” Browser for Exploring and Analyzing Large-Scale Biological Data Sets. Baxter I, editor. *PLoS One* 2:e718.
- Witztum A, Gutterman Y, Evenari M. 1969. Integumentary Mucilage as an Oxygen Barrier During Germination of *Blepharis persica* (Burm.) Kuntze. *Bot. Gaz.* 130:238–241.
- Wu A-M, Hörnblad E, Voxeur A, Gerber L, Rihouey C, Lerouge P, Marchant A. 2010. Analysis of the Arabidopsis IRX9/IRX9-L and IRX14/IRX14-L pairs of glycosyltransferase genes reveals critical contributions to biosynthesis of the hemicellulose glucuronoxylan. *Plant Physiol.* 153:542–54.
- Yang X, Baskin JM, Baskin CC, Huang Z. 2012. More than just a coating: Ecological importance, taxonomic occurrence and phylogenetic relationships of seed coat mucilage. *Perspect. Plant Ecol. Evol. Syst.* 14:434–442.
- Yang X, Dong M, Huang Z. 2010. Role of mucilage in the germination of *Artemisia sphaerocephala* (Asteraceae) achenes exposed to osmotic stress and salinity. *Plant Physiol. Biochem.* 48:131–135.
- Yapo BM. 2011. Pectic substances: From simple pectic polysaccharides to complex pectins - A new hypothetical model. *Carbohydr. Polym.* 86:373–385.
- Yin X-J, Volk S, Ljung K, Mehlmer N, Dolezal K, Ditengou F, Hanano S, Davis SJ, Schmelzer E, Sandberg G, et al. 2007. Ubiquitin Lysine 63 Chain Forming Ligases Regulate Apical Dominance in Arabidopsis. *Plant Cell Online* 19:1898–1911.
- Yin Y, Chen H, Hahn MG, Mohnen D, Xu Y. 2010. Evolution and function of the plant cell wall synthesis-related glycosyltransferase family 8. *Plant Physiol.* 153:1729–46.
- Yin Y, Huang J, Gu X, Bar-Peled M, Xu Y. 2011. Evolution of plant nucleotide-sugar interconversion enzymes. *PLoS One* 6:e27995.
- York WS, O’Neill MA. 2008. Biochemical control of xylan biosynthesis — which end is up? *Curr. Opin. Plant Biol.* 11:258–265.
- Young JA, Evans R. 1973. Mucilaginous seed coats. *Weed Sci.* 21:52–54.
- Young RE, McFarlane HE, Hahn MG, Western TL, Haughn GW, Samuels AL. 2008. Analysis of the Golgi Apparatus in Arabidopsis Seed Coat Cells during Polarized Secretion of Pectin-Rich Mucilage. *Plant Cell Online* 20:1623–1638.
- Yu L, Shi D, Li J, Kong Y, Yu Y, Chai G, Hu R, Wang J, Hahn MG, Zhou G. 2014. CELLULOSE SYNTHASE-LIKE A2, a glucomannan synthase, is involved in maintaining adherent mucilage structure in Arabidopsis seed. *Plant Physiol.* 164:1842–56.
- Yuan Y, Teng Q, Zhong R, Haghighat M, Richardson EA, Ye Z-H, Gille S, Pauly M, Pawar P-A, Koutaniemi S, et al. 2016. Mutations of Arabidopsis TBL32 and TBL33 Affect Xylan Acetylation and Secondary Wall Deposition. Zhang J-S, editor. *PLoS One* 11:e0146460.
- Yuan Y, Teng Q, Zhong R, Ye ZH. 2013. The arabidopsis DUF231 domain-containing protein ESK1 mediates 2-o- and 3-o-acetylation of xylosyl residues in xylan. *Plant Cell Physiol.* 54:1186–1199.
- Yuan Y, Teng Q, Zhong R, Ye Z-H. 2016a. TBL3 and TBL31, Two Arabidopsis DUF231 Domain

- Proteins, are Required for 3-O-Monoacetylation of Xylan. *Plant Cell Physiol.* 57:35–45.
- Yuan Y, Teng Q, Zhong R, Ye Z-H. 2016b. Roles of Arabidopsis TBL34 and TBL35 in xylan acetylation and plant growth. *Plant Sci.* 243:120–30.
- Zabotina OA, Avci U, Cavalier D, Pattathil S, Chou Y-H, Eberhard S, Danhof L, Keegstra K, Hahn MG. 2012. Mutations in multiple XXT genes of Arabidopsis reveal the complexity of xyloglucan biosynthesis. *Plant Physiol.* 159:1367–84.
- Žárský V, Cvrčková F, Potocký M, Hála M. 2009. Exocytosis and cell polarity in plants - exocyst and recycling domains. *New Phytol.* 183:255–272.
- Žárský V, Kulich I, Fendrych M, Pečenková T. 2013. Exocyst complexes multiple functions in plant cells secretory pathways. *Curr. Opin. Plant Biol.* 16:726–33.
- Zeng W, Jiang N, Nadella R, Killen TL, Nadella V, Faik A. 2010. A Glucurono(arabino)xylan Synthase Complex from Wheat Contains Members of the GT43, GT47, and GT75 Families and Functions Cooperatively. *Plant Physiol.* 154 :78–97.
- Zhang B, Liu X, Qian Q, Liu L, Dong G, Xiong G, Zeng D, Zhou Y. 2011. Golgi nucleotide sugar transporter modulates cell wall biosynthesis and plant growth in rice. *Proc. Natl. Acad. Sci. U. S. A.* 108:5110–5.
- Zhang F, Gonzalez A, Zhao M, Payne CT, Lloyd A. 2003. A network of redundant bHLH proteins functions in all TTG1-dependent pathways of Arabidopsis. *Development* 130:4859–69.
- Zhang Q, Shirley N, Lahnstein J, Fincher GB. 2005. Characterization and Expression Patterns of UDP- D -Glucuronate Decarboxylase Genes in Barley. *Plant Physiol.* 138:131–141.
- Zhong R, Ye ZH. 2015. Secondary cell walls: biosynthesis, patterned deposition and transcriptional regulation. *Plant Cell Physiol.* 56:195–214.
- Zhong R, Ye Z-H. 2012. MYB46 and MYB83 Bind to the SMRE Sites and Directly Activate a Suite of Transcription Factors and Secondary Wall Biosynthetic Genes. *Plant Cell Physiol.* 53:368–380.
- Zohuriaan-Mehr, M.J. and Kabiri K. 2008. Superabsorbent polymer materials: a review. *Iran. Polym. J.*:415–477.
- Zou H-F, Zhang Y-Q, Wei W, Chen H-W, Song Q-X, Liu Y-F, Zhao M-Y, Wang F, Zhang B-C, Lin Q, et al. 2013. The transcription factor AtDOF4.2 regulates shoot branching and seed coat formation in Arabidopsis. *Biochem. J.* 449:373–388.
- Zwieniecki MA, Melcher PJ, Michele Holbrook NM. 2001. Hydrogel control of xylem hydraulic resistance in plants. *Science* 291:1059–62.
- Zykwinska A, Thibault J-F, Ralet M-C. 2007. Organization of pectic arabinan and galactan side chains in association with cellulose microfibrils in primary cell walls and related models envisaged. *J. Exp. Bot.* 58:1795–802.
- Zykwinska A, Thibault J-F, Ralet M-C. 2008. Competitive binding of pectin and xyloglucan with primary cell wall cellulose. *Carbohydrate Polymers* 74: 957-961.
- Zykwinska AW, Ralet M-CJ, Garnier CD, Thibault J-FJ. 2005. Evidence for In Vitro Binding of Pectin Side Chains to Cellulose. *Plant Physiol.* 139:397–407.